1991-12-18

Spacecraft Design Project High Temperature Superconducting Infrared Imaging Satellite

Angus, Bill

SPACECRAFT DESIGN PROJECT
HIGH TEMPERTURE
SUPERCONDUCTING INFRARED
IMAGING SATELLITE

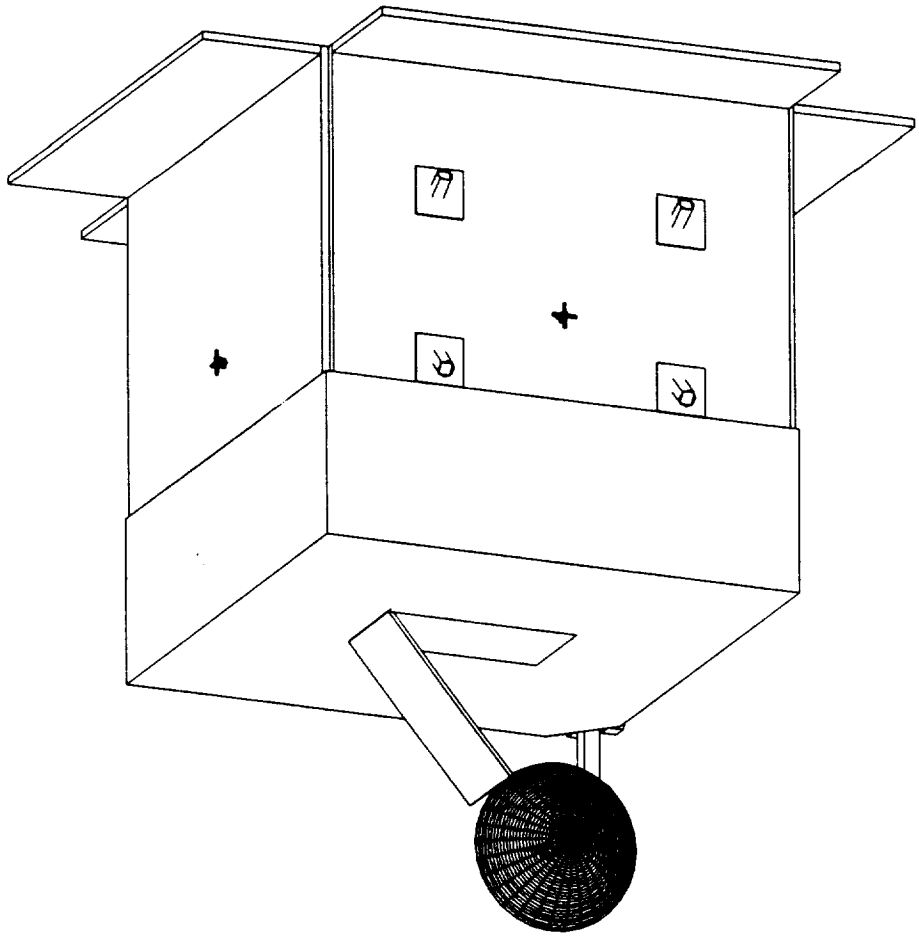

DECEMBER 18, 1991
NAVALPOSTGRADUATE SCHOOL
MONTEREY, CALIFORNIA

1991 SATELLITE DESIGN TEAM

Bill Angus

Jeff Covelli

Nick Davinic

Jeff Hailey

Evan Jones

Vince Ortiz

John Racine

Doug Satterwhite

Tom Spriesterbach

Dennis Sorensen

Chris Sortun

Rob Vaughan

Chon Yi

COURSE

AE4871

Advanced Spacecraft Design

Course Instructor

Professor Brij Agrawal

ACKNOWLEDGMENTS

The 1991 High Temperature Superconductor Infrared Imaging Satellite design team would like to thank Prof Brij Agrawal for his guidance and assistance throughout the 11 week quarter. His continuous support was sincerely appreciated and ensured the success of the project. We are also indebted to Professor Edward Euler and Mr Dan Sakoda of the Naval Postgraduate School, who consistently made themselves available to answer our questions. Dr. Alan Schaum, George Price, Woody Ewen, Nelson Hyman, and Porter Lyon of the Naval Research Laboratory provided valuable insight into all facets of the satellite design. Finally, we appreciate the continued interest and support of Dr. Kim Aaron, our NASA representative from the Jet Propulsion Laboratory.

TABLE OF CONTENTS

TABLES AND FIGURES

I. INTRODUCTION

A. SATELLITE DESCRIPTION

1. General

The High Temperature Super Conductor Infrared Imaging Satellite (HTSCIRIS) is designed to perform the space based infrared imaging and surveillance mission and is depicted in Figure 1.1.

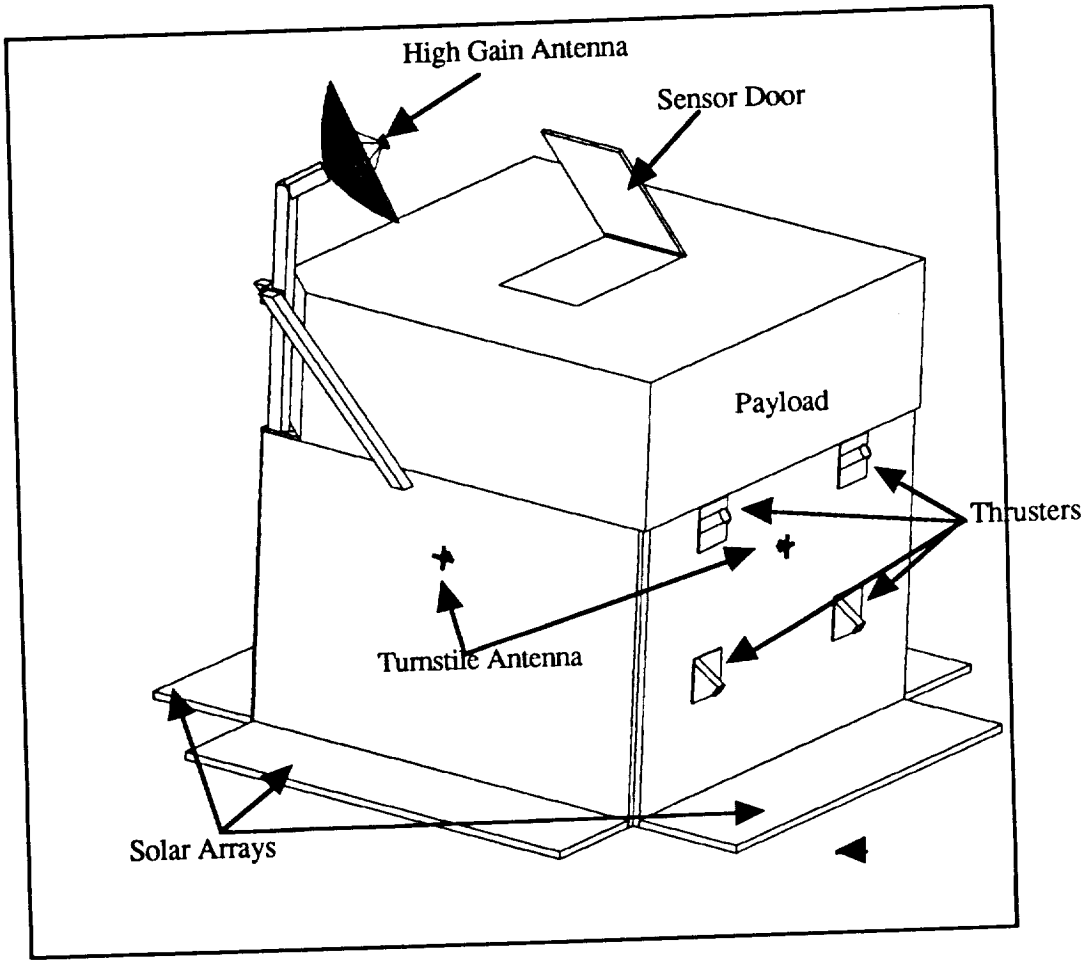

Figure 1.1 HTSCIRIS Satellite

The design of the satellite follows the 'black box' approach. The payload is a stand alone unit, with the spacecraft bus designed to meet the requirements of the payload as listed in the statement of work presented in appendix A.

2. Payload

The payload weighs 362.9 kg and has the dimensions of 1.52 x 1.52 x 0.51 meters. The payload attaches to the spacecraft bus on one 1.52 x 1.52 meter square surface. On the opposite face is mounted the infrared telescope and associated radiators. The infrared focal telescope has a 4 x 4° field of view, and is mounted at a 45° angle to the surface of the payload. The telescope has a hinged protective cover that opens approximately 50° after the satellite is deployed.

The entire cryogenic cooling system is contained within the payload, and is designed to maintain the infrared detector at 65 degrees Kelvin during sensing operations. When the detector is not sensing, the cryogenic refrigeration system is designed to replenish the cold reservoir of liquid nitrogen. During the sensing mode, the mechanical portion of the cryogenic cooling system is not operated and the cold reservoir is used to maintain the infrared detector at the required 65 degrees Kelvin.

The orientation of the payload continuously measured by an inertial measurement unit. This IMU is periodically updated through two star sensors which are mounted on the front (positive x -axis) face of the payload. Finally, a data processor is included within the payload to format the infrared data for transmission.

a. Payload Modes

The satellite has two modes of operation which include the sensing and standby modes. The 3 axis attitude control system is designed to track the sun in the standby mode and nadir point during the imaging periods.

(1) Sensing Mode

The satellite payload will be earth pointing during sensing. The spacecraft body frame will track the moving local vertical reference system, with a specified roll axis orientation for the infrared device to view the desired region. The system is designed for 15 minutes of sensing time for two consecutive orbits each 24 hour time period. This sensing time limitation is a function of the capacity of the cryogenic refrigeration system. 150 watts of power is required by the payload during this mode. Real time image data transmission to the mobile ground site also occurs during sensing. There is no store and dump capability on board the spacecraft for the infrared information.

(2) Standby Mode

In the standby mode, the spacecraft will track the sun, with the solar arrays to charge the batteries. Simultaneously, the payload and telescope are pointed away from the sun to optimize thermal control and cooling requirements for the payload. 100 watts of power is required by the payload during this mode.

3. Spacecraft Bus

a. General

The general configuration of the spacecraft is a 1.524 meter cube with the solar panels at the base and the payload located on the top as previously depicted in Figure 1.1. The four solar panels are folded for launch and deployed following separation from the launch vehicle. The high data rate antenna extends above the payload and the two pairs of omnidirectional turnstile antennas are placed on opposite sides of the the spacecraft. Total weight of the spacecraft is approximately 1000 kg. The launch vehicle adapter attaches to the central support cylinder and thrust cone at the base of the spacecraft.

b. Attitude Control

The attitude control system is designed to continuously stabilize the spacecraft while operating in the sensing and the standby modes. The attitude control system consists of four reaction wheels for three axis control. Three of the wheels are located on orthogonal axes, with a fourth wheel skewed at 45 degrees out of plane for redundancy. Momentum dumping is achieved via orthogonal magnetic torque rods. Eight hydrazine thrusters are used for despin after deployment from the launch vehicle and to provide orbital corrections to compensate for atmospheric drag. The thrusters are also available for detumble mode and as a backup to the torque rods. The attitude control computer receives data from the IMU, earth sensor, sun sensors, star trackers, and the long term gyro assembly.

c. Propulsion

The propulsion system is composed of two sets of four 1 Newton hydrazine thrusters. The system is designed for reboost and detumble operations, as well as backup to the torque rods for momentum wheel desaturation. Sufficient fuel is left over at end of life for deboost. The system is designed to maintain full capability in the event of single thruster failure.

d. Electric Power

The electric power system will provide power to the payload and the bus for all anticipated operating conditions. While operating in the sensing mode, the entire satellite is designed to operate completely on batteries. In the standby mode, the solar arrays provide the power required for housekeeping and to recharge the batteries prior to the next sensing period. Four 10 Ah nickle-hydrogen batteries provide power at the bus voltage of 28 ± 4 volts via a full shunt regulator. The solar arrays are mounted on four panels that deploy following

separation from the launch vehicle. Each panel has a sub-array with two partial shunt regulators. Only three of the sub-arrays are required for normal operation.

e. TT and C

The spacecraft utilizes the Air Force Satellite Control Network for satellite tracking, telemetry and control. Two sets of turnstile antenna pans provide omnidirectional coverage. Image data is sent to a mobile ground site via the wide band high data rate transmitter. The transmission frequency of 20 GHz was selected and utilized the binary phase shift keying (BPSK) modulation scheme. The system was designed with a 3dB safety margin. The antenna is a front fed parabolic antenna design. One 0.5 meter antenna on a tripod structure provides full coverage. The 2.1 degree half power band width provides a 19-63 km footprint.

f. Thermal

The thermal design utilized both passive and active techniques to maintain the bus with temperature limits. Strip heaters with temperature sensors are used to maintain the minimum temperature during the cold conditions. The batteries require louvers to maintain the temperature range. In addition, the payload is thermally isolated from the spacecraft bus.

g. Structures

The spacecraft structure was designed to withstand the launch loads of the Delta II launch vehicle. The predicted launch vehicle loads are 7.2 g axial and 2.5 g laterally. A factor of safety of 1.5 was used for all critical load carrying structures. The fundamental launch vehicle natural frequency is 35 Hz axial and 15 Hz lateral. The primary load carrying structure includes the central cylinder and conical adapter. The sides of the structure are made of aluminum honeycomb panels with equipment attached directly to those same panels. The spacecraft is designed for a 50 Hz minimum frequency.

B. MISSION REQUIREMENTS

1. General

Specifications influencing the design of the spacecraft bus were originated at the Naval Research Lab and are summarized below in Table 1.1.

Table 1.1 General Design Requirements

Design Life	3 Years
Orbit altitude	509.3 km
Orbit Inclination	70 Degrees

The designed lifetime of the satellite is three years. All bus subsystems were designed to meet this requirement. The satellite orbit will be circular with an altitude of 509.3 km and an inclination of 70 degrees. Launch vehicle selection will be discussed in greater detail later in the report and is based on the satellite weight and dimensions, as well as the specified orbit.

2. Attitude Control Subsystem

The attitude control subsystem has three principal tasks. The first is to slew the satellite between sun tracking in the standby mode orientation to the sensing mode orientation, and the second is to ensure the satellite is sufficiently stabilized in the sensing mode to ensure proper image resolution. Additionally, while in the sensing mode the control subsystem must orient the satellite about the roll axis for the telescope to view the desired geographic area. The Attitude Control System requirements are specified in Table 1.2

Table 1.2 Attitude Control Specifications

Method Of Control	3 Axis Stabilized
Pointing Accuracy	± 0.5 Degrees Each Axis (3σ)
Slew Time	90 Degrees In 15 Minutes
Settling Time	1 Minute
Rate stability	0.003 Degree Per Second

Information is also available to the spacecraft bus from the dual star sensors as well as the Inertial Measurement Unit that are contained within the payload.

3. Radio Frequency Communication Subsystem (RFCS)

a. Omnidirectional Transmit and Receive Capability

The communications subsystem is designed to provide dual redundant communications with the ground control station. The low data rate transmission is designed for omnidirectional command and control of the satellite and is capable of transferring data at a minimum rate of 16 KBPS. Information to be transmitted includes spacecraft operation and housekeeping data as well as pointing commands.

b. Directional High Data Rate Transmitting Capability

The high data rate downlink is designed to transmit image data in real time to a remote mobile ground station. Requirements for the Radio Frequency Communications Subsystem (RFCS) are specified in Table 1.3.

Table 1.3 Radio Frequency Communications Subsystem Requirements

Low Data Transfer Rate	16 Kbits(Minimum)
High Data Transfer Rate	150 Mbits
Bit Error Rate	10^{-11} (Encrypted)
	10^{-9} (Unencrpyted)
Minimum Elevation Angel (1)	10 Degrees
Link Availability Due To Rain Attenuation	99 Percent
Maximum Ground Antenna Diameter	20 Feet

4. Command and Telemetry Subsystem (CATS)

a. Command Receive

The information received by the RFCS from the ground site is used by the CATS subsystem to execute commands to the spacecraft subsystems. Specifically, the CATS subsystem will decrypt the ground commands, then validate, decode, and store them. The information is then distributed to the respective subsytem for implementation.

b. Transmission

The CATS system will perform the reverse operations as above for data transmission via the RFCS. The data to be processed, formatted, and encrypted includes the spacecraft operation and housekeeping information, and the image data.

5. Electric Power Subsystem (EPS)

The electric power subsystem must be sized to support 15 minutes of sensing time per orbit for two consecutive orbits during the worst case orbital

eclipse period. In the sensing mode 150 watts is required for payload. In the standby mode, 100 watts is required for payload operation.

C. LAUNCH VEHICLE DESCRIPTION

The Delta II launch vehicle with medium shroud was selected based on payload mass and dimensions. The ideal launch site is Vandenberg AFB, California. This site minimizes flight over populated areas during launch and is more suitable for high inclination launches.

II. SPACECRAFT CONFIGURATION

A. MISSION REQUIREMENTS

The spacecraft is comprised of two distinct subsections: the payload and the bus. The specifications and performance criteria for the payload were dictated to the design team by the representatives of the Naval Research Laboratory statement of work and the goal of the design was to define a bus that could support the payload from launch through end-of-life.

B. DESCRIPTION

1 General

The payload is described as a 1.524 meter square by 0.508 meter tall cubic structure and is depicted in Figure 2.1. The imaging system and radiators for the sensor thermal control system are located on one of the square faces. The payload-to-bus mounting interface is located on the other square face. Two star sensors are mounted on one of the side panels.

2. Satellite Bus

a. General

The bus is also a box-like structure that is 1.524 m square by 1.016 m tall. The bus is required to provide a stable platform to orient the sensor for imaging and standby modes. It is also required to provide electric power, command uplink, telemetry downlink as well as real time transmission of the imaging data. The bus is constructed around a cylindrical aluminum monocoque thrust tube that is attached to an aluminum monocoque conical adapter cone. The cone protrudes through the face opposite the payload (the bottom face) and provides the interface to the launch vehicle. The thrust tube and adapter carry the

spacecraft launch loads. Four aluminum honeycomb side panels surround and are attached to the thrust tube and cone. They act as mounting surfaces for equipment and provide radiating area for the thermal control of the bus. An additional panel is located along the payload mounting face and provides a mounting surface for the payload.

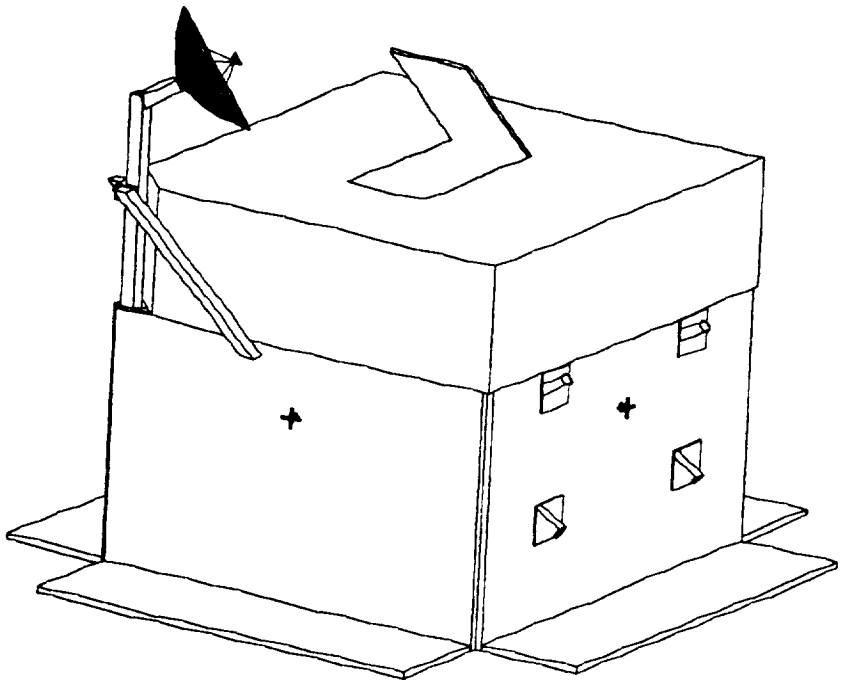

Figure 2.1 Overall Configuration

b. Solar Arrays

Fixed solar arrays are located parallel to the bottom face and are mounted on panels that extend outboard from the bus. The arrays are 0.38 m wide by 1.47 m long. The silicon solar cells are mounted parallel to the anti-earth face and are designed to provide maximum power to recharge the nickek hydrogen batteries as well as supply house keeping power while operating in the standby

mode. During the imaging mode the entire spacecraft power is provided by four rechargeable nickel hydrogen batteries.

c. TT & C and Comunications

Telemetry and communications are provide by the bus through one Wide Band Downlink antenna (WBDL) , two omni-directional transmit antennas and two omni directional receive antennas. The omni-directional transmit and receive antennas are paired up on the pitch and anti-pitch faces to provide continuous telemetry and command uplink communications capability. The WBDL antenna is gimbal mounted to a boom that extends along one corner of the spacecraft, past the payload face, to allow horizon to horizon coverage during imaging evolutions. The support equipment, transmit/receivers, and amplifiers are mounted interior to the bus. The high heat dissipating components are mounted to external panels. Two interior aluminum honeycomb equipment panels (oriented parallel to the square faces of the bus) provide mounting surfaces for the non-critical equipment.

d. Attitude Control

Attitude control for the spacecraft is provided by four reaction wheels and eight magnetic torque rods (for momentum desaturation). The reaction wheels are mounted near the top of the bus, three inside the adapter cone and the fourth (the yaw wheel) inside the bus on the top of the uppermost equipment panel. Three of the wheels are oriented on mutually orthogonal axes with the fourth at a 45 degree angle from the other three. The torque rods are mounted, two per axis, on opposite side panels of the bus toward the top surface. Initial orbit correction and emergency attitude control (despin) are provided by eight 1-lbf hydrazine thrusters, mounted in groups of four on the pitch and anti-pitch faces of the bus. The thrusters are utilized as a back-up to the primary attitude control system in addition to station keeping. The fuel and pressurant tank are located at the center

of the adapter cone with the surface of the tank aligned with the top face of the bus.

e. Thermal Control

The thermal control system is an active/passive design that maintains the bus and components at nominally low temperature, and provides active heating to maintain temperature within limits. The system is composed of passive radiating and insulating material, applied to the surfaces of equipment and structures, and electric heaters attached to temperature sensitive components. Louvers are attached to the batteries as an aditional measure to disapate more heat energy.

C. MASS SUMMARY

The mass properties for the principle subsystems are listed in Table 2.1.

Table 2.1 Satellite Mass Summary

SUBSYSTEM	MASS
PAYLOAD	362 kg
T T & C	148.5 kg
ELECTRIC POWER	97.0 kg
PROPULSION (DRY)	8.3 kg
ATTITUDE CONTROL	42.4 kg
THERMAL CONTROL	24.8 kg
STRUCTURE	164.9 kg
MECHANICAL INTEGRATION	73.3 kg
SUB TOTAL	921.2 kg
MASS MARGIN (20%)	184.2 kg
PROPELLANT	12.9 kg
TOTAL	1118.3 kg

D. MOMENT OF INERTIA CALCULATIONS

Moment of inertia and center of mass calculations for the spacecraft were conducted using the Microsoft Excel (ver. 2.2) spreadsheet software. The complete spread sheet is included in Appendix B. The reference coordinate system used to define the positions in that spread sheet is shown in Figure 2.2.

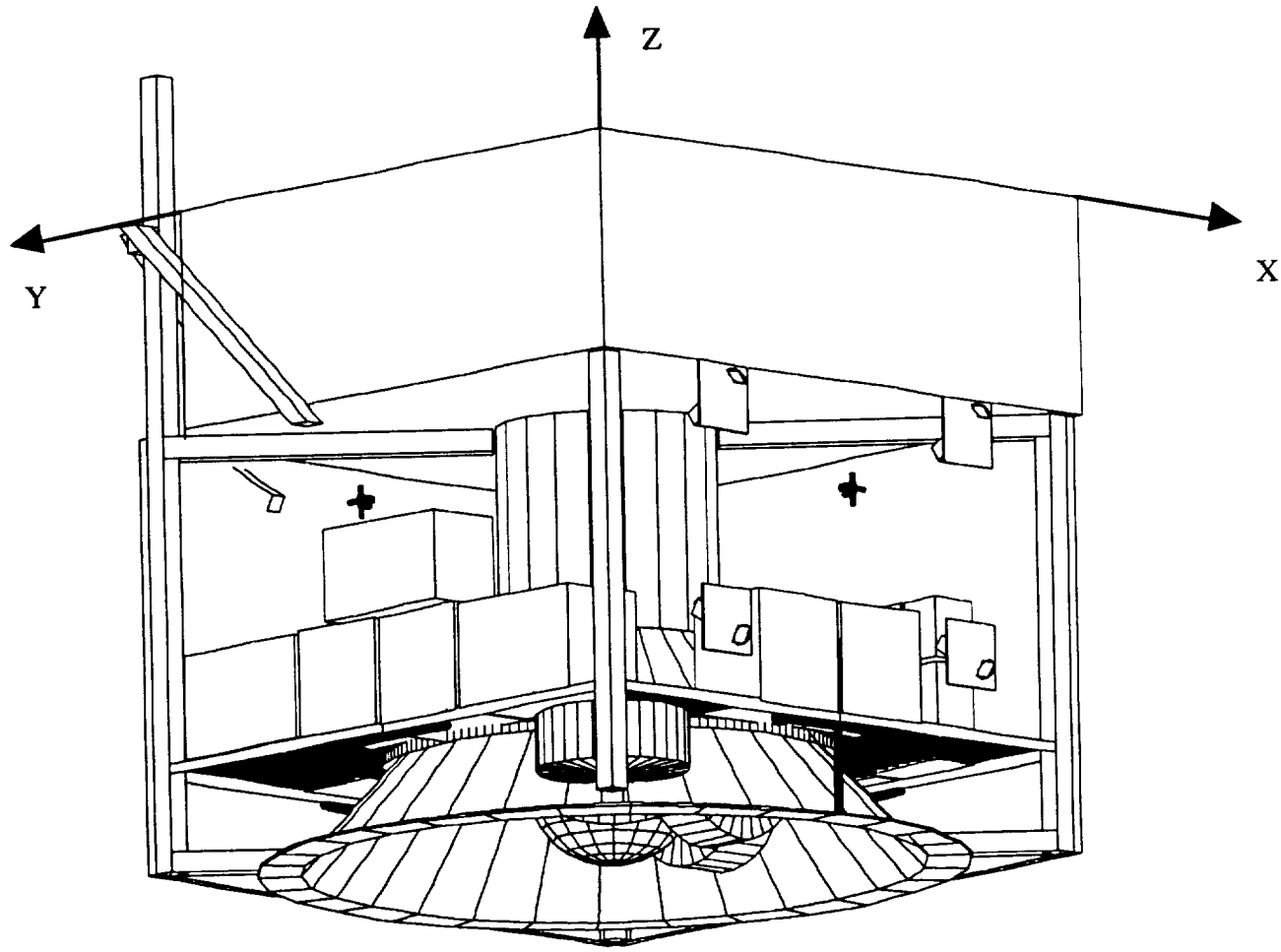

Figure 2.2 Moment Of Inertia Reference Frame

Calculations of the components were made by idealizing the components into one of several regular geometric shapes. Component moments of inertia were then calculated about the principle axes oriented parallel to the principle axes of the spacecraft. Parallel calculations were also made to determine the spacecraft center of mass. Smaller components of the spacecraft were modeled as point masses and only their displacement from the spacecraft axes were considered. The final calculation of the spacecraft moments of inertia were calculated with reference to axes that pass through the spacecraft center of mass and are perpendicular to the faces of the spacecraft. The location of the center of mass is listed in Table 2.2:

Table 2.2 Center of Mass Location

X = -0.0152 m	Y = 0.0106 m	Z = -0.0107 m

Note that X, Y, and Z pass through the geometric center of the 1.524 m cube and are oriented positive along the roll, pitch, and yaw axes. The moments of inertia for the system are summarized in Table 2.3:

Table 2.3 Moment of Inertia Summary

Ixx	Iyy	Izz	Ixy	Ixz	Iyz
476 kg-m^2	450 kg-m^2	432 kg-m^2	-6 kg-m^2	-32 kg-m^2	9 kg-m^2

E. ELECTRICAL POWER REQUIREMENTS

The spacecraft operates in two distinct modes: sensing and stand-by. During the sensing mode the sensor draws it's peak power, the data is being transmitted in real time and the bus is still drawing general maintenance power. During this mode the batteries supply the entire load to the spacecraft. In the stand-by mode the sensor and payload draw less power, however the solar arrays are required to

recharge the batteries for the next sensing period. The peak power requirements for the various subsystems are listed in the Table 2.4:

Table 2.4 Electrical Power Summary

SUBSYSTEM	STAND-BY LOAD (Watts)	SENSING LOAD (Watts)
PAYLOAD	100	150
ATTITUDE CONTROL	50	50
THERMAL CONTROL	70	30
PROPULSION	1	1
T T & C	25	25
DOWNLINK	0	140
TOTAL	246	406

E. EQUIPMENT LAYOUT

The following sections show the general layout of the equipment on the various structural panels. A more complete description of the individual components is provided in the following chapters.

1. Roll Face

Primary components of the roll face are depicted in Figure 2.3

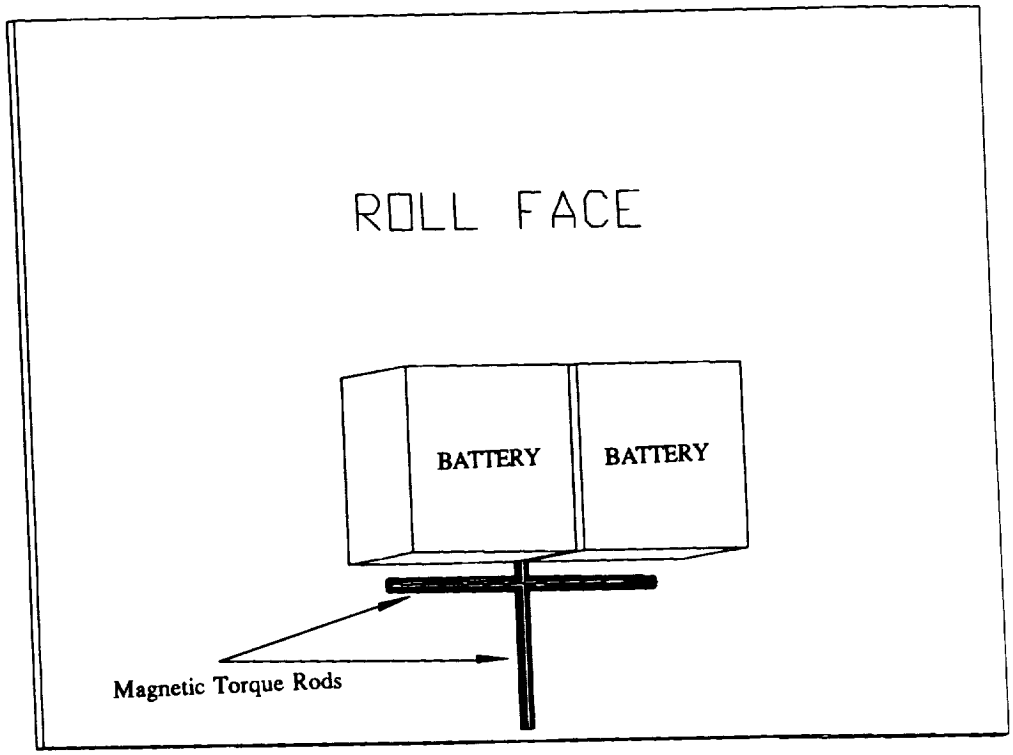

Figure 2.3 Primary Roll Face Components

2. Anti-Roll Face

Primary components mounted on the Anti-Roll face of the spacecraft are depicted in figure 2.4.

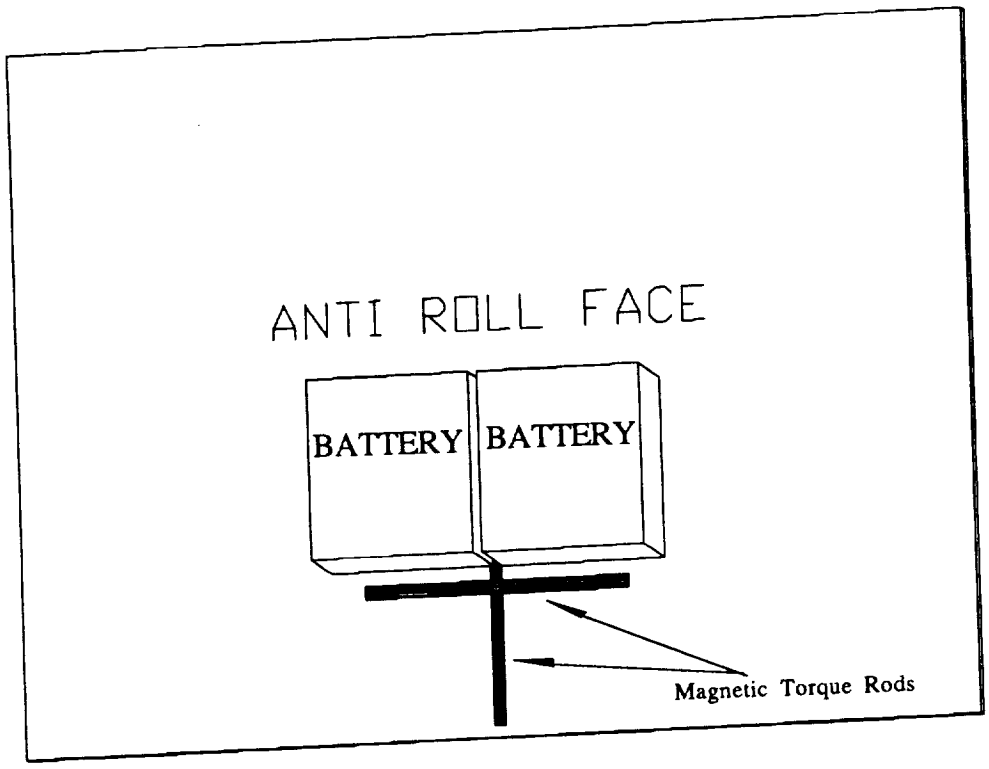

Figure 2.4 Primary Anti-Roll Face Components

3. Pitch Face

Primary components mounted on the Pitch face of the spacecraft are depicted in figure 2.5.

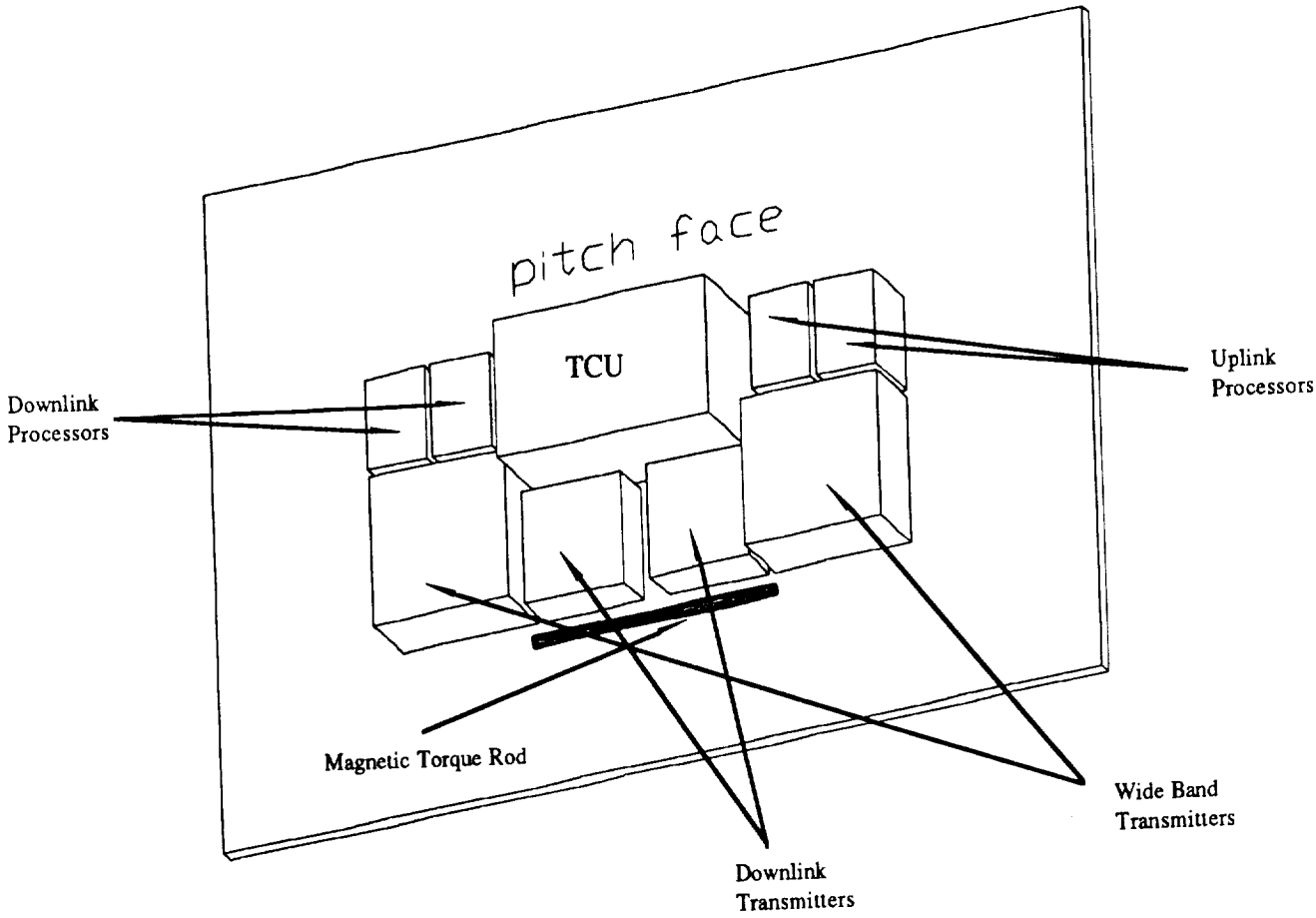

Figure 2.5 Primary Pitch Face Components

4. Anti-Pitch Face

Primary components mounted on the Anti-Pitch face of the spacecraft are depicted in figure 2.6.

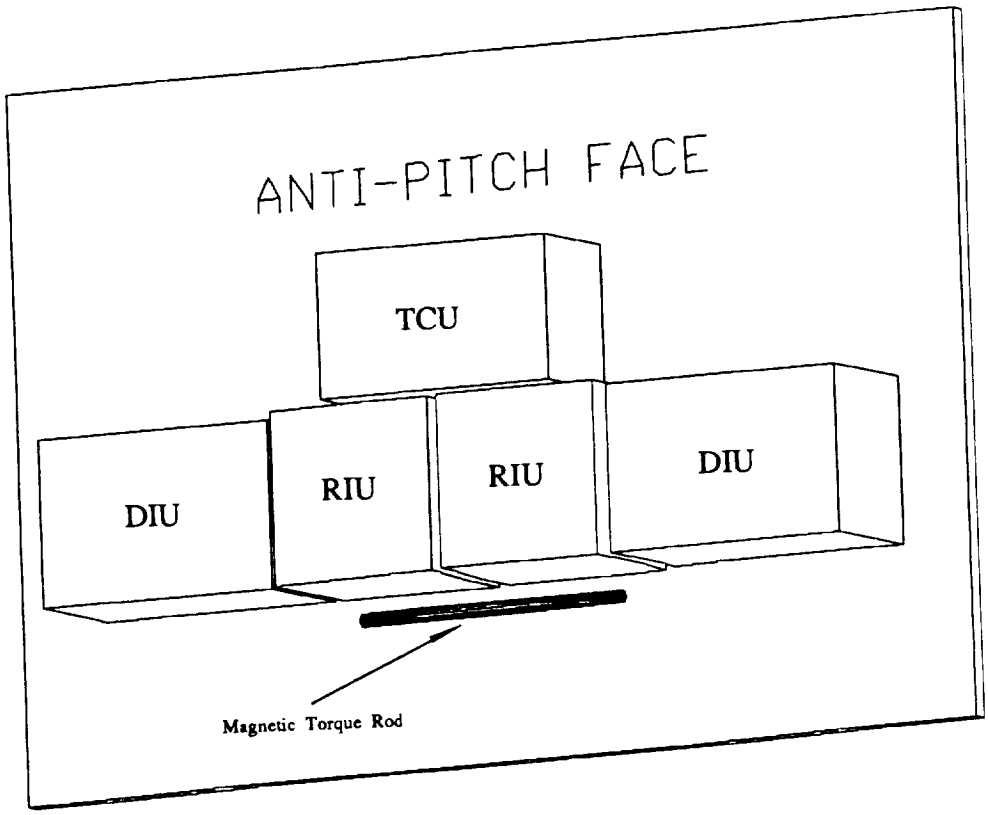

Figure 2.6 Primary Anti-Pitch Face Components

5. Anti-Earth Face

Primary components mounted on the Anti-Earth face of the spacecraft are depicted in figure 2.7.

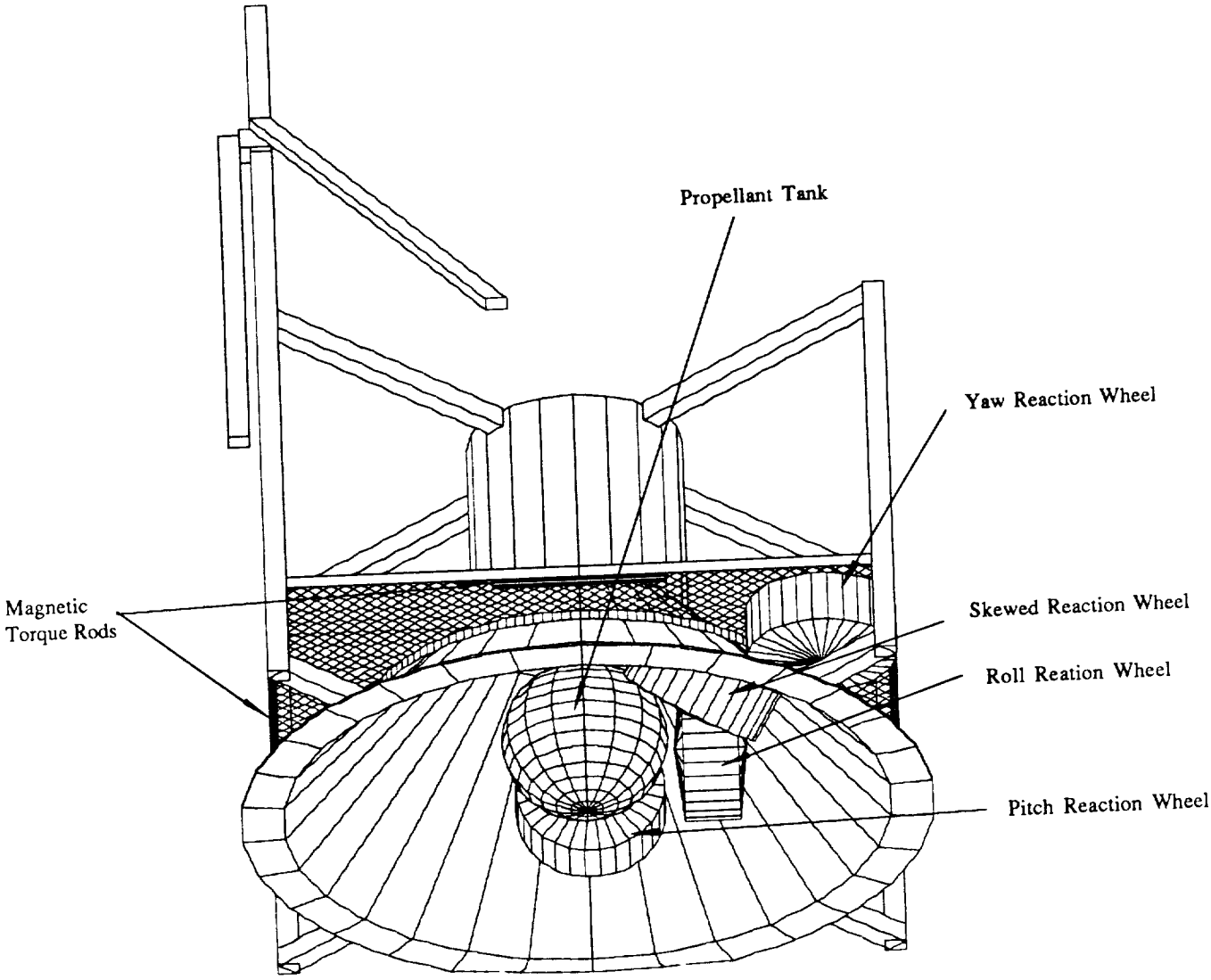

Figure 2.7 Anit-Earth Spacecraft Face

III. ORBITAL DYNAMICS

The infrared imaging mission of this satellite dictates the orbital parameters for this spacecraft. These parameters were defined within the statement of work by NRL and included in Appendix A. The orbit was given a 509.3 km altitude and a 70° inclination as summarized in Table 3.1. The ground path of this high inclination orbit is depicted in Figure 3.1 and shows that the satellite maximizes its time over land masses and passes over the majority of the habitable land on the Earth. These characteristics of this orbit make the choice ideal to successfully carry out the mission of imaging a wide variety of targets with both land and water backgrounds.

Table 3.1. Summary of Orbital Parameters

Parameter	Value	Parameter	Value
Apogee	6887.43 km	Perigee	6887.43 km
Period	1.58 hrs	Inclination	70 °
Argument of Perigee	N/A	Longitude of the Ascending Node	TBD (1)
Eccentricity	0.0	Altitude	509.3 km

Note: (1) Longitude of Ascending Node determined by launch date.

A. ORBITAL PERTURBATIONS

The statement of work defined the allowable tolerances and are defined as one nautical mile of orbital altitude (1.852 km) and 1° of inclination. For this particular satellite the drag force on the spacecraft is the primary factor in maintaining this tolerance over the three year lifetime. The inclination is effected by several different forces, these include the Earth's

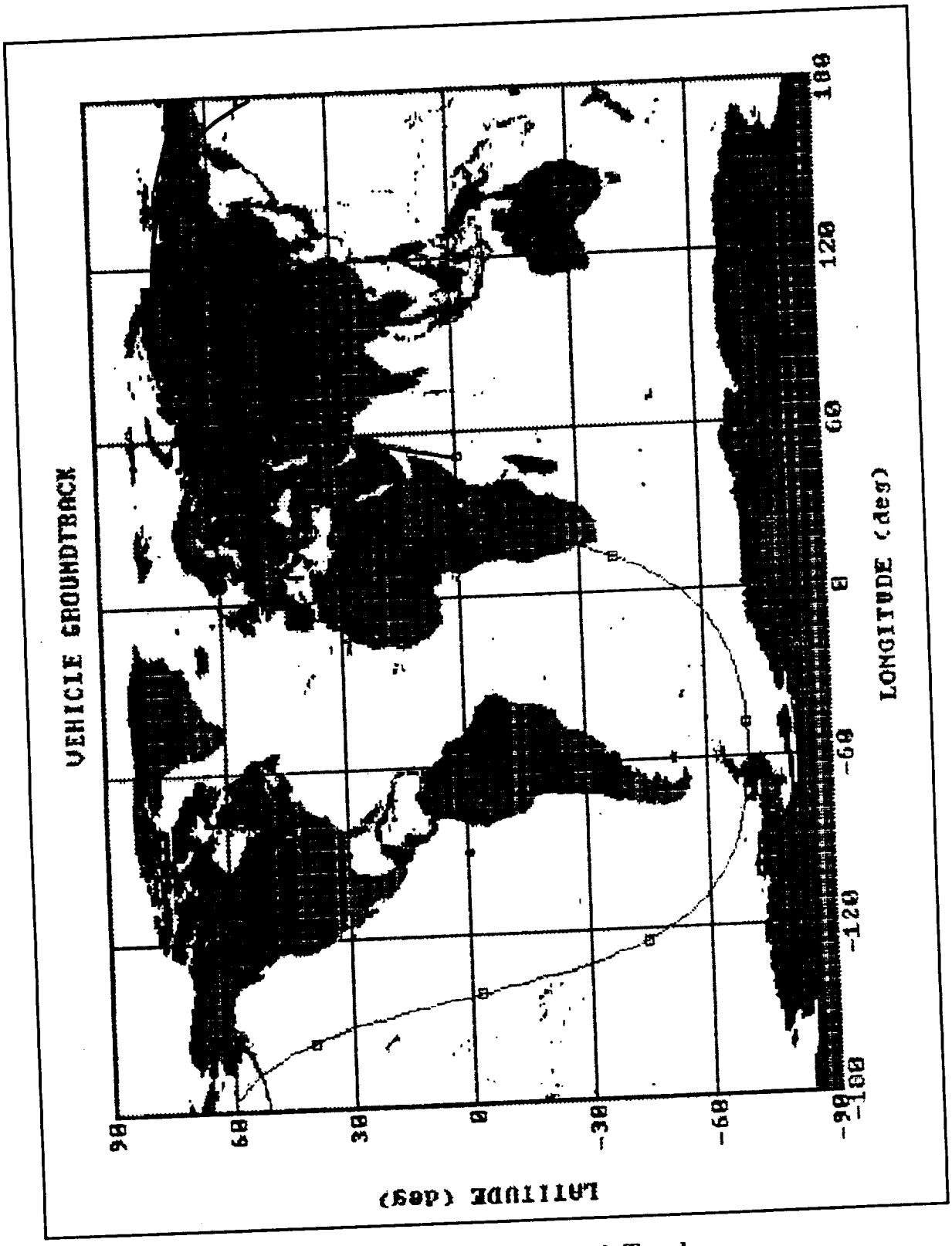

Figure 3.1 Orbit Ground Track

oblateness, and the attraction of the sun and moon. Since the orbit is circular and there is no perigee or rotation of the argument of perigee within the orbital plane however, the orbit's ground track is affected by the rotation of the longitude of the ascending node.

1. Drag

The accuracy of the drag force on the satellite and its effect on the orbit are as accurate as the prediction of the atmospheric density. Two methods, hand calculations and the ASAP program, are used to predict the drag perturbations on the orbit. The ASAP program estimated the largest altitude loss and will be used for orbital maintenance calculations. Detailed analysis can be found in Appendix C and the results are summarized below in Table 3.2

Table 3.2 Summary of Altitude Loss for Spacecraft

Method	Estimated Altitude Loss
Hand Calculations	1.65 km/yr
ASAP Program	4.50 km/yr

2. Inclination

The effect of the Earth, Sun, and Moon on the inclination of the orbit is complex in nature. These effects not only change as the satellite orbits around the Earth, but also change as the Moon rotates around the Earth and as the Earth rotates around the Sun. The total effect of inclination change on the orbit is based on the maximum represented values for effect from the Sun and Moon, it will be shown that for the circular orbit the perturbations from the Earth's oblateness has no effect on the inclination of the orbit.

a. Effects from Earth's Oblateness

As mentioned above there is no cumulative effect on the inclination of the orbit. The Earth's equatorial bulge does exert an influence on the satellite, but this is small

in nature and has a period equal to the orbital period of the satellite. A detailed derivation and analysis are include in Appendix C.

b. Effects from Sun

The Sun's influence on the inclination of the orbit depends on four parameters, the apparent inclination of the sun, the inclination of the orbit, the altitude of the orbit and the longitude of the ascending node. Because the altitude and inclination of the orbit are specified, the Sun's effect on the inclination will be influenced only by the apparent inclination of the sun and the position of the satellites longitude of the ascending node. For design purposes interest lies in the maximum value of di/dt, Equation 3.1 shows that the maximum value for di/dt will occur when the Sun's inclination is ± 23.5° and is a minimum when the Sun's inclination is 0°.

$$\frac{di}{dt} = \frac{3}{2}\frac{\mu_s}{h}\frac{r^2}{r_s^3}\left[\sin(\Omega)\cos(\Omega)\sin(i)\sin(i_s)^2 + \sin(\Omega)\cos(i)\sin(i_s)\cos(i_s)\right] \qquad (3.1)$$

Figure 3.2 shows the inclination change as a function of Ω when the Sun's apparent inclination is set to 23.5°, from the graph the maximum value is found to be .0084 deg/yr.

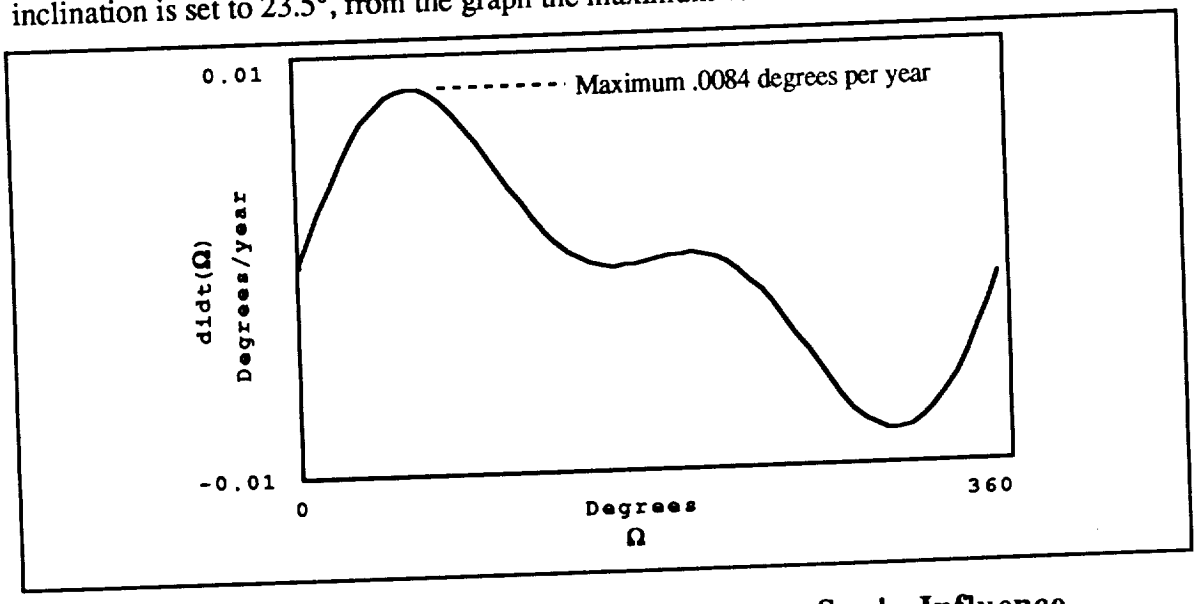

Figure 3.2. Perturbation Effect Due to Sun's Influence

c. Effects from Moon

The influence of the Moon on the orbital perturbation is similar to the effect of the Sun. The magnitude of the change in inclination per year is slightly higher for the Moon's influence than it is for the Sun's. The governing equation for di/dt is shown to be

$$\frac{di}{dt} = \frac{3}{4}\frac{\mu_1}{h}\frac{r^2}{r_1^3}[\sin(\Omega-\Omega_1)\cos(\Omega-\Omega_1)\sin(i)\sin(i_1)^2 + \sin(\Omega-\Omega_1)\cos(i)\sin(i_1)\cos(i_1)$$

$$+ \sin(2\theta_1)[-\cos(2(\Omega-\Omega_1))\sin(i)\cos(i_1) + \cos(\Omega-\Omega_1)\cos(i)\sin(i_1)]$$

$$+ \cos(2\theta_1)[\sin(\Omega-\Omega_1)\cos(\Omega-\Omega_1)\sin i + \sin(\Omega-\Omega_1)\cos(\Omega-\Omega_1)$$

$$\times \sin(i)\cos(i_1)^2 - \sin(\Omega-\Omega_1)\cos(i)\sin(i_1)\cos(i_1)]] \qquad (3.2)$$

where all of the 'l' subscripted variables apply to the Moon's orbit. Equation 3.2 contains both secular and period terms, the terms dependent on θ_l are periodic with a period of 14 days, half of the lunar cycle. Equation 3.3 shows only the secular terms and is dependent on both the inclination and the the Moon's longitude of the ascending node.

$$\frac{di}{dt} = \frac{3}{4}\frac{\mu_1}{h}\frac{r^2}{r_1^3}[\sin(\Omega-\Omega_1)\cos(\Omega-\Omega_1)\sin(i)\sin(i_1)^2 + \sin(\Omega-\Omega_1)\cos(i)\sin(i_1)\cos(i_1)] \qquad (3.3)$$

The lunar orbital inclination takes 9 years to complete a cycle of inclination change from a maximum value of 28.6° to a minimum value of 18.3°, during this nine years the longitude of the ascending node is varying ±13°. Fortunately, at the maximum and minimum inclinations the longitude of the ascending node is zero. Figures 3.3 and 3.4 show the inclination change on the satellite as a function of the satellites longitude of the ascending node. The maximum value occurs when the Moon's inclination is at 28.6° and contributes to the change in inclination .023 degrees per year. Because this is the maximum value encountered all orbital maintenance calculations will be based on the .023 degrees per year value.

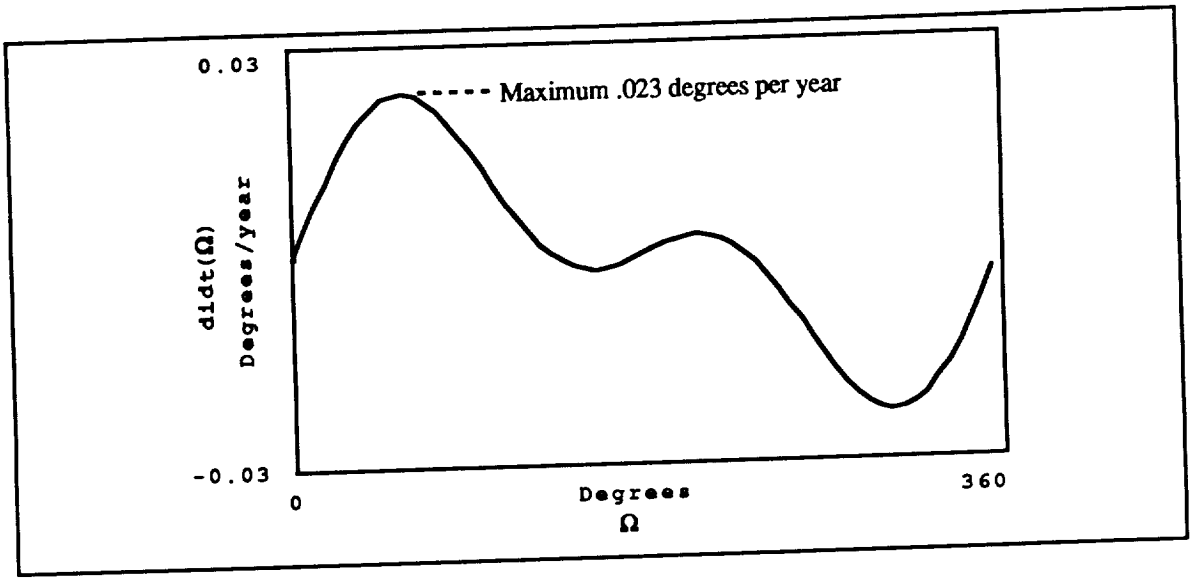

Figure 3.3 Moon's Influence on Di/dt (i_l=28.6°)

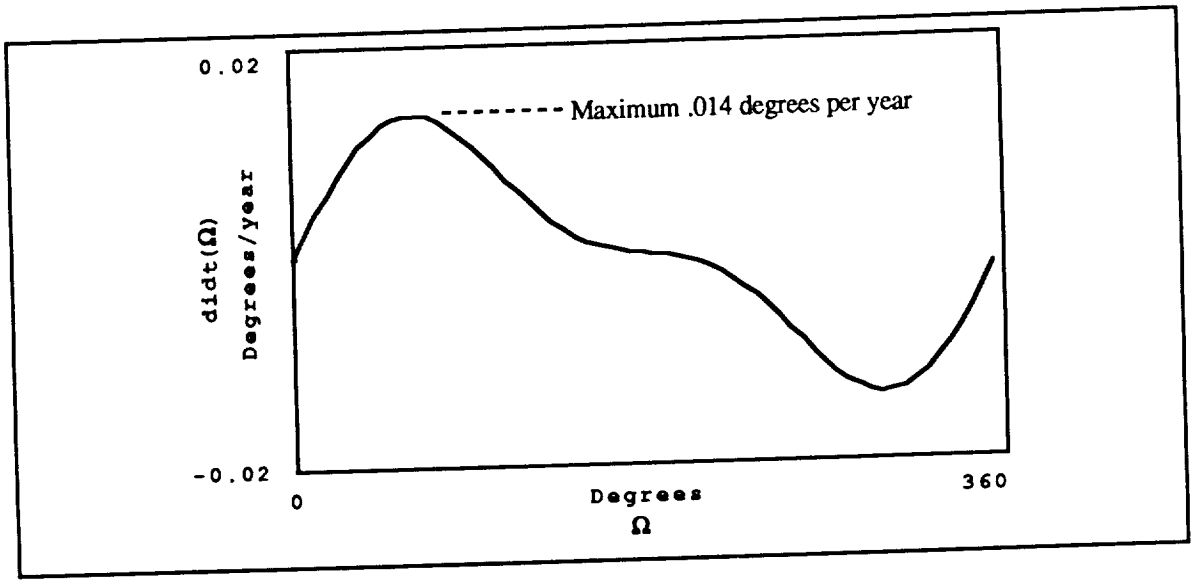

Figure 3.4 Moon's Influence on Di/dt (i_l=18.3°)

3. Longitude of the Ascending Node

We are interested in the longitude of the ascending node for the satellite for two reasons; first, all of the calculation for the inclination change are based on the spacecraft's longitude of the ascending node and second, it can be calculated how much the ground track shifts on daily basis. The equation governing the change in the longitude of the ascending node can be approximated by

$$\frac{d\Omega}{dt} = -2.062\times10^{14}\left[\frac{\cos(i)}{r^{3.5}}\right] \qquad (3.4)$$

For this orbit the longitude of the ascending node shifts -2.6 degrees per sidereal day. This orbit completes 15.14 orbits per sidereal day, computing the shift of the ascending node for 15 orbits (-2.57 degrees) and then computing the remaining degrees of rotation the Earth has at the 15 orbit point (+3.419 degrees) it can be shown that the orbit ground track shifts .84 degrees east every 15^{th} orbit. This orbit nearly passes over the same ground track every day and at the equator the subsatellite point shifts by 50 nm every 15^{th} orbit.

B. SWATH WIDTH

Because the satellite can only image within its visible horizon and transmission of data from the satellite to a ground station must occur when they are visible to each other, the swath width of the spacecraft is of interest. Defining three variables, ρ - angular radius of Earth, λ - Earth central angle, and η - nadir angle the swath width can be calculated (Figure 3.5). Equation 3.5 computes the angular radius of the Earth based on the orbital radius (r) of the satellite, where R equals 6378.14 km.

$$\sin(\rho) = \frac{R}{r} \qquad 3.5$$

At a 509.3 km altitude ρ (angular radius of Earth) is computed to be 67.8°, this is the angle off nadir the satellite sees the horizon. Because the grazing angle requirements for a ground station to communicate with the satellite is different than the grazing angle of the to observe

an object on the ground there will be two different swath widths to define. To compute the swath width the spacecraft will have for a ground station to observe the satellite at grazing angles greater than 10° a nadir angle of 65.7° will define the edge of the swath. While the statement of work restricts the grazing angle for observation of an object between 45° and 90°. Using Equation 3.6 the remaining Earth central angle can be found, this angle represents half the angle the swath subtends on the Earth's surface.

$$\tan(\eta) = \frac{\sin(\rho)\sin(\lambda)}{1 - \sin(\rho)\cos(\lambda)} \qquad 3.6$$

The Earth's central angle for the ground station to see the satellite is 14.2° and for observations it is 4.1°. This defines swath widths of 3165 km and 911 km for the ground station and observations respectively. Realizing that the subsatellite point is moving across the Earth's surface at 7.6 km/sec these distances become very important

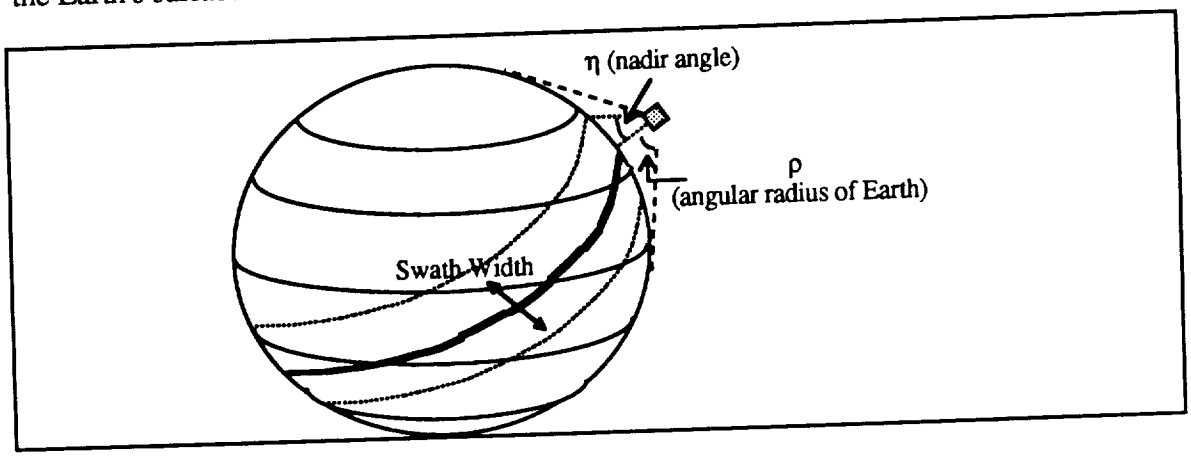

Figure 3.5 Satellite Swath Width

C. RESULTS

Drag on the satellite is a factor which must be accounted for in the fuel consumption for orbital maintenance, the predicted altitude loss for the 180 day period from the ASAP program was nearly equal to the allowed altitude perturbation and the spacecraft must be reboosted to maintain the orbit. The maximum inclination change seen by the satellite did

not exceed the allowed tolerance, the total for both the Sun and Moon influence is .0314 degrees per year and over the lifetime of the satellite is approximately 0.1 degree. No additional fuel is necessary for the shifting longitude of the ascending node, because it does not concern us that the ground track shifts and the calculations were done to inform on the nature of this orbit.

IV. RADIO FREQUENCY COMM SUBSYSTEM (RFCS)

A. MISSION REQUIREMENTS

The RFCS communication subsystem is the interface between the satellite and the ground station. The RFCS includes the Command and Telemetry Subsystem (CATS) which provides the interface between the payload, spacecraft bus and the ground station. As described in the statement of work, the Radio Frequency Communication Subsystem (RFCS) is required to provide the following capabilities:

- Omnidirectional command receiving capability:
- Omnidirectional low data rate (16 Kbps minimum) transmitting capability:
- Directional high data rate (150 Mbps maximum) transmitting capability:

The High Data Rate Down Link System (HDRDS) is required to provide the following capabilities:

- Optimal spectrum usage for 150 Mbps:
- Bit Error Rate (BER) 10e-11 encrypted
- Bit Error Rate (BER) 10e-9 unencrypted:
- 99% availability due to rain attenuation:
- Minimum elevation angle of 10 degrees at data collection terminal:
- 20 foot (6 meter) diameter receiver antenna is assumed for the ground station:

B. SYSTEM DESCRIPTION

1. System Integration

The communications subsystem is the interface between the satellite and the earth. The system's components are located as depicted in Figure 4.1. It generates a downlink RF signal that is phase coherent, transmits the downlink error

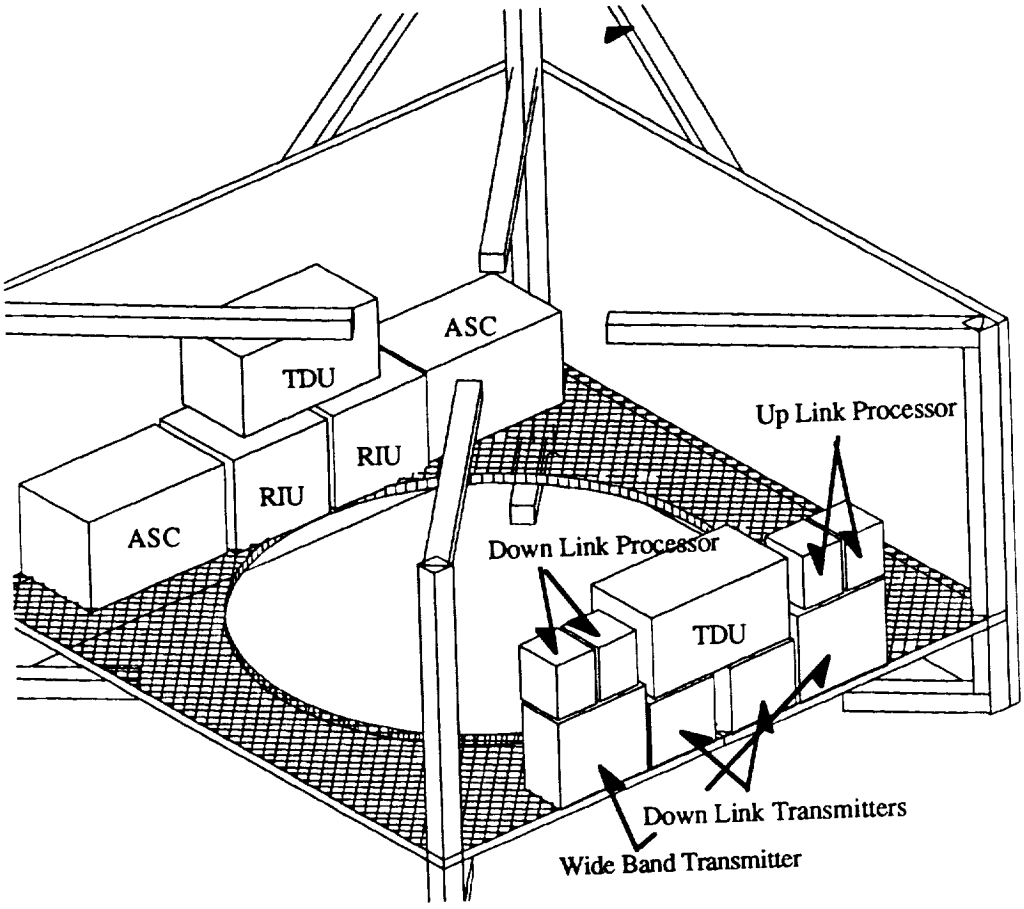

Figure 4.1 Communications Subsystem Components

so its phase synchronizes with the received phase of the uplink carrier. This is referred to as the coherent turnaround or two-way-coherent mode. The turnaround ratio using SGLS is 256/205. The two-way-coherent mode allows the ground station to know more precisely the downlink signal's frequency and to measure the

Doppler range rate. This allows a sweep of fewer frequencies and thus acquire the spacecraft more quickly. The spacecraft will have large volumes of data and a short field-of-view time to the ground station. To transmit maximum data on a direct downlink, the ground station must acquire the signal in a minimum amount of time. By using a ranging method of navigation, range-rate information is obtained from the Doppler shift of the coherent signal.

The communication subsystem's transponder is compatible with SGLS. It tracks the uplink carrier, receives and detects commands, and transmits telemetry. The communication subsystem contains two transponders with parallel transmit and receive signal paths for redundancy.

Command and Data Handling (C&DH) on board receives, decodes, processes and distributes spacecraft commands. It also gathers,formats, stores and transmits telemetry data from spacecraft measurement. As depicted in Figure 4.2, the C&DH

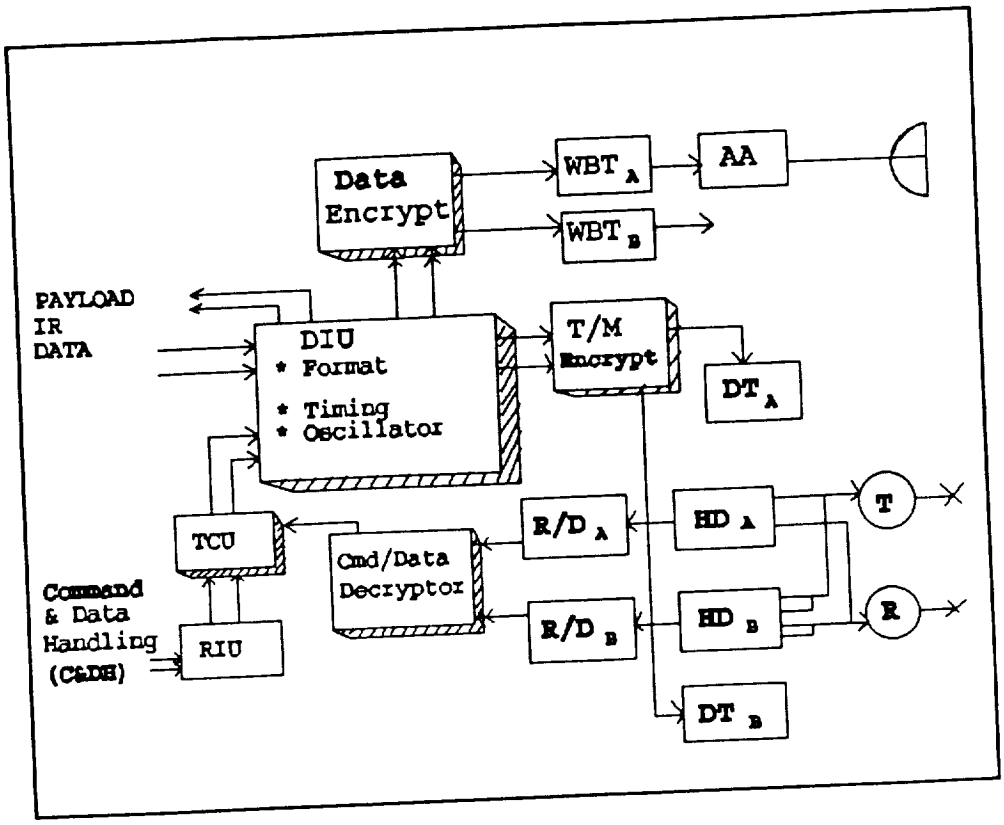

AA : Antenna Actuator
DIU : Data Interface Unit
DT : Downlink Transmitter
HD : Hybrid Divider
R : Receiver
R/D : Receiver/Domod
RIU : Remote Interface Unit
T : Transmitter
TCU : Telemetry Command Unit
WBT : Wide Band Transmitter

Figure 4.2 C&DH Subsystem

subsystem consists of a Remote Interface Unit (RIU), Tracking & Command Units (TCU), and Data Interface Units (DIU). Encryption and decryption devices are also included for which NSA distributes and regulates the keys. The TCU receives the demodulated uplink information and routes it to the DIU which also receives, formats and routes downlink telemetry, through encryptors, to the

transmitter. The TCU serves as decoder; authenticator for commands; and formatter. Remote Interface units receive and process commands and requests for data. The TCU has a built in processor that performs calculations, makes decision and issues commands. Pulse Code Modulation (PCM) subcarrier provided by DIU is sent to the downlink transmitter. (DT) Hybrid Dividers(HD) route the signal to or from the appropriate set of turnstile antennas The primary receive antenna could be used as a back up transmit antenna, and the primary transmit antenna could be used as a back up receive antenna. Dual redundancy is provided in the design.

2. High Data Rate Down Link

a. Description

The Wide Band High Data Rate (WBHD) Transmitter is designed to provide the capability of sending real time digital imagery data at a rate of 150 megabits per second (Mbps). The design includes a 3 db safety or link margin. The link margin is simply the difference between the received and required bit energy per noise power spectral density which yields a specified error probability. This margin becomes important when you consider the uncertainties involved with the receiver, a mobile platform (assumed to be a Van). There are increased noise problems with such platforms due to incalculable environmental interference and equipment calibration. This is especially true if you're using a mobile 20 foot diameter antenna (assumed to be a fold out umbrella design). The required bit energy per noise power spectral density was calculated based on Quadrature Phase Shift Keying (QPSK) modulation. This consists of using 0, 90 180 and 270 degree phase shifts for binary data transmission. Binary Phase Shift Keying (BPSK) and Multiple Frequency Shift Keying (MFSK) were also considered but the standard in industry is QPSK due to efficiency and reliability of digital signal

transmission. Using 20 GHz for a carrier frequency allows up to 1 MHz band width for data transmission.

b. Antenna Design

For the High Data Rate Wide Band Down-link antenna design, two parabolic antenna configurations were considered. Parabolic reflector antennas offer narrow beams over a wide range of frequencies. They are also simple to design, simple to construct and have a proven track record. For an offset parabolic antenna the reflected beam is not intercepted by the feed horn which reduces the side lobes The reduction in side lobes increases antenna efficiency. An offset parabolic antenna is depicted in Figure 4.3. Due to the fact that a feed horn can not be fixed

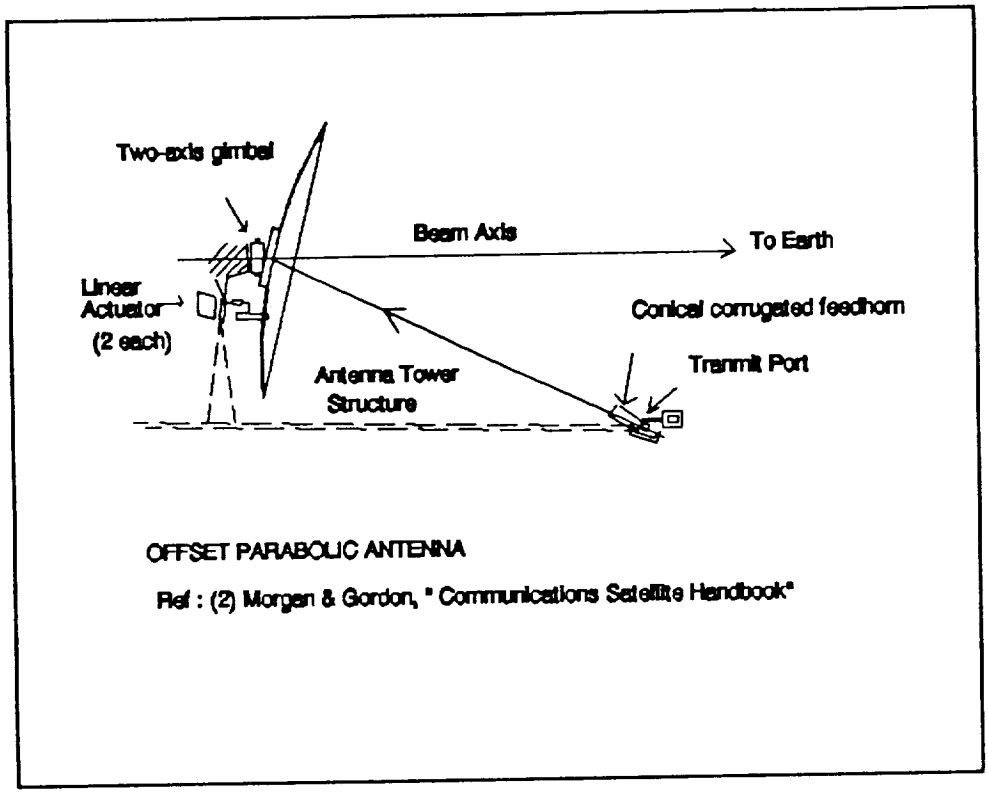

Figure 4.3 Offset Parabolic Antenna

to the payload, the decision was made to use a Front Fed (symmetric) Parabolic Antenna design as depicted in Figure 4.4.

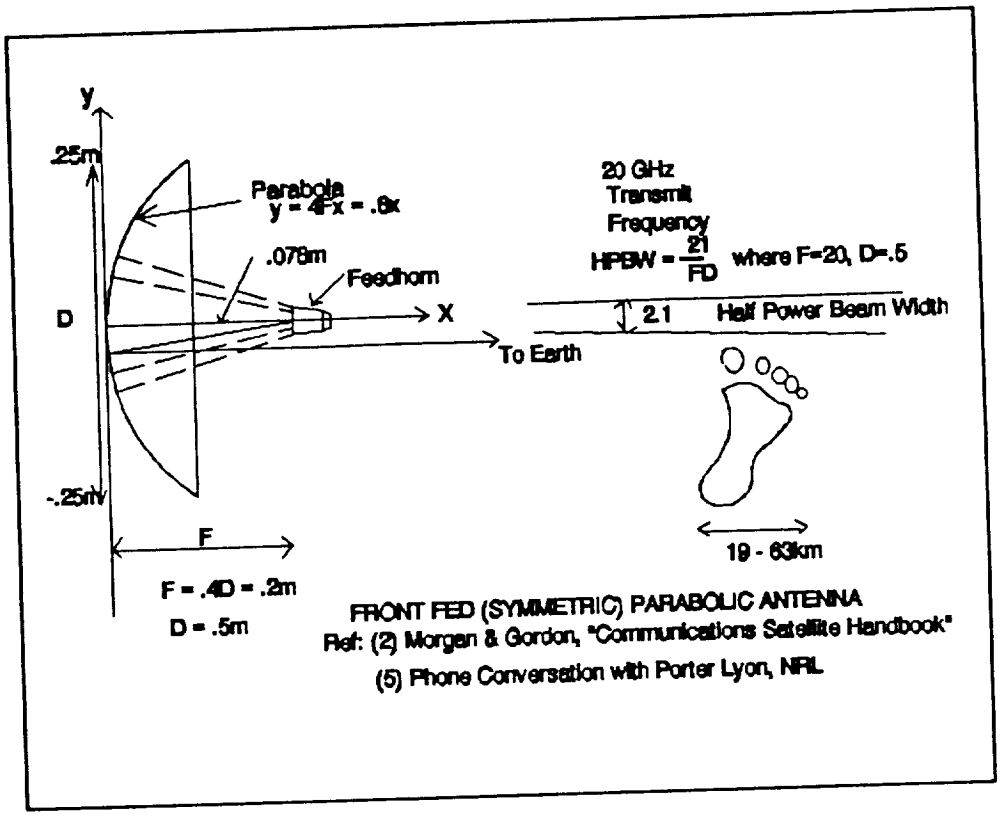

Figure 4.4 Parabolic Antenna Design

This simplified the antenna support structure design and allows a larger down-link FOV. The antenna will also have two three degree of freedom gimbal attachment to the supporting structure to provide a wider range of pointing angles. The Front Fed Parabolic Antenna will provide a 19 to 63 Km diameter footprint with a 2.1 degree Half Power Beam Width (HPBW) as depicted in Figure 4.4. Antenna pointing control will consist of an open loop, on-board attitude and computer steer. This design provides +/- 0.2 degrees of pointing accuracy with about 1 db loss, assuming the attitude and control system maintains within spacecraft attitude design tolerances. Using a closed loop system would require the use of an auto-

track receiver and a more complicated three dimensional up-link beacon which must be constantly tracked. It was desired that the additional cost and complexity of this system was not required for this mission.

2. Tracking, Telemetry, And Control

a. Description

The principal objectives for spacecraft TT&C or telemetry are to provide information of operational use, failure analysis, and prediction of spacecraft performance. In routine operations the telemetry verifies commands and equipment status and also alerts personnel of any unusual occurrences. In case of failures or anomalies, data is used to determine the causes, the events, and ways to counteract or alleviate the problems produced by failure. Telemetry can also be used to analyze any degradation that might affect performance and predict its effect on the spacecraft lifetime. For this spacecraft , TT&C consist of two sets of omnidirectional turnstile antennas, Command and Data Handling system (C&DH) and the Air Force Satellite Control Network (AFSCN).

b. Antenna Design

TT&C, omnidirectional transmit and receive antennas will consist of 2 sets of Turnstile Antenna Pans, one set for transmit and one set for receive. The turnstile antenna consists of two Half-wave Dipole Antennas intersecting in the middle and at a 90 angle from each other. This provides the necessary 180 arrangement for near omnidirectional coverage. They extend from the plane of the spacecraft a distance of $\lambda/4$ (0.0375 m) for optimal gain out to $\lambda/2$ (0.075 m) for minimal gain as depicted in Fig 4.5.

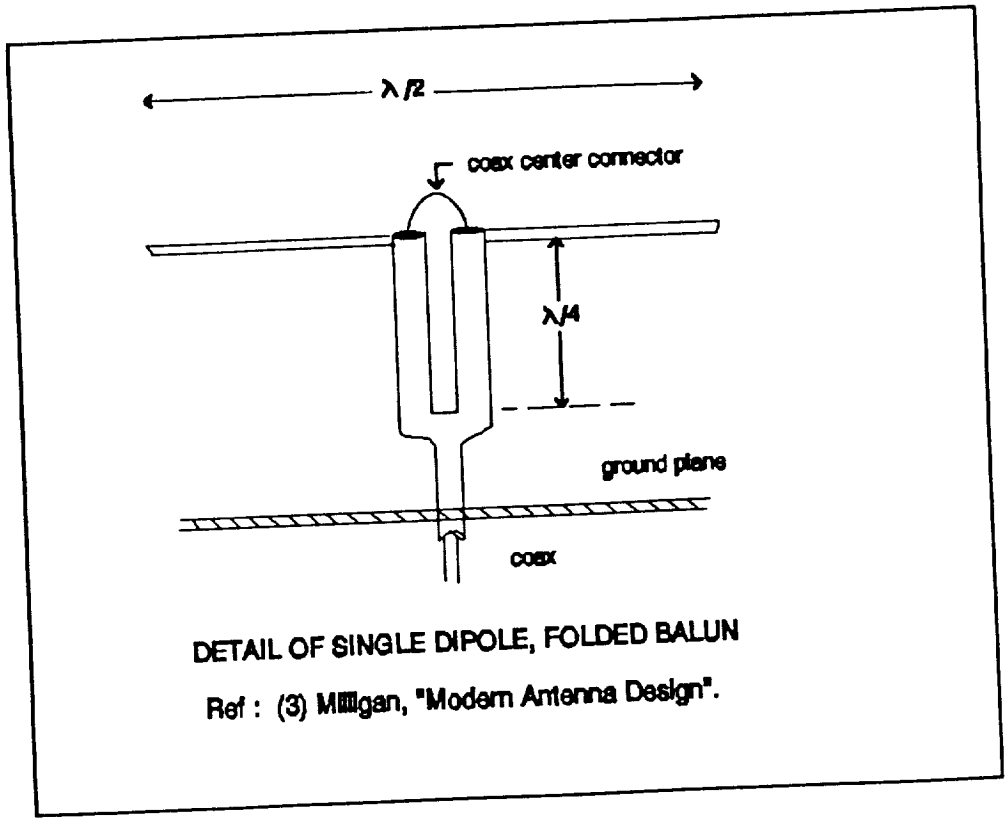

DETAIL OF SINGLE DIPOLE, FOLDED BALUN

Ref : (3) Milligan, "Modern Antenna Design".

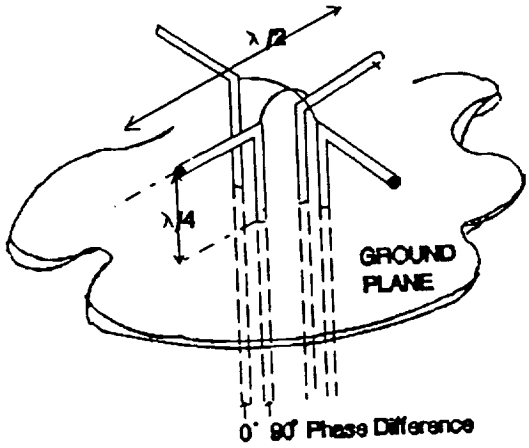

CLOSED DIPOLE (TURNSTILE) ANTENNA

Ref : (4) Johnson & Jasik, " Antenna Engineering Handbook".

Figure 4.5 Turnstile Antenna

The cone of coverage is +/- 125 degrees from center with a 4 db drop in gain at the 125 degree angle. The reason for using two pair of Turnstile Antenna is because of the different frequencies/wavelengths used for transmit and receive. The pattern for a three-axis-stabilized satellite is a cardroid of revolution and is an omnidirectional antenna except for a cone of silence where the spacecraft shadows the antenna 2.

3. Ground Control and Frequency Selection

The TT&C for the spacecraft was designed to be compatible with the Air Force Satellite Control Network (AFSCN)1. AFSCN consists of seven Remote Tracking Station (RTS) located throughout the world. The system of RF links with spacecraft is known as the S-Band Space-Ground Link Subsystem (SGLS). The downlinks provide telemetry and mission data rates up to 1.024 Mbps per channel. There are 40 downlink channels available with frequency range of 2197.5 - 2297.5 MHz. There are 20 uplink channels available with frequency range 1763.721 - 1839.795 MHz. TT&C was designed to operate at a primary SHF carrier frequency corresponding to channel 10 of the SGLS ground terminal:

Command Uplink : 1799.756 MHz

Telemetry Downlink: 2247.5 MHz

A back-up channel could be channel 9 or 11 to remain close to dipole design antennas. The high data downlink was designed to be compatible with 20 foot maximum diameter antenna. The frequency was selected to 20 GHz. The Ku-band frequency was chosen to provide wideband transmit data capability as specified in mission requirements.

D. MASS,POWER AND EQUIPMENT LIST

The systems power and weight are summarized in the Table 4.1 and 4.2 below.

Table 4.1 RFCS Power & Weight Summary

Unit	Quantity	Length (cm)	Width (cm)	Height (cm)	Weight (kg)	Power (Watts)
Downlink Transmitter	2	16.7	7.6	17.3	3	22
Wide Band Transmitter	2	22.8	22.8	11.4	19	75
WBDL Antenna	1				15	
Antenna Actuator	1				4.5	5
Omni Xmit Antenna	2				1.7	5
Omni Rcv Antenna	2				1.6	5
Hybrid Divider	2	5	5	0.6	0.25	
Receiver/Demod	2	17.8	17.2	17.8	6.8	2
RFCS Total:					51.85	114

Table 4.2 CATS Mass And Power Summary

Unit	Quantity	Length (cm)	Width (cm)	Height (cm)	Weight (kg)	Power (watts)
Data Interface (DIU)	2	35.5	21.6	24.1	19.9	25
Remote Interface (RIU)	2	24.4	23.1	24.9	29.9	6
Telem & Command (TCU)	2	21.1	35.6	19	8.1	15
Uplink Processor	2	9.9	14.2	11.7	3.6	9.5
Downlink Processor	2	9.9	14.2	11.7	3.6	9.5
CATS Total:					65.1	65
Total Comm/TTC	Weight	116.95	kg	Power	179	Watts

V. ELECTRICAL POWER SUBSYSTEM (EPS)

A. MISSION REQUIREMENTS

The electrical power subsystem must provide sufficient power for 30 minutes sensing time per day (15 minutes times two successive passes). During non-sensing periods, the spacecraft will be sun oriented, and for active periods, the spacecraft will slew to an earth seeking orientation, and will continue to track the earth until the active session is concluded.

The spacecraft, being sun oriented for approximately 21 hours out of each day is an attribute that is fully exploited in this design. The solar panels are fixed, and during the intervals of earth orientation, the batteries play a big role in powering the spacecraft's active and, if necessary, it's housekeeping load. Fixing the solar arrays provides a higher degree of simplicity and reliability, which is probably desirable considering the payload involves rather high risk technology.

The basic concept goes like this. Put fairly large batteries in the vehicle, capable of carrying the active load and housekeeping load for two consecutive orbits. After this event, return the vehicle to sun orientation, and begin charging the batteries and be back to full charge in 21 hours. During the development of the design, worst case scenarios were always assumed, battery and solar cell EOL, winter solstice, etc.

B. EPS DESCRIPTION

1. General

The satellite electrical power subsystem consists of four solar arrays that nominally generate 34.2V at 4.3A at end of life (EOL)., four 10Ah NiH_2 batteries, and the regulation devices to fully regulate the bus voltage.

2. Solar Array

There are four arrays mounted in a stationary, fixed manner. Each array is capable of filling the role as either charge array, or housekeeping array. Two arrays are required normally for battery charging, and one array is required for the housekeeping electrical load. The manipulation of the solar array's power distribution is done from ground control. via the CATS link.

3. Batteries

The batteries are designed to carry the electrical demand during eclipse and the additional load that arises during sensing and data transfer. Four 10Ah NiH_2 batteries are installed.

After a maximum possible demand event, the batteries were designed to be at 60%depth of discharge (DOD). The batteries will have approximately 21 hours to fully recharge after completion of this event.

4. Power Control Electronics

The spacecraft bus is regulated to 28(+/-4)V. The regulation is achieved by use of two partial shunt regulators on each solar panel and one series dissipative regulator at the battery discharge terminal.

a. Regulation of Housekeeping and Battery Charging Voltage

The partial shunt regulators were designed to shunt the voltage spikes that are experienced at BOL eclipse emergence, and dissipate the power surplus to space in the form of thermal energy.

One of the partial shunt regulators on the panel is to regulate the voltage supplied to the housekeeping bus when that array is aligned as such. The other partial shunt regulator is used to regulate the battery charging voltage, when the array is aligned for battery charging.

b. Regulation of Active Payload Voltage

A series dissipative regulator is connected in series between the battery discharge terminal and the payload input terminal. It must regulate the voltage from the battery discharge voltage at full charge (33V) down to the payload operating voltage of 28V. This regulator also regulates the voltage to the housekeeping bus during eclipse.

C. EPS DESIGN

1. Solar Arrays

Since each array must be capable of filling the role as either charge array, or housekeeping array, the voltage supplied from each array is fixed by the battery charging requirement (33.9V), and the current is fixed by the housekeeping load, since the housekeeping current draw (8.05A) is greater than the battery charging rate (4.0A).

2. Batteries

The batteries are 22 cell NiH_2 in individually encapsulated pressure vessels (CPV). This allows for an open circuit failure of one cell per battery. Minimum battery discharge voltage in the event of a cell failure is 24.1V, and maximum battery output voltage at full charge, no cell failure is 33V. See Appendix F for detailed development of battery design.

The storage device is divided into four 10 Ah batteries for purposes of mass distribution, battery margin, and redundancy.

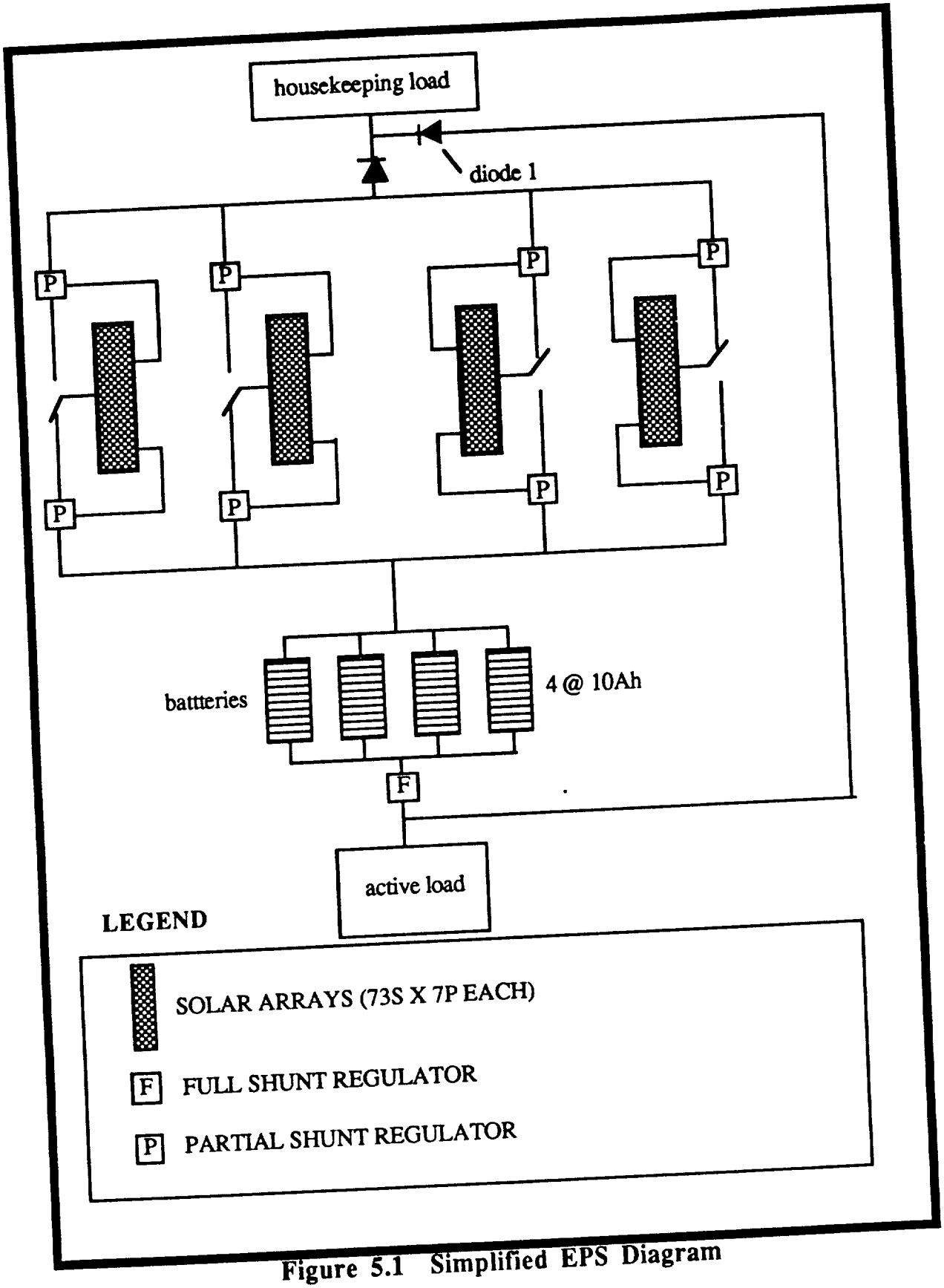

Figure 5.1 Simplified EPS Diagram

D. EPS PERFORMANCE

1. General

The worst possible case for EPS demand at end of life yields a 60% DOD and total battery recovery in a 24 hour cycle.

2. Solar Array

a. Radiation Degradation Of Solar Cells

Table 5.1 depicts the anticipated outputs of each array at EOL and BOL. A detailed evaluation of radiation degradation is provided in Appendix F.

Table 5.1. Subarray Output

	EOL	BOL
P_{MAX} (W)	148	158
V_{OC} (V)	42.8	44.4
I_{SC} (A)	4.69	4.74
I_{MP} (A)	4.34	4.36
V_{MP} (V)	34.2	36.6

b. Temperature Effects

Although the temperature range is severe (-60C to 50C), the most significant problem faced is the extreme voltage spike experienced when emerging from a 35.5.minute eclipse. The voltage output will nearly double it's nominal value for one or two minutes, and rapidly return to the nominal output value. The power control electronics are designed to accommodate this situation.

c. Array Sizing

As discussed, each subarray must provide one half of the current demand during spacecraft passive periods (8/2)A at the battery charging voltage (33.9V). The number of cells in series is determined by dividing the battery charging voltage by the voltage at max power point at EOL.

$$N_S = \frac{33.9}{0.469} = 72.3 \approx 73 \text{ cells}$$

The number of strings necessary is computed in the following manner.

$$N_P = \frac{4}{0.04 \times 2.5 \times 6.2} = 6.45 \approx 7 \text{ strings}$$

d. Solar Cell Arrangement And Panel Dimensions

The cells are arranged on a 3/8 inch sheet of aluminum. Inter-cell spacing is 1 mm in both directions. There are 531 cells mounted to each panel, arranged with the 6.2 cm side pointing in a radial fashion from the yaw axis.

3. Batteries

The spacecraft's design life is three years, and the batteries will be nominally cycled one time per day, yielding approximately 1000 cycles. Nickel Hydrogen batteries will be used at 60% depth of discharge (DOD). With only 1000 cycles, this battery could be cycled to a greater DOD, therein requiring a smaller battery, but selecting 60% DOD provides margin, and is an attempt to deal with the uncertainty that exists in the ability to maintain the battery's operating temperature because in the operating concept as outlined, no true "north and south faces" are maintained, and the sun will impinge upon the battery's thermal radiator at times, the full consequence of this on battery life has not been completely analyzed.in this report.

a. Requirements

The energy storage must be sufficient to carry the entire spacecraft electrical load for 220 minutes, once per day. This event also, of course includes two 15 minute periods of active sensing and high speed data link.

b. Battery Capacity And Sizing

The capacity of the storage device may now be evaluated in the following manner,

$$C = \frac{E_{OUT}}{V_{DB}DOD} = \frac{2 \times 10^6}{24.1 \times 0.6} = 38 \text{ Ah}$$

The storage device is divided into four 10 Ah batteries for purposes of mass distribution, battery margin, and redundancy.

c. Battery Charging

To determine a suitable charging voltage, the correct charging voltage (V_C) per cell must be obtained from the manufacturer of the battery, as well as the voltage drop across the bypass diodes (V_{DD}) in the event of a cell's open circuit failure.

$$V_{BC} = V_C(N\text{-}1) + N_D V_{DD} = 1.5(21) + 3(0.8) = 33.9\text{V}$$

Where N_D is the number of bypass diodes in series.

A BASIC code was written that simulated a worst case 24 hr day, winter solstice, EOL scenario. (Appendix F)

4. Power Control Electronics

a. Shunt Regulator

Each subarray is fitted with two partial shunt regulators (PSR). One to bring the supplied voltage down to the housekeeping load's bus voltage (nominally 27V) when the subarray is aligned to feed the housekeeping load. This PSR is called PSR_H.

The housekeeping must be regulated to 27V so that diode 1 (Figure 1) will remain reverse biased during sunlight periods, ensuring that the housekeeping does not draw it's power from the batteries.

The other PSR on the panel is to protect the batteries from the voltage spike at emergence from eclipse when the subarray is aligned to charge batteries. This PSR is called PSR_B. Their tap points are computed as follows:

$$TP\ (\%) = 100\ (1 - \frac{V_{BUS}}{V_{OC\,(ECLIPSE\ EMERGENCE)}})$$

Table 5.2. Partial Shunt Regulator Tap Points

	TP (%)	NUMBER OF CELLS PER STRING THAT ARE SHUNTED
PSR_H	37	27
PSR_B	24	18

b. Battery Charge And Discharge Regulator

A series dissipative regulator is incorporated at the battery discharge terminal, as the battery voltage output at full charge is well above the specified bus voltage. This regulator must reduce the voltage from 33V (full charge voltage) to the 28V payload voltage.

5. System Integration and Failure Recovery

Redundancy in the electrical power subsystem offers many options to recover from component casualties. The output terminals on all solar arrays lead to three position switches that will feed either the housekeeping load, charge batteries, or go to open circuit. These switches are ground controlled via an allotted word in the TT&C housekeeping link. Two subarrays must be placed in parallel for carrying the housekeeping load. One subarray is sufficient for battery charging, leaving one subarray idle for later use in the event of loss of any one of the remaining three subarrays. All major components are isolatable by switches, again through ground control. Table 9 lists the effects of various levels of electrical power subsystem failure.

Table 5.3. EPS Degradation Effects Matrix

Battery Loss	Array Loss	Effect
0	1	None
0	2	Mission Loss
1	0	1) Limit active sensing to 15 min. per day, or 2) Sacrifice lifetime due to higher battery DOD and higher charging rate
1	1	Same as above
1	2	Mission Loss
2	0	Mission Loss

D. MASS AND POWER SUMMARY

Table 5.4 illustrates the mass budget of the electric power subsystem.

Table 5.4 EPS Mass Budget

BATTERIES	43
SOLAR ARRAYS	17
DISCHARGE CONTROL	12
CHARGE CONTROL	10
WIRING	9
HOUSEKEEPING REGULATION	6
TOTAL EPS MASS	97 kg

VI. PROPULSION

A. MISSION REQUIREMENTS

A launch vehicle is required to place a satellite in a circular orbit that has a 509.3 kilometer altitude and a 70 degree inclination. This satellite is anticipated to weigh between 800 and 1200 kilograms. The satellite should be designed for a three year lifetime. Additionally, the requirement exists for the satellite to remain within 1 nautical mile of its given altitude and within 0.5 degrees of its inclination. It is anticipated that these requirements will make a propulsion subsystem necessary.

B. LAUNCH VEHICLE

1. Description

A Delta II (7320) launch vehicle was chosen for this mission. Appendix F gives the details of the selection process. This launch vehicle is a two stage liquid propelled rocket with three solid strap-on boosters. Typically a Delta II has nine solid strap-ons but these are not required since this satellite has such a small mass. If desired, the six other solids could remain attached and additional satellites could be included in the fairing space remaining. This multiple launch would reduce the launch costs.

2. Satellite Integration

a. Delta II Fairing

The Delta II standard shroud has a 2.184 meter diameter for a height of 1.448 meters. It then expands to 2.54 meters for 2.032 meters. The payload has dimensions of 1.524 meters by 1.524 meters and a height of 0.508 meters. The necessary internal shroud diameter therefore is 2.155 meters.

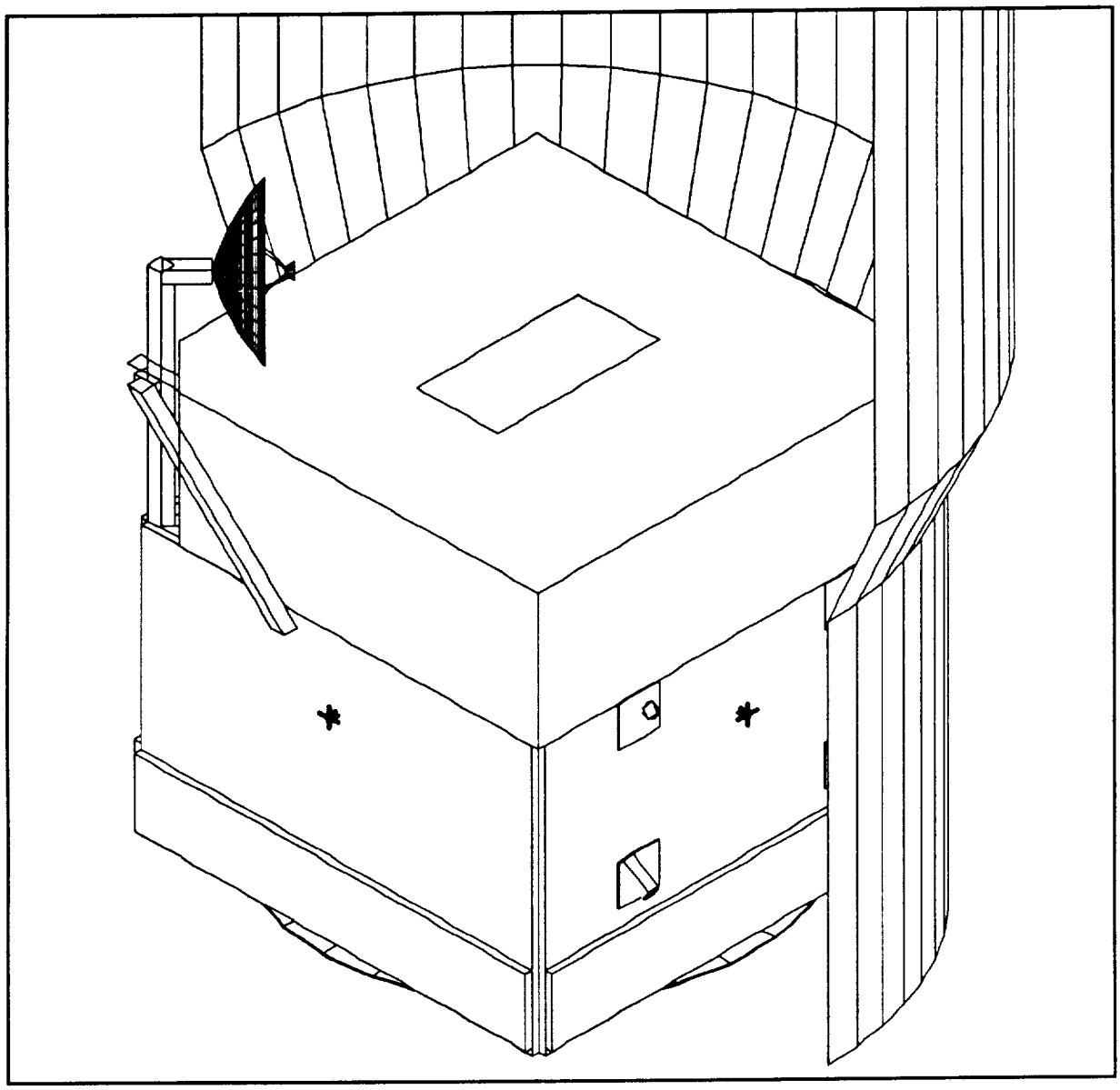

Figure 6.1 The Satellite Inside the Delta II Standard Shroud

Figure 6.1 shows that the payload will fit inside the shroud. The internal dimensions of the shroud includes the payload attachment fittings, the expected static and dynamic deflection tolerances (assumes that all significant spacecraft lateral vibration modes are above 15 Hertz), and the acoustic blanket thickness.

b. Spacecraft Attachment Assembly

The two stage Delta II (7320) vehicle normally uses the 6019 attachment fitting. It weighs 57 kilograms and has a 1.524 meter diameter (to the outside edge) at the attachment point. For more detail see Structural Design, Section IX.

3. Launch Profile

The Delta II can be launched from either Cape Canaveral or Vandenberg Air Force Base. Since the desired launch inclination is 70 degrees, a west coast launch is the best choice. The Delta II for this spacecraft will be launched from Vandenberg pad SLC-2W at a 158 degree launch azimuth.

The Delta II (7320) has two liquid stages as well as three solid strap-ons. The first stage RS-27 engine and the three solid rocket boosters are ignited on the ground at liftoff. Following burnout of the solids, the spent cases are then jettisoned about one second later. The RS-27 engine continues to burn until main engine cutoff (MECO). This takes approximately 255 seconds.

After a short coast period, the first to second stage separation bolts are blown, followed by second stage ignition approximately five seconds later. The next major event is the payload fairing separation, which occurs early in the second stage flight.

The second stage burns for approximately 410 seconds, at which time stage two engine cutoff (SECO 1) occurs. The vehicle then follows a Hohmann transfer trajectory to the desired low Earth orbit altitude. After SECO 1 occurs,

approximately 670 seconds later, the second stage is re-ignited and completes itsburn to circularize to the desired orbit. Satellite separation then begins approximately 200 seconds after stage two engine cutoff command (SECO 2). Figure 6.2 graphically presents this sequence of events.

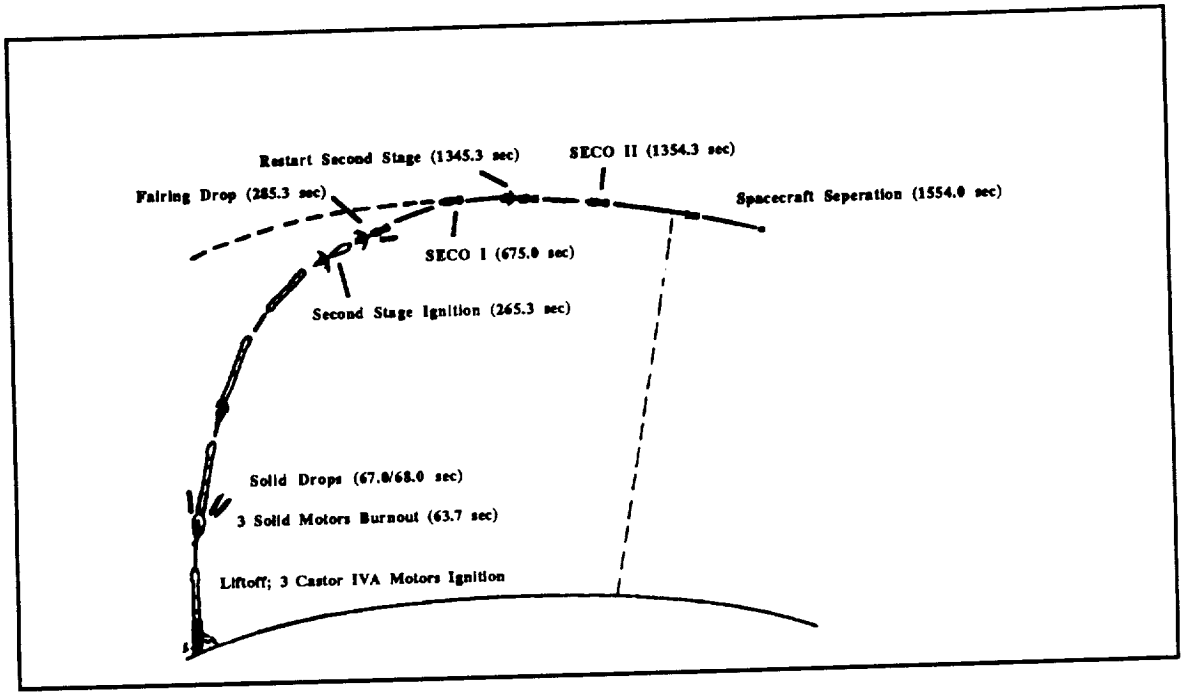

Figure 6.2 Launch Sequence

4. Spacecraft Separation

The launch vehicle and the spacecraft are attached by three attachment bolts and bolt catcher assemblies. "Upon separation, the bolts and catcher assemblies are retained by the spacecraft.... Following release of the three explosive nuts, the spacecraft/launch vehicle is stabilized by the launch vehicle attitude control system. Subsequently, three retaining latches are released followed

by retrofire of the launch vehicle yielding a minimal separation tip-off of the spacecraft."[1]

Fifteen seconds after the explosive bolts are fired the latches are released. This delay allows the angular rates to dissipate. At this point the second stage retro rocket fires providing the required relative separation velocity from the spacecraft. Expected, angular velocities at separation are a little more than 0.2 degrees per second. This can be reduced by employing additional steps in the separation process. The angular velocity can be increased to 30 degrees per second (within a 5% accuracy) by using control jets.

5. Launch Uncertainties

Table 6.1 lists the three sigma (3σ) injection error parameters. Worst case is the one guaranteed by McDonnell Douglas. The probable worst case is what they actually expect for this mission. The worst case was designed for.

Table 6.1 3σ Injection Parameters

	Worst Case	Probable Worst Case
Altitude (km)	±18.5	±9.5
Inclination (degrees)	±0.05	±0.02

6. Launch Vehicle Performance

The spacecraft load factors in table 6.2 represent the combined steady state and dynamic values with the three sigma maximum values applicable at the spacecraft center of gravity. These values should be multiplied by at least 1.25 to obtain ultimate loads.

---

[1] Commercial Delta II Payload Planners Guide, MDC H3224B, December 1989, p. 5-3.

Table 6.2 Spacecraft Limit Load Factors

	Second Stage (g's)	Main Engine Cut Off
Lateral Load	±2.0	
	±2.5 [1]	
Axial Load	±2.2/-0.2 [2]	6.7 to 7.2 [3]

1. Lateral load factor to provide correct bending moment at separation plane.
2. Plus indicates compression load, minus indicates tension load.
3. 6.7 is for a 2000 kg payload, 7.2 is for a 1000 kg payload.

C. PROPULSION SUBSYSTEM

1. Thruster Description

Eight MR-111C one lb_f thrusters built by Rocket Research Company were chosen. Figure 6.3 depicts the layout and physical dimensions of this thruster. Table 6.3 gives the design and performance characteristics.

Table 6.3 Characteristics of the MR-111C Thruster

Propellant	Hydrazine
Catalyst	Shell 405
Steady State Thrust (N)	5.338 - 1.334
Feed Pressure (MPa)	2.7579 - 0.5516
Chamber Pressure (MPa)	1.2066 - 0.3447
Expansion Ratio	74:1
Flow Rate (g/sec)	2.404 - 0.635
Mass (kg)	0.33113
Specific Impulse (sec)	229 - 226
Minimum Impulse Bit (N-s)	0.0845 @ 2.4132 MPa & 20 ms On

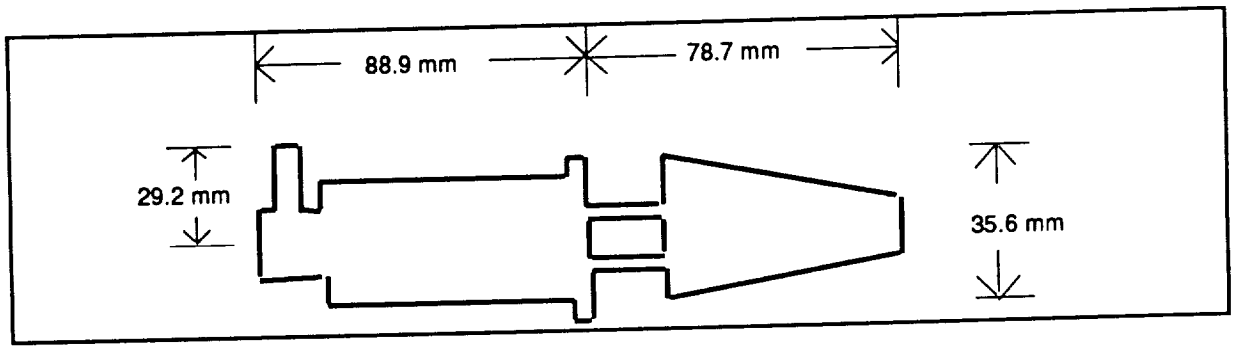

Figure 6.3 MR-111C One lbf Thruster

2. Thruster Locations

The analysis of the thruster placement was based on the mission requirements envisioned for the thrusters. The missions are broken down into primary and secondary missions with an emphasis on allowing for single point failure to complete all primary missions.

Primary Mission

Detumble of Spacecraft on orbit

Spin down

Delta V maneuver required for orbit maintenance

Secondary Mission

Backup for desaturation of reaction wheels

Slew maneuver

Deorbit

A single point failure of the thruster system is defined as the inability of a single thruster to operate in the mode for which it was intended. Two separate designs are presented each having their own strengths and weaknesses. The first design meets the design criteria of redundancy within the thruster system, but is more complicated to implement and requires more thrusters. A second design is also introduced which is much simpler to construct, but offers little redundancy. Both are proposed at this time allowing a trade-off between the actual need for redundancy and the requirement for simplicity.

a. Eight Thruster Design

The eight thruster design for the spacecraft is described as two sets of four thrusters, each set oriented on either the roll or anti-roll face and bracketing the center of mass of the spacecraft. The thrusters are canted 35.8° off vertical and oriented to thrust in the x-z plane (Figure 6.4). The canting of the thruster provides a moment arm with components in x, y and z. As shown in Table 6.4 any combination of two thrusters on either face creates a moment only about a primary axis. To produce an incremental velocity

Table 6.4 Thruster Operations

Operation	Thruster Number	Redundant Thrusters
Orbital Insertion	1, 2, 3, and 4	5, 6, 7, and 8
Atmospheric Drag	1, 2, 3, and 4	5, 6, 7, and 8
Positive Roll (+X)	2 and 3	7 and 6
Negative Roll (-X)	1 and 4	8 and 5
Positive Pitch (+Y)	2 and 4	7 and 5
Negative Pitch (-Y)	1 and 3	8 and 6
Positive Yaw (+Z)	1 and 2	8 and 7
Negative Yaw (-Z)	3 and 4	6 and 5

Table 6.5 Thruster Placement Summary

Thruster Number	Location[1] (meters)	Moment Arm[1] (meters)	Moment Created[1] (N*m)
(1) anti-roll face	[-.762,-.427,-.241]	[-.146,-.427,.203]	[-1.11,1.11,1.54]
(2) anti-roll face	[-.762,-.427,.241]	[-.146,-.427,-.203]	[1.11,-1.11,1.54]
(3) anti-roll face	[-.762,.427,-.241]	[-.146,.427,.203]	[1.11,1.11,-1.54]
(4) anti-roll face	[-.762,.427,.241]	[-.146,.427,-.203]	[-1.11,-1.11,-1.54]
(5) roll face	[.762,-.427,-.241]	[.146,-.427,.203]	[-1.11,-1.11,-1.54]
(6) roll face	[.762,-.427,.241]	[.146,-.427,-.203]	[1.11,1.11,-1.54]
(7) roll face	[.762,.427,-.241]	[.146,.427,.203]	[1.11,-1.11,1.54]
(8) roll face	[.762,.427,.241]	[.146,.427,-.203]	[-1.11,1.11,1.54]

Note (1): All distances are measured from the beginning of life center of mass for the spacecraft

change four thruster must be fired at once. In addition to the delta v created in the roll and anti-roll direction, a delta v can be created in the +Z and -Z direction by firing the top or bottom set of thruster, but this drops the effectiveness of the thruster down to below 60%. A summary of the thruster location, moment arm and moment created are shown in table 6.5. As stated earlier these eight thrusters give the satellite the ability to withstand a single point thruster failure. The thrusters are placed at positions and moments calculated which correspond to the beginning of life center of mass, the fuel requirements for this satellite are small compared to the mass of the satellite and will cause minimal changes to the center of mass. Appendix F shows a sample calculation of the moment created by the thruster #7.

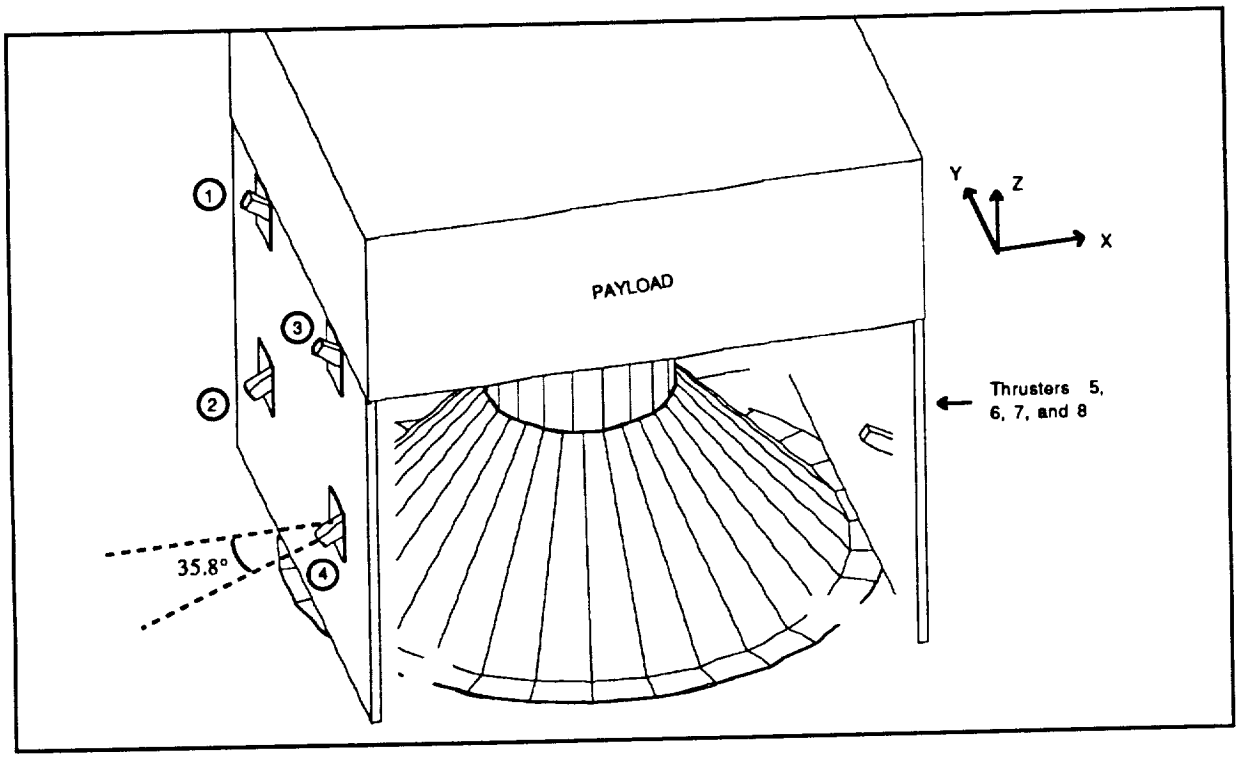

Figure 6.4 Thruster Placement Diagram

b. Six Thruster Design

Four thrusters oriented on the negative pitch face perpendicular to the x-y plane and bracketing the center of mass, along with two additional thruster on the positive yaw axis also bracketing the center of mass describes the six thruster design. The four thrusters on the negative pitch face when fired in pairs would be able to create moments about the X and Y

axis, all four thruster would be able to cause and incremental velocity change to the spacecraft. The two thruster on the the positive yaw axis would create the moment required for the Z axis. While this simple design is effective it does not provide the redundancy for rolling maneuvers, redundancy is provided for the delta v maneuver in that two of the four thrusters on the pitch face could be fired to create a translational movement.

The disadvantages to the eight thruster design are the complexity of two additional thrusters, the movement of the center of mass (slight as it may be), and the accuracy of the cant angle required. These disadvantages for the eight thruster system must be weighed against the major disadvantage for using only six thruster, no redundancy within the propulsion system. While the secondary missions of the propulsion system are themselves redundant to some other system, the primary missions listed for the propulsion system have no other means to complete the assigned tasks. A trade off between full redundancy and necessity to complete the primary objectives is required to be evaluated at this time and beyond the scope of this preliminary design.

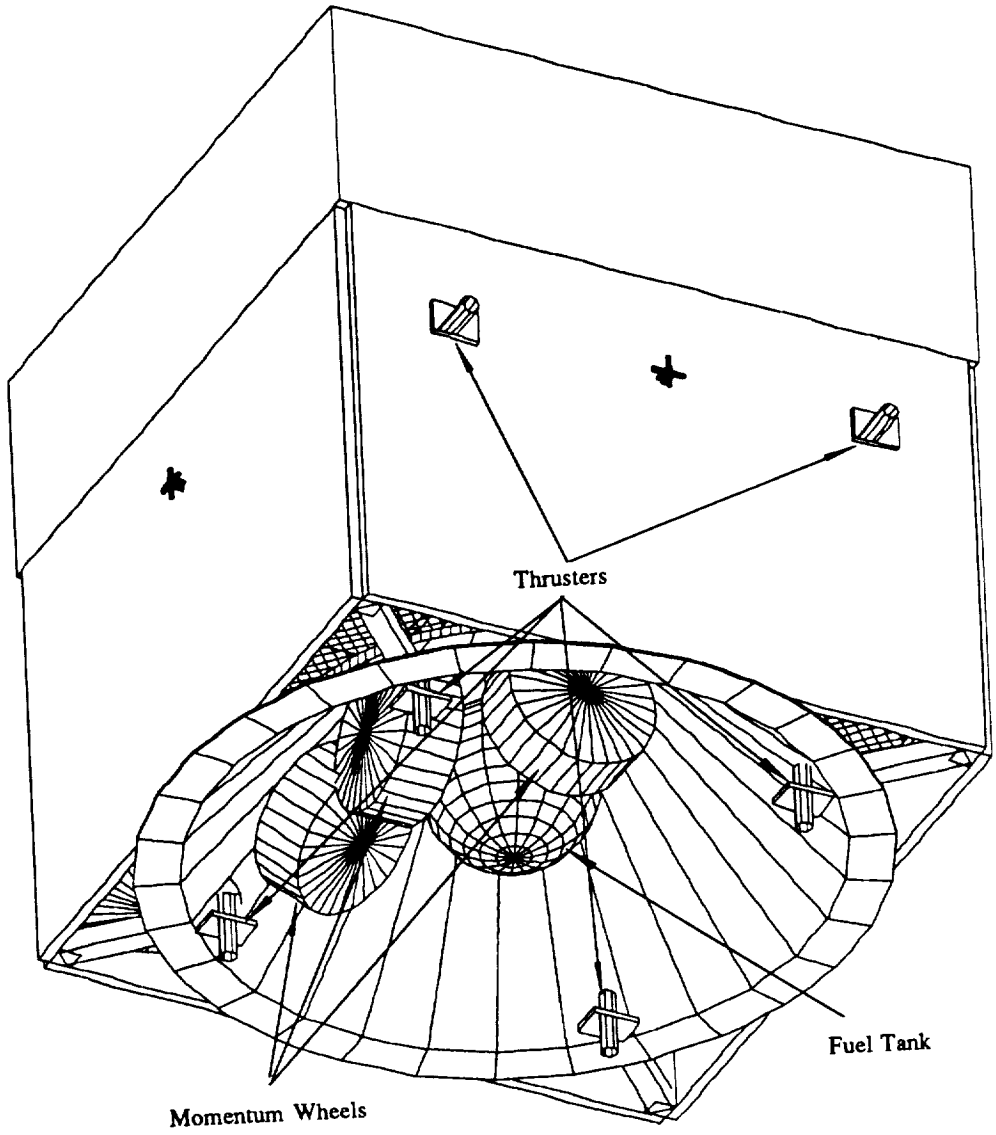

Figure 6.5 Thruster Placement Summary

3. Propellant Requirements

The amount of fuel required for maneuvers was anticipated to be small due to the mission, mission life, and orbit. One of the goals of the design is to keep everything as simple as possible. Combining these two thoughts it was decided to use monopropellant hydrazine (N_2H_4) as the fuel. For the anticipated steady state

low thrust maneuvers, hydrazine has a specific impulse, I_s, of 225 seconds. Calculations are included in Appendix G.

a. Spin Down and Detumble

The first maneuver is to despin the satellite for three axis stabilization. Typically, the second stage is spinning at 0.033 rpm upon spacecraft separation. A worst case of 5 rpm was designed for to include the possibility of tumbling upon separation (or later during the mission). If reorientation is required, the satellite would be despun to less than 0.05 rpm, then reoriented. This uses only a negligible amount of fuel - even if a worst case maneuver of 180 degrees is performed.

b. Orbital Insertion

The second maneuver is to correct for possible errors in launch vehicle orbital insertion. The worst case of 18.5 kilometers from the expected orbit was designed for. The orbital section shows that the delta v required is 10.238 m/s (includes apogee and perigee firings). To do this maneuver four 1 lb_f thrusters were used canted at 35.8 degrees from the thrust axis.

c. Atmospheric Drag Corrections

The next important consideration is correcting for atmospheric drag. The satellite must remain within 1 nmi (1.852 km) of its intended altitude. Drag calculations are included in the orbital section (Section III). The result is a delta v of 8.172 m/s.

d. Station Keeping

The satellite must remain within ± 0.5 degrees of a 70 degree inclination. The Delta II inserts the satellite to within ± 0.05 degrees. The change in inclination due to effects from the earth, moon, and sun over the three year life are ± 0.0942 degrees (calculations in the orbital section). Therefore the worst case change in inclination with respect to time is ± 0.1492 degrees. This is well within the allowable tolerances so no extra fuel is necessary for station keeping.

e. Deorbit

At the satellite's mission termination a decision is to be made regarding the disposition of the spacecraft. Previously the common practice was to leave the spacecraft dormant in their original orbits, considering them only as space junk. Now with space exploitation starting its fourth decade the heavens are beginning to fill with these expired satellites. An investigation was conducted into the most practical method to dispose of this satellite at the end of its lifetime. Three concepts governed the analysis; first, bring the satellite back into the Earth's atmosphere to be burned up on reentry, second, minimize the impact the plan will have on the original mission and third, minimize the time required to complete the deorbit process.

A controlled reentry into the Earth's atmosphere is defined as: upon command to terminate the mission the spacecraft would conduct a single deorbit burn bringing the spacecraft within 50 to 90 km perigee altitude. This would ensure atmospheric capture and enable accurate placement of the geographic point in which the destruction would occur. In order to meet these requirements the spacecraft would have to develop a 120.5 m/s delta v at end of life. To develop this much delta v the spacecraft would require approximately 75 kilograms of extra fuel on board, this is five times the mission's fuel requirement. While this idea meets the first and third concepts of spacecraft disposal, it would require the addition of two additional fuel tanks and ultimately a larger spacecraft bus.

An uncontrolled reentry of the spacecraft would be defined as: a deorbit of the spacecraft to a lower altitude and the satellite would complete more than one orbit before decay of the orbit was sufficient enough to cause the destruction of the satellite. This idea could be carried out with minimal impact to the mission requirement and while it is slower to achieve satellite destruction it is an order of magnitude faster than leaving the satellite in the original orbit. This idea would allow for a single deorbit burn at the end of mission life, the satellite would expend all of the remaining fuel on board to achieve the highest delta v possible. Prior to launch the fuel tank within the satellite would be filled to capacity, rather than filling only for

maximum mission requirement, this would give approximately 12.5 kg of fuel mass margin. Any fuel not used from the allotted maximum fuel requirement would only add to the fuel available at satellite end of life. Using the ASAP program the orbit was input for a satellite with a 509.3 km apogee and 430 km perigee, representing an end of life deorbit burn of 12.5 kg of fuel. The ASAP program computed a decay of the orbit and destruction of the satellite in less than 9 years. This time frame appears to be very reasonable for a satellite of this size and weight, The LDEF satellite, which was much larger and heavier, was launched into an orbit 20 nm less than this proposed orbit and its projected decay time to destruction was approximated to be 7 years. The idea of an uncontrolled reentry using the remaining on board fuel appears to be the better of the two concepts for destruction of the satellite.

f. Total Fuel Required

Since the worst case was designed for, the propulsion system is in reality a backup for the attitude control system. This provides a valuable redundancy. The total propellant required is calculated in table 6.6.

Table 6.6 Propellant Budget

1. Propellant for delta v maneuvers and control	11.03
2. Allowance for off-nominal performance	0.11
3. Allowance for off-nominal operations	0.11
4. Mission margin (reserves)	1.10
5. Contingency	1.10
6. Total required propellant	13.45
7. Residual propellant (trapped in motor case, tanks, lines, etc.)	0.27
8. Loading uncertainty	0.07
9. Total propellant load	13.79 kg

4. Propellant/Pressurant Tank Selection

To decide on a fuel tank from those available commercially, the required tank diameter was first determined to be 0.322 meters (see Appendix G).

A survey was conducted of off-the-shelf positive expulsion tanks based on the the above minimum fuel tank diameter and the diameter of the satellite cylinder ($\cong$ 0.5 meters) . The TRW 80225-1 sphere used by the OTS-Marex program was selected since it was the closest match in propellant capacity. Several other tanks were in the same range. Table 6.7 describes the features of this tank.

Table 6.7 Propellant/Pressurant Tank Characteristics

Expulsion Device	AF-E-322 Diaphragm
Volume (m^3)	0.0306
Propellant Capacity (kg)	24.1
Outside Diameter (m)	0.39
Minimum Wall Thickness (mm)	0.48
Weight (kg)	3.70
Pressure (P_o) (MPa)	2.20
Pressure (P_p) (MPa)	3.52
Pressure (P_b) (MPa)	4.70

5. Subsystem Operations

Figure 6.5 is a schematic of the propulsion subsystem. This schematic shows a single tank connected to eight thrusters. The propulsion subsystem includes a fill/drain valve for the pressurant and one for the propellant. These will be manually operated during prelaunch operations. Two pressure transducers - one for each tank exit line - are included to measure absolute pressures. One pressure regulator for each line is included. Also a filter is included near each tank exit to remove impurities from the lines before they reach the thrusters. As a safety feature, each thruster has an isolation valve in its line in case of line breaks or failures. Also note that the propellant regulation valve is an integral part of each thruster.

D. MASS AND POWER SUMMARY

Each thruster requires 9 watts during its operation. Since no more than four thrusters will be used at any one time, the power requirements will never exceed 36 watts. Also the use of thrusters will only occur during the standby mode so only a minimal power of approximately 1 watt will be used during payload operation. Table 6.8 shows a breakout of the propulsion system masses.

Table 6.8 Propulsion System Mass Summary (kg)

1 lbf thrusters (8)	2.65
Propellant/Pressurant Tank	3.70
Tubing	1.0
Valves, Filters, & Pressure Transducers	1.0
Propellant/Pressurant	13.89
Total	22.24

VII. ATTITUDE CONTROL SUBSYSTEM

A. MISSION REQUIREMENTS

The Attitude Control System (ACS) is designed to control Spacecraft orientation, either automatically or on command, in the presence of external disturbances by using torque producing devices. The equations of motion are analyzed by the designer and the external disturbances modeled in order to select a proper control system to manage the spacecraft angular momentum.

Listed below are the design specifications as provided by the statement of work:

(a) Three axis stability with slew capability for sensing and standby modes,

(b) Attitude accuracy: $\pm 0.5°$ / axis (3σ),

(c) Maximum time to slew: 90 degrees in 15 minutes,

(d) Slew settling time: 1 minute,

(e) Rate stability: $0.003°$ / second (3σ) per axis,

A payload supplied Inertial Measurement Unit (IMU) is available for short term attitude reference. It is aligned by a pair of star sensors contained within the payload.

Further requirements are added due to the choice of satellite configuration and the power collection method. The design selection of fixed solar arrays requires the ACS to operate in multiple modes to collect power and to point the payload for sensing. It must also be able to slew between these modes accurately and with adequate speed. Intermediate modes include acquisition/de-tumble and boost maneuvers. Mass and power are kept to the minimum required within the constraints, specifications, and component availability. The majority of the satellite

lifetime is spent in a relatively quiet mode with respect to the ACS, but it must be extremely reliable for mission success.

B. ACS CONCEPT

1. Configuration and Operation

The choice of configuration was driven mainly by the requirements to be able to slew about multiple axes in varying geometries and to maintain reasonably accurate three axis stability. Adequate redundancy is crucial because the ACS must be able to orient for both payload operations and power collection. Three orthogonal Reaction Wheel Assemblies (RWAs), one along each body axis, allows somewhat independent control of rotation about each axis. A fourth RWA is skewed 45 degrees out of plane with respect to the others to back up any single RWA failure. In the event of a RWA failure, the redundant rate will be commanded $\sqrt{3}$ times the normal rate to achieve the desired affect while the undesired components are temporarily taken up by the other wheels. Location of the major hardware is depicted in Figure 7.1.

Momentum dumping is accomplished by pairs of orthogonal magnetic torque rods. Normal operations call for the pairs to work simultaneously to rapidly desaturate the RWAs before slew maneuvers and to periodically activate to keep the RWA bias low. Specifically, automatic desaturation begins at 210 rpm. This minimizes dynamic coupling in the euler equations which are located in Appendix H. The rods can work singly in the event of a failure. Redundancy for momentum dumping is provided by the propulsion system, available in the event of complete torque rod failure. Both the magnetic dumping system and the propulsion system give limited three axis stable capability in the event of multiple RWA failure. The control system concept is depicted in Figure 7.2. Its algorithm contains all described failure modes.

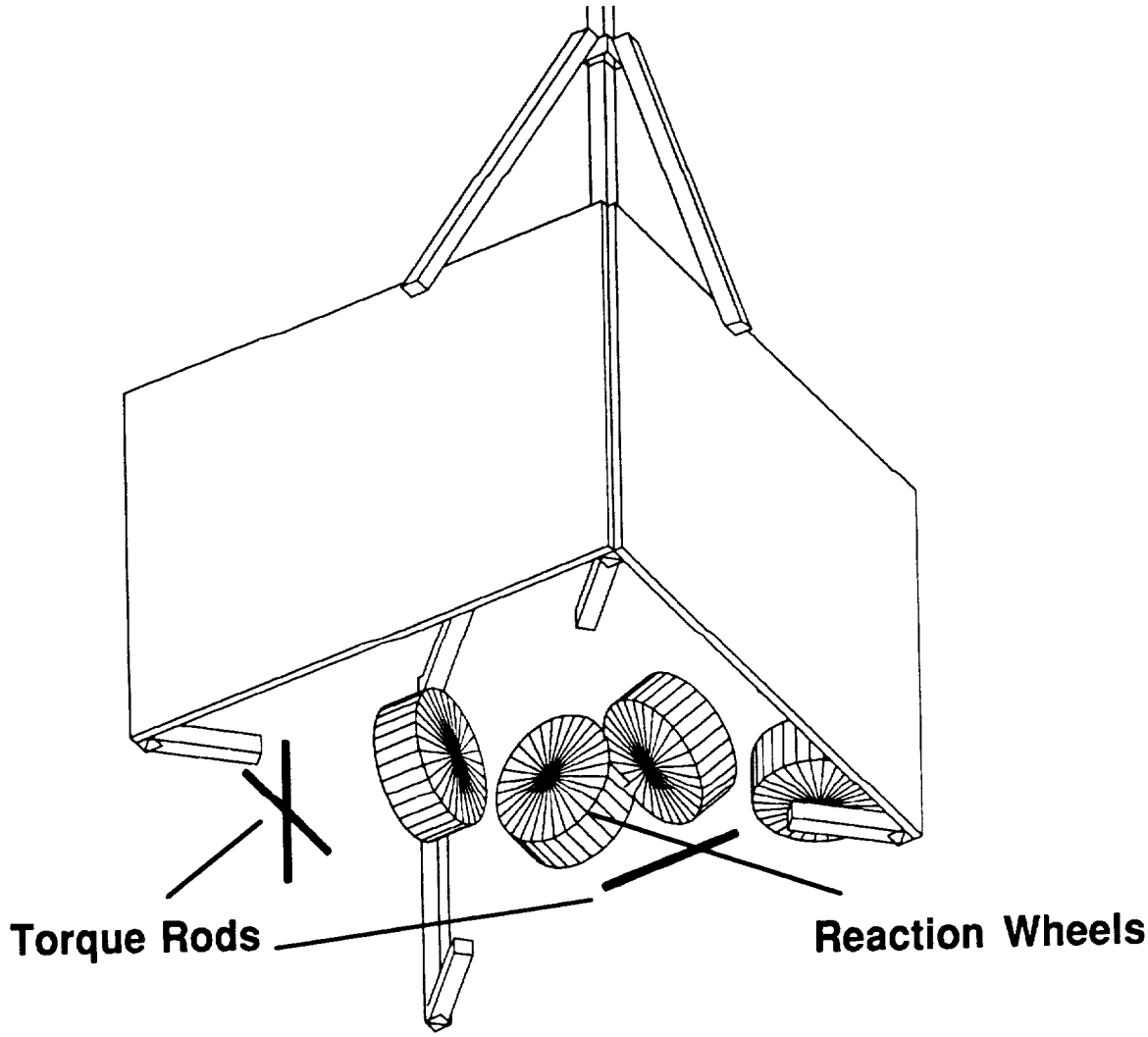

Figure 7.1 Location of Major Equipment

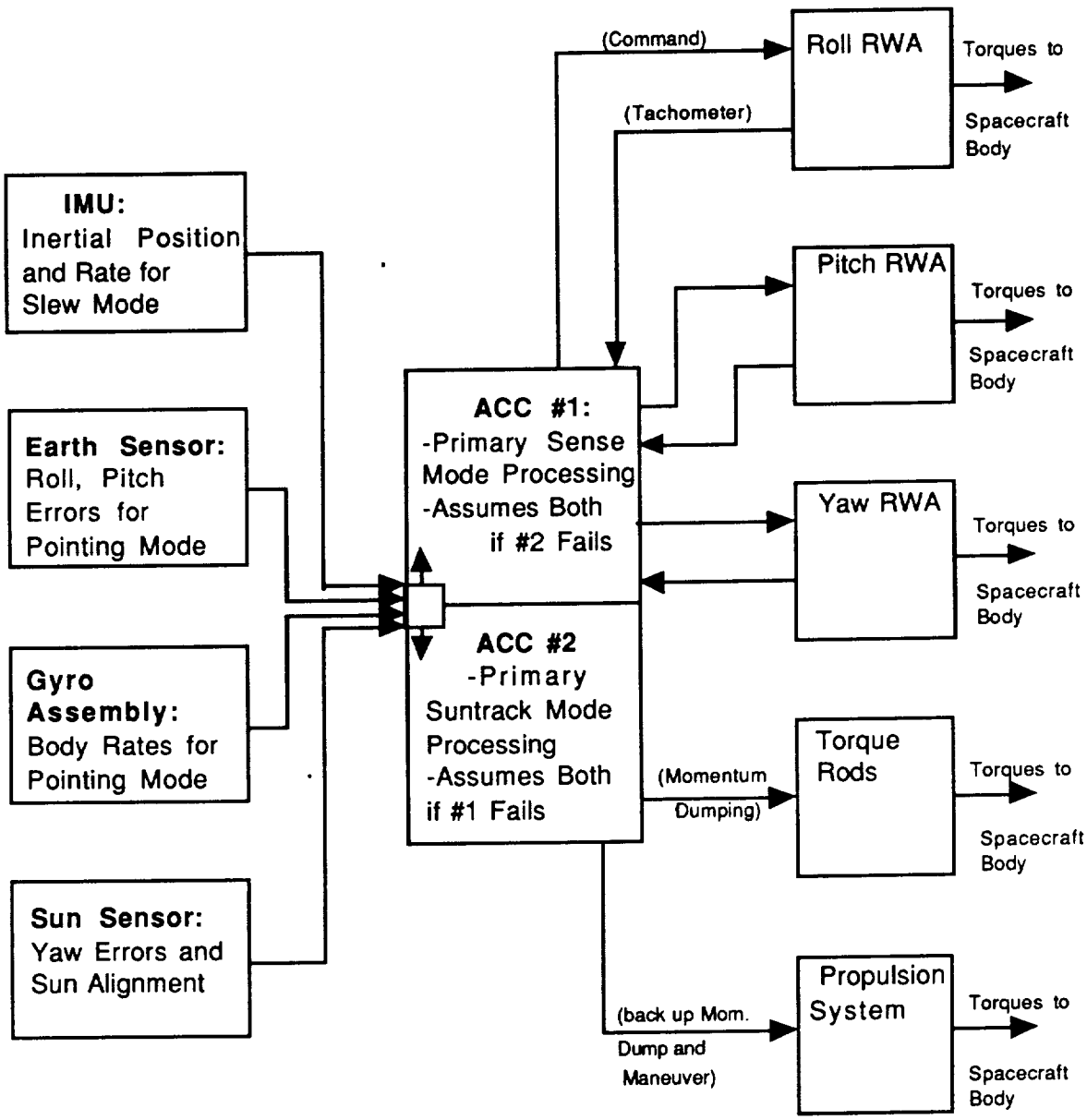

Figure 7.2 ACS Concept Block Diagram

Attitude errors are induced by solar, aerodynamic, gravity gradient, magnetic disturbance torques and perturbations during desaturation and Δv maneuvers. The two Attitude Control Computers (ACC) receive data from the IMU, the earth sensor, one of two sun sensors in view, and the back up gyro assembly to compute and store two sets of these errors: (1) the euler angles with respect to the standard nadir pointing sensing coordinates, and (2) the euler angles with respect to the suntracking coordinates which track the incoming sun vector and can be considered "inertially" fixed. From these, each computer can calculate the direction cosine matrix used in its duty slew direction. In the event of a single computer failure, the other assumes the load for both. The first set of errors include the orbital rate while the second set are fixed with respect to the orbit normal coordinate system. Twelve independent transformations exist in each case (sign ambiguities are removed), and the computer defaults to the one which results in the minimum total correction path (or slew path) but any specific direction cosine matrix can be chosen. The duty ACC then commands the RWAs to perform the chosen sequence of single axis slews to reach the target axes (i.e. to zero the euler angles). From here, smaller slews can be commanded to accomplish offset nadir pointing or to correct a thermal problem. Single axis slew sequences are not the fastest method but they simplify constraint checking, allow separate orthogonal error computation, and minimize dynamic coupling. A more detailed description of the coordinate systems used is in Appendix H.

2. Operating Modes

The spacecraft is deployed from the launch vehicle at or near desired orbit parameters with a spin of 0.2 RPM about the designated body Z- axis. Given the inertia properties of chapter II, this spin will remain stable in the absence of major dissipators. The propulsion system will slowly despin the satellite, if necessary, until a sun sensor acquires the sun. At this time the sun vector is used to control a slow

slew to roughly point the solar array face using the thrusters. At steady state, the solar arrays deploy, all components of the ACS power up and star data is linked to begin alignment of the IMU. The entire process is autonomous with the maneuvers time tagged shortly before launch. The detumble mode works in an identical manner. The RWAs shut down when the body rates indicate that for some reason three axis stability is lost and the last known sun position is used for search. If this doesn't work the ground controoler must link the data. The acquisition sequence then repeats to regain control.

Seven to eight orbits will be available to power up and self test all subsystems due to the small magnitude of the disturbance torques. When ready, the ACS begins a slow slew to align with suntracking coordinates. The majority of the lifetime will be spent in this mode, tracking the sun to irradiate the solar arrays and maintain thermal balance.

After successful power up, battery charge, and test of all systems the ACS is ready to perform slew maneuvers. When the command is received to sense, the ACS dumps any accumulated angular momentum to less than 2 RPM on each RWA and the commanded sequence of axis slews is performed to align with the sensing coordinates using the first set of errors. This maneuver may be time tagged if out of view of a controller. If offset nadir pointing is desired, a slow slew about the roll axis gives the commanded grazing angle. In this mode, noise effects suppression filtering is used to counteract sensor noise to provide the rate stability. Noise through motor vibrations and aeroelastic effects is damped by the control system. After a maximum of two orbits of sensing, the second set of errors is used to perform the slew back to suntracking.

During momentum dumping, the ACS holds its current mode and the RWAs are given a command to a small pre-bias to ensure near zero RPM on completion of the process. All Δv maneuvers are performed in the suntracking

mode using the required offsets for thruster alignment and the ACS maintains an inertially fixed posture during burns.

C. ACS DESIGN

1. Component Sizing and Selection

The equations of motion (EOM) for this attitude control configuration are well known and together with the specifications and the estimated disturbance torques, they are used to determine the required capabilities and sizes of the various components. Sensors must provide the required accuracy and noise levels, RWAs and torque rods must supply adequate torque at rapid response, and electronics must have sufficient speed and memory. Off-the-shelf components that satisfy these findings are then chosen and used. The sizing and selection process, EOM, disturbance torque estimation (all worst case scenarios), and calculations are given in Appendix H. The results are summarized in Table 7.1 along with the mass and power consumption of each component.

2. Control System Design

The design of two primary controllers covers the operation of all the modes and will be discussed here: (1) the sensing mode controller, and (2) the slew controller. Only subtle changes separate the controllers between suntracking and sensing mode; suntracking and Δv mode; slew and acquisition. Detailed analysis: assumptions, EOM reduction, controller type and gain selection is given in Appendix H. and the results are summarized below.

Table 7.1 (a) ACS Component Sizing and Selection Sensors and Electronics

Component	Mass (kg)	Power (W)	Manufacturer
Back Up Spring Restraint Gyro Assembly	1.3	19.5	Heritage: DMSP
Precision Pointing Earth Sensor	3.8	4.0	Barnes
Attitude Control Computers (2)	2.5ea	6.0ea	MIL STD 1750 (GPS Version)
Sun Sensor (Sense Mode)	0.04	1.0	Adcole
Sun Sensor (Sun-Track Mode)	0.04	1.0	Adcole

Table 7.1 (b) ACS Component Sizing and Selection Torque /Angular Momentum Devices

Component	Storage Capacity (Nms)	Peak Torque (Nm)	Mass (kg)	Power (W)	Manufacturer
Roll RWA	19.9	0.3	9.09	<140 Peak <10 Nom.	Honeywell
Pitch RWA	19.9	0.3	9.09	<140 Peak <10 Nom.	Honeywell
Yaw RWA	19.9	0.3	9.09	<140 Peak <10 Nom.	Honeywell
Redundant RWA	19.9	0.3	9.09	<140 Peak <10 Nom.	Honeywell
Torque Rods (6)	N/A	.003 max @ $10Am^2$	1.76ea	1.6ea	Ithaco

In the sensing mode the attitude errors are limited to a small range leading to linearized and uncoupled EOM. Each axis can have its own proportional and rate feedback controller (PD). Using the disturbance torque estimates the gains are selected to provide the required pointing accuracy. Using noise models the rate stability characteristics are analyzed. The main source of noise is small and random structural mode vibration excited by the gimbaled transmit antenna which tracks during sensing. Inertia effects from aeroelasticity, and RWA motors plus noisy references from the sensors enter the control system. A circuit to detect jitter out of limits is included to signal a gain change adjusting controller bandwidth to suppress the noise effects. Control parameters for each axis are summarized in Table 7.2

Table 7.2 Controller Parameters for Pointing Modes

Loop	Gain (NM/rad)	Time Constant (s)	Control Bandwidth by Cutoff Freq.
roll	46.37	5.82	0.0546 Hz
pitch	38.896	6.395	0.0498 Hz
yaw	26.45	7.491	0.0425 Hz

For large angle slews the EOM are no longer linear and are doubly coupled: (1) significantly by the off-axis slew rates, and (2) weakly by small off-axis momenta stored in the RWAs (not completely dumped prior to slew). Given the appropriate set of errors for the slew direction, the computer transposes the direction cosine matrix to determine the target change in angle for each axis to align the body axes with the desired axes. During each single axis portion of the sequence, the controller exploits the independent axis capability and commands the off-axis rates to zero to minimize the time that coupling affects the single axis rotation .

The scheme for each axis is a nonlinear saturation feedback controller with variable gain on the rate depending on the initial errors. It is described by:

$$U_{command} = - N \text{ sgn} (\text{ position } + \text{ gain } * \text{rate }) ,$$

where N is the selected torque level. Gain selection is also based on the axis (primary or off-axis). Torque switching levels are also variable based on initial error magnitude and entry /exit torques are shaped to prevent structural excitation and actuator wear. Estimates from the structural team (chapter IX) indicate the fundamental frequency around 22-25 Hz, relatively rigid interms of the low operating torques and slew rates of the ACS. Enough so that rigid body assumptions are made for this preliminary design.

A capture box is established at 2 degrees and 0.05 degrees per second signaling the slew controller transition to the pointing controller. This prevents chatter and actuator wear. The selection and mathematical models for this controller are given in Appendix H.

D. PERFORMANCE PREDICTION

1. Pointing Modes

The well known EOM and designed controllers are simulated for various conditions using MATLAB and its associated SIMULAB for the MAC IIsi. These programs are located in Appendix H. Additional results which may be of interest to the reader are also located in Appendix H, such as disturbance torques for various modes, off-axis responses during slew, phase plane plots, and wheel speed histories.

The time responses to the estimated disturbance torques for both the sensing and suntracking modes are shown in figure 7.3. This is a worst case

scenario i.e. maximum disturbance torques which occur during RWA desaturation and a certain orbit configuration. The pointing accuracy specifications of less than one half a degree per axis are satisfied by these predictions.

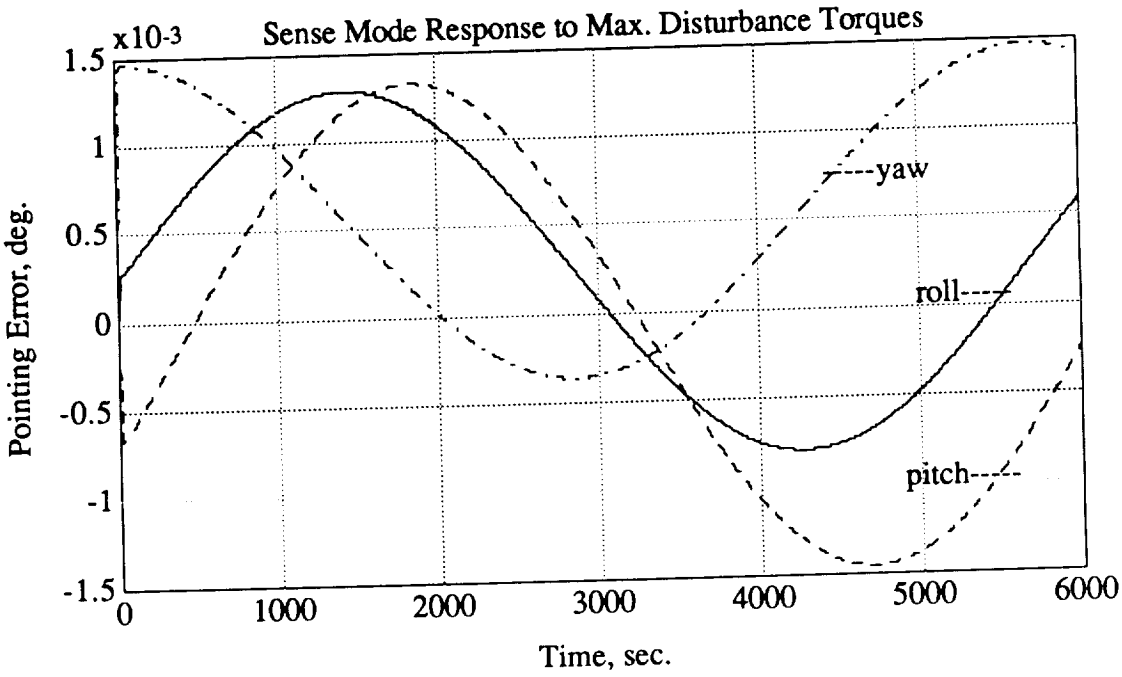

Figure 7.3(a) Time Response to Disturbance Torques in Sensing Mode

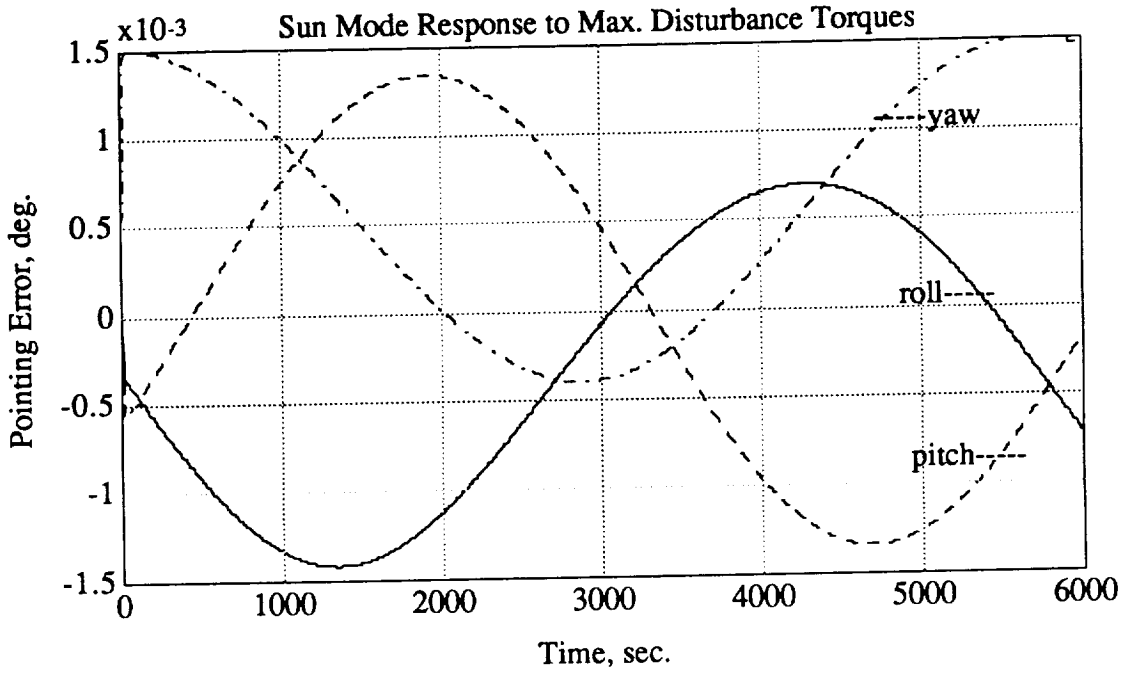

Figure 7.3(b) Time Response to Disturbance Torques in Suntrack Mode

The rate stability characteristics are shown in Figure 7.4 for each axis near its noise threshold i. e. that maximum level still within specs. A typical model for sensors is exponentially correlated noise. The threshold levels for this noise is approximately $\sigma = 67$ rad/sec in the PSD which corresponds to 10^{-4} degree rms magnitude in the time domain. Torque noise is modeled by white noise at low intensity. These level far exceed the normal levels encountered so the rate stability specs are met for this preliminary design.

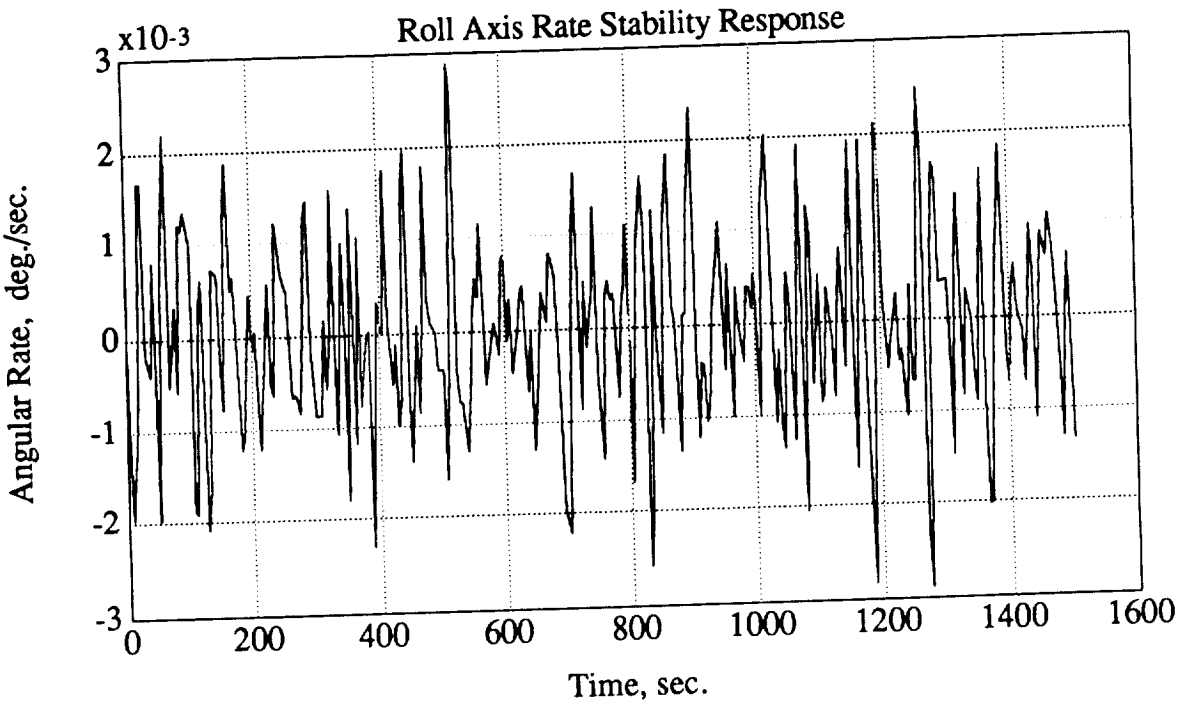

Figure 7.4(a) Rate Stability Response for Roll Near Limit

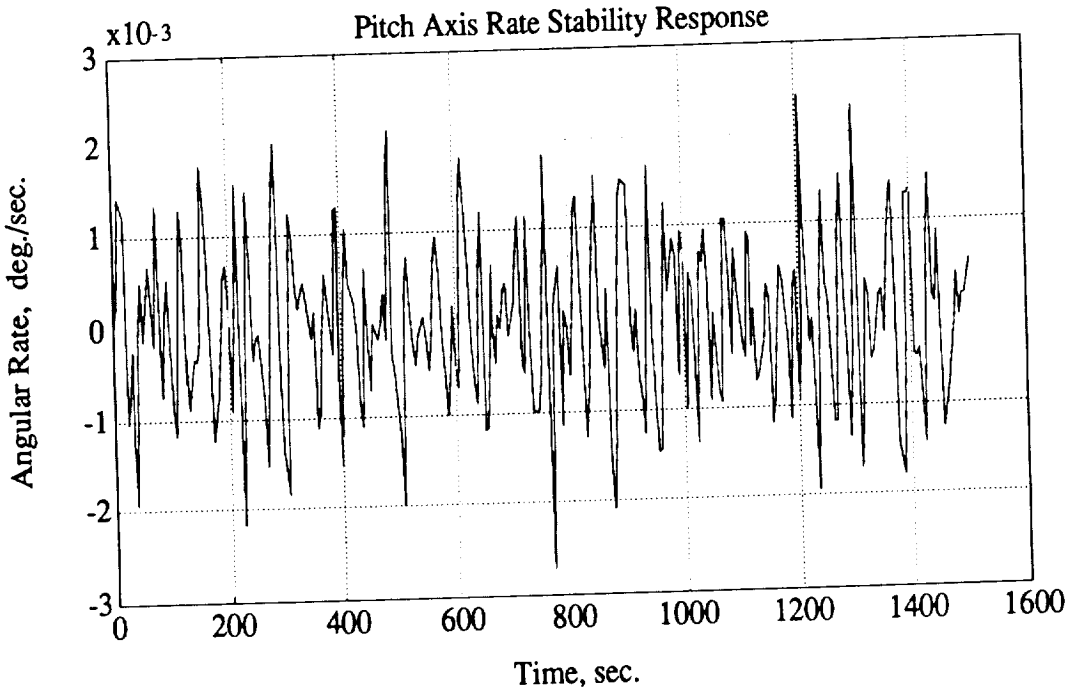

C-2

Figure 7.4(b) Pitch Rate Stability Response Near Limit

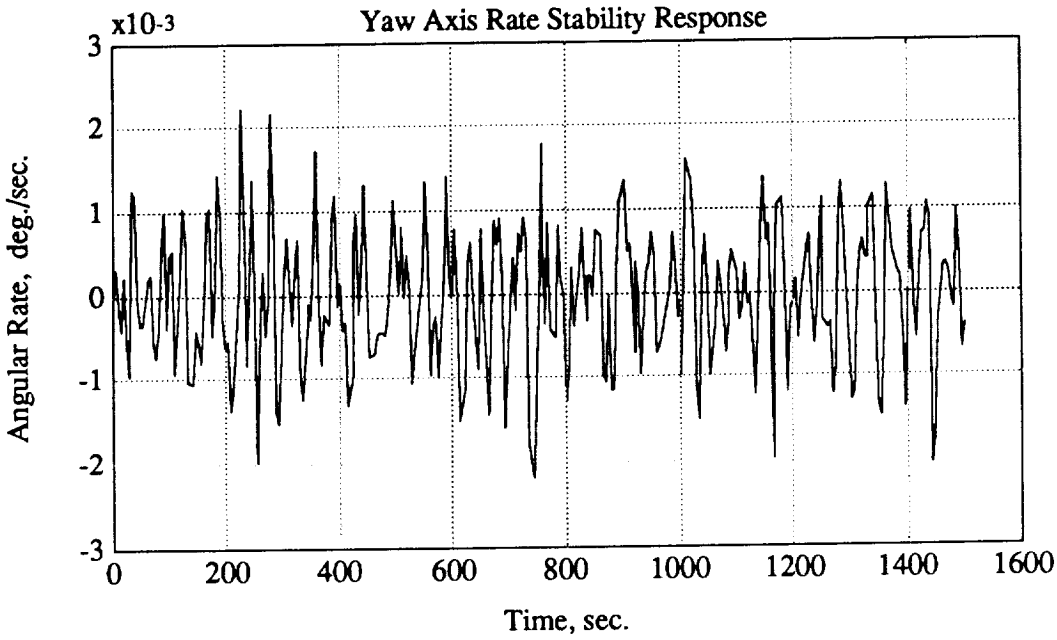

Figure 7.4(c) Yaw Rate Stability Response Near Limit

2. Sensing Modes

A typical single axis slew is depicted in Figure 7.5. Slew rates of approximately one degree per second are attainable well within the required rate. Slower rates can be used and will consume less power. The time response shows nice damping characteristics. Once the spacecraft is slewed into the capture box, the individual axis PD controllers take over to settle the slew. The settling time is approximately twenty-five seconds, well within the requirements.

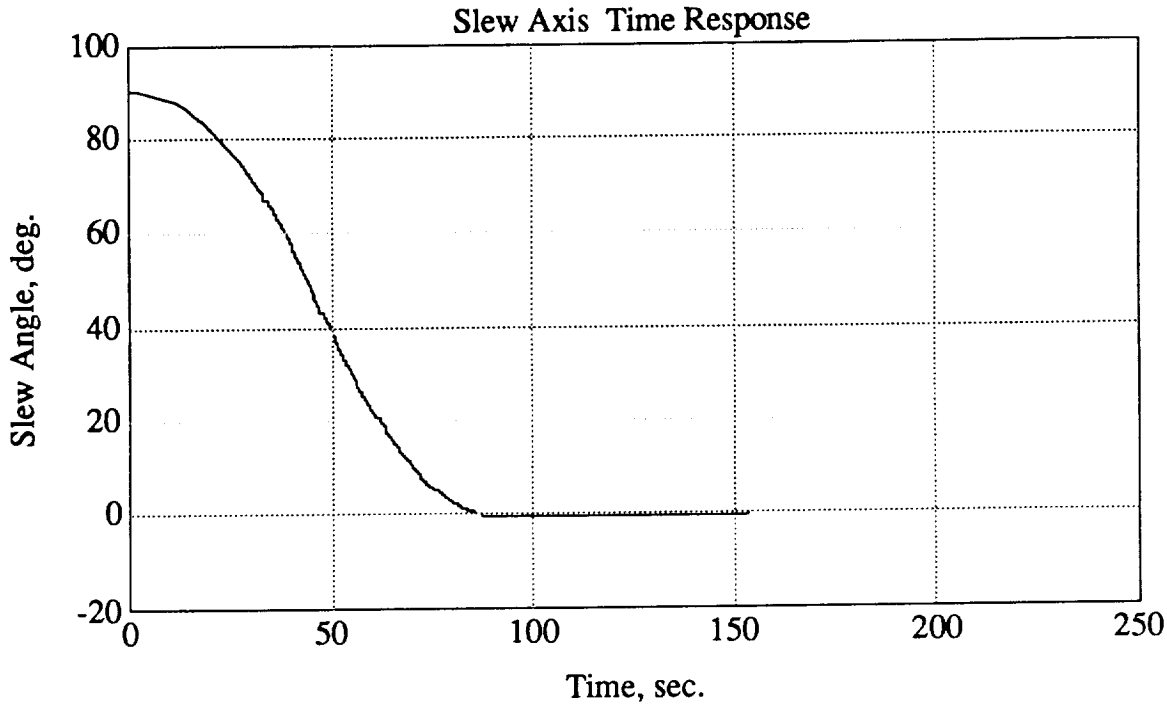

Figure 7.5(a) Typical 90 Degree Slew Response About Roll Axis

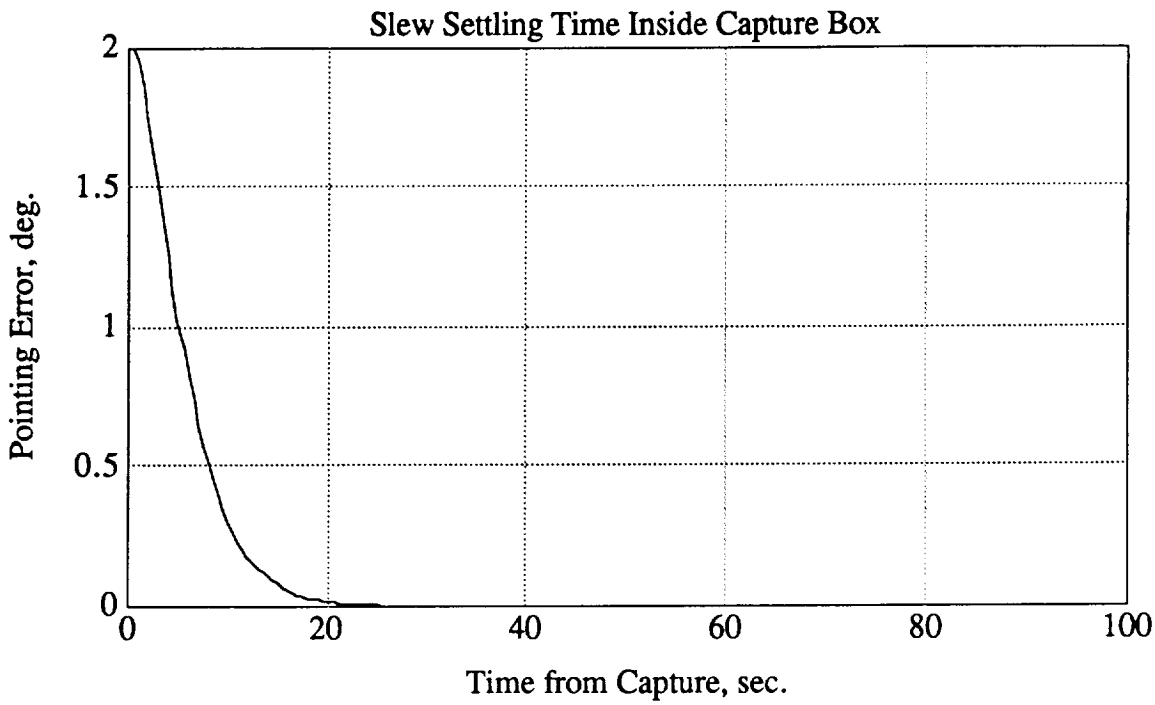

Figure 7.5(b) Capture Initial Conditions; 2 degrees and 0.5 dps

As mentioned previously the ACS has redundancy exhibits excellent performance within the specifications in this preliminary design. The degraded modes all perform favorably but do not meet the normal specs. They can, however, maintain an operating satellite.

The rate stability requirement is key and must be validated by a more advanced model. Further testing on subsequent design should focus here because from this report, it appears the other requirements are easily met. In addition, the slew rate and pointing accuracies far exceed the specs so that reduction in available control effort can be investigated. In its present condition, however, this bus could slew and control a much heavier payload.

VIII. THERMAL CONTROL

A. MISSION REQUIREMENTS

A spacecraft thermal control subsystem provides for adequate conduction and radiation heat paths between all spacecraft elements so that temperature sensitive components remain within specified temperature limits during all mission phases. This generic definition applies to this spacecraft bus as well as the cryogenic payload, however the bus thermal control subsystem is designed to function independently from that of the payload. The payload is equipped to provide its own cooling and heating for both sensing and stand-by modes. The only payload imposed thermal constraint on the bus was to maintain the bus/payload interface temperature between 0 and 30 degree Celsius. No bus components are required to maintain cryogenic temperatures, and in fact some bus components may go above the 30 degree celsius but the interface between the bus and payload will always be in the required range. Specific temperature range requirements for selected bus component and subsystems are given as Table 8.1. The references for the table are given in Appendix I.

B. THERMAL ENVIRONMENT

Spacecraft orientation and configuration will vary throughout the lifetime of the system. The vehicle will go through various transfer, acquisition, and slewing modes. Solar arrays and the antenna will be deployed early in the mission. Thermal analysis, however, is done only for the two primary mission modes; on orbit stand-by and earth sensing. Theses two mode also represent the two extreme thermal cases for the system.

Table 8.1 Component Allowabel Temperature Ranges

COMPONENT / REGION	ALLOWABLE TEMPERATURES MIN / MAX (°C)
PAYLOAD/BUS INTERFACE	0 / +30
BATTERIES	0 / +10
FUEL TANK	-10 / + 50
THRUSTERS/PIPING/ VALVES	-10 / +50
SOLAR ARRAYS	-160 / +80
ANTENNA	-170 / +90
TT&C ELECTRONICS	-55 / +125
EPS ELECTRONICS	-55 / +125
ADCS ELECTRONICS	-55 / +125
REACTION WHEELS	-45 / + 55
SENSORS	-30 / +55

The hot case is defined as the earth sensing mode during which the payload is acquiring and transmitting data. In this mode the high data rate transmitter is active and the batteries discharge providing their greatest thermal output. Other TT&C and ADCS components operate in this mode intermittently. The spacecraft is earth pointing with the payload side facing earth. With an orbit altitude of 275 NM, inclination of 70 deg., and longitude of ascending node at 90 deg, we find that the spacecraft does not experience an eclipse period during this orbit.

The cold case is defined as the standby mode during which the spacecraft is sun pointing (solar arrays are normal to sun vector). The batteries are being

charged in this mode and the high data rate transmitter is non-operational. The low data rate transmitter and a variety of other components will operate intermittently. The orbit altitude and inclination are the same as in the hot case, however with the longitude of the ascending node at 0 degrees the satellite experiences a 37 minute eclipse period per orbit.

The significant thermal environment inputs of the system are given as Table 8.2. A number of smaller electrical components are not identified

Table 8.2 Spacecraft Bus Thermal Environment

ELEMENT	HOT CASE (EARTH SENSING)	COLD CASE (STAND-BY)
SOLAR INPUT	1390 W/m^2	1310 W/m^2
EARTH REFLECTED IR	76 W/m^2	72 W/m^2
ALBEDO	325 W/m^2	306 W/m^2
BATTERIES	27 W	
HIGH DATA RATE XMTR	75 W	5 W
LOW DATA RATE XMTR	5 W	22 W
GTU RFCS	17 W	17 W
ASC	25 W	25 W
RIU	6 W	25 W
REACTION WHEELS/ TORQUE RODS	20 W	20 W
GYRO ASSEMBLY	19 W	19 W
UPLINK PROCESSOR	9.5 W	9.5 W
DOWNLINK PROCESSOR	9.5 W	9.5 W

explicitly but are modeled later as an aggregate. Due to the 275 NM altitude the effects of aerodynamic heating have been ignored. Due to the location of nozzles plume impingement by the spacecraft propulsive elements is also ignored.

C. THERMAL CONTROL SYSTEM DESIGN CONCEPT

Thermal control of the spacecraft bus is achieved using a near passive thermal control system. Passive control systems are simpler, more reliable, and more cost effective than active systems. The most attractive of these features are the simplicity and reliability. It was decided that the majority of the mission risk should be with the experimental payload, therefore all of the bus subsystems are as simple and reliable as possible. Passive components of the system include Optical Solar Reflectors (OSR), Multi Layer Insulation (MLI), temperature sensors, fiberglass standoffs, and space qualified coatings/paints. Temperature sensors are used to control strip heaters located on critical elements. A pair of temperature sensor controlled louvers is used for thermal control of the batteries. All items are readily available and generally "off the shelf" hardware. A thermal control subsystem schematic is shown in Figure 8.1.

The spacecraft bus radiates excess heat to cold space by way of OSR radiators. OSR's are bonded to the aluminum honeycomb outboard panels. They have a clear view to space and effectively dissipate heat since they have high (0.8) emissivity, while absorbing little incident energy due to low absorptivity (0.12). Heat dissipating hardware is mounted directly to the inside face of the honeycomb panels. A good conductive path is maintained by using thermal grease at the box to panel interface. The sizing of the radiators is based on the hot case.

During the cold situations critical components are kept above their low temperature limits by applying heater power. The bus is equipped with 15

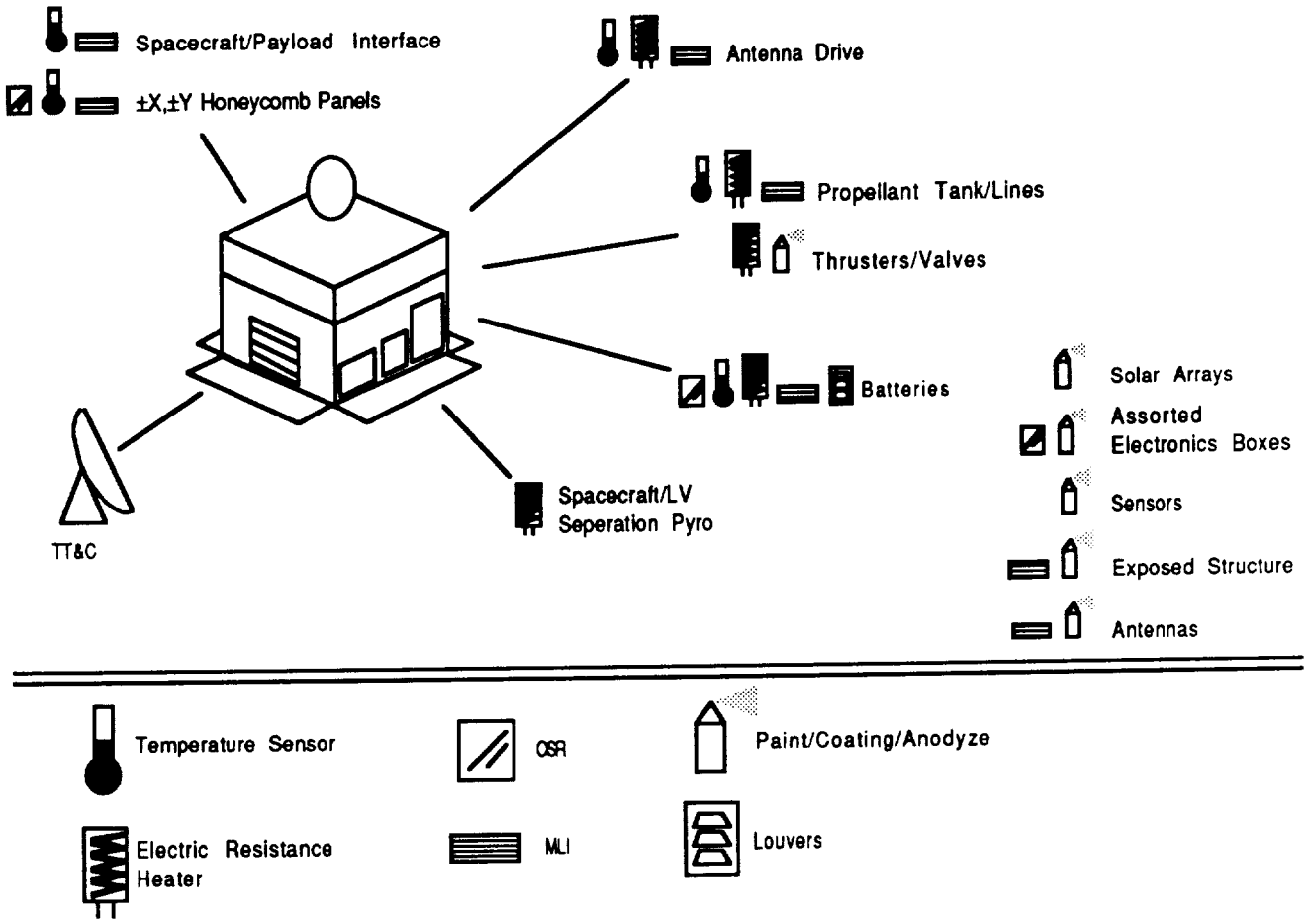

Figure 8.1 Thermal Control System

heaters and range in size from 2.5 W to 20 W watts. Spacecraft heaters are electrical resistance elements which are mounted directly to the exterior surface of the critical component. The heaters are controlled by a closed loop system which includes local temperature sensors. Although the heaters function autonomously the provision has been made for ground controlled operation and adequate telemetry channels are available.

The Nickel/Hydrogen batteries used in our spacecraft have a very narrow operating range (0-10 deg C). Based on preliminary hand analyses a simple OSR/heater system was deemed feasible. After further computer modeling and optimizing the batteries were placed on the ±X panels and the need for louvers for

was demonstrated. These active elements provide for a variable absorptivity/emissivity ratio which, in combination with battery mounted strip heaters, will ensure that the batteries will remain in the appropriate range (see analysis results in section D). Additionally the batteries are thermally decoupled from the rest of the spacecraft to eliminate spurious heat inputs from other components. The mounting of the battery, using thermal stand-offs, is shown as Figure 8.2.

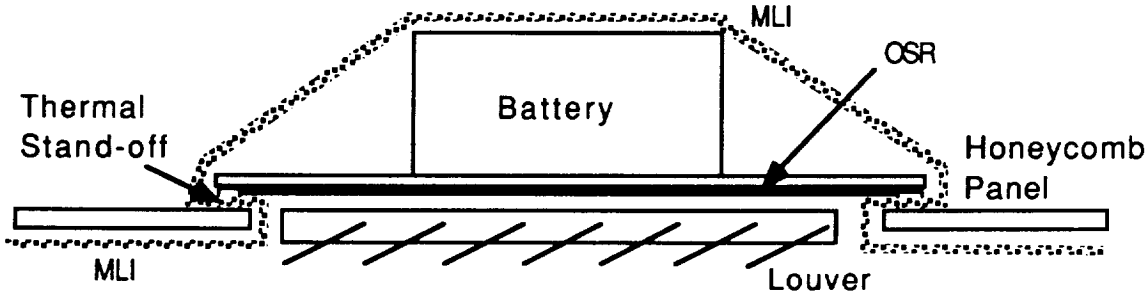

Figure 8.2 Battery Mounts

A similar isolation concept is applied at the payload/bus interface to isolate the payload. A detail of the interface is given as Figure 8.3.

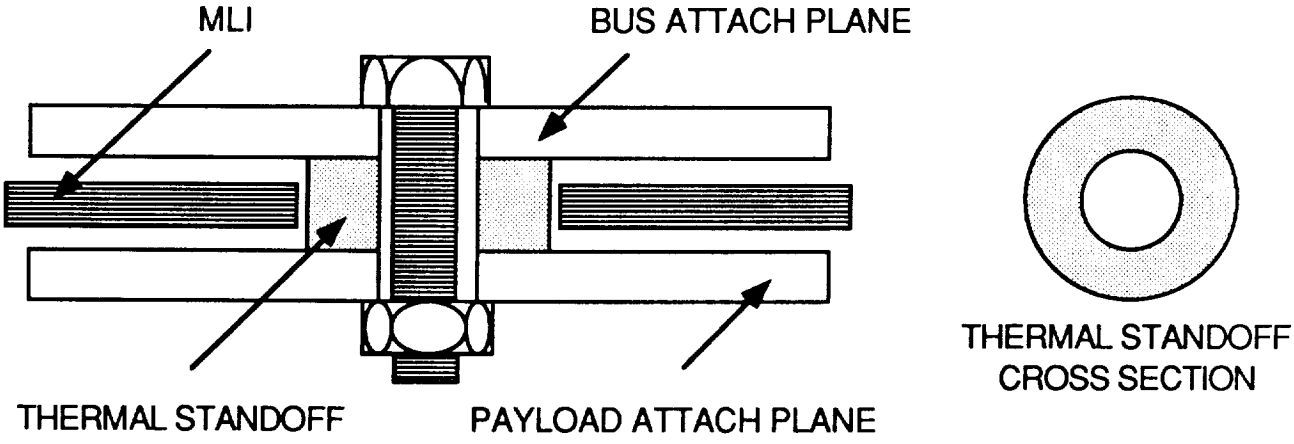

Figure 8.3 Bus Payload Isolation Schematic

To provide additional heat to cold sensitive components electrical strip heaters are applied directly to the surface of these components. Heaters are closed loop controlled by selected temperature sensors. Downlink telemetry is provided for critical temperature sensors while uplinks for the heaters and louvers provide for ground control of these components.

A full summary of all thermal hardware is given as Table 8.3. All properties listed are BOL, the models include degraded values based on mission life and other factors.

Table 8.3 Thermal Hardware Summary

COMPONENT	IMPORTANT CHARACTERISTICS
HEATERS	- Electrical strip heaters - Temperature sensor controlled - Ground control available - "Off the shelf", industry standard equipment - Total heater count of 120 W - Locations: Batteries / 40W (20 W per battery) Antenna drive / 20W Launch vehicle separation pyro / 5W Propellant tank / 20W Propellant lines and valves / 15W (total) Thrusters / 20W (2.5W each)
LOUVERS	- Only for battery OSR's - Temperature sensor controlled - Ground control available - Special made hardware for this mission - Developed and flight proven technology - 20 x 25 in. area covered - Surface properties when closed: absorptivity = 0.36 emissivity = 0.45 - Surface properties when open (underlying OSR properties): absorptivity =0.08 emissivity = 0.8

OSR	- Body mounted (exterior honeycomb panels) - "Off the shelf", industry standard equipment - Applied in 1 x 1 in. squares, allow for variable geometry - Roll panels (±X): 20 x 25 in. area on each panel, used for battery heat rejection - Pitch panels (±Y): net 20 x 55 in. area on each panel, used for electronics boxes heat rejection - Surface properties: absorptivity = 0.08 emissivity = 0.8
MLI	- Mounted on virtually all exposed areas: honeycomb panels, aft face of antenna, antenna support structure,bus/payload interface, used to closeout the anti-earth side of bus, propellant lines and thrusters - 10 to 15 layer construction - 1 to 2 mil aluminized kapton inner/outer layers - Dacron spacer layers - "Off the shelf", industry standard equipment - Surface properties: absorptivity = 0.35 emissivity = 0.53
TEMP. SENSORS	- Used for control of heaters and louvers - "Off the shelf", industry standard equipment, available in a variety of temperature ranges.
STAND-OFFS	- Used to isolate batteries from bus, and payload from bus - G-10 of generic fiberglass construction - Not an "Off the shelf" item but very easy manufacture
COATINGS	- A variety of anodyzes and paints used to tailor surface properties where required

D. THERMAL ANALYSIS

The thermal analysis done in support of this design is intended to be used as a preliminary sizing of hardware and an initial validation of the thermal control concept.

1. Preliminary Analysis

Preliminary thermal hand analyses were done in the following areas: 1) Battery temperatures , and 2) Solar array temperatures. The results of these analyses, done early in the design process, indicated that a passive thermal control system was feasible. The important results were the following:

Solar array temperature extremes:

Hot 40 deg C

Cold -44 deg C

Solar cell performance is not degraded within these temperature limits.

Battery temperature extremes:

Hot 10 deg C

Cold 0 deg C

These limits are set as the required operating temperature range of the batteries by the manufacturer. To maintain these extremes each battery is required to have a dedicated 0.25 sq. meter OSR radiator for the hot case and 21 watts of heater power. The complete analyses and all simplifying assumptions are included in Appendix I.

2. Thermal Analysis Modeling

A detailed lumped-parameter analytical model was developed using the PC-ITAS (Version 7.0) thermal analysis software developed by ANALYTIX, Inc.. The software is a PC based, modular, menu driven finite difference program which is capable of interfacing with other industry standard codes such as SINDA and TRASYS.

The model developed for the spacecraft consisted of a system of thermally coupled nodes which represent significant spacecraft components. The model is essentially divided into two submodels. The first is developed by the geometry definition module within PC-ITAS and is a geometric representation of the

spacecraft exterior. The interior of the spacecraft is modeled by the user as a set of nodes and associated conductances which represent the electronics boxes, batteries, fuel tanks, reaction wheels, etc., and the way in which they are mounted. The two submodels are then coupled using appropriate conductance terms. Thermal parameters such as optical properties and internal thermal dissipations are defined for all nodes in separate modules. Orbital parameters are set and then the entire model is submitted for processing to the internal analysis module. The model developed for this spacecraft is shown in Figure 8.4.

The model used in our analyses consisted of 80 active nodes. Detailed model information is provided in Appendix I

A full thermal analysis is carried out for only two orientations, the earth sensing and the on orbit stand-by modes. The spacecraft configuration is the same during both cases, antenna and solar arrays deployed.

Based on current thruster placement plume impingement analysis is considered unnecessary at this time. Aerodynamic heating was not a concern at the 275 NM altitude.

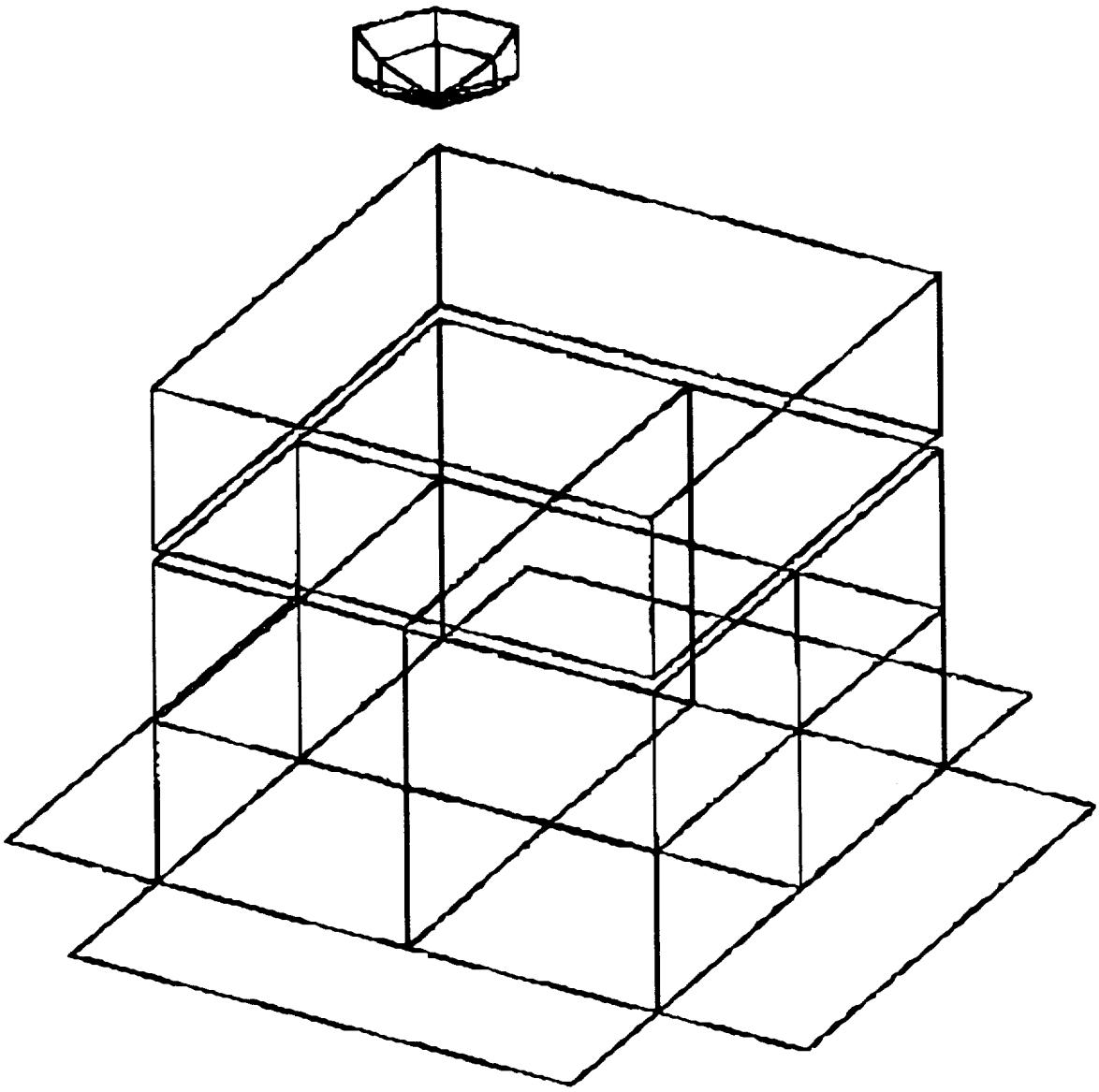

Figure 8.4 Thermal Model

3. Results of Detailed Analyses

The results of the detailed model are given in Table 8.4. The temperature extremes experienced by specific components are given for the earth sensing and stand-by modes.

Table 8.4 Analysis Results

COMPONENT	EARTH SENSING MIN / MAX (°C)	STAND-BY MODE MIN / MAX (°C)
PAYLOAD/BUS/ INTERFACE	+3/+11	0/+30
BATTERIES	0/+13	0/+18
FUEL TANK	-11/+10	-9/+29
SOLAR ARRAYS	-57/+13	-44/+66
ANTENNA	-14/-13	-43/-27
ADCS ELECTRONICS	-40/-10	-39/-10
TT&C ELECTRONICS	-49/+91	-46/-14
EPS ELECTRONICS	-37/+33	-46/+4
REACTION WHEELS	-40/-10	-39/-10

4. Conclusions

The results of the current models show that critical hardware is maintained within required temperature limits.

The batteries are the most temperature sensitive components, and consequently required the most detailed work. After sizing the radiators for the sensing mode, which was the hot case for the batteries, the batteries were running too cold in stand-by mode. The two possible solutions were to include very large heaters (up to 60W per battery) or to have a louver system which would allow for different surface properties for the hot and cold cases. To keep the power requirements lower the louvers are chosen.

The payload/bus interface is controlled by the payload. For early versions of the thermal model the payload was modelled using knowledge of it's exterior and

the electrical power drawn. Modeled in this manner the interface temperature was very cold, -40 deg C. After discussions with NRL we were told to treat the payload as a temperature controlled node, which meant that the ITAS program would not allow the node to make excursions beyond the 0 to 30 deg C limits. The mechanism by which this is accomplished is internal to the payload, and is therefore not a primary concern of the bus design.

In general the bus electronics are running cold, but within limits. This problem would be alleviated by reducing the size of the radiators. Due to the coarseness of the model, and time constraints, the electronics boxes mounted to the honeycomb panels were lumped together and attached to the OSR's, modeled at 20 x 30 in areas. A finer detailed model could separate each box and its associated radiator patch. The overall radiator size would area would consequently go down, thereby the operating temperature ranges would drift upward.

The solar arrays experience the greatest temperature fluctuations of the entire system, however they still remain within their required limits for optimal operation.

Some temperature sensitive components such as thruster, sensors, and tank piping/valves are not explicitly defined in the model. These components are too small to have an effect on the over all system temperates but should be modeled at a later date due to their sensitive nature.

E. MASS AND POWER SUMMARY

A mass and power summary for the thermal control subsystem is given as Table 8.5. The total power shows all the component requirements, however not all the heaters will be active at the same time. The highest active power requirement is 80 W and occurs during the stand-by mode.

Table 8.5. Thermal Control System Mass And Power Summary

COMPONENT	MASS (KG)	POWER (W)
MULTI LAYER INSUL.	8.2	-
OPTICAL SOLAR REFL.	1.8	-
COATINGS / PAINTS	0.45	-
HEATERS	2.3	120.0
TEMP. SENSORS	1.4	2.0
LOUVERS	5.0	5.0
ELECTRONICS	3.6	5.0
STAND-OFFS	2.0	-
TOTALS	24.8	132.0

IX. STRUCTURAL DESIGN

A. MISSION REQUIREMENTS

The structural subsystem must be designed to withstand the dynamic loads of the Delta II launch vehicle. During launch, the Delta II experiences axial loads of 7.2 g's and lateral loads of 2.5 g's. To ensure that the spacecraft bus can adequately withstand these loads, a factor of safety of 1.5 is used. The natural fundamental frequencies of the launch vehicle are 35 Hz axially and 15 Hz laterally. To prevent dynamic coupling between the launch vehicle and the spacecraft, the spacecraft's modal frequencies must be above the launch vehicle's natural frequency in the thrust axis. If payloads are unable to meet this criteria, the structural design must be coordinated closely with the MDAC Delta Program Office so that appropriate analyses can be performed.

B. DESIGN OVERVIEW

The structural configuration of the spacecraft appears as Figures 9.1 and 9.2. The primary load carrying members for axial compressive loads and bending moments are the central cylinder and conical adapter. These are monocoque shells of 6061-T6 Aluminum designed to withstand the ultimate quasi-static loads during launch. The loads are assumed to be a factor of safety of 1.5 times the axial and lateral limit loads of 7.2 and 2.5 g's of the Delta II launch vehicle. Aluminum 6061-T6 was chosen for its ease of machining and large strength-to-weight ratio. There are seven panels made of honeycomb sandwich material with aluminum skins and core. The top panel supports the load of the payload and transmits it to the central cylinder and cone. The two

equipment panels support the subsystem components. The remaining panels make up the body of the spacecraft bus. The panels are designed for stiffness to meet the design criteria for a minimum natural frequency of 50 Hz and stress due to dynamic loads. The adapter ring transfers the loads from the conical section to the 6019 adapter of the Delta II. The frame of the spacecraft bus is made of aluminum square tubing. It provides the mounting surfaces for the side panels and the parabolic antenna. Dimensions for the various components appear in Table 9.1.

1. Central Support Assembly

The central support assembly consists of the cylinder and conical sections. These are designed to support the dynamic loads on the spacecraft during launch. The procedure used to design these components appear in Appendix J.

2. Honeycomb Panels

The honeycomb panels are designed for stiffness to meet a natural frequency of 50 Hz. This frequency was chosen to prevent resonance between the launch vehicle and the spacecraft. The panel which must support the largest mass is the one between the payload and the bus. The procedure used to find the core depth assuming a skin thickness of 1 mm appears in Appendix J. All other honeycomb panels are made from the same material so that costs could be reduced by buying in larger quantities. Calculations in Appendix J show that the core depth chosen is adequate for all equipment and side panels.

C. FINITE ELEMENT MODEL

A finite element model of the spacecraft bus was created on GIFTS (Graphics-Oriented Interactive Finite-element Transportable System Version

6.5.2). GIFTS is a program used to analyze and design structures for static and dynamic loads. It is available on the VAX system of the Computational Instruction Laboratory of the Aero/Astronautics Department of NPS. GIFTS obtains displacements, stresses, stress contours, bending moment and shear forces, and associated normal and shearing stresses for each element. Free vibration response mode shapes and frequencies and forced responses may also be obtained..

All components listed in Table 9.1 were modeled on GIFTS. The central support assembly and all honeycomb panels were modeled as membranes, while all the struts were modeled as hollow beams. The payload and all other subsystem components such as attitude control and electric power were modeled as distributed masses on the equipment panels. The parabolic antenna was modeled as a point mass. The data files used to create the model appear in Appendix J.

1. Modal Analysis

The first eight modal frequencies of the spacecraft are given in Table 9.2. In the first mode, the central support assembly moves opposite to the box framework which supports the side panels. The second through fifth modes show bending and twisting of the antenna support. These modes are similar to the first and second modes of a cantilever beam. Because the second and third modes have frequencies which are close to the launch vehicle natural frequency, the antenna support structure should be stiffened to raise these frequencies. This should be considered in refinement of this design but will not be considered at this time. The sixth through eighth modes show warping of

the equipment shelves. These modes are similar to the first and second modes of a membrane.

2. Deflections and Stresses

A static analysis of the spacecraft under loads equal to those experienced during launch was also performed. The maximum translational deflection occurs at the tip of the antenna support. This deflection is only 1.2 mm. The maximum rotational deflection of 2.2 mm also occurs at this point. The maximum stress in the spacecraft is 87.9% of the maximum yield stress using Von Mises yield criterion. This results in a margin of safety of 13.8%.

D. MASS SUMMARY

The individual masses of each structural component appear in Table 9.1. These total to 164.97 kg. Assuming fittings, brackets, and other attachment devices add an additional 25% mass and assuming another 10% margin for growth, the total mass of the spacecraft bus structural subsystem is 226.8 kg.

Table 9.1 Structural Dimensions (length - m; mass - kg)

Cylinder:		Cone:	
Outer Radius	0.254	Out Low Rad	0.709
Height	0.491	Out Up Rad	0.254
Thickness	0.002	Height	0.508
Mass	4.39	Thickness	0.005
		Mass	21.52
Payload Panel:		Adapter Ring:	
Length	1.524	Inner Radius	0.680
Width	1.524	Outer Radius	0.809
Skin Thick	0.001	Thickness	0.025
Core Depth	0.023	Mass	42.24
Mass	15.24		
Low Equip Panel:		Up Equip Panel:	
Length	1.524	Length	1.524
Width	1.524	Width	1.524
Skin Thick	0.001	Skin Thick	0.001
Core Depth	0.023	Core Depth	0.023
Hole Radius	0.530	Hole Radius	0.254
Mass	9.56	Mass	14.08
Side Panel:		Verticle Struts:	
Length	1.016	Sides	0.050
Width	1.524	Thickness	0.003
Skin Thick	0.001	Length 3@	1.016
Core Depth	0.023	1@	1.864
Mass	10.28	Mass 3@	1.60
		1@	2.94
Antenna Support:		Horizontal Struts:	
Sides	0.050	Sides	0.050
Thickness	0.003	Thickness	0.003
Length 2@	0.800	Length 4@	0.300
Mass 2@	1.22	4@	0.753
		Mass 4@	0.47
		4@	1.19

Table 9.2 Modal Frequencies (Hz)

Mode	Frequency
1	22.76
2	31.72
3	32.14
4	40.31
5	40.98
6	67.40
7	70.18
8	70.63

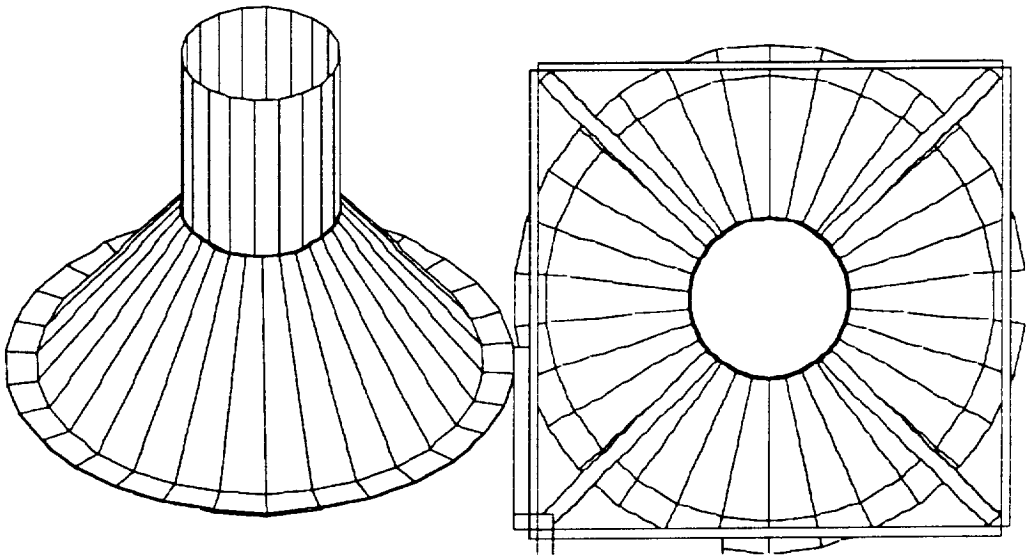

Figure 9.1 Adaptor Cone and Cylinder

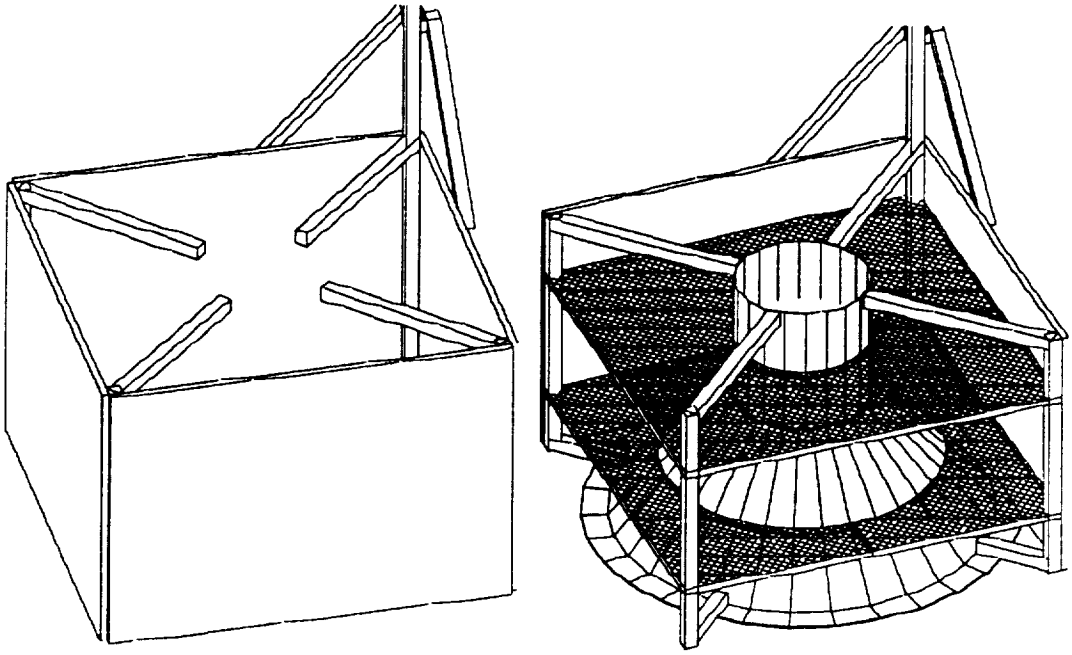

Figure 9.2 Honeycomb Panels and Box Frame

X. TESTING

A. INTRODUCTION

Due to the high risk nature of the proposed payload, the decision was made to minimize risk and cost for the bus design. To this extent, simplicity of design and testing was paramount. To minimize cost a modofied proto-flight test plan has been developed. The United States Air Force Military Standard Test Requirement for Space Vehicles (MIL-STD-1540B) was adopted as the basic guideline for developing testing requirements and acceptance levels.

B. TESTING PHILOSOPHY

All spacecraft development programs include intensive testing of all hardware to ensure proper operation during all mission phases. Testing is divided between system level tests and component/subsystem level tests.

For system level tests a dedicated qualification unit is usually constructed and used to qualify the design before the flight unit is completed. The qualification unit is built to the same demanding standards as the flight article. With production satellites this cost is usually acceptable, however with a unique, one of a kind, spacecraft the cost is excessive. Under these circumstances a "proto-flight" test plan is usually developed. This plan calls for building only one vehicle, to flight hardware standards, which is used in all system level testing and subsequently flown as the mission flight unit. The testing is usually done to levels which are lower than qualification levels but higher than flight levels. This standard industry practice is outlined in great detail in MIL-STD-1540B.

The deficiency of the proto-flight testing philosophy is that certain tests cannot be undertaken until the proto-flight unit is at least partially completed. This generally requires a great deal of time due to the strict standards of procuring, manufacturing, assembling, inspecting, and accepting flight hardware. For this reason it is proposed that early in the development of this system a full scale "test" model is developed for early development tests.

The test model would include primary structure such as the central cylinder and cone, external honeycomb panels, internal decks, and internal framework. Additionally mass simulators of the significant bus components would be included, as well as a mass model of the payload. This unit could be easily constructed and used in dynamic testing such as acoustic or random vibration tests which not only are an indicator of the structural system performance but can be used to derive component test levels for critical equipment. With slight modifications, such as the addition of some heaters, multi-layer insulation, and optical solar reflectors, the test model could be used as a development system for the thermal control system which may be critical.

A flowchart for the proposed testing is shown as Figure 10.1. Appropriate functional tests are performed before and after all environmental tests. The modified proto-flight testing philosophy speaks primarily to the system level tests. Component level testing is done as required to accept critical hardware. All mission specific electronics packages are to be tested on a component, and subsystem level. All other components will be off the shelf and flight proven. These components will be tested on a subsystem and space vehicle level only. All component and subsystem testing of the payload is done by the

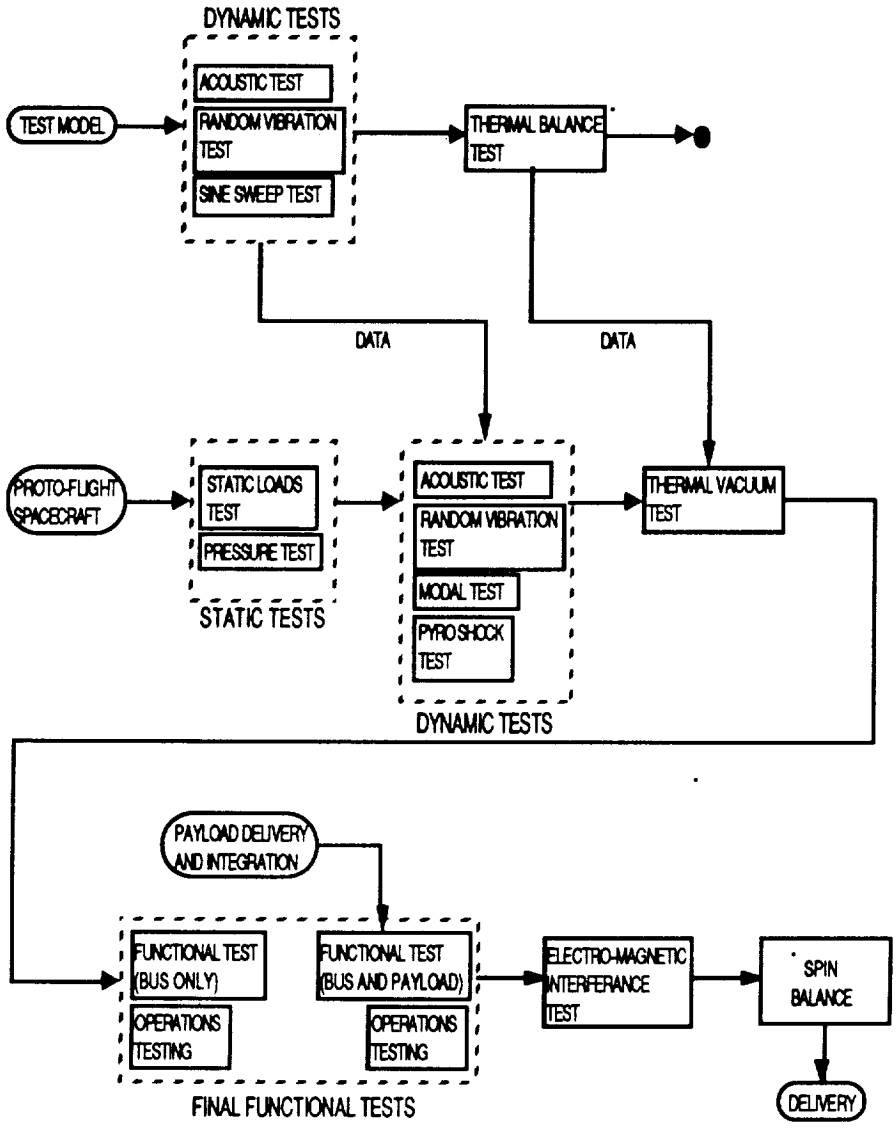

Figure 10.1 System Level Test Flow Chart

payload supplier. Only those tests required to ensure proper integration of the payload and bus are considered in the bus test plan.

C. SYSTEM LEVEL TESTING

System level tests are done on both the test model as well as the proto-flight model. Not all tests are done on both.

1. Proto-Flight Unit

a. Functional Test

Purpose: This test verifies that mechanical and electrical performance of the space vehicle meets specification requirements and validates all test techniques and software algorithms used in computer assisted commanding and processing.

Mechanical Functional Test: Mechanical devices, valves, deployables, and separable entities shall be functionally tested, with the spacecraft in the launch, or orbital configuration appropriate to the function. The maximum and minimum operating limits shall be determined with respect to mechanics, time, and other applicable requirements. Where operation at 1-g environment cannot be performed, a suitable ground test fixture shall be utilized to permit operation and evaluation of the devices. Fit checks shall be made of the space vehicle physical interfaces with the launch vehicle by means of launch vehicle master gages or interface assemblies.

Electrical Functional Test: The space vehicle shall be in its flight configuration with all components and subsystems connected except pyrotechnic elements. The operation of all thermally controlled components, such as heaters and thermostats, shall be verified by test. The test shall verify the integrity of all electrical circuits in the initiating stimulus and confirmation of the successful completion of the event. Wherever possible, equipment performance parameters (such as power, voltage, gain, frequency, command and data rates) shall be varied over specification ranges to demonstrate the performance margins. A segment of this test shall operate the space vehicle through a mission profile with all events occurring in actual flight sequence to

the extent practical. this sequence shall include final countdown, launch, ascent, separation from the launch vehicle, orbital injection, and orbital operation as appropriate.

b. Acoustic Test

Purpose: This test demonstrates the ability of the space vehicle to withstand the design level acoustic environment which is the maximum level imposed during launch plus a design margin. This test also verifies the adequacy of component vibration qualification criteria.

Test Description: The mass model used for this test shall be of identical structural quality and design as the flight vehicle. It shall be mounted to a flight-type support structure. The model shall represent the space vehicle in the stowed launch configuration. Adequate dynamic instrumentation shall be installed to measure vibration responses at attachment points of critical and representative components.

Test Levels and Duration: The acoustic test spectrum shall be the design environment which is the maximum predicted flight environment plus the design margin (3dB). The overall sound pressure level of the test shall not be less than 141 dB. Exposure time shall be at least three times the expected flight exposure time to the maximum flight environment, but not less than 3 minutes. Operating time shall be divided equally between redundant circuits.

c. Pyro Shock Test

Purpose: This test demonstrates the capability of the space vehicle to withstand the design level pyro shock environments which are the

levels predicted for flight plus a design margin. This test also verifies the adequacy of component pyro shock criteria.

Test Description: In this test all pyrotechnically operated devices shall be operated. Separation subsystem shocks are often more severe than those from other pyrotechnic devices, and operation of the separation subsystem is therefore especially significant. For this test the vehicle shall be suspended or otherwise supported to prevent the possibility of recontact between the separated portions thereof. The launch vehicle separation adapter shall be attached and appropriate pyrotechnics used to impose the required shock. Adequate dynamic instrumentation shall be installed to measure pyro shock responses in 3 axes at attachment points of critical and representative components.

Test Levels and Duration: All pyrotechnic devices shall be fired at once. Those pyrotechnic devices producing levels within 6 dB of the maximum shock response measured from any of the devices shall be fired an additional two times to provide the expected variability in the shock environment.

d. Pressure Test

Purpose: This test demonstrates the capability of fluid subsystems to meet the flow, pressure, and leakage rate requirements specified.

Test Description: Tests shall be performed to verify compatibility with the test setup and to ensure that proper control of the equipment and test functions provided. The requirements of the subsystem including flow, leakage, and regulation shall be measured while operating applicable valves, pumps, and motors. The flow checks shall verify that the plumbing configurations are

adequate. Checks for subsystem cleanliness, moisture levels, and pH shall also be made.

In addition to the high pressure test, propellant tanks and thruster valves shall be tested for leakage under propellant servicing conditions. The system shall be evacuated to the internal pressure normally used for propellant loading and the systems pressure monitored for any indication of leakage.

Test Levels and Duration: The subsystem shall be pressurized to 1.5 times the maximum predicted operating pressure and held there for 5 minutes, then the pressure shall be reduced to the maximum operating pressure. This sequence shall be repeated three times. Inspection for leakage after these cycles shall be made at the maximum operating pressure. The duration of the evacuated propulsion system leak test shall not exceed the time that this condition is normally experienced during propellant loading.

e. Thermal Vacuum Test

Purpose: This test demonstrates the ability of the space vehicle to meet design requirements under vacuum conditions and temperature extremes which simulate those predicted for flight plus a design margin.

Test Description: The space vehicle shall be placed in a thermal vacuum chamber and a functional test conducted to assure readiness for chamber closure. Equipment that does not operate during launch shall have power applied after the test pressure has been reached. A temperature cycle begins with the space vehicle at ambient temperature (23 +/- 10 deg C). The temperature is reduced to the specified low level and stabilized. Temperature stabilization has been achieved when the rate of temperature change is no more than 3 deg C/hour. Following the cold soak. the temperature shall be raised to

the highest specified temperature and stabilized. Following the high temperature soak, the space vehicle shall be returned to ambient temperatures to complete one temperature cycle. Functional tests shall be performed during the first and last temperature cycle at both the low and high temperature limits with functional operation and monitoring of perceptive parameters during all other cycles. In addition to the temperature cycles, the chamber shall be programmed through various orbital operations. Strategically placed temperature monitors shall assure attainment of temperature limits. Strategically placed witness plates and quartz crystal microbalances shall be installed in the test chamber to assure that outgassing from the space vehicle and test equipment does not degrade system performance beyond specified limits.

Test Levels and Duration: The temperature extremes shall be established by a survey of predicted temperatures in various equipment areas. Temperatures on the components shall not be allowed to exceed the design level of 0 - 30 deg C. The pressure shall be maintained at 0.0133 pascals (0.0001 Torr) or less. All orbital operational conditions and all equipment functional modes shall be tested. The test shall include six complete hot-cold cycles ate the maximum predicted orbital rate of temperature change and with an 8-hour soak at each temperature extreme. Operating time shall be divided equally between redundant circuits.

1. **Test Model**

   a. Thermal Balance Test

   Purpose: This test verifies the analytical thermal model and demonstrates the ability of the space vehicle thermal control subsystem to

maintain components, subsystems, and the entire space vehicle within specified operating temperature limits. This test also verifies the adequacy of component thermal design criteria.

Test Description: The mass model shall be tested to simulate the thermal environment seen by the space vehicle during the transfer orbit and orbital mission phases. Tests shall be conducted over the full range of seasons, equipments duty cycles, solar angles, and eclipse combinations so as to include the worst case high and low temperature extremes for all space vehicle components. Special emphasis shall be placed on defining the maximum and minimum battery temperatures. The power requirements for all thermostatically controlled heaters shall be verified during the test. The test chamber pressure, with the test item installed, shall provide a pressure of 0.0133 pascals (0.0001 Torr). The space vehicle thermal environment will be supplied by the Incident Flux method, where the intensity, spectral content, and angular distribution of the incident solar, albedo, and planetary irradiation is simulated.

Test Levels and Duration: For this space vehicle two modes of operation will exist. The first, Earth sensing, shall be used during sensing period which will be two consecutive orbits per day. The second, Sun sensing, shall be used during all other periods. The worst case temperature extremes for each case shall be predicted and used for the test. The worst case high temperature will be predicted with all heat producing components operating at full power and the space vehicle receiving maximum solar irradiation. The worst case low temperature will be predicted at maximum eclipse and minimum heat production by onboard equipment. The test duration will be

dependent on the thermal time constant of the subsystems and orbital maneuvering.

All tests are to be conducted at the Naval Research Laboratory (NRL).

D. COMPONENT AND SUBSYSTEM LEVEL TESTING

A component is a functional unit that is viewed as an entity for purposes of analysis, manufacturing, maintenance, or record keeping. Examples are hydraulic actuators, valves, batteries, electrical harnesses, and individual electronics packages such as transmitters, receivers, or multiplexers. A subsystem is an assembly of two or more components including the supporting structure to which they are mounted, and any interconnecting cables or tubing. A subsystem is composed of functionally related components that perform one or more prescribed functions. Typical space vehicle subsystems are electrical power, attitude control, thermal control, telemetry, structure, and propulsion.

Component level random vibration testing is done as required to accept critical hardware. All mission specific electronics packages and mechanical devices are to be tested to appropriate random vibration levels. Levels are to be determined from the test model acoustic and random vibe system level tests and any analytical models available. Electronics packages and mechanical devices should alsoAll other components will be off the shelf, flight tested and validated quality and will be tested on a subsystem and space vehicle level only.

XI. COST ANALYSIS

A. INTRODUCTION

Program costs can be estimated using one of three standard methods -- engineering build-up, analogy, parametrics -- or a combination of the three. Cost modeling for this project was performed using the Unmanned Space Vehicle Cost Model, Revision 6 (USCM6).

B. PARAMETRICS

The USCM6 is a parametric estimating tool. Parametric estimates, also known as "top-down" estimates, or Cost Estimating Relationship (CER) estimates, are based on mathematical expressions relating cost as the dependent variable to selected, independent cost driver variables. The mathematical expression is derived by statistically correlating the historical cost data of several related or similar systems to physical and/or performance characteristics of those same systems. The implicit assumption of this approach is that the forces that affect cost in the past will continue to affect cost in the future.

1. Advantages

Parametric estimating has four advantages.

a. Provides unbiased, objective, and consistent estimates.

b. Once the parametric relatinships have been defined, the estimating process can be performed numerous times varying the cost sensitive physical or performance characteristic.

c. Since parametrics are derived from actual program cost history, they inherently account for the impact of schedule changes, engineering changes, system growth, and redirection.

d. Since most of the parametric relationships are based on the advance design characteristics, and most cost estimates are reguired during the concept formulation phase of the program, the parametric approach provides a feasible means for performing an estimate.

2. Disadvantages

The main disadvantage of parametric estimates stem from several factors:

a. The underlying assumption that what affects cost in the past will affect cost in the future.

b. The need for a sufficient data base that is representative of the particular products developement, production, and technology environment.

c. The parametric relationships may become obsolete, and require continual re-evaluation of the CERs and expansion of the data base.

d. The estimate lacks program peculiarity.

e. There is the limitation that extrapolation beyond the range of historical data becomes risky.

C. USCM6 SCOPE

The USCM6 provides CERs for estimating hardware costs for earth orbiting, unmanned space vehicle programs. These CERs are limited within the following boundary conditions:

a. The model addresses only unmanned earth-orbiting space vehicles, with the following exceptions -- the stucture and thermal CER data bases include data points for large structures such as the Apollo Adapter, Apollo Module, Lunar Module Descent, Shuttle , Spacelab, ERBS, STOTA, UARS, COBE, GRO, and Space Telescope.

b. The model is an approximation of the real world based upon mathematical relationships derived from the analysis of historical cost data. Implicit in this approach is the assumption that historical costs will properly reflect current and future costs.

c. All costs included in the model are end-of-program costs or estimates of mature programs (at least one launch).

d. The model's emphasis is on space vehicle hardware costs. It does not address specific missin payload costs other than communications payloads.

5) Launch vehicle, launch adapters, and their associated ground support are not addressed in the model.

e. CERs are based on burdened cost (direct plus indirect) with General and Administrative (G&A) costs included.

f. A 95% cumulative learning curve is used to derive data base first unit costs.

g. All CERs with the exception of Program Level CERs represent first unit cost and require appropriate consideration for production learning. Program Level recurring CERs estimate total recurring costs.

h. The cost model provides for an estimate calculated in U.S. Government Fiscal Year 1986 dollars, and must have the appropriate inflation costs added if costs are to be expressed as future expenditures.

i. Target and incentive fee costs are not included in the model.

j. The model yields an "average" starting point estimate which represents and "average" program with "average" problems, "average" technology, "average" schedule, "average" engineering changes, etc.(Ref. USCM6)

D. ANALYSIS

The USCM6 has provisions for subsystem and component cost estimating. Due to the preliminary design nature of this project and the limited component information the subsystem cost estimating approach was determined sufficient. Since the USCM6 provides for cost estimates in FY 1986 dollars, a constant 7 percent annual inflation rate was applied to convert to FY 1991 dollars. The complexity factor was also set to one (1) due to the simple design concept used for this project. Most cost drivers associated with the cost model were dependent on subsystem mass and/or power requirements. A summary of mass and power requirements can be found in Chapter II.

1. Non-recurring Costs

The non-recurring costs associated with the subsystems are listed in Table 11.1. Appendix L shows the actual non-recurring cost estimate with inflation and complexity taken into account. The High Estimate and Low Estimate are calculated by taking the Most Likely Estimate and either adding

or subtracting, as appropriate, a correction factor derived from the Standard Error (SE) as a percentage of the calculated subsystem cost.

Table 11.1 Non-recurring Costs

Cost Estimating Relationship (CER)Category	Most Likely Cost ($millions)	Low Estimate ($million)	High Estimate ($millions)
Integration and Assembly (I&A)	3.34	2.81	3.88
Structure	15.27	12.60	17.94
Attitude Control System (ACS)	10.41	5.31	15.50
Thermal Control	1.64	0.86	2.42
Electrical Power Supply (EPS)	4.20	2.29	6.11
Communications/ TT&C	20.97	11.39	30.55
TOTAL	55.83	35.26	76.40

2. Recurring Cost

The recurring costs associated with the subsystems are listed in Table 11.2. Appendix L shows the actual recurring cost estimate with inflation and complexity taken into account. The High and Low estimates are derived in the same manner as for non-recurring costs.

Table 11.2 Recurring Costs

Cost Estimating Relationship (CER) Category	Most Likely Cost ($millions)	Low Estimate ($millions)	High Estimate ($millions)
Integration and Assembly (I&A)	1.20	1.05	1.36
Structure	2.60	2.29	2.92
Attitude Control System (ACS)	4.19	2.05	6.32
Thermal Control	0.49	0.32	0.66
Electrical Power Supply (EPS)	0.14	0.08	0.19
Communications/ TT&C	8.98	6.92	11.03
TOTAL	17.60	12.71	22.48

3. Launch Vehicle Costs

Table 11.3.below is a cost comparison between the Titan 2 or Delta II launch vehicles. The Titan 2 figures are based on the Operational development Model (ODM) Freeflyer presentation given at the Naval Postgraduate School by Charlie Merk and P. Regeon of the Naval Research Laboratory on October 22, 1991. They were verified to be reasonable figures by Martin Marietta. The Delta II figures were provided by McDonnell Douglas.

Table 11.3 Launch Vehicle Cost Comparison ($millions)

Titan IIG(1)		Delta II(7320) (2)	
Booster	20.6	Booster	21.3
Extended ACS	1.0	Failure Liability	1.6
Integration	8.4	Integration	9.3
Launch Services	9.6	Launch Operation	3.9
		Range Support	1.9
Mgmt Reserve (5%)	1.0	Mgmt Reserve	1.1
TOTAL	$40.6		$39.1

Notes: (1) Costs provided by Martin Marietta

(2) Costs provided by McDonnell-Douglas

E. CONCLUSIONS

As with all cost estimating schemes the use of parametrics is not without errors. The payload, and on orbit operation support costs are not included with the overall cost figure. Launch cost, as previously noted, are approximaltely $40 million. Payload and on orbit operation support costs were unavailable for incorporation in this cost analysis. The spacecraft bus, design and production, and launch costs represent an overall most likely cost of approximatley $160 million. Program level, aerospace ground equipment and launch & orbital support are included in the total program costs along

with the non-recurring and recurring hardware costs. This cost is within realistic limits for a space vehicle of similar mass and complexity. A cost summary is provided in Table 11.4.

Table 11.4 Cost Summary

Category	Most LikelyCost ($millions)	Low Estimate ($millions)	High Estimate ($millions)
Satellite	73.43	47.97	98.88
Launch	39.1	39.1	39.1
Program Level	29.59	22.68	36.50
Aerospace Ground Equipment (AGE)	9.64	7.14	12.15
Launch & Orbital Ops Support (LOOS)	3.53	2.71	4.36
TOTAL	155.29	119.60	190.99

REFERENCES

1. Agrawal, Brij N., *Design of Geosynchronous Spacecraft*, Prentice-Hall, 1986.

2. Air Force Military Standard 1582, *Low Data Rate EHF Communications Standards*, 18 April 1990.

3. Johnson & Jasik, *Antenna Engineering Handbook*, McGraw-Hill Book Company, 1983.

4. Josefson, C. et. al., *Spacecraft Design Porject; High Latitude Communications Satellite*, Naval Postgraduate School, December 1989.

5. JPL and NASA, *Solar Cell Array Design Handbook*, Volumes 1, 2, and 3., JPL Publication SP43-38. October 1976.

6. Kellman, L. et. al., *Spacecraft Design Project: Mulitpurpose Satellited Bus*, Naval Postgraduate School, December 1990.

7. Lee H. F. and Markus J. L., *Optimal Control Theory*, Academic Press, 1964.

8. Milligan, *Modern Antenna Design*, McGraw-Hill Book Company, 1979.

9. Morgan & Gordon, *Communications Satellite Handbook*, John Wiley & Sons, 1989.

10. Space Systems Control Division, Space Flight Operations, *Air Force Satellited Control facility Space/Ground Interface*, Aerospace Report No. TOR-0059(6110-01)-3 Reissue H., June 1987.

11. Tada, H. Y., et al., *Solar Cell Handbook*, Third Addition, JPL Publication 82-69. November 1, 1982.

12. Wheeler, P. C., *Methods in Attitude Control*, NASA CR - 313, 1975

13. Wertz, James R., *Spacecraft Attitude Determination and Control*, Kluwer Academic Publishers, 1978.

14. Wertz & Larson, *Space Mission Analysis and Design*, Kluwer Academic Publishers, 1989.

APPENDIX A - STATEMENT OF WORK

A. SCOPE

This document establishes the preliminary requirements for an infrared (IR) surveillance spacecraft.

B. REQUIREMENTS

1. Mission

This spacecraft will be used to sense areas of the earth subtended by a 4 by 4 degree field of view (FOV) for footprint toe grazing angle of 90 to 45 degrees. The spacecraft orbit shall be circular, with a height of 275 nautical miles and an inclination of 70 degrees.

2. Threat

Classified

3. System Functions

a. Payload Subsystem

The payload is an IR sensor which consist of the following:

- Telescope
- Dewar/IR focal plane array
- Cryogenic cooler (65 degrees K)
- Data Processor
- Pointing controller and sensors
- Structure/Optical Bench

b. Physical Characteristics

(1) Weight 800 pounds

(2) Volume

Width 60 Inches

Length 60 Inches

Height 20 Inches

Note: Use one 60 by 60 inch side for mounting the spacecraft buys and leave the other 60 by 60 inch side clear for payload thermal radiators and the telescope aperture. The boresight of the telescope FOV is at a 45 degree angle with respect to the plane of this side.

(3) Power

Standby Mode - 100 watts

Sensing Mode - 150 watts

c. Attitude Control Subsystem

A three-axis stabilization capability shall be provide to provide nadir and offset-pointing for payload operation (sensing mode). In the nadir pointing mode, the spacecraft body frame tracks the rotating local vertical reference system (pitch, roll, and yaw = zero). The sensor boresight may then be offset, as require, about the roll axis to achieve grazing angles of between 90 degrees and 45 degrees, for the toe of the footprint of the telescope FOV.

Output form an inertial measurement unit (IMU), which is part of the payload subsystem, is available for short term attitude reference, The IMU is initialized by a pair of star sensor, which are also part of the payload.

- Attitude Accuracy ± 5 Degrees Per Axis (3σ)
- Time To Slew 90 Degrees in 15 minutes
- Slew Settling Time 1 Minute
- Rate Stability 0.003 Degrees/Sec (3σ) Per Axis

d. Command and Telemetry Subsystem (CATS)

The CATS shall:

a. Decrypt, validate, decode, store and execute commands to the spacecraft subsystems in accordance with commands and data received from the ground sited via the RFCS (see below); and

b. Process, format and encrypt spacecraft subsystem housekeeping data for transmission to the ground via the RFCS.

e. Radio Frequency Communications Subsystem (RFCS)

The RFCS shall provide redundant:

a. Omnidirectional command receiving capability;

b. Omnidirectional low data rate (16 Kbps minimum) transmitting capability; and

c. Directional high data rate (150 Kbps maximum) transmitting capability.

For the high data rate downlink, design, for:

a. Optimal spectrum usage;

b. BER 10^{-11} encrypted (10^{-9} unencrypted);

c. Minimum Elevation angle of 10 degrees at data collection terminal;

d. 99 Percent link availability due to rain attenuation;

e. Assume a 20 foot maximum diameter ground antenna.

f. Electrical Power Subsystem (EPS)

The electrical power system shall be designed to provide 30 minutes of sensing time per day. Initial sizing should assume 15 minutes of sensing time per orbit, for two contiguous orbits. This will allow some warm up time and as much data collection as the pass geometry allows. The solar array and battery shall be sized to proved energy balance for day and/or night sensing during the maximum orbital eclipse season.

STRUCTURAL SUBSYSTEM

The 1,2,3 Dimensions of component are parallel to the X,Y,Z coordinate system of the spacecraft.

Coordinates of component cg from reference frame

Coordinates of component cg from center of mass of spacecraft.

Component coordinate system

COMPONENT	DIM 1	DIM 2	DIM 3	X	Y	Z	X'	Y'	Z'	MASS	I 11	I 22	I 33
PAYLOAD PANEL	1.524	1.524	0.017	0.762	0.762	-0.5165	0.02122781	-0.0073005	0.23478264	14.32	2.77195223	2.77195223	5.54321472
SIDE #1 PANEL	0.017	1.524	1.016	1.5155	0.762	-1.016	0.77472781	-0.0073005	-0.2647174	9.75	2.725801	0.83894281	1.88732781
SIDE #2 PANEL	1.524	0.017	1.016	0.762	1.5155	-1.016	0.02122781	0.74619949	-0.2647174	9.75	0.83894281	2.725801	1.88732781
SIDE #3 PANEL	0.017	1.524	1.016	0.0085	0.762	-1.016	-0.7322722	-0.0073005	-0.2647174	9.75	2.725801	0.83894281	1.88732781
SIDE #4 PANEL	1.524	0.017	1.016	0.762	0.0085	-1.016	0.02122781	-0.7608005	-0.2647174	9.75	0.83894281	2.725801	1.88732781
							-0.7407722	-0.7693005	0.75128264				
CENTRAL CYLINDER				0.762	0.762	-0.7705	0.02122781	-0.0073005	-0.0192174	4.39	0.244	0.244	0.292
CONE				0.762	0.762	-1.355	0.02122781	-0.0073005	-0.6037174	21.52	3.05	3.05	5.41
RING				0.762	0.762	-1.5365	0.02122781	-0.0073005	-0.7852174	42.24	9.217	9.217	18.435
EQUIP PANEL #1	1.524	1.524	0.017	0.762	0.762	-0.7535	0.02122781	-0.0073005	-0.0022174	13.36	2.58612303	2.58612303	5.17160256
EQUIP PANEL #2	1.524	1.524	0.017	0.762	0.762	-1.3325	0.02122781	-0.0073005	-0.5812174	9.07	1.7556988	1.7556988	3.51096072
							-0.7407722	-0.7693005	0.75128264				
CONE STRUT #1	0.3	0.05	0.05	1.3691	0.1549	-1.499	0.62832781	-0.6144005	-0.7477174	0.47	0.00019583	0.00362292	0.00362292
CONE STRUT #2	0.3	0.05	0.05	1.3691	1.3691	-1.499	0.62832781	0.59979949	-0.7477174	0.47	0.00019583	0.00362292	0.00362292
CONE STRUT #3	0.05	0.3	0.05	0.1549	1.3691	-1.499	-0.5858722	0.59979949	-0.7477174	0.47	0.00362292	0.00019583	0.00362292
CONE STRUT #4	0.05	0.3	0.05	0.1549	0.1549	-1.499	-0.5858722	-0.6144005	-0.7477174	0.47	0.00362292	0.00019583	0.00362292
							-0.7407722	-0.7693005	0.75128264				
CYLINDER STRUT #1	0.753	0.05	0.05	1.2076	0.3164	-0.55	0.46682781	-0.4529005	0.20128264	1.19	0.00049583	0.05647631	0.05647631
CYLINDER STRUT #2	0.753	0.05	0.05	1.2076	1.2076	-0.55	0.46682781	0.43829949	0.20128264	1.19	0.00049583	0.05647631	0.05647631
CYLINDER STRUT #3	0.05	0.753	0.05	0.3164	1.2076	-0.55	-0.4243722	0.43829949	0.20128264	1.19	0.05647631	0.00049583	0.05647631
CYLINDER STRUT #4	0.05	0.753	0.05	0.3164	0.3164	-0.55	-0.4243722	-0.4529005	0.20128264	1.19	0.05647631	0.00049583	0.05647631
							-0.7407722	-0.7693005	0.75128264				
VERTICAL STRUT #1	0.05	0.05	1.016	1.482	0.042	-1.016	0.74122781	-0.7273005	-0.2647174	1.6	0.13796747	0.13796747	0.00066667
VERTICAL STRUT #2	0.05	0.05	1.016	1.482	1.482	-1.016	0.74122781	0.71269949	-0.2647174	1.6	0.13796747	0.13796747	0.00066667
VERTICAL STRUT #3	0.05	0.05	1.864	0.042	1.482	-1.016	-0.6987722	0.71269949	-0.2647174	2.94	0.85186402	0.85186402	0.001225
VERTICAL STRUT #4	0.05	0.05	1.016	0.042	0.042	-1.016	-0.6987722	-0.7273005	-0.2647174	1.6	0.13796747	0.13796747	0.00066667
							-0.7407722	-0.7693005	0.75128264				
							-0.7407722	-0.7693005	0.75128264				
							-0.7407722	-0.7693005	0.75128264				
							-0.7407722	-0.7693005	0.75128264				
FASTENERS AND WIRING				1.5155	0.762	-1.016	0.77472781	-0.0073005	-0.2647174	3.957			
FASTENERS AND WIRING				0.762	1.5155	-1.016	0.02122781	0.74619949	-0.2647174	3.957			
FASTENERS AND WIRING				0.0085	0.762	-1.016	-0.7322722	-0.0073005	-0.2647174	3.957			
FASTENERS AND WIRING				0.762	0.0085	-1.016	0.02122781	-0.7608005	-0.2647174	3.957			
TOTAL										174.108			

	A	B	C	D	E	F	G	H	I	J	K	L	M	N
53														
54														
55														
56				Spacecraft coordinate system					componets for CM calc's					
57														
58	COMPONENT	I XX	I YY	I ZZ	I XY	I XZ	I YZ	Xi*Mi	Yi*Mi	Zi*Mi				
59		3.56207523	3.56776489	5.55043082	-0.0022192	0.07136976	-0.0245449	10.91184	10.91184	-7.39628				
60		3.40955462	7.37415784	7.73982852	-0.0551451	-1.999568	0.01884256	14.776125	7.4295	-9.906				
61		6.95111022	3.41342852	7.32065479	0.15444179	-0.0547889	-1.9259366	7.4295	14.776125	-9.906				
62		3.40955462	6.75034669	7.11601737	0.05212308	1.88999029	0.01884256	0.082875	7.4295	-9.906				
63		7.16564653	3.41342852	7.5351911	-0.1574638	-0.0547889	1.96362172	7.4295	0.082875	-9.906				
64		0	0	0	0	0	0	0	0	0				
65		0.24585523	0.24759948	0.2942122	-0.0006803	-0.0017909	0.0006159	3.34518	3.34518	-3.382495				
66		10.8946414	10.9031918	5.4208443	-0.003335	-0.2757917	0.09484815	16.39824	16.39824	-29.1596				
67		35.2630117	35.2797946	18.4562855	-0.0065461	-0.7040752	0.24214011	32.18688	32.18688	-64.90176				
68		2.58690077	2.592209	5.1783349	-0.0020704	-0.0006289	0.00021627	10.18032	10.18032	-10.06676				
69		4.8201517	4.82375542	3.51553125	-0.0014056	-0.1119054	0.03848565	6.91134	6.91134	-12.085775				
70		0	0	0	0	0	0	0	0	0				
71		0.44038337	0.45194515	0.36659631	-0.1814411	-0.2208115	0.21591702	0.643477	0.072803	-0.70453				
72		0.43205095	0.45194515	0.3582639	0.17712923	-0.2208115	-0.2107858	0.643477	0.643477	-0.70453				
73		0.43547804	0.42428974	0.33403557	-0.1651607	0.2058914	-0.2107858	0.072803	0.643477	-0.70453				
74		0.44381045	0.42428974	0.34236799	0.16918128	0.2058914	0.21591702	0.072803	0.072803	-0.70453				
75		0	0	0	0	0	0	0	0	0				
76		0.29279978	0.36402337	0.55990233	-0.2515976	0.11181756	-0.1084816	1.437044	0.376516	-0.6545				
77		0.277315	0.36402337	0.54441755	0.24348637	0.11181756	0.10498428	1.437044	1.437044	-0.6545				
78		0.33329548	0.26301751	0.49939217	-0.2213425	-0.1016483	0.10498428	0.376516	1.437044	-0.6545				
79		0.34878026	0.26301751	0.51487695	0.22871607	-0.1016483	-0.1084816	0.376516	0.376516	-0.6545				
80		0	0	0	0	0	0	0	0	0				
81		1.09643355	1.12915779	1.72608218	-0.8625526	-0.3139454	0.30804651	2.3712	0.0672	-1.6256				
82		1.06279282	1.12915779	1.69244145	0.8452363	-0.3139454	-0.3018623	2.3712	2.3712	-1.6256				
83		2.55123061	2.49343609	2.93012102	-1.4641629	0.54383275	-0.5546719	0.12348	4.35708	-2.98704				
84		1.09643355	1.03134002	1.62826442	0.81314778	0.2959634	0.30804651	0.0672	0.0672	-1.6256				
85		0	0	0	0	0	0	0	0	0				
86		0	0	0	0	0	0	0	0	0				
87		0	0	0	0	0	0	0	0	0				
88		0	0	0	0	0	0	0	0	0				
89		0.27749878	2.65229188	2.3752149	-0.0223804	-0.811517	0.00764718	5.9968335	3.015234	-4.020312				
90		2.48059963	0.27907098	2.20509486	0.06267961	-0.0222359	-0.781634	3.015234	5.9968335	-4.020312				
91		0.27749878	2.39912053	2.12204355	0.02115395	0.76704529	0.00764718	0.0336345	3.015234	-4.020312				
92		2.56766837	0.27907098	2.29216359	-0.0639061	-0.0222359	0.79692832	3.015234	0.0336345	-4.020312				
93	TOTAL	92.722571	92.764874	88.618609	-0.694114	-1.128517	0.2205466	131.7055	133.6351	-195.9979				

THERMAL CONTROL SUBSYSTEM

The 1,2,3 Dimensions of component are parallel to the X,Y,Z coordinate system of the spacecraft.

Coordinates of component cg from reference frame

Coordinates of component cg from center of mass of spacecraft.

Component coordinate system

	O	P	Q	R	S	T	U	V	W	X	Y	Z	AA	AB
10	COMPONENT	DIM 1	DIM 2	DIM 3	X	Y	Z	X'	Y'	Z'	MASS	I 11	I 22	I 33
11	THERMAL MASS				0.762	0.762	-0.508	0.02122781	-0.0073005	0.24328264	4.183			
12	THERMAL MASS				0.762	0.762	-1.524	0.02122781	-0.0073005	-0.7727174	4.183			
13	THERMAL MASS				0.762	0	-1.016	0.02122781	-0.7693005	-0.2647174	4.183			
14	THERMAL MASS				0.762	1.524	-1.016	0.02122781	0.75469949	-0.2647174	4.183			
15	THERMAL MASS				0	0.762	-1.016	-0.7407722	-0.0073005	-0.2647174	4.183			
16	THERMAL MASS				1.524	0.762	-1.016	0.78322781	-0.0073005	-0.2647174	4.183			
17								-0.7407722	-0.7693005	0.75128264				
18								-0.7407722	-0.7693005	0.75128264				
19								-0.7407722	-0.7693005	0.75128264				
20								-0.7407722	-0.7693005	0.75128264				
21								-0.7407722	-0.7693005	0.75128264				
22								-0.7407722	-0.7693005	0.75128264				
23								-0.7407722	-0.7693005	0.75128264				
24								-0.7407722	-0.7693005	0.75128264				
25								-0.7407722	-0.7693005	0.75128264				
26								-0.7407722	-0.7693005	0.75128264				
27								-0.7407722	-0.7693005	0.75128264				
28								-0.7407722	-0.7693005	0.75128264				
29								-0.7407722	-0.7693005	0.75128264				
30								-0.7407722	-0.7693005	0.75128264				
31								-0.7407722	-0.7693005	0.75128264				
32								-0.7407722	-0.7693005	0.75128264				
33								-0.7407722	-0.7693005	0.75128264				
34								-0.7407722	-0.7693005	0.75128264				
35								-0.7407722	-0.7693005	0.75128264				
36								-0.7407722	-0.7693005	0.75128264				
37								-0.7407722	-0.7693005	0.75128264				
38								-0.7407722	-0.7693005	0.75128264				
39								-0.7407722	-0.7693005	0.75128264				
40								-0.7407722	-0.7693005	0.75128264				
41	FASTENERS AND WIRING				1.5155	0.762	-1.016	0.77472781	-0.0073005	-0.2647174	0.62745			
42	FASTENERS AND WIRING				0.762	1.5155	-1.016	0.02122781	0.74619949	-0.2647174	0.62745			
43	FASTENERS AND WIRING				0.0085	0.762	-1.016	-0.7322722	-0.0073005	-0.2647174	0.62745			
44	FASTENERS AND WIRING				0.762	0.0085	-1.016	0.02122781	-0.7608005	-0.2647174	0.62745			
45	TOTAL										27.6078			

	O	P	Q	R	S	T	U	V	W	X	Y	Z	AA	AB
53														
54														
55														
56				Spacecraft coordinate system					componets for CM calc's					
57														
58	COMPONENT	I XX	I YY	I ZZ	I XY	I X2	I YZ	XI*MI	YI*MI	ZI*MI				
59		0.24779984	0.24946184	0.00210789	-0.0006483	0.02160251	-0.0074294	3.187446	3.187446	-2.124964				
60		2.49785926	2.49952126	0.00210789	-0.0006483	-0.0686142	0.02359725	0.08879594	3.187446	-6.374892				
61		2.76872162	0.29500984	2.47748167	-0.0683108	-0.0235058	0.85185622	0.08879594	0	-4.249928				
62		2.67564175	0.29500984	2.3844018	0.06701425	-0.0235058	-0.8356883	0.08879594	6.374892	-4.249928				
63		0.29334784	2.58851867	2.29561672	0.02262171	0.82026645	0.00808394	-3.0986501	3.187446	-4.249928				
64		0.29334784	2.85916871	2.56626676	-0.0239182	-0.8672781	0.00808394	3.27624194	3.187446	-4.249928				
65		0	0	0	0	0	0	0	0	0				
66		0	0	0	0	0	0	0	0	0				
67		0	0	0	0	0	0	0	0	0				
68		0	0	0	0	0	0	0	0	0				
69		0	0	0	0	0	0	0	0	0				
70		0	0	0	0	0	0	0	0	0				
71		0	0	0	0	0	0	0	0	0				
72		0	0	0	0	0	0	0	0	0				
73		0	0	0	0	0	0	0	0	0				
74		0	0	0	0	0	0	0	0	0				
75		0	0	0	0	0	0	0	0	0				
76		0	0	0	0	0	0	0	0	0				
77		0	0	0	0	0	0	0	0	0				
78		0	0	0	0	0	0	0	0	0				
79		0	0	0	0	0	0	0	0	0				
80		0	0	0	0	0	0	0	0	0				
81		0	0	0	0	0	0	0	0	0				
82		0	0	0	0	0	0	0	0	0				
83		0	0	0	0	0	0	0	0	0				
84		0	0	0	0	0	0	0	0	0				
85		0	0	0	0	0	0	0	0	0				
86		0	0	0	0	0	0	0	0	0				
87		0	0	0	0	0	0	0	0	0				
88		0	0	0	0	0	0	0	0	0				
89		0.04400218	0.42056622	0.37663093	-0.0035488	-0.1286799	0.00121259	0.48610297	0.4781169	-0.6374892				
90		0.39334148	0.04425148	0.34965549	0.00993892	-0.0035259	-0.1239414	0.01331939	0.95090048	-0.6374892				
91		0.04400218	0.38042158	0.33648628	0.00335432	0.12162814	0.00121259	-0.4594642	0.4781169	-0.6374892				
92		0.40714772	0.04425148	0.36346173	-0.0101334	-0.0035259	0.12636661	0.01331939	0.00533333	-0.6374892				
93	TOTAL	9.6652117	9.6761809	11.154217	-0.004278	-0.155138	0.053354	3.6847033	21.037144	-28.04952				

ATTITUDE CONTROL SUBSYSTEM

The 1,2,3 Dimensions of component are parallel to the X,Y,Z coordinate system of the spacecraft.

Coordinates of component cg from reference frame

Coordinates of component cg from center of mass of spacecraft.

Component coordinate system

	COMPONENT	DIM 1	DIM 2	DIM 3	X	Y	Z	X'	Y'	Z'	MASS	I 11	I 22	I 33
11	ROLL TORQUE ROD #1	0.4064	0.01778	0.01778	0.762	0.0254	-1.3208	0.02122781	-0.7439005	-0.5695174	0.36	0.00495483		
12	ROLL TORQUE ROD #2	0.4064	0.01778	0.01778	0.762	1.4986	-1.3208	0.02122781	0.72929949	-0.5695174	0.36	0.00495483		
13	PITCH TORQUE ROD #1	0.01778	0.4064	0.01778	0.0254	0.762	-1.3208	-0.7153722	-0.0073005	-0.5695174	0.36		0.00495483	
14	PITCH TORQUE ROD #2	0.01778	0.4064	0.01778	1.4986	0.762	-1.3208	0.75782781	-0.0073005	-0.5695174	0.36		0.00495483	
15	YAW TORQUE ROD #1	0.01778	0.01778	0.4064	0.0508	0.762	-1.3208	-0.6899722	-0.0073005	-0.5695174	0.36			0.00495483
16	YAW TORQUE ROD #2	0.01778	0.01778	0.4064	1.4732	0.762	-1.3208	0.73242781	-0.0073005	-0.5695174	0.36			0.00495483
17	PITCH RWA	0.3505	0.1702	0.3505	1.3235	0.1105	-1.17855	0.58272781	-0.6588005	-0.4272674	9.09	0.55112048	0.1395886	0.55112048
18	ROLL RWA	0.1702	0.3505	0.3505	1.4135	0.58675	-1.29795	0.67272781	-0.1825505	-0.5466674	9.09	0.1395886	0.55112048	0.55112048
19	YAW RWA	0.3505	0.3505	0.1702	1.34875	1.34875	-1.3881	0.60797781	0.57944949	-0.6368174	9.09	0.55112048	0.55112048	0.1395886
20	SKEWED RWA*	0.3505	0.1702	0.3505	1.381	0.93725	-1.3	0.64022781	0.16794949	-0.5487174	9.09	0.326	0.326	0.326
21								-0.7407722	-0.7693005	0.75128264				
22								-0.7407722	-0.7693005	0.75128264				
23								-0.7407722	-0.7693005	0.75128264				
24								-0.7407722	-0.7693005	0.75128264				
25								-0.7407722	-0.7693005	0.75128264				
26								-0.7407722	-0.7693005	0.75128264				
27								-0.7407722	-0.7693005	0.75128264				
28								-0.7407722	-0.7693005	0.75128264				
29								-0.7407722	-0.7693005	0.75128264				
30								-0.7407722	-0.7693005	0.75128264				
31								-0.7407722	-0.7693005	0.75128264				
32								-0.7407722	-0.7693005	0.75128264				
33								-0.7407722	-0.7693005	0.75128264				
34								-0.7407722	-0.7693005	0.75128264				
35								-0.7407722	-0.7693005	0.75128264				
36								-0.7407722	-0.7693005	0.75128264				
37								-0.7407722	-0.7693005	0.75128264				
38								-0.7407722	-0.7693005	0.75128264				
39								-0.7407722	-0.7693005	0.75128264				
40								-0.7407722	-0.7693005	0.75128264				
41	FASTENERS AND WIRING				1.5155	0.762	-1.016	0.77472781	-0.0073005	-0.2647174	0.963			
42	FASTENERS AND WIRING				0.762	1.5155	-1.016	0.02122781	0.74619949	-0.2647174	0.963			
43	FASTENERS AND WIRING				0.0085	0.762	-1.016	-0.7322722	-0.0073005	-0.2647174	0.963			
44	FASTENERS AND WIRING				0.762	0.0085	-1.016	0.02122781	-0.7608005	-0.2647174	0.963			
45	TOTAL										42.372			
46														
47														
48														
49														
50														
51														
52														

	AC	AD	AE	AF	AG	AH	AI	AJ	AK	AL	AM	AN	AO	AP
53														
54														
55														
56				Spacecraft coordinate system				componets for CM calc's						
57														
58	COMPONENT	I XX	I YY	I ZZ	I XY	I XZ	I YZ	Xi*Mi	Yi*Mi	Zi*Mi				
59	ROLL TORQUE ROD #1	0.3209405	0.11692823	0.19938189	-0.0056849	-0.0043523	0.15251913	0.27432	0.009144	-0.475488				
60	ROLL TORQUE ROD #2	0.31319683	0.11692823	0.19163821	0.00557332	-0.0043523	-0.1495255	0.27432	0.539496	-0.475488				
61	PITCH TORQUE ROD #1	0.11678519	0.30595349	0.18425184	0.00188013	0.14667008	0.0014968	0.009144	0.27432	-0.475488				
62	PITCH TORQUE ROD #2	0.11678519	0.32846991	0.20676827	-0.0019917	-0.1553746	0.0014968	0.539496	0.27432	-0.475488				
63	YAW TORQUE ROD #1	0.11678519	0.28814819	0.1763562	0.00181337	0.14146241	0.0014968	0.018288	0.27432	-0.475488				
64	YAW TORQUE ROD #2	0.11678519	0.30988819	0.1980962	-0.001925	-0.1501669	0.0014968	0.530352	0.27432	-0.475488				
65	PITCH RWA	6.15579178	4.88574211	7.58305187	-3.4896635	-2.2632334	2.55868911	12.030615	1.004445	-10.71302				
66	ROLL RWA	3.15901286	7.38141839	4.96783694	-1.1163138	-3.3429233	0.90713112	12.848715	5.3335575	-11.798366				
67	YAW RWA	7.28951987	7.5974464	6.55166313	3.20233825	-3.5193828	-3.3542418	12.2601375	12.2601375	-12.617829				
68	SKEWED RWA*	3.31931673	6.78882994	4.30831706	0.97741077	-3.1933544	-0.8377053	12.55329	8.5196025	-11.817				
69		0	0	0	0	0	0	0	0	0				
70		0	0	0	0	0	0	0	0	0				
71		0	0	0	0	0	0	0	0	0				
72		0	0	0	0	0	0	0	0	0				
73		0	0	0	0	0	0	0	0	0				
74		0	0	0	0	0	0	0	0	0				
75		0	0	0	0	0	0	0	0	0				
76		0	0	0	0	0	0	0	0	0				
77		0	0	0	0	0	0	0	0	0				
78		0	0	0	0	0	0	0	0	0				
79		0	0	0	0	0	0	0	0	0				
80		0	0	0	0	0	0	0	0	0				
81		0	0	0	0	0	0	0	0	0				
82		0	0	0	0	0	0	0	0	0				
83		0	0	0	0	0	0	0	0	0				
84		0	0	0	0	0	0	0	0	0				
85		0	0	0	0	0	0	0	0	0				
86		0	0	0	0	0	0	0	0	0				
87		0	0	0	0	0	0	0	0	0				
88		0	0	0	0	0	0	0	0	0				
89		0.06753382	0.64547816	0.57804699	-0.0054466	-0.1974958	0.00186107	1.4594265	0.733806	-0.978408				
90		0.60369407	0.06791644	0.53664553	0.0152541	-0.0054115	-0.1902233	0.733806	1.4594265	-0.978408				
91		0.06753382	0.58386481	0.51643365	0.00514816	0.18667289	0.00186107	0.0081855	0.733806	-0.978408				
92		0.62488366	0.06791644	0.55783511	-0.0155526	-0.0054115	0.19394541	0.733806	0.0081855	-0.978408				
93	TOTAL	22.388565	29.484929	26.756323	-0.42716	-12.36665	-0.709702	54.273902	31.698887	-53.71277				

T T & C SUBSYSTEM

The 1,2,3 Dimensions of component are parallel to the X,Y,Z coordinate system of the spacecraft.

Coordinates of component cg from reference frame

Coordinates of component cg from center of mass of spacecraft.

Component coordinate system

	AQ	AR	AS	AT	AU	AV	AW	AX	AY	AZ	BA	BB	BC	BD
10	COMPONENT	DIM 1	DIM 2	DIM 3	X	Y	Z	X'	Y'	Z'	MASS	I 11	I 22	I 33
11	DOWNLINK TRANSMITTER #1	0.076	0.173	0.167	0.6355	0.03	-1.18	-0.1052722	-0.7393005	-0.4287174	3	0.0144545	0.00841625	0.00892625
12	DOWNLINK TRANSMITTER #2	0.076	0.173	0.167	0.8885	0.03	-1.18	0.14772781	-0.7393005	-0.4287174	3	0.0144545	0.00841625	0.00892625
13	W/B TRANSMITTER #1	0.228	0.114	0.228	0.6185	0.114	-1.159	-0.1222722	-0.6553005	-0.4077174	19	0.102885	0.164616	0.102885
14	W/B TRANSMITTER #2	0.228	0.114	0.228	0.9055	0.114	-1.159	0.16472781	-0.6553005	-0.4077174	19	0.102885	0.164616	0.102885
15	WBDL ANTENNA				0.1	1.5	0.34	-0.6407722	0.73069949	1.09128264	15			
16	ANTENNA ACTUATOR				0.1	1.5	0.34	-0.6407722	0.73069949	1.09128264	4.5			
17	OMNI XMIT ANTENNA #1							-0.7407722	-0.7693005	0.75128264	0.95			
18	OMNI XMIT ANTENNA #2							-0.7407722	-0.7693005	0.75128264	0.95			
19								-0.7407722	-0.7693005	0.75128264				
20								-0.7407722	-0.7693005	0.75128264				
21	OMNI RCV ANTENNA #1							-0.7407722	-0.7693005	0.75128264	0.75			
22	OMNI RCV ANTENNA #2							-0.7407722	-0.7693005	0.75128264	0.75			
23	HYBRID DIVIDER #1				0.4	0.4	-0.853	-0.3407722	-0.3693005	-0.1017174	0.125			
24	HYBRID DIVIDER #2				1.1	1.1	-0.853	0.35922781	0.33069949	-0.1017174	0.125			
25	RECEIVER/DEMOD #1				0.4	1.1	-0.853	-0.3407722	0.33069949	-0.1017174	3.4			
26	RECEIVER/DEMOD #2				0.4	1.1	-0.853	-0.3407722	0.33069949	-0.1017174	3.4			
27								-0.7407722	-0.7693005	0.75128264				
28	ASC	0.216	0.241	0.355	0.8825	1.416	-1.09	0.14172781	0.64669949	-0.3387174	19.9	0.30530912	0.28636266	0.17368886
29								-0.7407722	-0.7693005	0.75128264				
30	RIU	0.231	0.249	0.244	0.6375	1.4085	-1.1513	-0.1032722	0.63919949	-0.4000174	29.9	0.30282969	0.28130169	0.28744365
31								-0.7407722	-0.7693005	0.75128264				
32	TDU	0.19	0.356	0.211	0.762	0.095	-1.0008	0.02122781	-0.6743005	-0.2495174	4.05	0.05779924	0.02720959	0.05495715
33	UPLINK PROCESSOR #1	0.117	0.099	0.142	0.9155	0.071	-0.9958	0.17472781	-0.6983005	-0.2445174	1.8	0.00449475	0.00507795	0.0035235
34	UPLINK PROCESSOR #2	0.117	0.099	0.142	1.0325	0.071	-0.9958	0.29172781	-0.6983005	-0.2445174	1.8	0.00449475	0.00507795	0.0035235
35	DOWNLINK PROCESSOR #1	0.117	0.099	0.142	0.6085	0.071	-0.9958	-0.1322722	-0.6983005	-0.2445174	1.8	0.00449475	0.00507795	0.0035235
36	DOWNLINK PROCESSOR #2	0.117	0.099	0.142	0.4915	0.071	-0.9958	-0.2492722	-0.6983005	-0.2445174	1.8	0.00449475	0.00507795	0.0035235
37								-0.7407722	-0.7693005	0.75128264				
38								-0.7407722	-0.7693005	0.75128264				
39								-0.7407722	-0.7693005	0.75128264				
40								-0.7407722	-0.7693005	0.75128264				
41	FASTENERS AND WIRING				1.5155	0.762	-1.016	0.77472781	-0.0073005	-0.2647174	3.375			
42	FASTENERS AND WIRING				0.762	1.5155	-1.016	0.02122781	0.74619949	-0.2647174	3.375			
43	FASTENERS AND WIRING				0.0085	0.762	-1.016	-0.7322722	-0.0073005	-0.2647174	3.375			
44	FASTENERS AND WIRING				0.762	0.0085	-1.016	0.02122781	-0.7608005	-0.2647174	3.375			
45	TOTAL										148.5			
46														
47														
48														
49														
50														
51														
52														

	AQ	AR	AS	AT	AU	AV	AW	AX	AY	AZ	BA	BB	BC	BD
53														
54														
55														
56				Spacecraft coordinate system					componets for CM calc's					
57														
58	COMPONENT	I XX	I YY	I ZZ	I XY	I XZ	I YZ	Xi*Mi	Yi*Mi	Zi*Mi				
59		2.20554593	0.59305867	1.68186866	0.23348335	0.13539604	0.95085288	1.9065	0.09	-3.54				
60		2.20554593	0.62528249	1.71409248	-0.3276457	-0.1900004	0.95085288	2.6655	0.09	-3.54				
61		11.4202767	3.60711069	8.54590056	1.52237548	0.94719736	5.07637041	11.7515	2.166	-22.021				
62		11.4202767	3.83862122	8.7774111	-2.0509782	-1.2760854	5.07637041	17.2045	2.166	-22.021				
63		25.8722934	24.022302	14.1676612	-7.0231787	-10.488953	11.9609951	1.5	22.5	5.1				
64		7.76168801	7.20669061	4.25029836	-2.1069536	-3.146686	3.58829854	0.45	6.75	1.53				
65		1.09843643	1.05751059	1.08353836	0.5413826	-0.5287028	-0.549064	0	0	0				
66		1.09843643	1.05751059	1.08353836	0.5413826	-0.5287028	-0.549064	0	0	0				
67		0	0	0	0	0	0	0	0	0				
68		0	0	0	0	0	0	0	0	0				
69		0.86718666	0.83487678	0.85542502	0.42740731	-0.417397	-0.4334716	0	0	0				
70		0.86718666	0.83487678	0.85542502	0.42740731	-0.417397	-0.4334716	0	0	0				
71		0.01834116	0.01580901	0.03156357	0.01573092	0.00433281	0.00469553	0.05	0.05	-0.106625				
72		0.01496357	0.01742388	0.02980085	0.01484956	-0.0045675	-0.0042047	0.1375	0.1375	-0.106625				
73		0.40700916	0.43000515	0.76665865	-0.3831568	0.11785232	-0.1143688	1.36	3.74	-2.9002				
74		0.40700916	0.43000515	0.76665865	-0.3831568	0.11785232	-0.1143688	1.36	3.74	-2.9002				
75		0	0	0	0	0	0	0	0	0				
76		10.9110078	2.96920546	8.89599834	1.82394058	-0.9553128	-4.359062	17.56175	28.1784	-21.691				
77		0	0	0	0	0	0	0	0	0				
78		17.3036671	5.3846047	12.8227537	-1.9737447	1.23518894	-7.6451577	19.06125	42.11415	-34.42387				
79		0	0	0	0	0	0	0	0	0				
80		2.15140658	0.28118319	1.89824091	-0.0579714	-0.0214517	0.6814112	3.0861	0.38475	-4.05324				
81		0.98983695	0.16765133	0.93619963	-0.2196225	-0.0769032	0.30734387	1.6479	0.1278	-1.79244				
82		0.98983695	0.26588689	1.03443518	-0.3666846	-0.1283985	0.30734387	1.8585	0.1278	-1.79244				
83		0.98983695	0.14419035	0.91273865	0.16625832	0.05821712	0.30734387	1.0953	0.1278	-1.79244				
84		0.98983695	0.2245436	0.99309189	0.31332041	0.10971248	0.30734387	0.8847	0.1278	-1.79244				
85		0	0	0	0	0	0	0	0	0				
86		0	0	0	0	0	0	0	0	0				
87		0	0	0	0	0	0	0	0	0				
88		0	0	0	0	0	0	0	0	0				
89		0.23668395	2.26218982	2.02586563	-0.0190887	-0.6921582	0.00652243	5.1148125	2.57175	-3.429				
90		2.11575026	0.23802491	1.88076703	0.05346062	-0.0189654	-0.6666704	2.57175	5.1148125	-3.429				
91		0.23668395	2.04625519	1.809931	0.01804261	0.65422741	0.00652243	0.0286875	2.57175	-3.429				
92		2.19001282	0.23802491	1.9550296	-0.0545067	-0.0189654	0.67971521	2.57175	0.0286875	-3.429				
93	TOTAL	104.76876	58.792844	79.774892	-8.867647	-15.53067	15.343079	93.868	122.905	-131.5595				

ELECTRICAL POWER SUBSYSTEM

The 1,2,3 Dimensions of component are parallel to the X,Y,Z coordinate system of the spacecraft.

Coordinates of component cg from reference frame

Coordinates of component cg from center of mass of spacecraft.

Component coordinate system

COMPONENT	DIM 1	DIM 2	DIM 3	X	Y	Z	X'	Y'	Z'	MASS	I 11	I 22	I 33
							-0.7407722	-0.7693005	0.75128264				
							-0.7407722	-0.7693005	0.75128264				
WIRING				0.762	0.762	-1.499	0.02122781	-0.0073005	-0.7477174	15			
SHUNT				0.3	0.3	-1.45	-0.4407722	-0.4693005	-0.6987174	3			
CHARGE CONTROL							-0.7407722	-0.7693005	0.75128264	0.6			
DISCHARGE CONTROL							-0.7407722	-0.7693005	0.75128264	6			
							-0.7407722	-0.7693005	0.75128264				
BATTERY #1	0.25	0.26	0.21	0.175	0.637	-1.1683	-0.5657722	-0.1323005	-0.4170174	10.9			
BATTERY #2	0.25	0.26	0.21	1.348	0.637	-1.1683	0.60722781	-0.1323005	-0.4170174	10.9			
BATTERY #3	0.25	0.26	0.21	1.348	0.887	-1.1683	0.60722781	0.11769949	-0.4170174	10.9			
BATTERY #4	0.25	0.26	0.21	0.175	0.887	-1.1683	-0.5657722	0.11769949	-0.4170174	10.9			
							-0.7407722	-0.7693005	0.75128264				
							-0.7407722	-0.7693005	0.75128264				
SOLAR ARRAY #1	0.381	1.4732	0.013	2.303	0.762	-1.535	1.56222781	-0.0073005	-0.7837174	5			
SOLAR ARRAY #2	1.4732	0.381	0.013	0.762	2.303	-1.535	0.02122781	1.53369949	-0.7837174	5			
SOLAR ARRAY #3	0.381	1.4732	0.013	-0.19	0.762	-1.535	-0.9307722	-0.0073005	-0.7837174	5			
SOLAR ARRAY #4	1.4732	0.381	0.013	0.762	-0.19	-1.535	0.02122781	-0.9593005	-0.7837174	5			
							-0.7407722	-0.7693005	0.75128264				
							-0.7407722	-0.7693005	0.75128264				
							-0.7407722	-0.7693005	0.75128264				
							-0.7407722	-0.7693005	0.75128264				
							-0.7407722	-0.7693005	0.75128264				
							-0.7407722	-0.7693005	0.75128264				
							-0.7407722	-0.7693005	0.75128264				
							-0.7407722	-0.7693005	0.75128264				
							-0.7407722	-0.7693005	0.75128264				
							-0.7407722	-0.7693005	0.75128264				
							-0.7407722	-0.7693005	0.75128264				
							-0.7407722	-0.7693005	0.75128264				
							-0.7407722	-0.7693005	0.75128264				
							-0.7407722	-0.7693005	0.75128264				
FASTENERS AND WIRING				1.5155	0.762	-1.016	0.77472781	-0.0073005	-0.2647174	2.205			
FASTENERS AND WIRING				0.762	1.5155	-1.016	0.02122781	0.74619949	-0.2647174	2.205			
FASTENERS AND WIRING				0.0085	0.762	-1.016	-0.7322722	-0.0073005	-0.2647174	2.205			
FASTENERS AND WIRING				0.762	0.0085	-1.016	0.02122781	-0.7608005	-0.2647174	2.205			
TOTAL										97.02			

	BE	BF	BG	BH	BI	BJ	BK	BL	BM	BN	BO	BP	BQ	BR
53														
54														
55														
56				Spacecraft coordinate system					componets for CM calc's					
57														
58	COMPONENT	I XX	I YY	I ZZ	I XY	I XZ	I YZ	X(*MI	Y(*MI	Z(*MI				
59		0	0	0	0	0	0	0	0	0				
60		0	0	0	0	0	0	0	0	0				
61		8.38701815	8.39297799	0.00755876	-0.0023246	-0.2380861	0.08188072	11.43	11.43	-22.485				
62		2.12534673	2.0474582	1.24356925	0.62056383	0.92392553	0.98372523	0.9	0.9	-4.35				
63		0.69374933	0.66790142	0.68434002	0.34192585	-0.3339176	-0.3467773	0	0	0				
64		6.93749327	6.67901425	6.8434002	3.4192585	-3.3391757	-3.4677727	0	0	0				
65		0	0	0	0	0	0	0	0	0				
66		2.08633521	5.38461791	3.67985734	0.81588621	2.57171136	0.60137052	1.9075	6.9433	-12.73447				
67		2.08633521	5.91465712	4.20989655	-0.8756684	-2.7601475	0.60137052	14.6932	6.9433	-12.73447				
68		2.04654745	5.91465712	4.1701088	0.77902743	-2.7601475	-0.5350018	14.6932	9.6683	-12.73447				
69		2.04654745	5.38461791	3.64006958	-0.725843	2.57171136	-0.5350018	1.9075	9.6683	-12.73447				
70		0	0	0	0	0	0	0	0	0				
71		0	0	0	0	0	0	0	0	0				
72		3.07133097	15.2738432	12.2030452	-0.0570253	-6.1217253	0.02860766	11.515	3.81	-7.675				
73		14.8322352	3.07331758	11.7634238	0.16278544	-0.083183	-6.0099346	3.81	11.515	-7.675				
74		3.07133097	7.40274879	4.3319508	0.03397554	3.64731159	0.02860766	-0.95	3.81	-7.675				
75		7.67235178	3.07331758	4.6035404	-0.1018193	-0.083183	3.75910228	3.81	-0.95	-7.675				
76		0	0	0	0	0	0	0	0	0				
77		0	0	0	0	0	0	0	0	0				
78		0	0	0	0	0	0	0	0	0				
79		0	0	0	0	0	0	0	0	0				
80		0	0	0	0	0	0	0	0	0				
81		0	0	0	0	0	0	0	0	0				
82		0	0	0	0	0	0	0	0	0				
83		0	0	0	0	0	0	0	0	0				
84		0	0	0	0	0	0	0	0	0				
85		0	0	0	0	0	0	0	0	0				
86		0	0	0	0	0	0	0	0	0				
87		0	0	0	0	0	0	0	0	0				
88		0	0	0	0	0	0	0	0	0				
89		0.15463351	1.47796401	1.32356554	-0.0124713	-0.45221	0.00426132	3.3416775	1.68021	-2.24028				
90		1.38229017	0.15550961	1.22876779	0.03492761	-0.0123907	-0.435558	1.68021	3.3416775	-2.24028				
91		0.15463351	1.33688672	1.18248825	0.01178784	0.42742857	0.00426132	0.0187425	1.68021	-2.24028				
92		1.43080838	0.15550961	1.277286	-0.035611	-0.0123907	0.4440806	1.68021	0.0187425	-2.24028				
93	TOTAL	58.178987	72.334999	62.392868	4.4093755	-6.054469	-4.792778	70.43724	70.45904	-117.434				

OTHER SPACECRAFT COMPONENTS

The 1,2,3 Dimensions of component are parallel to the X,Y,Z coordinate system of the spacecraft.

Coordinates of component cg from reference frame

Coordinates of component cg from center of mass of spacecraft.

Component coordinate system

	BS	BT	BU	BV	BW	BX	BY	BZ	CA	CB	CC	CD	CE	CF
10	COMPONENT	DIM 1	DIM 2	DIM 3	X	Y	Z	X'	Y'	Z'	MASS	I 11	I 22	I 33
11	THRUSTER #1	0.1	0.2	0.1	0.9398	0	-0.508	0.19902781	-0.7693005	0.24328264	0.31			
12	THRUSTER #2	0.1	0.2	0.1	0.5842	0	-0.508	-0.1565722	-0.7693005	0.24328264	0.31			
13	THRUSTER #3	0.1	0.2	0.1	0.9398	0	-1.106	0.19902781	-0.7693005	-0.3547174	0.31			
14	THRUSTER #4	0.1	0.2	0.1	0.5842	0	-1.106	-0.1565722	-0.7693005	-0.3547174	0.31			
15	THRUSTER #5	0.1	0.2	0.1	0.9398	1.524	-0.508	0.19902781	0.75469949	0.24328264	0.31			
16	THRUSTER #6	0.1	0.2	0.1	0.5842	1.524	-0.508	-0.1565722	0.75469949	0.24328264	0.31			
17	THRUSTER #7	0.1	0.2	0.1	0.9398	1.524	-1.106	0.19902781	0.75469949	-0.3547174	0.31			
18	THRUSTER #8	0.1	0.2	0.1	0.5842	1.524	-1.106	-0.1565722	0.75469949	-0.3547174	0.31			
19	THRUSTER #9	0.1	0.2	0.1	0	0.762	-0.762	-0.7407722	-0.0073005	-0.0107174	0.31			
20	TANK #1	0.195	0.195	0.195	0.762	0.762	-1.329	0.02122781	-0.0073005	-0.5777174	18.7			
21								-0.7407722	-0.7693005	0.75128264				
22								-0.7407722	-0.7693005	0.75128264				
23	PAYLOAD	1.524	1.524	0.508	0.762	0.762	-0.254	0.02122781	-0.0073005	0.49728264	362	77.8493067	77.8493067	140.128752
24								-0.7407722	-0.7693005	0.75128264				
25								-0.7407722	-0.7693005	0.75128264				
26								-0.7407722	-0.7693005	0.75128264				
27								-0.7407722	-0.7693005	0.75128264				
28								-0.7407722	-0.7693005	0.75128264				
29								-0.7407722	-0.7693005	0.75128264				
30								-0.7407722	-0.7693005	0.75128264				
31								-0.7407722	-0.7693005	0.75128264				
32								-0.7407722	-0.7693005	0.75128264				
33								-0.7407722	-0.7693005	0.75128264				
34								-0.7407722	-0.7693005	0.75128264				
35								-0.7407722	-0.7693005	0.75128264				
36								-0.7407722	-0.7693005	0.75128264				
37								-0.7407722	-0.7693005	0.75128264				
38								-0.7407722	-0.7693005	0.75128264				
39								-0.7407722	-0.7693005	0.75128264				
40								-0.7407722	-0.7693005	0.75128264				
41	FASTENERS AND WIRING				1.5155	0.762	-1.016	0.77472781	-0.0073005	-0.2647174	9.58725			
42	FASTENERS AND WIRING				0.762	1.5155	-1.016	0.02122781	0.74619949	-0.2647174	9.58725			
43	FASTENERS AND WIRING				0.0085	0.762	-1.016	-0.7322722	-0.0073005	-0.2647174	9.58725			
44	FASTENERS AND WIRING				0.762	0.0085	-1.016	0.02122781	-0.7608005	-0.2647174	9.58725			
45	TOTAL										421.839			

	BS	BT	BU	BV	BW	BX	BY	BZ	CA	CB	CC	CD	CE	CF
53														
54														
55														
56				Spacecraft coordinate system					componets for CM calc's					
57														
58	COMPONENT	I XX	I YY	I ZZ	I XY	I XZ	I YZ	X1*Mi	Yi*Mi	Zi*Mi				
59		0.20181301	0.03062754	0.19574495	-0.0474648	0.0150102	-0.0580188	0.291338	0	-0.15748				
60		0.20181301	0.0259474	0.19106482	0.03733983	-0.0118083	-0.0580188	0.181102	0	-0.15748				
61		0.22247078	0.05128531	0.19574495	-0.0474648	-0.0218856	0.08459412	0.291338	0	-0.34286				
62		0.22247078	0.04660517	0.19106482	0.03733983	0.01721705	0.08459412	0.181102	0	-0.34286				
63		0.19491491	0.03062754	0.18884685	0.04656392	0.0150102	0.05691764	0.291338	0.47244	-0.15748				
64		0.19491491	0.0259474	0.18416671	-0.0366311	-0.0118083	0.05691764	0.181102	0.47244	-0.15748				
65		0.21557268	0.05128531	0.18884685	0.04656392	-0.0218856	-0.0829886	0.291338	0.47244	-0.34286				
66		0.21557268	0.04660517	0.18416671	-0.0366311	0.01721705	-0.0829886	0.181102	0.47244	-0.34286				
67		5.2129E-05	0.17014607	0.17012699	0.00167648	0.00246113	2.4255E-05	0	0.23622	-0.23622				
68		6.24225901	6.24968894	0.00942326	-0.002898	-0.2293307	0.07886966	14.2494	14.2494	-24.8523				
69		0	0	0	0	0	0	0	0	0				
70		0	0	0	0	0	0	0	0	0				
71		167.38759	167.531421	140.31117	-0.0561005	3.82135284	-1.3142101	275.844	275.844	-91.948				
72		0	0	0	0	0	0	0	0	0				
73		0	0	0	0	0	0	0	0	0				
74		0	0	0	0	0	0	0	0	0				
75		0	0	0	0	0	0	0	0	0				
76		0	0	0	0	0	0	0	0	0				
77		0	0	0	0	0	0	0	0	0				
78		0	0	0	0	0	0	0	0	0				
79		0	0	0	0	0	0	0	0	0				
80		0	0	0	0	0	0	0	0	0				
81		0	0	0	0	0	0	0	0	0				
82		0	0	0	0	0	0	0	0	0				
83		0	0	0	0	0	0	0	0	0				
84		0	0	0	0	0	0	0	0	0				
85		0	0	0	0	0	0	0	0	0				
86		0	0	0	0	0	0	0	0	0				
87		0	0	0	0	0	0	0	0	0				
88		0	0	0	0	0	0	0	0	0				
89		0.6723402	6.42612721	5.75480896	-0.0542246	-1.9661906	0.01852804	14.5294774	7.3054845	-9.740646				
90		6.01014123	0.67614943	5.34263221	0.1518638	-0.0538743	-1.8937883	7.3054845	14.5294774	-9.740646				
91		0.6723402	5.81272891	5.14141066	0.05125303	1.85844199	0.01852804	0.08149163	7.3054845	-9.740646				
92		6.22109643	0.67614943	5.55358742	-0.1548353	-0.0538743	1.93084434	7.3054845	0.08149163	-9.740646				
93	TOTAL	188.87536	187.85134	163.80281	-0.063649	3.3760527	-1.160195	321.2051	321.44132	-158.0005				

	CG	CH	CI	CJ	CK	CL	CM	CN	CO	CP	CQ	CR	CS	CT
1														
2														
3					SPACECRAFT TOTALS									
4														
5														
6														
7		The 1,2,3 Dimensions of component are parallel			Coordinates of component cg			Coordinates of component cg from				Component coordinate system		
8		to the X,Y,Z coordinate system of the spacecraft.			from reference frame			center of mass of spacecraft.						
9														
10	COMPONENT	DIM 1	DIM 2	DIM 3	X	Y	Z	X'	Y'	Z'	MASS	I 11	I 22	I 33
11	STRUCTURAL										174.108			
12	THERMAL										27.6078			
13	ACS										42.372			
14	TT&C										148.5			
15	ELECTRICAL										97.02			
16	OTHER										421.839			
17														
18														
19														
20														
21														
22														
23														
24														
25														
26														
27														
28														
29														
30														
31														
32														
33														
34														
35														
36														
37														
38														
39														
40														
41														
42														
43														
44														
45	TOTAL										911.4468			
46														
47														
48														
49														
50														
51														
52														

	CG	CH	CI	CJ	CK	CL	CM	CN	CO	CP	CQ	CR	CS	CT
53														
54														
55														
56				Spacecraft coordinate system					componets for CM calc's					
57														
58	COMPONENT	I XX	I YY	I ZZ	I XY	I XZ	I YZ	Xi*Mi	Yi*Mi	Zi*Mi				
59	STRUCTURAL	92.7225714	92.7648744	88.6186095	-0.6941141	-1.1285169	0.22054664	0	0	0				
60	THERMAL	9.66521169	9.67618091	11.1542172	-0.0042785	-0.1551383	0.05335402	0	0	0				
61	ACS	22.3885647	29.4849288	26.7563227	-0.4271601	-12.366653	-0.7097018	0	0	0				
62	TT&C	104.768756	58.792844	79.7748924	-8.8676472	-15.530671	15.3430789	0	0	0				
63	ELECTRICAL	58.1789872	72.334999	62.3928683	4.40937546	-6.0544685	-4.7927782	0	0	0				
64	OTHER	188.875362	187.851342	163.802806	-0.0636495	3.3760523	-1.1601953	0	0	0				
65								0	0	0				
66								0	0	0				
67								0	0	0				
68								0	0	0				
69								0	0	0				
70								0	0	0				
71								0	0	0				
72								0	0	0				
73								0	0	0				
74								0	0	0				
75								0	0	0				
76								0	0	0				
77								0	0	0				
78								0	0	0				
79								0	0	0				
80								0	0	0				
81								0	0	0				
82								0	0	0				
83								0	0	0				
84								0	0	0				
85								0	0	0				
86								0	0	0				
87								0	0	0				
88								0	0	0				
89								0	0	0				
90								0	0	0				
91								0	0	0				
92								0	0	0				
93	TOTAL	476.59945	450.90517	432.49972	-5.647474	-31.8594	8.9543042	0	0	0				

	CU	CV	CW	CX	CY
1					
2					
3					
4		CENTER OF MASS CALCULATIONS			
5					
6		relative to reference frame at corner of payload			
7					
8					
9					
10		X BAR	Y BAR	Z BAR	
11		0.74077219	0.76930051	-0.7512826	
12					
13					
14					
15					
16					
17					
18					
19					
20					
21					
22					
23					
24					
25					
26					
27					
28					
29					
30					
31					
32					
33					
34					
35					
36					
37					
38					
39					
40					
41					
42					
43					
44					
45					
46					
47					
48					
49					
50					
51					
52					

	CU	CV	CW	CX	CY
53					
54					
55					
56					
57					
58					
59					
60					
61					
62					
63					
64					
65					
66					
67					
68					
69					
70					
71					
72					
73					
74					
75					
76					
77					
78					
79					
80					
81					
82					
83					
84					
85					
86					
87					
88					
89					
90					
91					
92					
93					

APPENDIX C - ORBITAL ANALYSIS

I. ESTIMATION OF ALTITUDE LOSS DUE TO DRAG USING MANUAL CALCULATIONS

A back of the envelope prediction of the orbital decay encountered by drag forces is computed below. A simple atmospheric model based on an exponential atmosphere with a reference altitude and scale height is used and shown

$$\beta = .0476 \text{ km}$$

$$r_0 = 140 \text{ km}$$

$$\rho_0 = 3.0 \times 10^{-6} \text{ kg/m}^3$$

$$\rho = \rho_0 e^{-\beta (r - r_0)} \qquad \text{(C.1)}$$

Using the computed density of 7.0 x 10^{-14} kg/m^3 for 509.3 km orbital altitude, the decay of the orbit can be estimated using Equation C.2.

$$\Delta r = -2\left[\frac{C_D A}{m}\right] a^2 (1 + e) \int_0^{2\pi} \rho \, dv \qquad \text{per orbit} \qquad \text{(C.2)}$$

$$\Delta r = 1.657 \text{ km/year}$$

Using a coefficient of drag equal to 2.4 and an effective area of 3.0 m^2 the orbit will decay 1.657 km per year. Over a three year lifetime this will exceed the allowable altitude perturbation.

II. ESTIMATION OF ALTITUDE LOSS DUE TO DRAG USING ASAP PROGRAM

The ASAP program also computed the orbital decay caused by the atmospheric drag. The atmospheric model used within the program is the 1976 Standard Atmospheric model. The program was executed with all of the internal models, except drag, turned off to ensure

all the effects seen were due only to the atmosphere. The estimated altitude decay is approximated to be 4.5 km per year, indicating a need to reboost the satellite at six month intervals to maintain the orbit within defined specifications. Selected outputs from the ASAP program are include below and are summarized in Table C.2

Table C.2. ASAP Orbital Perturbations from Drag

Geocentric Radius (km)	Change in Altitude (km)	Time from epoch (days)
6889.00	0.00	0
6888.15	0.85	90
6887.38	1.62	180

A coefficient of drag on the satellite was estimated to be 2.4, slightly more than the recommended 2.0 to 2.2, this was to ensure that the perturbation was of a maximum value. The effective area used by the program was 3.0 m^2, the average value of the minimum planform area of 2.25 m^2 and the maximum value of 3.75 m^2. An exponential extrapolation of the data yields a decay in the orbit of approximately 4.5 km per year. This decay clearly exceeds the allowable 1.852 km for the lifetime of the satellite. Because the value for altitude decay from the ASAP program is larger than the hand calculation value, the ASAP value will be used in on orbit fuel consumption calculations.

```
   PRINTING INFORMATION AT APOAPSIS OF REV #      1

       0 DAYS     0.395186 HOURS FROM EPOCH
   CARTESIAN COORD X, Y, Z, XD, YD, ZD
5.31690111300030E+00  2.35762252690094E+03  6.47302144898769E+03 -7.60098081125
   EQUINOCTIAL ELEMENTS A, H, K, P, Q, MEAN LONG
6.87885527846071E+03 -1.47580129893126E-03 -1.56895096830383E-06 -5.23613596427
   CLASSICAL ELEMENTS E, I, NODE, W, MA, TA, EA, TRUE LONG, ECC LONG, ARG OF LA
1.47580213292105E-03  6.99871927975374E+01  3.59957144149593E+02  2.69981943697
1.79988502260349E+02  1.79988485279421E+02  8.99275901071035E+01  8.99275731261
   OTHER PARAMETERS R, V, ENODE, LONG, LAT, HOUR ANGLE/ ALT, ELLIPSOIDAL ALT, P
6.88900710754771E+03  7.60098495404533E+00  3.09013129113831E+02  3.89267719651
5.10867107547710E+02  5.29758681020809E+02  4.90563449168706E+02  1.57718534913

   PRINTING INFORMATION AT APOAPSIS OF REV #  2268

      89 DAYS     5.237573 HOURS FROM EPOCH
   CARTESIAN COORD X, Y, Z, XD, YD, ZD
-1.86428788340464E+03 -1.44274574639411E+03  6.47221655213690E+03  4.64607355879
   EQUINOCTIAL ELEMENTS A, H, K, P, Q, MEAN LONG
6.87804182773981E+03  8.98520115784012E-04  1.16377556745873E-03  5.54119594165
   CLASSICAL ELEMENTS E, I, NODE, W, MA, TA, EA, TRUE LONG, ECC LONG, ARG OF LA
1.47027615429293E-03  6.99870938732084E+01  1.27668977690547E+02  2.70001796514
1.80021063889814E+02  1.80021094882349E+02  2.17691838095118E+02  2.17691869087
   OTHER PARAMETERS R, V, ENODE, LONG, LAT, HOUR ANGLE/ ALT, ELLIPSOIDAL ALT, P
6.88815444794196E+03  7.60147642265765E+00  2.76170803513895E+02  6.23760150029
5.10014467941964E+02  5.28905999770507E+02  4.89789206852251E+02  1.57690559518

   PRINTING INFORMATION AT APOAPSIS OF REV #  4542

     180 DAYS     1.214861 HOURS FROM EPOCH
   CARTESIAN COORD X, Y, Z, XD, YD, ZD
2.21644190656460E+03 -8.02884466447513E+02  6.47138192919904E+03  2.48450313443
   EQUINOCTIAL ELEMENTS A, H, K, P, Q, MEAN LONG
6.87720372364524E+03  4.89581373271614E-04 -1.39658508894820E-03 -6.62835000483
   CLASSICAL ELEMENTS E, I, NODE, W, MA, TA, EA, TRUE LONG, ECC LONG, ARG OF LA
1.47991210270305E-03  6.99869655709817E+01  2.51034228144984E+02  2.69647347324
1.80028649695619E+02  1.80028692126068E+02  3.40710225165420E+02  3.40710267595
   OTHER PARAMETERS R, V, ENODE, LONG, LAT, HOUR ANGLE/ ALT, ELLIPSOIDAL ALT, P
6.88738137919248E+03  7.60186634200863E+00  1.03512152418559E+01  9.94045616761
5.09241379392481E+02  5.28132302108056E+02  4.88886066621866E+02  1.57661737999
```

III. EFFECTS ON INCLINATION FROM EARTH'S OBLATENESS

As mentioned earlier there is no cumulative effect on the inclination of the orbit. The Earth's equatorial bulge does exert an influence on the satellite, but this is small in nature and has a period equal to the orbital period of the satellite. This effect can be shown by relating two equations which evaluate the rotation of the longitude of the ascending node. Equation C.3 relates $d\Omega/dt$ with the force the Earth's bulge exerts and Equation C.4 relates $d\Omega/dt$ with other orbital parameters.

$$\frac{d\Omega}{dt} = \frac{r\, F_{J2} \sin(u)}{n\, a^2 \sqrt{(1 - e^2)} \sin(i)} \tag{C.3}$$

$$\frac{d\Omega}{dt} = \frac{-3\pi J_2 \left[\frac{R}{r}\right]^2 \cos(i)}{\sqrt{\frac{\mu}{r}}} \tag{C.4}$$

These two equations are equated and an expression for the J2 force is found this expression is then substitute into Equation C.5 and an expression for di/dt can be found based only on orbital parameters (Equation C.6).

$$\frac{di}{dt} = \frac{r\, F_{J2} \cos(u)}{n\, a^2 \sqrt{(1 - e^2)}} \tag{C.5}$$

$$\frac{di}{dt} = \frac{-3\pi J_2 \cos(i) \sin(i)}{\tan(u) \sqrt{\mu}} \left[\frac{R^2}{r^{1.5}}\right] \tag{C.6}$$

It now can easily be shown that di/dt varies with the parameter u (the argument of latitude). The effect is periodic with a period equal to the orbital period and singularities at u=0° and 180°.

IV. COMMENTS ON PROGRAMS USED

1. ASAP

This program was useful in the drag estimations. The input file was modified for our particular satellite and the requested data displayed on the screen in a scrolling fashion. The display of the data was very hard to cope with and modification should be made to have selected data dump into an output file for retrieval and manipulation.

2. Orbital Workbench (Version 1.01 Cygnus Engineering)

This program was useful in modeling the launch vehicle sequence (discussed later) and general orbit and ground track manipulation. The input sequence to execute a problem requires the entry and exit of about 8 submenus making it hard to keep track of what has been changed. The output data is displayed in a graphical format, which is very useful, and into a data file for further manipulation. The drag of the satellite was not modeled with this program because the time overhead associated with the graphical display slowed down the computation enough to make it impractical.

This MathCAD document calculates the effects of the sun and the moon on the inclination of a satellite. The first portion sets up necessary constants and then is followed by calculations for the sun and then the moon.

$$is := \frac{23.5}{180}\cdot\pi \qquad i := \frac{70}{180}\cdot\pi \qquad \Omega := 0, .1 \ldots 6.3$$

$$\mu := 1.32686\cdot 10^{11} \qquad k := 31536000\cdot\frac{180}{\pi}$$

$$h := 6887\cdot 7.610 \qquad k = 1.807\cdot 10^{9}$$

$$r := 6887$$

$$rs := 1.49592\cdot 10^{8}$$

$$rl := 3.844\cdot 10^{5}$$

Di/dt for sun influence

$$didt(\Omega) := \frac{3}{4}\cdot\frac{\mu}{h}\cdot\left(\frac{r}{rs}\right)^{2}\cdot\left[\sin(\Omega)\cdot\cos(\Omega)\cdot\sin(i)\cdot\sin(is)^{2} + \sin(\Omega)\cdot\cos(i)\cdot\sin(is)\cdot\cos(is)\right]$$

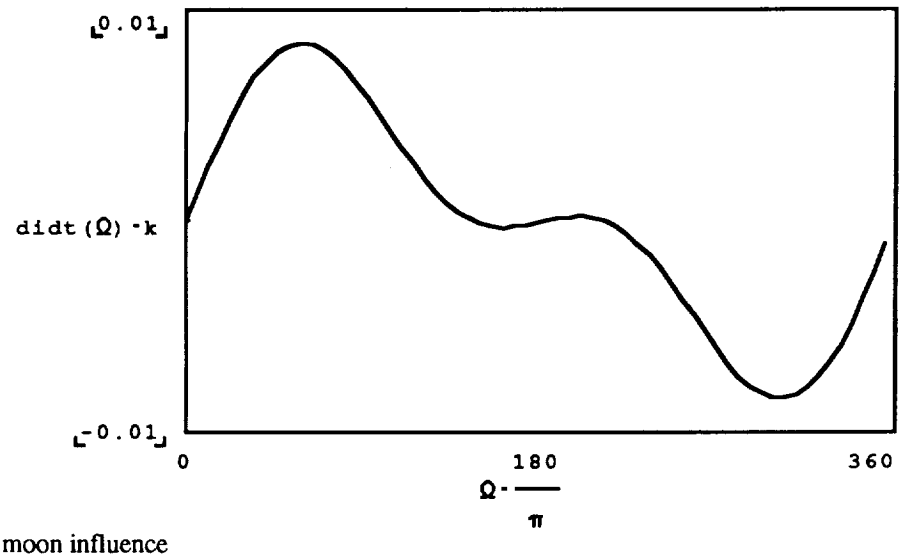

Di/dt for moon influence

$$\mu l := 4.9028\cdot 10^{3} \qquad \Omega l := 0$$

$$il := \frac{28.6}{180}\cdot\pi$$

$$dummy(\Omega) := \left[\sin(\Omega - \Omega l)\cdot\cos(\Omega - \Omega l)\cdot\sin(i)\cdot\sin(il)^{2} + \sin(\Omega - \Omega l)\cdot\cos(i)\cdot\sin(il)\cdot\cos(il)\right]$$

$$didt(\Omega) := \frac{3}{4}\cdot\frac{\mu l}{h}\cdot\left(\frac{r}{rl}\right)^{2}\cdot(dummy(\Omega))$$

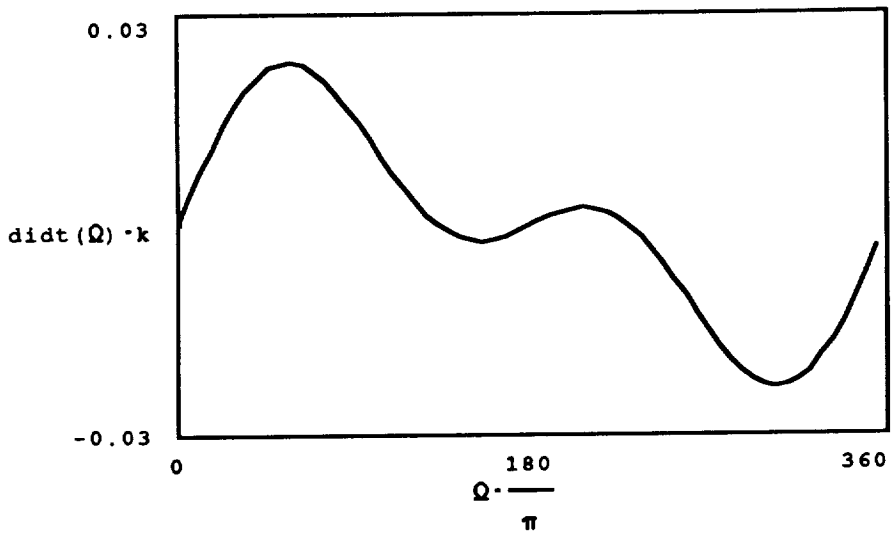

didt(.98)·k = 0.023

This MathCAD document calculates the precession of the longitude of the ascending node for a circular orbit. It also displays the degrees the ground track will move at the equator - based on the precession of the orbit and the rotation of the earth.

For circular orbits the precession of the orbital plane can be expressed as:

$$i := \frac{70}{180}\cdot\pi \qquad R := 6378.14 \qquad h := 509.3 \qquad \mu := 3.986\cdot 10^{14}$$

$$\Omega := -2.0626785\cdot 10^{14}\cdot\left[\frac{\cos(i)}{(R+h)^{\frac{7}{2}}}\right] \qquad \Omega = -2.602 \quad \text{Degrees/sidereal day}$$

$$\tau := \frac{2\cdot\pi}{3600}\cdot\frac{((R+h)\cdot 1000)^{1.5}}{\mu^{.5}} \qquad \tau = 1.58 \quad \text{Hours/orbit}$$

$$Orbits := \frac{23.93}{\tau} \qquad Orbits = 15.144 \quad \text{Orbits/siderial day}$$

$$deg1 := \frac{15}{Orbits}\cdot\Omega \qquad deg2 := 359\cdot(Orbits - 15)\cdot\frac{\tau}{23.93}$$

$$deg1 = -2.577 \qquad deg2 = 3.419$$

$$\Delta deg := deg1 + deg2 \qquad \Delta deg = 0.842$$

$fx := -.811 \qquad tx := 30$

$fy := -.00001 \qquad ty := 16.8$

$fz := .585 \qquad tz := -9.5$

$k1 := \frac{fx}{fy} \qquad k2 := \frac{fx}{fz} \qquad F := \begin{bmatrix} fx \\ fy \\ fz \end{bmatrix}$

$i := 0 \,..\, 5 \qquad j := 0 \,..\, 2$

$x := -20 \qquad y := 10 \qquad z := 0$

$a := 8 \qquad b := -10 \qquad c := -10$

$\sin\left[\operatorname{atan}\left[\frac{1}{k2}\right]\right] = -0.585$

Given

$x \approx \frac{-(y \cdot b + z \cdot c)}{a}$

$\cos\left[\operatorname{atan}\left[\frac{1}{k2}\right]\right] = 0.811$

$x \approx k1 \cdot y$

$x \approx k2 \cdot z$

$x \approx a - tx$

$y \approx b - ty$

$z \approx c - tz$

$\begin{bmatrix} X \\ Y \\ Z \\ r_0 \\ r_1 \\ r_2 \end{bmatrix} := \text{find}(x, y, z, a, b, c)$

$X = -24.24$

$r = \begin{bmatrix} 5.76 \\ 16.8 \\ 7.985 \end{bmatrix} \qquad M := r \mathbin{\text{⤫}} F \qquad F \cdot r = 0$

$Y = -2.989 \cdot 10^{-4}$

$Z = 17.485$

$M = \begin{bmatrix} 9.828 \\ -9.845 \\ 13.625 \end{bmatrix}$

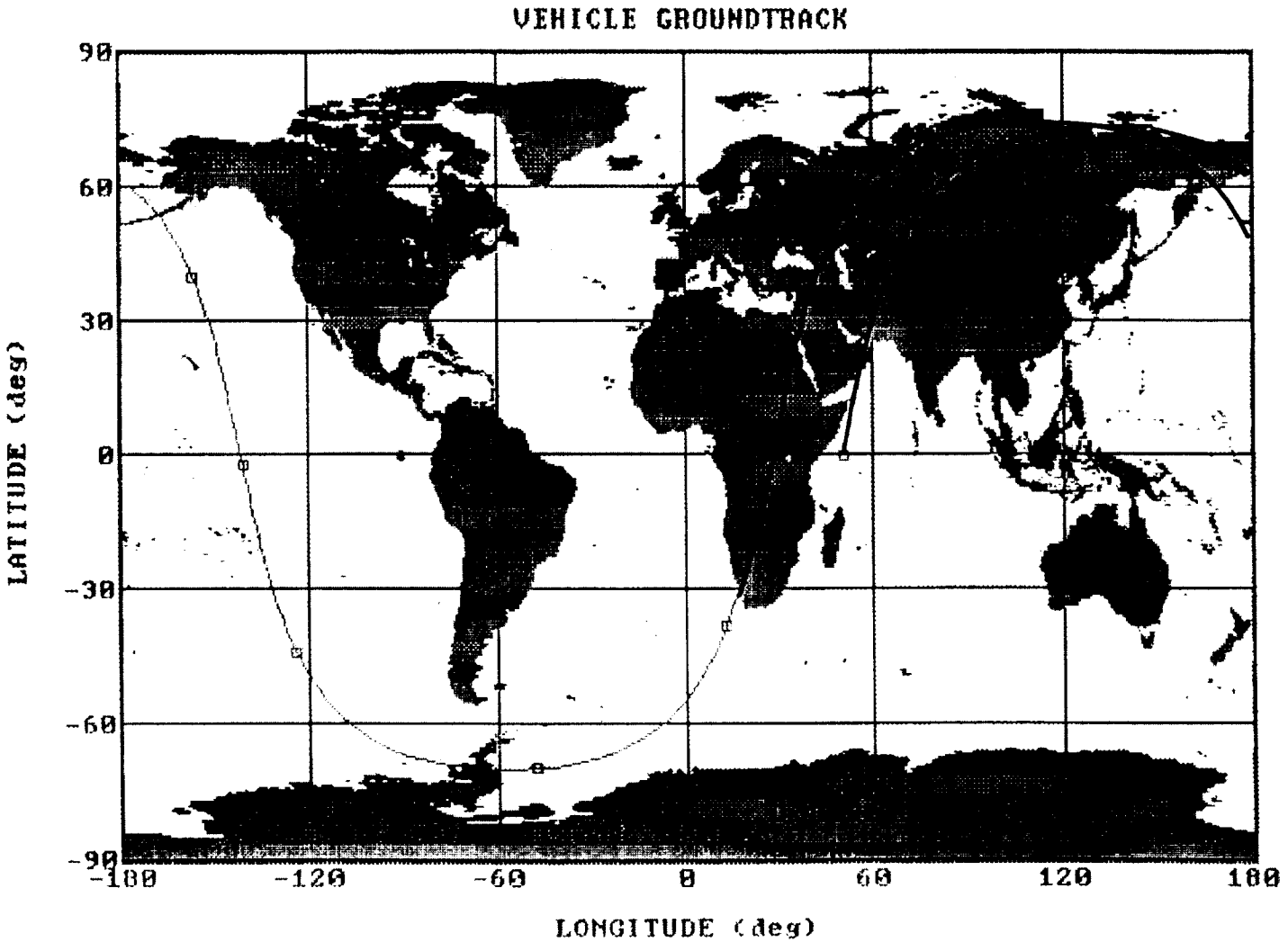
VEHICLE GROUNDTRACK
90
60
30
0
-30
-60
-90
LATITUDE (deg)
-180
-120
-60
0
60
120
180
LONGITUDE (deg)

APPENDIX D - LINK MARGIN CALCULATIONS

Specification		*Value*	*(Units)*
Omni-directional Low Data Rate		16	kbps
Directional High Data Rate		150	Mbps
Bit Error Rate (BER):			
Encrypted		1E-11	
Unencrypted		1E-09	
Data Collection Terminal (DCT):			
minimum elevation angle		10	deg
Satellite Orbit Altitude		275	nmi
		509643.39	m
link distance (R)		1718156.3	m
Assume receiver antenna diameter		20	ft
		6.096	m
Assume antenna effeciency of		0.45	
Effective receiver antenna area		13.133858	m^2
99% Avail. due to rain attenuation		-10	dB
Omni-directional Link Calculations:			
Down-Link Telemetry Frequency		2247.5	MHz
Corresponding wavelength		0.1334816	m
Signal:			
Power of Transmitter (Pt)		43.537235	dBm
		22.579976	Watts
Turnstile Antenna Gain (Gt)		1	dB
Gain of Receiver (Gr)		39.667591	dB
Directional Link Calculations:			
Down-Link transmitter freq		20	Ghz
corresponding wavelength		0.015	m
Signal:			
Power of Transmitter (Pt)		48.757616	dBm
		75.121038	Watts
Gain of Transmitter (Gt)		37.804199	dB
antenna diameter (m):	0.5		
Gain of Receiver (Gr)		37.362723	dB

APPENDIX D
Frequency Communication Subsystem (RFCS)

Losses:			
Loss due to medium (rain)		-10	dB
Signal/Path Loss (Ls)		-183.16363	dB
Incidental Loss (Li)		-1	dB
Transmission Line (Lt)		-3	dB
Actual Transmitted Power (Ca)			
Low Data Rate		-112.9588	dBm
High Data Rate		-73.239087	dBm
Receiver Noise Density:			
k		-198.6	dBm/Hz-K
250W Traveling Wave Tube Amp. (Te)		1000	K
10*log(Te)		30	dBK
Noise Power Spectral Density (No)		-168.6	dBm/Hz
Data Rate (B):	PCM		
Omni-directional	1E-09	42.0412	dB-Hz
Directional	1E-11	81.760913	dB-Hz
Eb/No Available		16.6	dB
Eb/No = (Ca - B) - No		13.6	dB
Margin		3	dB

APPENDIX E - ELECTRICAL POWER SUBSYSTEM (EPS)

A. RADIATION DEGRADATION

From the "Solar Array Radiation Degradation Handbook", for a 275 NM, 70° inclination, circular orbit, the annual 1 MeV equivalent electron fluences are as shown in Table 4.

Table E.1. Annual 1 MEV Equivalent Electron Fluence

	I_{SC}	V_{OC} & P_{MAX}
Electrons	3.95×10^{11}	3.95×10^{11}
Protons	2.11×10^{12}	4.08×10^{12}
TOTAL	2.51×10^{12}	4.48×10^{12}

After three years (spacecraft design life) the anticipated fluences are as shown in table E.2.

Table E.2 1 MEV Equivalent Electron Fluence At EOL

I_{SC}	V_{OC} & P_{MAX}
7.53×10^{12}	1.34×10^{13}

The cells selected are 2.5 x 6.2 cm Si, back surface reflector, 0.02 cm thick (8 mil), 10 Ω μ, with a 3 mil shield and Ti Ox Al_2O_3 anti-reflective coating.

The effects of radiation on the solar cells are summarized in table E.3 below.

Table E.3 Radiation Effect On Solar Cells

	EOL	BOL
P_{MAX} (mW/cm^2)	18.7	20
V_{OC} (mV)	587	608
I_{SC} (mA/cm^2)	43.2	43.7
I_{MP}(mA/cm^2)	40	40.2
V_{MP} (mV)	469	502

B. BATTERY DESIGN

The payload voltage specified is 28 ($\pm$ 4) VDC. Since 24V is the minimum allowable bus voltage, V_{DB} is 24V. Assuming an open circuit failure of one battery cell :

$$V_{DB} = (N-1)V_D - V_{DD}$$

V_D = 1.2V (Ref: *AN IMPROVED, HIGH SPECIFIC ENERGY (LIGHTWEIGHT) SPACE BATTERY SYSTEM* , Mr. Lee Miller, Eagle-Picher Industries)

V_{DD} = 1.1V (Bypass diode voltage drop in event of open circuit failure of one cell)

Therefore, N = 21.9 or 22

Now, recomputing for V_{DB} yields V_{DB} = 24.1V.

To determine the battery capacity necessary to accomplish this objective, first the initial "energy deficit" (E_{out}) must be determined by computing the energy that is drawn by the payload and bus in the earth oriented mode with the two active events mentioned earlier and subtracting the incidental solar input during this period.

$$E_{out} = \Sigma P_h t_h + \Sigma P_a t_a \quad (1)$$

Table E.4 Housekeeping Power Budget (Watts)

LOAD	P_h
Payload (Sensor Idle)	100
Attitude Determination and Control	50
Thermal Control	80
Propulsion	1
TT & C	5
TOTAL	256

Table E.5 Active Power Budget (Watts)

LOAD	P_a
Payload (Sensor Active)	50
Datalink	80
Margin	20
TOTAL	150

Table E.6 Time Intervals During Earth Seeking Event

EVENT	TIME (MINUTES)
Passive (t_h)	194.6
Active (t_a)	30

Evaluating Equation 1 and using data contained in Tables E.1-E.3 yields an energy deficit of approximately 2 X 10^6 Joules. The capacity of the storage device may now be evaluated in the following manner,

$$C = \frac{E_{OUT}}{V_{DB} DOD} = \frac{2 \times 10^6}{24.1 \times 0.6} = 38 \text{ Ah}$$

C. EPS SIMULATION

A simulator was developed to evaluate the demands placed on the energy storage system and to visualize the nature of the DOD cycle for a nominal active event under worst case conditions (EOL, winter solstice, maximum possible eclipse, etc.)

```
10 REM ************************************************
20 REM SIMULATION OF BATTERY DOD
30 REM ************************************************
40 REM SIMULATION RUNS FOR A 24 HOUR DAY (1440 MINS), MAX ECLIPSE SEASON, AT EO
 BATTERY DOD STARTS AT ZERO AND PROCEEDS ACCORDING TO PARAMETERS THAT HAVE BEEN
INPUT
50 REM ********************************************************************
30 REM ********************************************************************
60 REM VDB = MINIMUM BATTERY DISCHARGE VOLTAGE
70 REM VBC = BATTERY CHARGING VOLTAGE
80 REM ERATE IS ANGULAR VELOCITY OF SPACECRAFT AROUND EARTH
90 REM C = BATTERY CAPACITY (AH)
100 REM PH = HOUSEKEEPING POWER
110 REM PA = ACTIVE POWER
120 REM UNITPWR = MAX POWER AT EOL (mW/CM^2)
130 REM ************************************************
140 REM OUTPUT GOES TO A FILE CALLED DCALC.PRN IN ASCII
150 REM ************************************************
160 DIM DOD(1440)
170 VDB=24.1
180 VBC=34.2
190 PI=3.1415926540
200 ERATE=.0664887330
210 C=40
220 TC=0
230 PC=C/10*VBC
240 PH=180
250 PA=230
260 PC=PC/.95
270 UNITPWR=18.7/1000*100^2
280 AREA=PC/UNITPWR
290 K=VDB*C*60
300 DOD(0)=0
310 FOR T=1 TO 229
320 IF T<6 THEN SFR=1:PO=0:GOTO 400
330 IF T<47 THEN SFR=0:PO=PH:GOTO 400
340 IF T<62 THEN SFR=COS(ERATE*(T-47)-PI/2):PO=PA+PH*SQR(1-SFR^2):GOTO 400
350 IF T<95 THEN SFR=COS(ERATE*(T-47)-PI/2):PO=PH*SQR(1-SFR^2):GOTO 400
360 IF T<142 THEN SFR=0:PO=PH:GOTO 400
370 IF T<157 THEN SFR=COS(ERATE*(T-142)-PI/2):PO=PA+PH*SQR(1-SFR^2):GOTO 400
380 IF T<189 THEN SFR=COS(ERATE*(T-142)-PI/2):PO=PH*SQR(1-SFR^2):GOTO 400
390 SFR=0:PO=PH
400 DOD(T)=DOD(T-1)-(SFR*UNITPWR*AREA-PO)/K
410 NEXT T
420 FOR T =230 TO 1440
430 IF T=230+TC*95 THEN SFR=1:PO=0:GOTO 450
440 IF T=289+TC*95 THEN SFR=0:PO=PH:TC=TC+1
450 DOD(T)=DOD(T-1)-(SFR*UNITPWR*AREA-PO)/K
460 NEXT T
470 OPEN "C:\DCALC\DCALC.PRN" FOR OUTPUT AS #1
480 FOR I=0 TO 1440
490 PRINT #1,DOD(I)
500 NEXT I
510 END
```

Figure E.1 Battery Simulator

APPENDIX F - LAUNCH VEHICLE SELECTION

A survey of available launch vehicles was conducted (see table F.1). The preliminary launch vehicle selection was based on a spacecraft mass of 800 to 1400 kilograms, a circular orbit of 509.3 kilometers, and a 70 degree inclination. Based on the sensitive nature of the payload, choices were limited to American vehicles. Launch vehicles such as Scout and Pegasus were found to be too small while Atlas Centaur, Titan 3, and Titan 4 were too big. The closest matches were Atlas E, Titan 2, and Delta II. The Atlas E was immediately eliminated since the program is soon to be cancelled and has very few launch vehicles available. Additionally, the Delta II (6920) will not be available when the spacecraft is launched. The best choices were the Titan 2 and the Delta II (7320).

Additionally, the option of using the space shuttle was considered. The shuttle normally releases satellites between 200 to 400 kilometers at about a 28.5 degree inclination. A kick motor such as the PAM series (developed by McDonnell Douglas for the Delta launch vehicles) would be required to adjust the altitude and inclination. This option was decided against due to the extra costs associated with the human safety features required by space shuttle payloads.

Since both Titan 2 and Delta II can place the spacecraft at the correct altitude, they were compared in four areas: orbital insertion, cost, limit loads, and performance records. A two stage Delta II rocket would place the satellite in a circular orbit very close to that desired. The Titan 2 requires an apogee kick motor to circularize its orbit, adding a measure of complexity. Both launch vehicles cost virtually the same (see cost section Chapter 11). The limit loads of both launch vehicles are similar on the lateral axis but vary greatly on the vertical axis - Delta II is 7.2 g's while Titan II is 12.5 g's (based on a 1000 kg payload). The Delta

program has had over two hundred launches since 1960 and has a 98% success rate over the last twelve years. Titan 2 has had only three launches since the Gemini program. These factors lead to the choice of the Delta II (7320).

Table F.1 Launch Vehicle Survey*

Launch Vehicle	Launch Sites	Satellite Mass (kg)	Insertion Altitude (km)	Notes
Atlas Centaur				
Atlas E	E/WSMC	2350	185	1
Atlas 1	ESMC	5900	185	2
Atlas 2	ESMC	6780	185	
Scout				
Scout 1	WSMC	165-220	550	3
Scout 2	WSMC	353-451	555	
Titan				
Titan 2	WSMC	2177	185 polar	4
Titan 2	WSMC	3400	648 km & 70 deg incl	5
Titan 3	E/WSMC	14742	185	
Titan 4	ESMC	17690	185	
Delta II				
Delta 6920	E/WSMC	3983	185	6
Delta 7320	E/WSMC	2100	510 km & 70 deg incl	
Delta 7920	E/WSMC	6700	648 km & 70 deg incl	
Pegasus	NA	408	463	

Note 1: Includes a Star 20 motor. Only two vehicles remain as of June 1991. Program scheduled to be terminated in 1993.
Note 2: ESMC = Cape Canaveral
Note 3: WSMC = Vandenberg Air Force Base
Note 4: Only three Titan 2 launches since 1966.
Note 5: Includes a Star 37 kick stage.
Note 6: Replaced by the 7000 series in late 1992.

* Only US launch vehicles were considered due to the sensitive nature of the payload.

APPENDIX G - PROPULSION SUBSYSTEM

A. CALCULATION OF REQUIRED PROPELLANT

Monopropellant hydrazine (N_2H_4) with a specific impulse, I_s, of 225 seconds was used as the fuel. An estimated mass of 1050 kg for the satellite was used throughout the following equations.

1. Spin Down and Detumble

A worst case of 5 rpm was designed for to include the possibility of tumbling upon separation (or later on). The following inputs and calculations determined the propellant expended by this maneuver:

Approximate Spacecraft Spin Moment of Inertia = I_M= 475 kg-m^2

Thruster Moment Arm = r = 0.5 m

$$m_d = \frac{I_M * \Delta\omega}{I_s * g_0 * r} = \frac{475 * (5 * (\frac{2 * \pi}{60}))}{225 * 9.806 * 0.5} = 0.225 \text{ kg}$$

2. Orbital Insertion

The worst case of an 18.5 km insertion error was designed for. The orbital section (Section III) shows that the delta v required is 10.238 m/s (includes apogee and perigee firings). To do this maneuver four 1 lb_f thrusters were used canted at 35.8 degrees from the thrust axis. The following equations determine the fuel required and the time to station.

$$F = m * a = m * \frac{dv}{dt}$$

$$T * \cos\theta = \frac{dm}{dt} * v_2 * \cos\theta = I_s * g_0 * (\frac{dm}{dt}) * \cos\theta$$

Where F is the axial force, T is the thrust produced, and θ is the cant angle of the thrusters. When the cant angle is zero, F equals T. Otherwise F equals T * cos θ. Plugging into the equations:

$$T = 4 * (1\ lb_f) * (4.448\ N/lb_f) = 17.792\ N$$

$$T = \frac{m}{\cos\theta} * \left(\frac{\Delta v}{\Delta t}\right) = \frac{1050}{\cos 35.8} * \left(\frac{10.238}{\Delta t}\right) = 17.792$$

$$\Delta t = 745\ sec$$

$$T = I_s * g_0 * \left(\frac{\Delta m}{\Delta t}\right) = 17.792 = 225 * 9.806 * \left(\frac{\Delta m}{745}\right)$$

$$\Delta m = 6.01\ kg$$

3. Atmospheric Drag Corrections

Drag calculations are included in the orbital section (Section III). The result is a delta v of 8.172 m/s. The equations above apply. Using compact forms of these equations:

$$\Delta m = \frac{m * \Delta v}{I_s * g_0 * \cos\theta} = 4.80\ kg \qquad \Delta t = \frac{\Delta m * I_s * g_0}{T} = 595\ sec$$

B. PROPELLANT/PRESSURANT TANK REQUIRED DIAMETER

To decide on a fuel tank from those available commercially, the required tank diameter was determined below. The tank volume was assumed to be 90% fuel and 10% pressurant.

$$\text{Density} = \rho = 876.2\ kg/m^3$$

$$\text{Tank Volume} = V = \frac{m}{\rho} = \frac{13.79}{876.2} = 0.0157\ m^3$$

$$\text{Tank Diameter} = D = 2 * \sqrt[3]{\frac{V}{0.9 * \left(\frac{4}{3}\right) * \pi}} = 0.322\ m$$

C. DEORBIT CALCULATIONS USING THE ASAP PROGRAM

```
    RUN STARTS ON JULIAN DATE                =    2.44992450000000000E+06
    RUN ENDS ON JULIAN DATE                  =    2.45722950000000000E+06
    REFERENCE JULIAN DATE OF PM AND EPHEM =    2.44992450000000000E+06

        0 DAYS     0.000000 HOURS FROM EPOCH
    CARTESIAN COORD X, Y, Z, XD, YD, ZD
 6.81293826504205E+03  0.00000000000000E+00  0.00000000000000E+00  0.000000(
    EQUINOCTIAL ELEMENTS A, H, K, P, Q, MEAN LONG
 6.85647370178488E+03  0.00000000000000E+00  6.34953747893688E-03  0.000000(
    CLASSICAL ELEMENTS E, I, NODE, W, MA, TA, EA, TRUE LONG, ECC LONG, ARG (
 6.34953747893688E-03  7.00130717169308E+01  0.00000000000000E+00  0.000000(
 0.00000000000000E+00  0.00000000000000E+00  0.00000000000000E+00  0.000000(
    OTHER PARAMETERS R, V, ENODE, LONG, LAT, HOUR ANGLE/ ALT, ELLIPSOIDAL AI
 6.81293826504205E+03  7.67319245670377E+00  3.15000000000000E+02  3.150000(
 4.34798265042048E+02  4.34798265042048E+02  4.34798265042048E+02  1.569494:

      365 DAYS     0.000000 HOURS FROM EPOCH
    CARTESIAN COORD X, Y, Z, XD, YD, ZD
-2.67245331340190E+03  6.11307382623370E+03  1.60102362248374E+03 -1.7713818
    EQUINOCTIAL ELEMENTS A, H, K, P, Q, MEAN LONG
 6.84818276482983E+03 -4.38277941839643E-03 -3.23545774199522E-03  6.6373996
    CLASSICAL ELEMENTS E, I, NODE, W, MA, TA, EA, TRUE LONG, ECC LONG, ARG (
 5.44765474590269E-03  7.00103118090051E+01  1.08605572273694E+02  1.249589:
 2.49418414128877E+02  2.49710901050654E+02  1.22982909259365E+02  1.232753(
    OTHER PARAMETERS R, V, ENODE, LONG, LAT, HOUR ANGLE/ ALT, ELLIPSOIDAL AI
 6.86111907468798E+03  7.61484086803961E+00  6.38570964976474E+01  6.886503(
 4.82979074687983E+02  4.84149075656875E+02  4.32736229490193E+02  1.566648:

      730 DAYS     0.000000 HOURS FROM EPOCH
    CARTESIAN COORD X, Y, Z, XD, YD, ZD
 2.74638112869590E+03 -9.05581184536786E+02  6.22696343905423E+03  5.741067:
    EQUINOCTIAL ELEMENTS A, H, K, P, Q, MEAN LONG
 6.82556149289003E+03  5.46896376789193E-03 -3.02071378898686E-03 -3.854251(
    CLASSICAL ELEMENTS E, I, NODE, W, MA, TA, EA, TRUE LONG, ECC LONG, ARG (
 6.24774171116973E-03  6.99867047062779E+01  2.13406815154228E+02  2.655067(
 1.99640768542655E+02  1.99761445986203E+02  3.18554285373984E+02  3.186749(
    OTHER PARAMETERS R, V, ENODE, LONG, LAT, HOUR ANGLE/ ALT, ELLIPSOIDAL AI
 6.86569444828140E+03  7.59706959990528E+00  1.68909863602135E+02  2.972537(
 4.87554448281402E+02  5.05161338085073E+02  4.04777147648743E+02  1.558892(

     1095 DAYS     0.000000 HOURS FROM EPOCH
    CARTESIAN COORD X, Y, Z, XD, YD, ZD
 4.67261772554053E+03 -4.93634260084055E+03 -1.61596798173121E+02  2.013502(
    EQUINOCTIAL ELEMENTS A, H, K, P, Q, MEAN LONG
 6.83231582868964E+03 -2.24178026696187E-03  4.75798163233606E-03 -5.044273(
    CLASSICAL ELEMENTS E, I, NODE, W, MA, TA, EA, TRUE LONG, ECC LONG, ARG (
 5.25965473952302E-03  7.00096508283337E+01  3.13923405235067E+02  2.084856:
 3.37702193789004E+02  3.37816257723682E+02  3.12474160777036E+02  3.125882:
    OTHER PARAMETERS R, V, ENODE, LONG, LAT, HOUR ANGLE/ ALT, ELLIPSOIDAL AI
 6.79904024161415E+03  7.67538372182930E+00  2.69677977906928E+02  2.691824(
 4.20900241614150E+02  4.20912383026455E+02  4.18240206359354E+02  1.561206:

     1460 DAYS     0.000000 HOURS FROM EPOCH
    CARTESIAN COORD X, Y, Z, XD, YD, ZD
 3.31785439398445E+03  5.38518767676673E+02 -5.95655875473560E+03  3.858722:
    EQUINOCTIAL ELEMENTS A, H, K, P, Q, MEAN LONG
 6.80702412514308E+03 -1.06413393865491E-03 -5.39633075671409E-03  5.316834(
    CLASSICAL ELEMENTS E, I, NODE, W, MA, TA, EA, TRUE LONG, ECC LONG, ARG (
 5.50025151018166E-03  6.99856599846952E+01  4.94223376122076E+01  1.417330:
```

APPENDIX H - ATTITUDE CONTROL TOPICS

A. COORDINATE SYSTEMS

Four coordinate systems were used to perform the analyses in the different modes: (1) the spacecraft body, (2) the nadir pointing/sensing, (3) the sun tracking, and (4) the orbit normal.

The body Z-axis is the outward normal from the payload with the origin at the center of mass. The body X-axis is the outward normal from the freestream face and the Y-axis is orthogonal to X and Z.

The sensing coordinates are the standard satellite nadir pointing coordinates with the Z-axis nadir pointing, X in the direction of flight, and Y orthogonal to both. The origin is coincidental with the body coordinates.

The Z-axis of the sun tracking coordinates tracks parallel with the incoming sun vector, X is orthogonal in the equatorial plane , and Y completes the right hand set. For the purposes of analysis, these coordinates are an "inertially" fixed frame because of the slow change in the earth-orbit-sun orientation.

As a base for coordinate transformations between modes, the orbit normal system was used. The Z- axis in this system points out the normal for the orbital plane, X is orthogonal out the ascending node, and Y completes the right hand set. This also can be considered "inertially" fixed because of the slow rotation of the orbital plane.

B. THE EQUATIONS OF MOTION

The general equations for a three axis stabilized, three reaction wheel system in terms of euler angles are quite lengthy and involved. For this particular design, assumptions reduced these equations to two forms: (1) the pointing mode form

where the attitude errors remain in a small linear range, and (2) the slew mode form where the disturbance torques are small compared to the slewing torques.

In the pointing mode equations the small products of inertia are neglected as well as the small stored angular momentum in the RWAs. The control torque produced by the RWA is governed by the standard position plus rate feedback law leading to an uncoupled second order system for each axis. These are described by the following:

$$(H.1)\quad I_{xx}\,\phi + K_{\phi}\,\tau_{\phi}\,\phi + K_{\phi}\phi = \Sigma M_x$$

$$(H.2)\quad I_{yy}\theta + K_{\theta}\tau_{\theta}\theta + K_{\theta}\theta = \Sigma M_y$$

$$(H.3)\quad I_{zz}\psi + K_{\psi}\tau_{\psi}\psi + K_{\psi}\psi = \Sigma M_z\ ,$$

where M_i are the external torques acting on the spacecraft, I_{ii} are the principal moments of inertia, and K_i and τ_i are the respective system gain and time constant.The derivation of these equations can be found in ref. (1).

In the slew mode equations, the gravity gradient, aerodynamic, and solar disturbance torques are 3 - 4 orders of magnitude lower than the slewing torques and are neglected for the slew analysis. Assuming the products of inertia are negligable, the three axis / three reaction wheel equations reduce to:

$$(H.4)\quad I_{xx}\Omega_x + \Omega_y\Omega_z(\,I_{zz} - I_{yy}\,) + \Omega_y h_z - \Omega_z h_y = -h_x$$

$$(H.5)\quad I_{yy}\Omega_y + \Omega_x\Omega_z(\,I_{xx} - I_{zz}\,) + \Omega_z h_x - \Omega_x h_z = -h_y$$

$$(H.6)\quad I_{zz}\Omega_z + \Omega_x\Omega_y(\,I_{yy} - I_{xx}\,) + \Omega_x h_y - \Omega_y h_x = -h_z\ ,$$

where Ω_i are the angular velocities about each body axis described in terms of one of 12 euler transformations in terms of ϕ, θ, and ψ, the roll. pitch and yaw errors respectively. The h_i are the angular momenta produced about each axis by the RWAs. The various euler forms of the Ω_i, along with the general forms of equations G4 - G6 can be found in ref. (2). It is easy to see that even these simplified forms are highly coupled.

C. DISTURBANCE TORQUE MODELS

The following MATLAB code contains the disturbance torque models used in this design for both the sensing and sun tracking modes. The sense mode gravity gradient equations are derived in reference (1). The gravity gradient torque model for the sun track mode was developed by this designer. The aerodynamic moments model was developed by this designer assuming the cubic geometric center to be the center of pressure. Solar torque equations are derived in Ref (1) for geosynchronous spacecraft. Using suitable coordinate transformations these equations are applied to this design. Finally , the magnetic torques available for momentum dumping are included. This model was also developed by the designer.

```
%          PROG  DISTURBANCE TORQUES

% THIS PROGRAM CALCULATES THE DISTURBANCE TORQUES FOR
HTSI IN BOTH SENSING AND  %  SUNTRACKING MODES. ( NOTE IF
USED AS A SUBROUTINE, THE SUBROUTINE FLAG MUST  %  BE SET
AND A TIME VECTOR DEFINED )

sflag=input(' subroutine use = 1, not = 0');

% A.   SENSING MODE :

% THE GRAVITY GRADIENT CONTRIBUTION IS SECULAR IN THIS
MODE FOR STEADY STATE
% TRACKING ERRORS AS IN OFFSET NADIR POINTING. WERE
NEGLECTING THE CONTRIBUTION
% FROM SMALL TRANSIENT ERRORS. USE WORST CASE SCENARIO.

err=input('steady state offset angles as a row vector; roll pitch yaw in deg.');
err=(pi/180)*err;
h=input('enter orbital altitude in meters');
I=input('enter principal moments as a row; x y z in kg-m^2');

w0=sqrt(3.987464e14/((6378e3 + h)^3));
Mg(1) = (3*w0^2)*(I(3)-I(2))*sin(err(1))*cos(err(1))*cos(err(2));
Mg(2) = (3*w0^2)*(I(3)-I(1))*sin(err(2))*cos(err(2))*cos(err(1));
Mg(3) = (3*w0^2)*(I(1)-I(2))*sin(err(2))*cos(err(2))*sin(err(1));
```

```
% THE AERODYNAMIC DRAG IS ALSO SECULAR IN THIS MODE. BEGIN BY ESTIMATING THE
% DRAG FORCE: D=Cd*rho/2*v^2*A

cd=input('enter drag coefficient');
rho=input('enter estimated density at altitude, kg/m^3');
A=input('enter crosssectional area of spacecraft, m^2');

v=(6370e3+h)*w0;
D=.5*cd*rho*A*v^2;

% NEXT DEFINE THE FORCE DIRECTION AND MOMENT ARM. IN THIS MODE BOTH ARE FIXED IN % THE BODY NEGLECTING SMALL CHANGES DUE TO TRACKING ERRORS.

Du=input('enter drag direction cosines as a row, x y z');
cp=input('enter the cp-cm offset as a row vector; x y z');
Md=D.*[0 -cp(3) cp(2);cp(3) 0 -cp(1);-cp(2) cp(1) 0]*Du';

% THE SOLAR TORQUES ARE BOTH CYCLIC AND SECULAR IN THIS MODE. THEY ARE
% CALCULATED USING AGRAWAL P  ADJUSTED FOR COORDINATE SYSTEMS AND SELECTING THE % WORST CASE ORBIT AND SUN ANGLE

% SECULAR TERMS AND CYCLIC AMPLITUDES
```

```
del=input('enter sun declination in degrees');
del=(pi/180)*del;
ps=input('enter coefficient of specular reflection');
pd=input('diffuse reflection');
inc=input('enter orbit inclination in deg.');
inc=(pi/180)*inc;
dele= -(inc-del);
k1=((1-ps)*cos(dele) + 2*(ps +.33*pd))*cos(dele);
k2=(1-ps)*cos(dele)*sin(dele);

PA=4.644e-6*A^2;
Mxcos= PA*cp(2)*k1;Mbx=-PA*cp(3)*k2;
Mysin=PA*cp(3)*k1;Mycos=-PA*cp(1)*k1;
Mbz=PA*cp(1)*k2;Mzsin=-PA*cp(2)*k1;

if sflag==1  % COMPUTE TIME HISTORY OF TORQUES AND SUM

t=input('enter time as a row vector in seconds');
Ms(:,1)=Mxcos*cos(w0.*t')+Mbx;
Ms(:,2)=Mysin*sin(w0.*t')+Mycos.*cos(w0.*t');
Ms(:,3)=Mzsin*sin(w0.*t')+Mbz;

Msum=Mg+Md';
Madd(:,1)=Msum(1)*ones(t)';Madd(:,2)=Msum(2)*ones(t)';Madd(:,3)=Msum(3)*o
nes(t)';Mtot=Ms+Madd;
end
```

```
% NOISE DISTURBANCES ARE CALCULATED AND USED IN
% ANOTHER ROUTINE DUE TO THEIR VARIABLE AND SPECIAL CASE
NATURE. BE AWARE
% THAT Mtot CONTAINS AERO, SOLAR AND GRAVITY GRADIENT
ONLY.

% NEXT WE PERFORM SIMILAR ANALYSIS IN THE SUNTRACKING
MODE, WHERE THE DIS.
% TORQUES WILL CHANGE DUE TO DIFFERENT ORIENTATION AND
THE "INERTIAL" NATURE OF % THE COORDINATES

%    SUNTRACKING MODE

% THE SOLAR TORQUES ARE STRICTLY SECULAR IN THIS MODE

F=PA*cos(del).*[0;(1-ps-pd)*sin(del);(1-ps-pd)*cos(del)+2*ps];
Msst=([0 -cp(3) cp(2);cp(3) 0 -cp(1);-cp(2) cp(1) 0]*F)';

% GRAVITY GRADIENT TERMS ARE CYCLIC AND QUITE INVOLVED IN
THIS MODE AND THE
% DERIVATION IS GIVEN IN  THIS APPENDIX. THERE ARE NO PURELY
SECULAR TERMS.

 if sflag ==1

nu=input('enter angle between sunvector projection and ascend. node in deg.');
nu=(pi/180)*nu - 90;
```

```
arg=180-inc;
ste=input(' small steady state tracking errors in deg. as a row');
ste=(pi/180)*ste;

% CALCULATE AVAILABLE TORQUES FOR MAGNETIC DESATURATION ALSO

myu=input('earth rotation angle wrt ascending node, in deg.');
myu=(pi/180)*myu;
bmag=8e15/((6370e3+h)^3);

lintran=[1 ste(3) -ste(2);-ste(3) 1 ste(1);ste(2) -ste(1) 1];
xrot=[1 0 0;0 cos(del) sin(del);0 -sin(del) cos(del)];
yrot=[cos(nu) 0 sin(nu);0 1 0;-sin(nu) 0 cos(nu)];
xrot2=[1 0 0;0 cos(arg) sin(arg);0 -sin(arg) cos(arg)];
ttran=xrot*yrot*xrot2;

sighz=size(t);

for k=sighz(1):sighz(2)

c=cos(w0*t(k));
s=sin(w0*t(k));
r0=(-(6370e3+h).*ttran'*[c;s;0])';
r0t=(lintran*r0')';
magr0=(r0t(1)^2 + r0t(2)^2 + r0t(3)^2)^2.5;
mul=3*3.987464e14/magr0;
```

```
Mgst(k,1)=mul*(r0t(2)*r0t(3)*(I(2)-I(3)));
Mgst(k,2)=mul*(r0t(1)*r0t(3)*(I(3)-I(1)));
Mgst(k,3)=mul*(r0t(1)*r0t(2)*(I(1)-I(2)));

% NEXT CALCULATE AERO DRAG TERMS WHICH ARE CYCLIC IN THIS
FRAME. THE DERIVATION % IS GIVEN IN THIS APPENDIX

dvec=(D.*ttran'*[s;-c;0])';
Mdst(k,:)=([0 -cp(3) cp(2);cp(3) 0 -cp(1);-cp(2) cp(1) 0]*dvec')';

Mtotst(k,:)=Mgst(k,:)+Mdst(k,:)+Msst;

%CONTINUE WITH AVAILABLE DESATURATION TORQUE (PLUS OR
MINUS)

B1=bmag*(.9816*sin(inc)*c-.1908*sin(myu)*c-.1908*cos(myu)*cos(inc)*c);
B2=-bmag*(.9816*cos(inc)+.1908*sin(inc)*cos(myu));
B3=2*bmag*(.9816*sin(inc)*s+.1908*sin(myu)*c-.1908*cos(myu)*cos(inc)*s);
Bst=(ttran'*[B1 B2 B3]')';
Mmag(k,:)=20*[B3-B2 B1-B3 B2-B1];
Mmagst(k,:)=20*[Bst(3)-Bst(2)  Bst(1)-Bst(3)  Bst(2)-Bst(1)];

end
end

save dtq t Mg Md Mbx Mbz Ms Mtot Msst Mgst Mdst Mtotst Mmag Mmagst
clear
```

Figure H-1 shows the behavior of these disturbance torques for each mode over one orbit for a typical orbit - sun orientation.

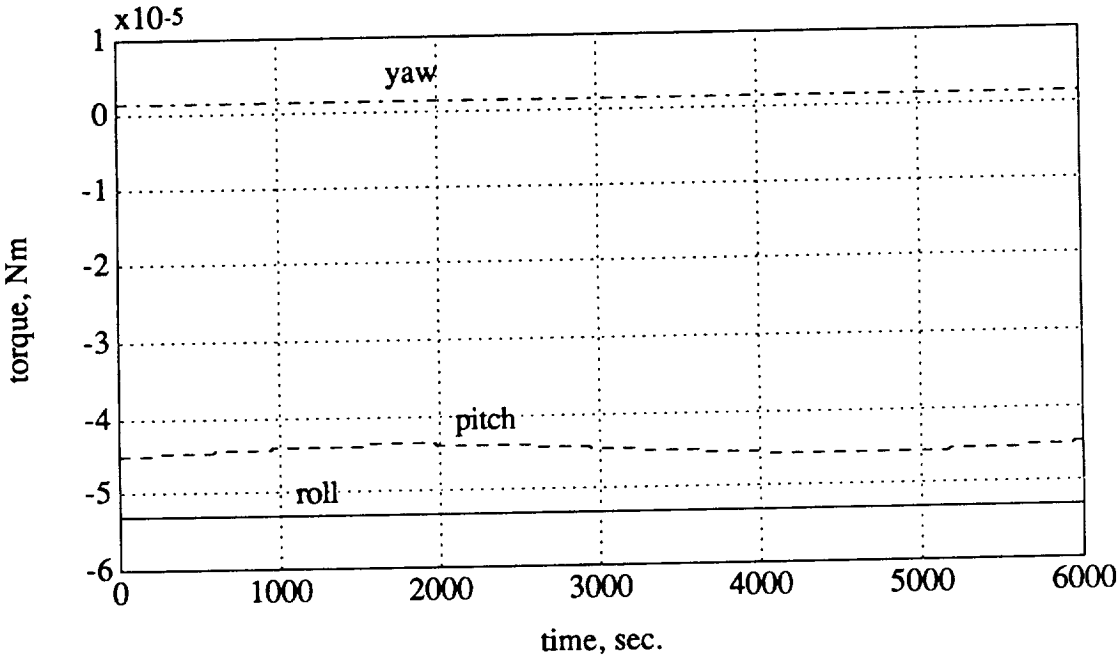

Figure H-1(a) Sense Mode Sum Of Disturbance Torques For One Orbit In ATypical Orbit-Sun Orientation

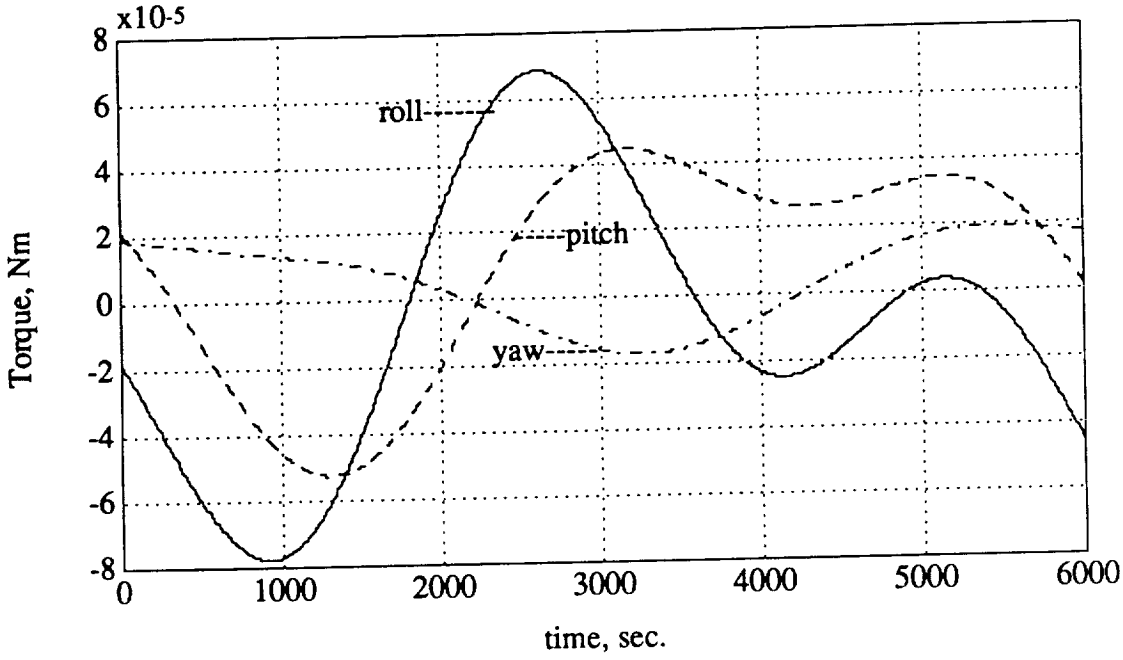

Figure H-1(b) Sun Track Mode Sum of Disturbance Torques For One Orbit In A Typical Orbit - Sun Orientation

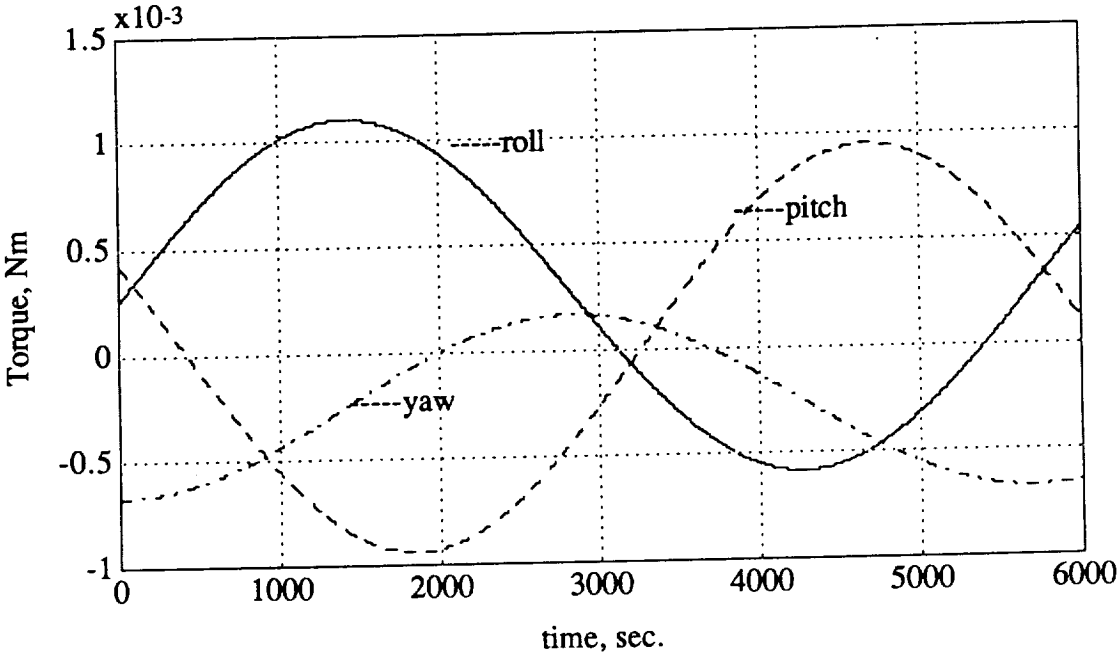

Figure H-1(c) Available Fixed Polarity Magnetic Torque Available for Desaturation in a Typical Orbit-Sun Orientation

D. SIZING OF RWAS AND TORQUE RODS

The required torque producing and angular momentum storage capabilities for the RWAs are governed by the slew rate and pointing accuracy requirements. A simple model for the slew dynamics is used for the purposes of sizing:

$$I_S \, \Delta\omega_S / \Delta t = \Sigma M_W \,, \tag{H.7}$$

where the subscript s indicates the properties about the slew axis, the subscript w indicates the properties of the wheel, and ω is the respective angular velocity . When driven by constant torque levels, the angular position and velocity of this simplified model will follow parabolic trajectories in the phase plane. This allows the designer to obtain average slew rates as a function of constant torque for fixed inertia properties.

Once the required torque level is determined a 100% margin for design uncertainty is added and a search for an off-the-shelf RWA is made that satisfies the design torque. In addition to the torque level, these factors must be considered: (1) mass, (2) power consumption, and (3) angular momentum storage capacity (peak RPM). Designers of the other subsystems need to know about the first two and the RWA must be able to absorb the increase in angular momentum over the time the slewing torque is applied.

The final check is in the area of pointing accuracy. Given the selected RWA and the disturbance torque models a check is made to see if the RWA can produce the required response to maintain pointing accuracies within the specified goal. This procedure is explained in the next section. The magnetic torque rods must be able to dump the accumulated angular momentum due to disturbance torques. The torque produced by a magnetic torque rod is described simply by:

$$(H.8)\quad T = m \times B,$$

where T= torque produced, m= dipole moment of the torque rod, and B = the earth magnetic field strength. Using the canted dipole model for the earth magnetic field, and the disturbance torque models, the dipole moment size of the torque rods can be found as follows:

$$(H.9)\quad m_x = -(B_z M_y - B_y M_z) / |B|^2$$

$$(H.10)\quad m_y = (B_z M_x - B_x M_z) / |B|^2$$

$$(H.11)\quad m_z = -(B_y M_x - B_x M_y) / |B|^2$$

The canted dipole model and detailed derivation of these equations can be found in ref (3). Once the dipole moment required is determineed, as in the RWA an off-the -shelf component is sought after a design margin of 100% is added.

E. . CONTROL SYSTEM DESIGN

The gain K_i, and time constant τ_i are determined by the following equations found in ref (1):

$$\tau = 2\alpha I e / M \quad , \tag{H.12}$$

$$K = I / (\tau / 2)^2 \quad , \tag{H.13}$$

where I= the moment of inertia of the axis in question, α = the maximum allowable pointing error, e = the natural exponent, and M = the maximum torque impulse acting about the axis. These gains are then fed into the following simulation code written in MATLAB. It takes the previously calculated disturbance torque models, adds in the noise models discussed in chapter VII, and simulates the system for the control parameters selected.

```
%   THIS PROGRAM DOES THE STEADY STATE POINTING ANALYSIS
%   TO BE CALLED FROM DTORQUE IF NO DTQ FILE RESIDENT

rand('normal')
mflag=input('sense mode=1, strack mode=0');
z=input('enter axis no. 1, 2 or 3');
I=input('enter I,K,tau as a row vector in consistent units');
n=input('enter white noise tau and intensity as arow');
An=[0 1 0;-(I(2)/I(1)) -(I(2)*I(3)/I(1)) I(2)/I(1);0 0 -1/n(1)];
Bn=[0 0;1/I(1) 0;0 1];
Ab=An(1:2,1:2);
Bb=Bn(1:2,1);
Bnw=Bn(1:3,2);
cb=eye(Ab);cn=[1 0 0;0 1 0];d=[0 0]';dn=[0 0;0 0];

load dtq
clear Ms Msst Mg Mgst Md Mdst

%  MODE RESPONSES DEPENDING ON FLAG
% (A) BASIC DTORQUES, NO NOISE

x0=input('enter initial error in deg. as a row');
x0=(pi/180)*x0';
if mflag==1
nflag=input('add a noisy torque?1-y 0-n')
if nflag==1
```

```
Mtot=Mtot+1e-8*rand(Mtot);
end
[eab,stb]=lsim(Ab,Bb,cb,d,Mtot(:,z),t,x0);
else
[eab,stb]=lsim(Ab,Bb,cb,d,Mtotst(:,z),t,x0);
end

% (B) BASIC W/ DESATURATION

if mflag==1
M=Mtot+ [Mmag(:,1) -Mmag(:,2) -Mmag(:,3)];
Msim=M(:,z);
[ead,std]=lsim(Ab,Bb,cb,d,Msim,t,x0);
else
M=Mtotst-Mmag;
clear Mmag
Msim=M(:,z);
clear M Mtotst
[ead,std]=lsim(Ab,Bb,cb,d,Msim,t,x0);
end
ead=(180/pi)*ead;
eab=(180/pi)*eab;
%plot(t,eab);
%pause
%plot(t,ead);
```

```
% WE ARE ONLY INTERESTED IN JITTER EFFECTS FOR THE SENSING
MODE

w=n(2)*rand(t);
if mflag==1

% NOISE EFFECTS ONLY

[ean,stn]=lsim(An,Bnw,cn,d,w,t);

% NOISE PLUS BASIC DTORQUES

unb=[Mtot(:,z) w'];
[eanb,stnb]=lsim(An,Bn,cn,dn,unb,t);

% NOISE PLUS DESATURATION ADDED

unb=[Msim w'];
[eand,stnd]=lsim(An,Bn,cn,dn,unb,t);

ean=(180/pi)*ean;
eanb=(180/pi)*eanb;
eand=(180/pi)*eand;

%plot(t,ean(:,2))
end
```

This code generated figures 7.3 and 7.4 in chapter VII. Figure H-2 shows the control system response to a thruster impulse in the event of torque rod failure and in the presence of system noise.

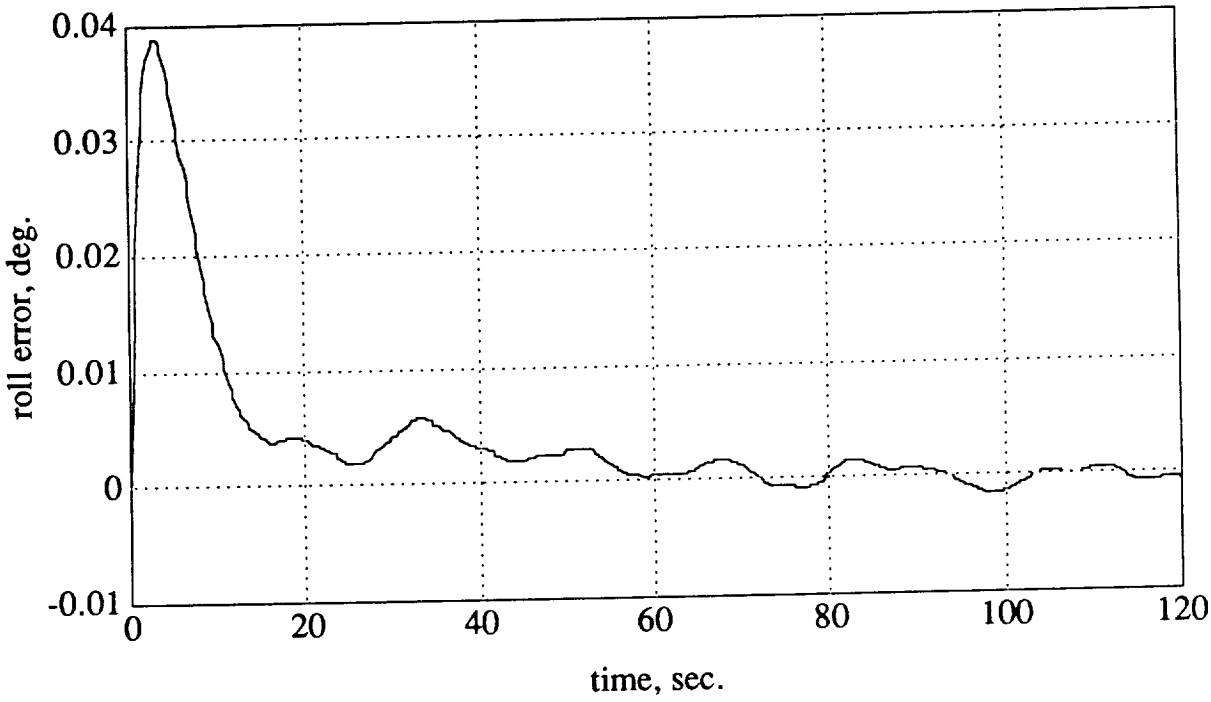

Figure H-2 Response to Thruster Impulse as Back Up Desaturation

The design of a saturating non-linear controller is found in ref (4). The gain selection algorithm is given in the following MATLAB code. It is adaptively selected from the initial errors and effort desired to steer phase trajectories with minimum chatter.

```
% STORES DIFFERENTIAL EQUATIONS TO BE SOLVED

function xdot=slew(t,x)

xdot(1)=x(2);
xdot(2)=k1.*x(4).*x(6) + (Iw/I(1))*(x(6).*x(8)-x(4).*x(9))- ...
      (N(1)/I(1))*sign(x(1) + gain.*x(2));
xdot(3)=x(4);
xdot(4)=k2.*x(2).*x(6) + (Iw/I(2))*(x(2).*x(9)-x(6).*x(7))-...
      (N(2)/I(2))*sign(x(3) + (gain/2).*x(4));
xdot(5)=x(6);

xdot(6)=k3.*x(2).*x(4) + (Iw/I(3))*(x(7).*x(4) - x(2).*x(8))-...
      (N(3)/I(3))*sign(x(5) + (gain/2).*x(6));
xdot(7)= -(N(1)/I(1))*sign(x(1) + gain.*x(2));
xdot(8)= -(N(2)/I(2))*sign(x(3) + (gain/2).*x(4));
xdot(9)= -(N(3)/I(3))*sign(x(5) + (gain/2).*x(6));

% THIS PROGRAM EXECUTES THE R-K INTEGRATOR


I=[392.7 397.7 371.1] %input('enter princ. inertias, 1 2 3');
Iw=.0884 %input('enter wheel inertia');
k1=(I(2)-I(3))/I(1);k2=(I(3)-I(1))/I(2);k3=(I(1)-I(2))/I(3);
%hnom=Iw*wnom;
N=input('enter torque limits, Nm');
```

```
global I Iw k1 k2 k3 N gain

t0=0;tf=225;
x0=[(pi/2) .001 .26 .00005 .26 .00005 0 0 0];gain=22.5;
[t,x]=ode23('slew',t0,tf,x0,1e-4);
x=(180/pi).*x;
x(:,7)=(1/6)*x(:,7);

plot(t,x(:,1)),title('roll slew angle response'),xlabel('time')
pause
plot(x(:,1),x(:,2)),title(' phase plane response'),xlabel('x1')
pause
plot(t,x(:,3)),title('2-axis intermediate response')
pause
plot(t,x(:,5)),title('3-axis intermediate response')
pause
plot(t,x(:,7)),title('wheel speed')
pause
```

Figure H-3 shows the phase plane response of the slew axis, Figure H-4 shows the corresponding wheel speed response, and Figure H-5 shows a typical off-axis slew response.

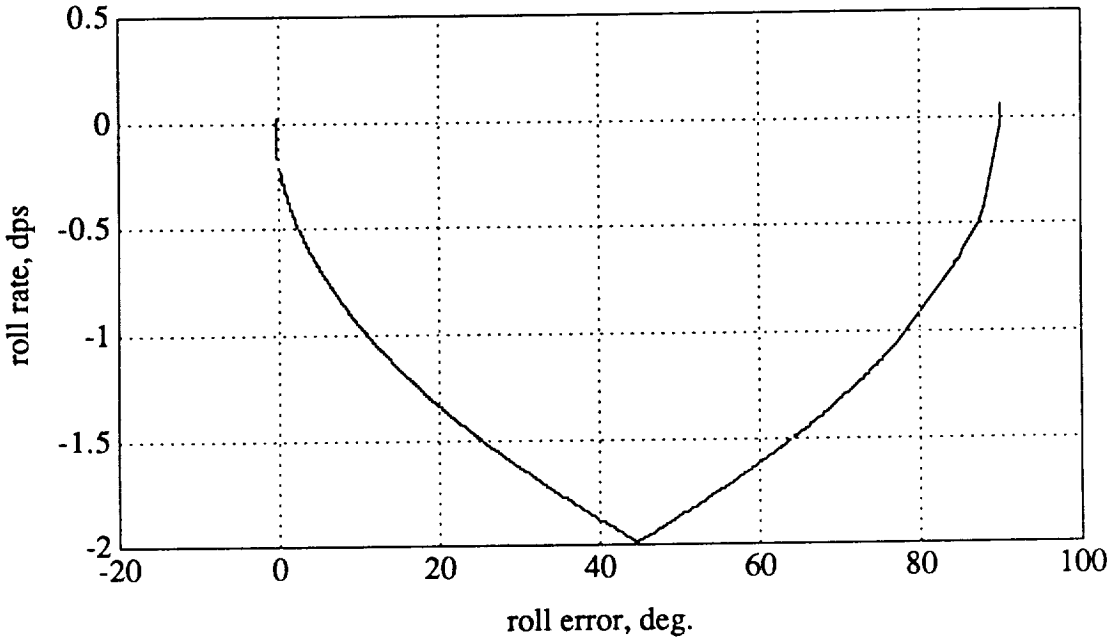

Figure H-3 Phase Plane Response for a Typical Slew

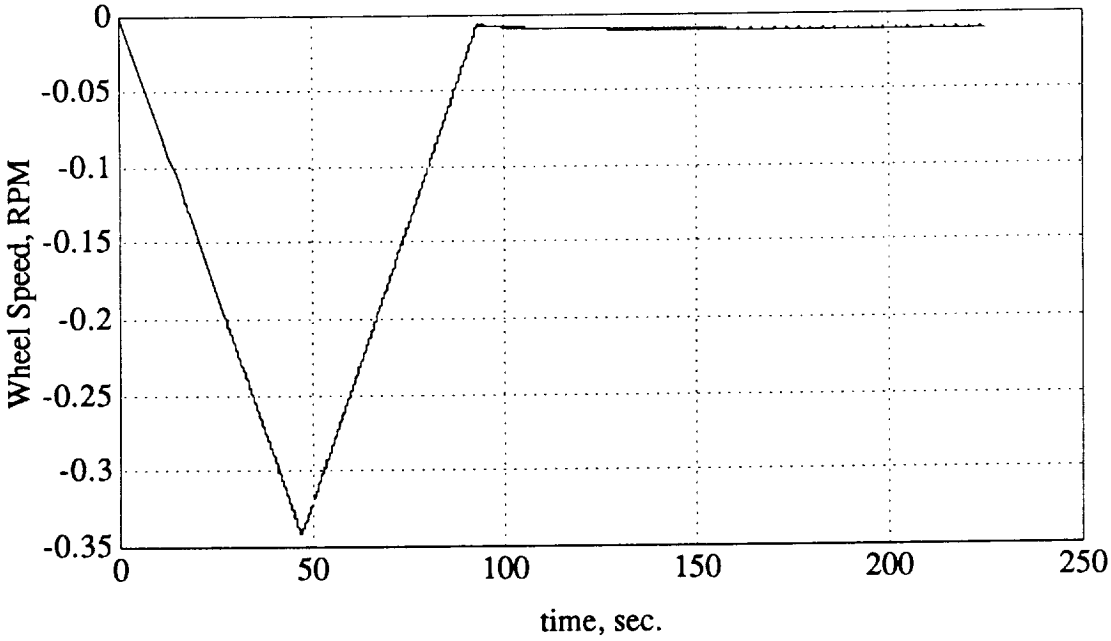

Figure H-4 Wheel Speed for a Typical Slew

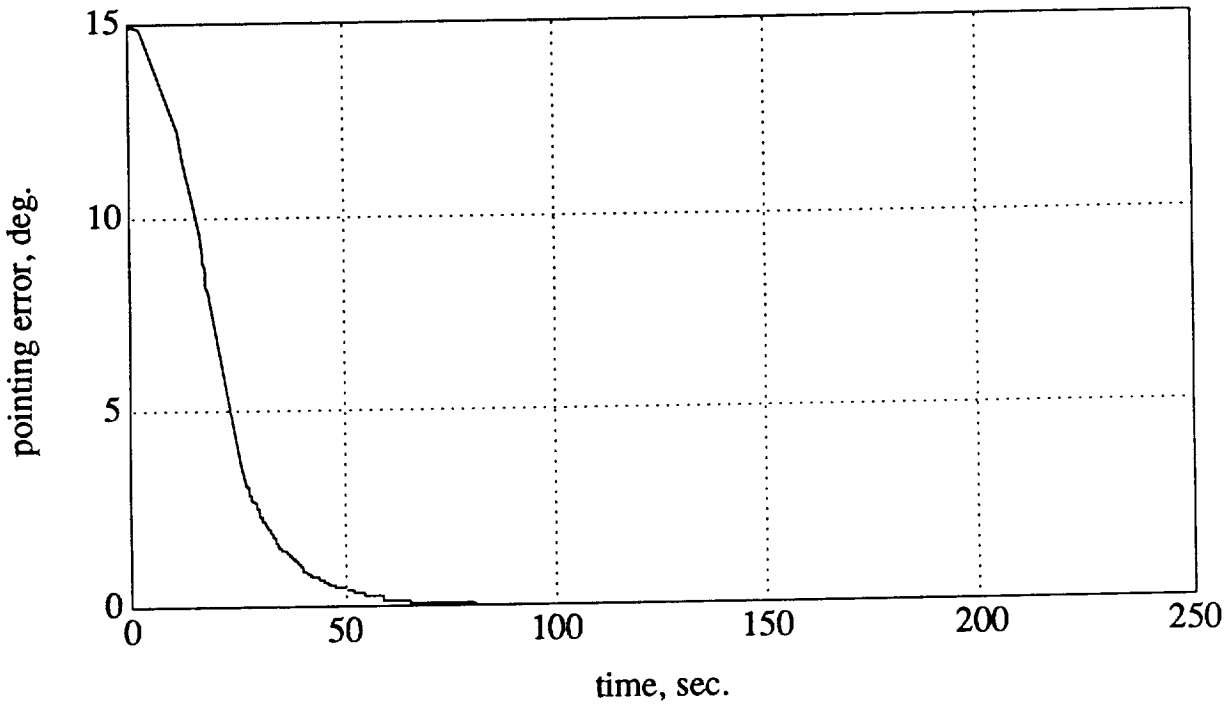

Figure H-5 Corresponding Off-Axis Response

APPENDIX I - THERMAL ANALYSIS

This Mathcad calculation sheet is used to solve thermal balance equations set for the spacecraft bus solar arrays. These sheets were done prior to the development of the PC-ITAS stand alone thermal model. The sheets included a several used in a trade study conducted to see what the temperature of the s arrays would be given certain conditions. Design variations included array locations (body mounted .vs. deployed), area of array, density of cell arranger coatings to be used on aft side of deployed arrays, and others. The associated geometries are given in Figure A8.1

Geometry A

This calculation is for a 60 in diam cell layout ignoring emmitance of corners. is similar to mounting the cells on the central bay since no radiation of heat be allowed into the S/C bus. All values EOL and sun line is normal to surface

Area (60 in Diam) $A := 1.824$

Emittance $E := 0.8$

Absorptance $a := 0.75$

Cell Packing Factor $F := 0.9$

Cell Efficiency $N := 0.15$

Boltzmans Constant $Sig := 5.67 \cdot 10^{-8}$

Solar Flux $S := 1397$

Effective Solar Absorptance $a_e := a - N \cdot F$

Operating Temperature. $$T_{op} := \left[\frac{\left[a_e \cdot A \cdot S \right]}{(E \cdot A) \cdot Sig} \right]^{0.25}$$

$T.op = 370.979$.

APPENDIX I - THERMAL ANALYSIS

Geometry B

This calculation is for a 60x60 in panel which is covered with a 60 in diam

Area $A := 2.323$

Emittance $E_{cell} := 0.8 \quad E_{OSR} := 0.8$

Absorptance $a_{cell} := 0.75 \quad a_{OSR} := 0.145$

Cell Packing Factor $F := 0.9$

Cell Efficiency $N := 0.15$

Boltzmans Constant $Sig := 5.67 \cdot 10^{-8}$

Solar Flux $S := 1397$

Averaged Solar Absorptance

$$a_{avg} := \frac{a_{cell} \cdot 1.824 + a_{OSR} \cdot .499}{2.323}$$

Effective Averaged Solar Absorptance $a_{eavg} := a_{avg} - N \cdot F$

Operating Temperature.

$$T_{op} := \left[\frac{a_{eavg} \cdot A \cdot S}{\left[E_{cell} \cdot A \right] \cdot Sig} \right]^{0.25}$$

$T_{op} = 349.603$

Geometry C

This calculation is for a 60x60 in panel which is covered with a 60 in diam patch of solar cells and the rest covered with OSR, with an additional 10 in strip of white paint added to the sides of the S/C looking into space and assumed to be totally effective as a radiator (conductively coupled to the solar cell area). Values are EOL

Areas (front and white strip)

$$A_f := 2.323 \qquad A_b := 1.548$$

Emittances (front and white strip)

$$E_f := 0.8 \qquad E_b := 0.9$$

Absorptance

$$a_{cell} := 0.75 \qquad a_{OSR} := 0.145$$

Cell Packing Factor

$$F := 0.9$$

Cell Efficiency

$$N := 0.15$$

Boltzmans Constant

$$Sig := 5.67 \cdot 10^{-8}$$

Solar Flux

$$S := 1397$$

Averaged Solar Absorptance

$$a_{avg} := \frac{a_{cell} \cdot 1.824 + a_{OSR} \cdot .499}{2.323}$$

Effective Averaged Solar Absorptance

$$a_{eavg} := a_{avg} - N \cdot F$$

Operating Temperature.

$$T_{op} := \left[\frac{a_{eavg} \cdot A_f \cdot S}{\left[E_f \cdot A_f + E_b \cdot A_b \right] \cdot Sig} \right]^{0.25}$$

$$T_{op} = 303.974$$

Geometry D

This would be the solar array steady state temp if we use the deployed peta array configuration (4 arrays each 60x12 in). Front covered with solar cell, l painted white. The main advantage to this design is that the arrays are only conductively coupled to the S/C . Values again EOL.

Areas (cells front and white back)

$$A_f := 1.858 \qquad A_b := 1.858$$

Emittances (front and back)

$$E_f := 0.8 \qquad E_b := 0.9$$

Absorptance

$$a := 0.75$$

Cell Packing Factor

$$F := 0.9$$

Cell Efficiency

$$N := 0.15$$

Boltzmans Constant

$$Sig := 5.67 \cdot 10^{-8}$$

Solar Flux

$$S := 1397$$

Effective Averaged Solar Absorptance

$$a_e := a - N \cdot F$$

Operating Temperature.

$$T_{op} := \left[\frac{a_e \cdot A_f \cdot S}{\left[E_f \cdot A_f + E_b \cdot A_b \right] \cdot Sig} \right]^{0.25}$$

$$T_{op} = 307.263$$

Geometry E

This would be the solar array steady state temp if we use the deployed petal solar array configuration (4 arrays each 60x15 in). Front covered with solar and 3 inch strip of white paint, back painted white. The main advantage to th design is that the arrays are only partially conductively coupled to the S/C . Values again EOL.

Areas (cells/paint front and white back)

$$A.f := 2.32 \qquad A.b := 2.32$$

Emittances (front and white strip)

$$E.cell := 0.82 \qquad E.paint := 0.9$$

Average Emmitance of the Front

$$E.eff := \frac{\left[E.cell \cdot 1.858 + E.paint \cdot 0.4\right.}{2.32}$$

Absorptance

$$a.cell := 0.75 \qquad a.paint := 0.4$$

Average Absorptance for Front Side

$$a.avg := \frac{\left[a.cell \cdot 1.858 + a.paint \cdot 0.4\right.}{2.32}$$

Cell Packing Factor

$$F := 0.9$$

Cell Efficiency

$$N := 0.15$$

Boltzmans Constant

$$Sig := 5.67 \cdot 10^{-8}$$

Solar Flux

$$S := 1397$$

Effective Averaged Solar Absorptance

$$a_{eavg} := a_{avg} - N \cdot F$$

Operating Temperature

$$T_{op} := \left[\frac{a_{eavg} \cdot A_f \cdot S}{\left[E_{eff} \cdot A_f + E_{paint} \cdot A_b \right] \cdot Sig} \right]$$

$$T.op = 296.626$$

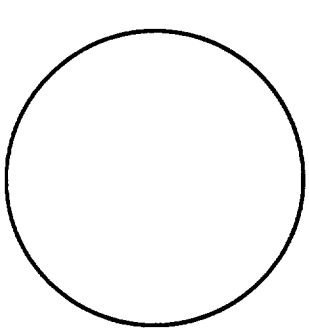

Geometry A

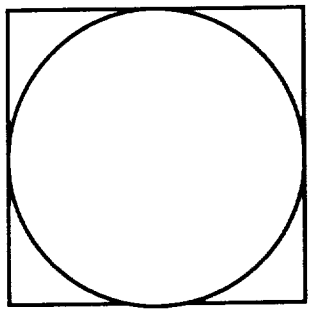

Geometry B

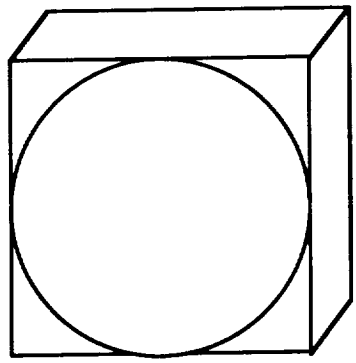

Geometry C

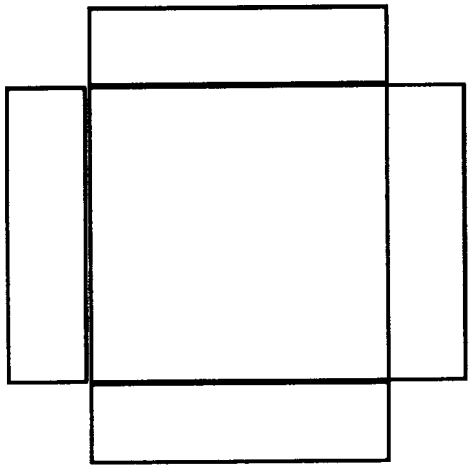

Geometry D

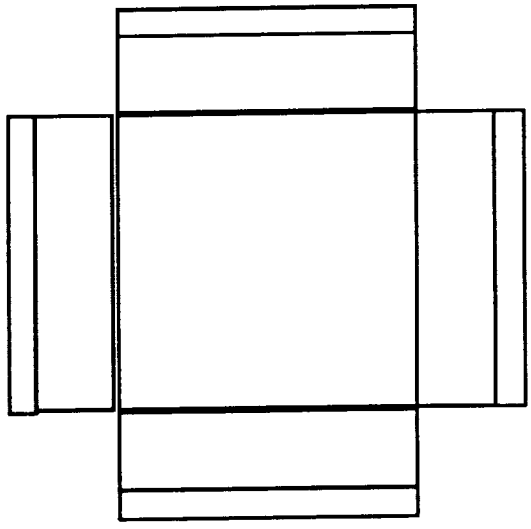

Geometry E

Figure A8.1

APPENDIX I - THERMAL ANALYSIS

This Mathcad calculation sheet is used for estimating the operating temperature of the batteries. These sheets were done prior to the developmen of the PC-ITAS stand alone thermal model. The sheets were used for initial sizing estimates of the battery radiator area and battery heaters.

Battery Temperature File

Battery parameters:

Radiator mounted surface
0.23x0.32 m

$A1 := 0.04$

Required watts dissipated
27 watts at 5 deg C

$W1 := 27$
$T1 := 283$

OSR radiator parameters:

Emissivity (EOL)
Absortivity (EOL)
Radiator efficiency

$e := 0.8$
$a := 0.145$
$n := .95$

Other parameters:

Boltzmans constant
Sun incident angle
Solar flux
Albedo flux

$sig := 5.67 \cdot 10^{-8}$
$È := 90$
$S := 1397$
$Alb := 79.4$

For a first cut at sizing assume that the radiator is the same size as battery face and that it looks into space without any solar impingement irradiation by other components. The heat balance equation is then:

$$T := \left[\frac{W1}{e \cdot sig \cdot n \cdot A1} \right]^{\frac{1}{4}}$$

$T = 353.775$ Too Hot!

Redefining the problem, what radiator area is required for 54 watts a
5 deg C?

$$A := \left[\frac{W1}{e \cdot sig \cdot n \cdot T1^4}\right] \qquad A = 0.098$$

This means that the radiator is 3 times bigger than the conduction path area. This can be done but radiator efficiency will be lower so try problem with lower assumed efficiency.

$$n := .85$$

$$A := \left[\frac{W1}{\left[e \cdot sig \cdot n \cdot T1^4\right]}\right] \qquad A = 0.109$$

$$Side := \sqrt{A} \qquad Side = 0.33$$

The battery heats up during discharge which means that it is in earth sensing mode not sun pointing. In earth pointing it is likely that the radiator will be in sun view at least for some part of the orbit therfore we need a heat balance equation that includes sun impingement (assume a 90 deg incidence) and earth reflection (assume all reflected energy hits the radiator) .

$$È1 := \frac{È}{360} \cdot 2 \cdot$$

$$T := \left[\frac{(W1 + a \cdot A \cdot S \cdot \sin(È1) + a \cdot A \cdot Alb)}{(e \cdot sig \cdot n \cdot A)}\right]^{\left[\frac{1}{4}\right]} \qquad T = 330.74$$

Too Hot!

If we are at an average theta of only 30 degrees, which is reasonable when in earth pointing mode we are not inertially fixed, then

$$È := 30$$

È

$$T := \left[\frac{(W1 + a \cdot A \cdot S \cdot \sin(È1) + a \cdot A \cdot Alb)}{(e \cdot sig \cdot n \cdot A)}\right]^{\left[\frac{1}{4}\right]}$$

T = 310.87

Too Hot!

Again redefining the problem, what radiator area is required for 54 watts at 5 deg C with sun impingement at theta = 30 deg ? (even smaller efficiency)

n := .75

$$A := \left[\frac{W1}{e \cdot sig \cdot n \cdot T1^{4} - a \cdot S \cdot \sin(È1) - a \cdot Alb}\right]$$

A = 0.

Side :=

Side =

Finally we need to consider any other heat sources which may affect th battery such as internal radiation from other components or conduction heat leaks from components mounted on the same panel. Combining these make a guess of an additional 50 watts which would need to be dissipat (still maintain the radiator at 5 deg C).

$$A := \left[\frac{W1 + 50}{e \cdot sig \cdot n \cdot T1^{4} - a \cdot S \cdot \sin(È1) - a \cdot Alb}\right]$$

A = 0.73

Side := \

Side = 0.

This results in a radiator that is approximately 0.92 square meter (pe: battery).

Since only the battery is required to be at less than 5 deg C we may s: able to go with a 0.30 sq. meter radiator if we were to mount the batt that it was adiabatic with respect to the S/C bus.

Additionally what power is required for the heater to maintain the batteries at C in full shadow , ie now other thermal inputs except charging heat plus. done f radiator of 0.256 sq m area

$P := 21.5$

$A := 0.256$

$$T := \left[\frac{W1 + P}{e \cdot sig \cdot n \cdot A}\right]^{\frac{1}{4}}$$

$T = 273.176$

APPENDIX I - THERMAL ANALYSIS

The PC-ITAS thermal analysis program was used to develop an analytical model of the spacecraft. The model consists of user defined geometric nodes and associated internal nodes which together represent the spacecraft system. Table A8.1 is a listing of major components and the nodes which represent them in the model.

NODE NUMBER	COMPONENT
63	SPACE SINK
101 - 106	PAYLOAD BOX
199	PAYLOAD BOX CENTRAL NODE (FOR MASS)
301 - 304	+X HONEYCOMB PANEL
501 - 504	-X HONEYCOMB PANEL
701 - 704	+Y HONEYCOMB PANEL
901 - 904	-Y HONEYCOMB PANEL
1101 - 1104	PAYLOAD INTERFACE PANEL
1301 - 1304	CLOSEOUT BLANKETS ON ANTI EARTH SIDE
1401 - 1408	SOLAR ARRAYS
1199,1299,1399	CENTER CYLINDER AND INTERNAL HARDWARE
2201 - 2299	ANTENNA
20304 and 20504	BATTERIES
20702 and 20902	EPS ELECTRONICS
20704 and 20904	TT&C ELECTRONICS
All other 20xxx	VARIOUS LOW DISSIPATION HARDWARE

TABLE A8.1

APPENDIX I - THERMAL ANALYSIS

Additionally values need to be set for a number of parameters. These include:

1) Orbital parameters

2) Incident flux settings

3) Component thermal masses

4) Optical surface properties

5) Conductive and radiative conductances

The parameters are different for the hot (earth sensing) and cold(stand-by) cases. The following pages are a summary of parameters used in the development of the PC-ITAS thermal model.

1) Orbital parameters:

Hot case:

Earth pointing vehicle

Non-spinning

Altitude = 275 NM

Longitude of ascending node = 90 deg

Inclination = 70 deg

Sun inclination = 23 deg

S/C rotations X=90/Y=00/Z=00

Cold case:

Sun pointing vehicle

Non-spinning

Altitude = 275 NM

Longitude of ascending node = 0 deg

Inclination = 70 deg

Sun inclination = 23 deg

S/C rotations X=0/Y=-90/Z=90

2) Incident flux settings:

Solar flux hot case = 1340 W/m^2

Solar flux cold case = 1310 W/m^2

Albedo hot case:

$$f_A = \frac{(S \cdot a)}{8} \cdot \left(1 - \sqrt{1 - \frac{R_e^2}{d^2}}\right) = \frac{(1390 \cdot 3)}{8} \cdot \left(1 - \sqrt{1 - \frac{6378^2}{6886^2}}\right) = 325 \ \frac{W}{m^2}$$

Albedo cold case:

$$f_A = \frac{(S \cdot a)}{8} \cdot \left(1 - \sqrt{1 - \frac{R_e^2}{d^2}}\right) = \frac{(1310 \cdot 3)}{8} \cdot \left(1 - \sqrt{1 - \frac{6378^2}{6886^2}}\right) = 306 \ \frac{W}{m^2}$$

Thermal radiation of earth hot case:

$$f_T = \frac{1}{2} \cdot f_r \cdot \left(1 - \sqrt{1 - \frac{R_e^2}{d^2}}\right) = \frac{1}{2} \cdot 244 \cdot \left(1 - \sqrt{1 - \frac{6378^2}{6886^2}}\right) = 76 \frac{W}{m^2}$$

Thermal radiation of earth hot case:

$$f_T = \frac{1}{2} \cdot f_r \cdot \left(1 - \sqrt{1 - \frac{R_e^2}{d^2}}\right) = \frac{1}{2} \cdot 230 \cdot \left(1 - \sqrt{1 - \frac{6378^2}{6886^2}}\right) = 72 \frac{W}{m^2}$$

3) Component thermal masses:

The inner workings of most electrical boxes and mechanical devices vary in composition. It was not possible to determine exact materials used in all components so for developing their thermal masses it is assumed that their total mass is made from aluminum. Most components use aluminum as part of the housing at the minimum. For a more realistic analysis each component thermal mass would need to be calculated individual based on the inner workings and construction of the piece. The following formula was used to generate our thermal masses:

$$\text{Thermal mass } \left(\frac{W \cdot \min}{°C}\right) = \text{Mass (kg)} \cdot \text{Al Specific heat } \left(\frac{kJ}{kg \cdot °C}\right) \cdot \frac{1000}{60}$$

4) Optical surface properties:

The PC-ITAS software come with a 350+ catalog of often used surface materials. The following materials were used through out the development of the model:

MATERIAL	ABSORPTIVITY	EMISSIVITY
OPTICAL SOLAR REFLECTORS	0.08 to 0.12	0.8

MULTI LAYER INSULATION	0.35	0.5
WHITE PAINT	0.5	0.8
BLACK PAINT	0.94	0.9
ANODYZE	0.36	0.68
ALUMINUM 6061-T6	0.41	0.04

TABLE A8.2

5) Conductances:

In addition to the radiative coupling that occurs between components aboard the spacecraft a number of conductive coupling terms have to be defined as well. Among these are the panel conductances between adjacent panel nodes, electronics box to mounting surface, payload to bus, etc.. Examples of these types of calculations are given below.

Panel conductances terms: The conductive heat path on a 4 node pane is a function of the cross sectional area of the path, the distance between the nodes, and the material of which the panel is constructed. For the side honeycomb panels of the bus we have the following situation:

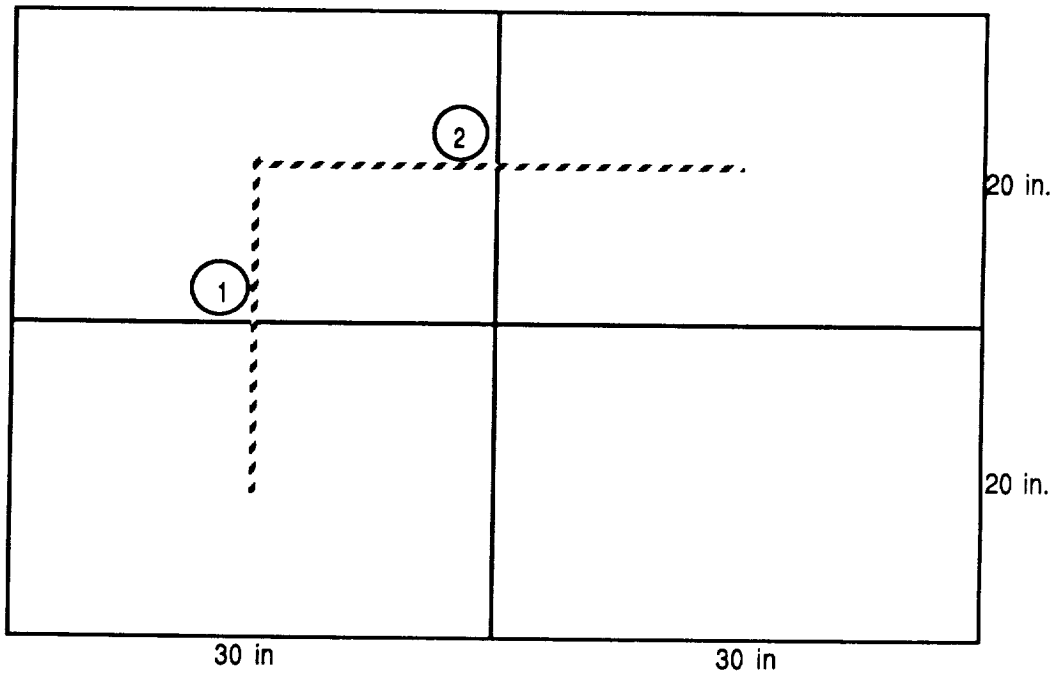

Figure A8.2

For conductance path 1 we have,

$$\text{Conductance} = \frac{K \cdot A}{L} = \frac{2.04 \frac{W}{cm \cdot °C} \cdot 15.2\ cm^2}{50.8\ cm} = 0.61 \frac{W}{°C}$$

similarly for path 2 we have,

$$\text{Conductance} = \frac{2.04 \frac{W}{cm \cdot °C} \cdot 10.1\ cm^2}{76.2\ cm} = 0.27 \frac{W}{°C}$$

assuming a 1 mm skin thickness and ignoring the cell material contribution.

APPENDIX I - THERMAL ANALYSIS

Hardware mounting terms: It is assumed that all hardware mounting is done with #10 screws or 0.25 in bolts. The number of bolts attaching the hardware will depend on the mass of the box and was estimated for the model. The conductance is again a function of the area of the heat path, the distance traversed, and the bolt material. Some boxes are mounted so that one of their sides is flush against the mounting surface. In these cases the temperature gradient between the box and the mounting surface would be negligible, this means that the conductance term is very high. We used 100 $\frac{W}{°C}$ for the conductance which is several orders of magnitude higher than if just the bolts were used as the heat paths.

In situations where the hardware is mounted using stand-offs, or if only a small area of the equipment comes in contact with the mounting surface, then the conductance is determined by looking at the attachment bolts. Looking at Figure A8.3

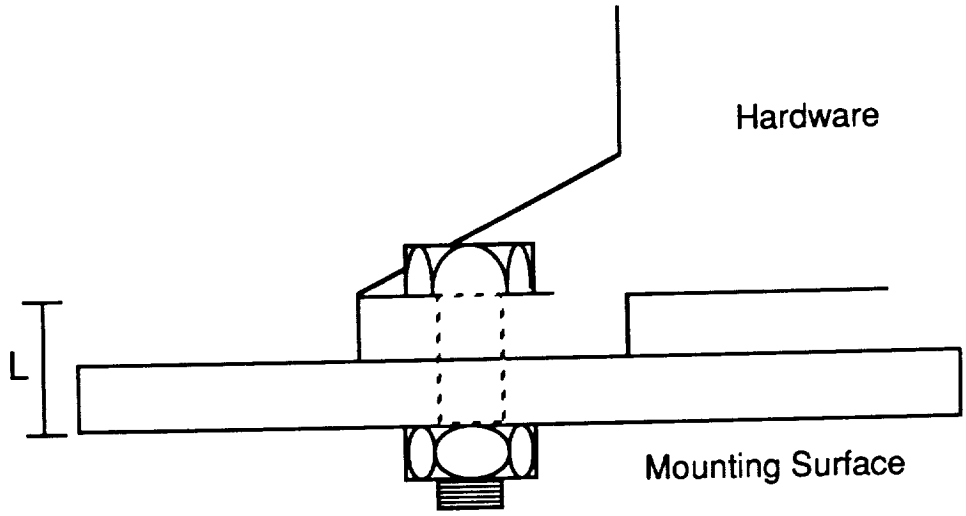

Figure A8.3

APPENDIX I - THERMAL ANALYSIS

The following output is generated by the PC-ITAS program the first file is the stand alone thermal model output which lists all the information regarding the node network and important parameters. The second file is the results file which is a tabular record of the results from a steady stste analyses. Tabular hardcopy of transient analyses was not available in ascii format.

These files are representative of the output form PC-ITAS but are not the latest versions of the model, and are included for completeness only.

FILE 1:

```
!   #OF THERMAL NODES, #OF SURFACES, ORBIT PERIOD(MIN)
        84        84   94.7700
!   ACTUAL NODE NUMBERS
       101       102       103       104       105       106
       301       302       303       304       501       502
       503       504       701       702       703       704
       901       902       903       904      1101      1102
      1103      1104      1301      1302      1303      1304
      1401      1402      1403      1404      1405      1406
      1407      1408      2201      2202      2203      2204
      2205      2206      2207      2208      2209      2210
      2211      2212      2213      2214      2215      2216
      2217      2218      2219      2220      2221      2222
      2223      2224        63       199      2299     20301
     20302     20303     20304     20501     20502     20503
     20504     20701     20702     20703     20704     20901
     20902     20903     20904      1199      1299      1399
!   ACTUAL NODE NUMBER POINTERS
         1         2         3         4         5         6
         7         8         9        10        11        12
        13        14        15        16        17        18
        19        20        21        22        23        24
        25        26        27        28        29        30
        31        32        33        34        35        36
```

```
      37      38      39      40      41      42
      43      44      45      46      47      48
      49      50      51      52      53      54
      55      56      57      58      59      60
      61      62      63      64      65      66
      67      68      69      70      71      72
      73      74      75      76      77      78
      79      80      81      82      83      84
!-------------------------------------------------------------
---------
!     POWR: orbital_absorbed_POWeR
!     MASS: thermal_MASS
!    COND: linear_CONDuctance
!     RAD : RADiative_conductance
!    NODE: boundary_NODE
!-------------------------------------------------------------
---------
POWR          101    94.77    110.85
                0.00    48.83
                7.90    48.71
               15.79    49.45
               23.69    50.09
               31.59   142.31
               39.49   209.12
               47.38   234.76
               55.28   216.37
               63.18   153.65
               71.08    62.44
               78.97    60.10
               86.87    54.32
               94.77    48.83
POWR          102    94.77     51.12
                0.00    48.15
                7.90    48.20
               15.79    48.18
               23.69    48.10
               31.59    48.18
               39.49    48.20
               47.38    48.16
               55.28    51.81
```

```
                63.18    56.91
                71.08    58.82
                78.97    56.91
                86.87    51.81
                94.77    48.15
POWR      103   94.77   459.76
                0.00   412.25
                7.90   471.44
                15.79  514.73
                23.69  536.07
                31.59  522.74
                39.49  476.31
                47.38  412.66
                55.28  426.44
                63.18  438.28
                71.08  442.52
                78.97  437.86
                86.87  425.87
                94.77  412.25
POWR      104   94.77   109.51
                0.00   234.02
                7.90   208.31
                15.79  135.72
                23.69   49.28
                31.59   48.61
                39.49   47.84
                47.38   47.92
                55.28   53.31
                63.18   59.09
                71.08   61.59
                78.97  152.84
                86.87  215.62
                94.77  234.02
POWR      105   94.77   562.42
                0.00   558.84
                7.90   556.14
                15.79  556.61
                23.69  556.87
                31.59  556.69
                39.49  556.32
```

```
                47.38    559.11
                55.28    566.31
                63.18    571.51
                71.08    573.31
                78.97    571.33
                86.87    566.03
                94.77    558.84
POWR        106    94.77    74.22
                0.00     7.46
                7.90    94.51
                15.79    51.16
                23.69    47.66
                31.59    51.16
                39.49    94.53
                47.38     7.49
                55.28   148.96
                63.18    81.73
                71.08    75.30
                78.97    81.73
                86.87   148.97
                94.77     7.46
POWR        301    94.77    37.33
                0.00    14.92
                7.90    15.31
                15.79   16.21
                23.69   17.18
                31.59   49.42
                39.49   72.31
                47.38   80.46
                55.28   74.02
                63.18   52.02
                71.08   20.01
                78.97   19.12
                86.87   16.97
                94.77   14.92
POWR        302    94.77    40.53
                0.00    15.83
                7.90    18.48
                15.79   22.62
                23.69   27.32
```

		31.59	59.47
		39.49	79.80
		47.38	83.77
		55.28	69.43
		63.18	47.21
		71.08	22.53
		78.97	21.37
		86.87	18.57
		94.77	15.83
POWR	303	94.77	37.19
		0.00	14.92
		7.90	15.31
		15.79	16.21
		23.69	17.18
		31.59	49.42
		39.49	72.31
		47.38	80.46
		55.28	74.02
		63.18	50.39
		71.08	20.01
		78.97	19.12
		86.87	16.97
		94.77	14.92
POWR	304	94.77	32.54
		0.00	22.33
		7.90	23.55
		15.79	25.44
		23.69	27.51
		31.59	42.28
		39.49	51.58
		47.38	53.39
		55.28	40.36
		63.18	30.34
		71.08	25.32
		78.97	24.86
		86.87	23.59
		94.77	22.33
POWR	501	94.77	37.25
		0.00	80.40
		7.90	72.22

		15.79	49.32
		23.69	17.10
		31.59	16.12
		39.49	15.22
		47.38	14.82
		55.28	16.86
		63.18	19.02
		71.08	19.95
		78.97	51.96
		86.87	73.96
		94.77	80.40
POWR	502	94.77	40.51
		0.00	83.77
		7.90	79.77
		15.79	59.42
		23.69	27.29
		31.59	22.59
		39.49	18.45
		47.38	15.80
		55.28	18.54
		63.18	21.33
		71.08	22.52
		78.97	47.21
		86.87	69.43
		94.77	83.77
POWR	503	94.77	37.17
		0.00	80.45
		7.90	72.28
		15.79	49.27
		23.69	17.16
		31.59	16.19
		39.49	15.29
		47.38	14.90
		55.28	16.94
		63.18	19.10
		71.08	20.00
		78.97	50.39
		86.87	74.01
		94.77	80.45
POWR	504	94.77	32.52

```
                0.00    53.37
                7.90    51.55
               15.79    42.24
               23.69    27.49
               31.59    25.40
               39.49    23.51
               47.38    22.30
               55.28    23.55
               63.18    24.83
               71.08    25.30
               78.97    30.32
               86.87    40.35
               94.77    53.37
POWR          701    94.77    196.69
                0.00   194.93
                7.90   194.88
               15.79   195.72
               23.69   196.06
               31.59   195.73
               39.49   194.89
               47.38   194.95
               55.28   197.43
               63.18   199.22
               71.08   199.85
               78.97   199.20
               86.87   197.41
               94.77   194.93
POWR          702    94.77    101.74
                0.00   107.87
                7.90   109.88
               15.79   111.83
               23.69   112.56
               31.59   111.84
               39.49   109.89
               47.38   107.87
               55.28    95.42
               63.18    86.28
               71.08    82.82
               78.97    87.76
               86.87    96.86
```

```
                94.77   107.87
POWR        703   94.77   196.71
                0.00   194.94
                7.90   194.91
                15.79   195.76
                23.69   196.10
                31.59   195.77
                39.49   194.92
                47.38   194.96
                55.28   197.43
                63.18   199.23
                71.08   199.86
                78.97   199.22
                86.87   197.42
                94.77   194.94
POWR        704   94.77   101.77
                0.00   107.89
                7.90   109.92
                15.79   111.87
                23.69   112.59
                31.59   111.87
                39.49   109.92
                47.38   107.90
                55.28   96.90
                63.18   87.80
                71.08   82.84
                78.97   86.31
                86.87   95.45
                94.77   107.89
POWR        901   94.77   15.80
                0.00   14.66
                7.90   14.72
                15.79   14.71
                23.69   14.64
                31.59   14.71
                39.49   14.72
                47.38   14.66
                55.28   16.07
                63.18   17.98
                71.08   18.69
```

```
                78.97    17.97
                86.87    16.07
                94.77    14.66
POWR      902   94.77    22.91
                0.00     22.16
                7.90     22.27
                15.79    22.26
                23.69    22.12
                31.59    22.26
                39.49    22.27
                47.38    22.16
                55.28    23.10
                63.18    24.25
                71.08    24.67
                78.97    24.25
                86.87    23.10
                94.77    22.16
POWR      903   94.77    15.80
                0.00     14.66
                7.90     14.72
                15.79    14.71
                23.69    14.64
                31.59    14.71
                39.49    14.72
                47.38    14.66
                55.28    16.07
                63.18    17.98
                71.08    18.69
                78.97    17.97
                86.87    16.07
                94.77    14.66
POWR      904   94.77    22.91
                0.00     22.16
                7.90     22.27
                15.79    22.26
                23.69    22.12
                31.59    22.26
                39.49    22.27
                47.38    22.16
                55.28    23.10
```

```
                63.18    24.25
                71.08    24.67
                78.97    24.25
                86.87    23.10
                94.77    22.16
POWR      1101  94.77    30.04
                0.00     0.00
                7.90     0.00
                15.79    0.00
                23.69    0.00
                31.59    0.00
                39.49    0.00
                47.38    0.02
                55.28    48.31
                63.18    83.66
                71.08    96.59
                78.97    83.64
                86.87    48.28
                94.77    0.00
POWR      1102  94.77    30.04
                0.00     0.00
                7.90     0.00
                15.79    0.00
                23.69    0.00
                31.59    0.00
                39.49    0.00
                47.38    0.02
                55.28    48.31
                63.18    83.66
                71.08    96.59
                78.97    83.64
                86.87    48.28
                94.77    0.00
POWR      1103  94.77    30.04
                0.00     0.00
                7.90     0.00
                15.79    0.00
                23.69    0.00
                31.59    0.00
                39.49    0.00
```

		47.38	0.02
		55.28	48.31
		63.18	83.66
		71.08	96.59
		78.97	83.64
		86.87	48.28
		94.77	0.00
POWR	1104	94.77	30.04
		0.00	0.00
		7.90	0.00
		15.79	0.00
		23.69	0.00
		31.59	0.00
		39.49	0.00
		47.38	0.02
		55.28	48.31
		63.18	83.66
		71.08	96.59
		78.97	83.64
		86.87	48.28
		94.77	0.00
POWR	1301	94.77	23.49
		0.00	3.90
		7.90	42.92
		15.79	31.25
		23.69	29.31
		31.59	28.75
		39.49	41.18
		47.38	3.85
		55.28	26.36
		63.18	16.23
		71.08	15.37
		78.97	16.28
		86.87	26.45
		94.77	3.90
POWR	1302	94.77	23.51
		0.00	3.87
		7.90	41.20
		15.79	28.78
		23.69	29.33

```
                31.59    31.28
                39.49    42.94
                47.38     3.91
                55.28    26.46
                63.18    16.30
                71.08    15.38
                78.97    16.25
                86.87    26.38
                94.77     3.87
POWR            1303     94.77    17.62
                 0.00     3.78
                 7.90    36.20
                15.79    13.85
                23.69     9.96
                31.59    10.52
                39.49    33.89
                47.38     3.73
                55.28    26.12
                63.18    15.98
                71.08    15.12
                78.97    16.03
                86.87    26.20
                94.77     3.78
POWR            1304     94.77    17.62
                 0.00     3.74
                 7.90    33.88
                15.79    10.52
                23.69     9.96
                31.59    13.85
                39.49    36.20
                47.38     3.78
                55.28    26.20
                63.18    16.03
                71.08    15.11
                78.97    15.98
                86.87    26.13
                94.77     3.74
POWR            1401     94.77   132.22
                 0.00    96.41
                 7.90   118.76
```

		15.79	151.03
		23.69	188.52
		31.59	187.22
		39.49	161.80
		47.38	120.29
		55.28	119.86
		63.18	117.26
		71.08	112.69
		78.97	109.56
		86.87	103.20
		94.77	96.41
POWR	1402	94.77	82.37
		0.00	0.01
		7.90	0.01
		15.79	0.01
		23.69	0.01
		31.59	0.01
		39.49	0.01
		47.38	0.05
		55.28	132.44
		63.18	229.35
		71.08	264.81
		78.97	229.31
		86.87	132.38
		94.77	0.01
POWR	1403	94.77	131.16
		0.00	119.34
		7.90	160.82
		15.79	186.16
		23.69	187.39
		31.59	149.94
		39.49	117.66
		47.38	95.32
		55.28	102.07
		63.18	108.47
		71.08	111.60
		78.97	116.29
		86.87	118.91
		94.77	119.34
POWR	1404	94.77	82.37

```
                0.00    0.01
                7.90    0.01
               15.79    0.01
               23.69    0.01
               31.59    0.01
               39.49    0.01
               47.38    0.05
               55.28  132.44
               63.18  229.35
               71.08  264.81
               78.97  229.31
               86.87  132.38
               94.77    0.01
POWR    1405   94.77  193.30
                0.00  165.99
                7.90  210.25
               15.79  244.27
               23.69  256.56
               31.59  244.27
               39.49  210.24
               47.38  166.04
               55.28  165.11
               63.18  164.34
               71.08  163.20
               78.97  164.28
               86.87  165.06
               94.77  165.99
POWR    1406   94.77   82.37
                0.00    0.01
                7.90    0.01
               15.79    0.01
               23.69    0.01
               31.59    0.01
               39.49    0.01
               47.38    0.05
               55.28  132.44
               63.18  229.35
               71.08  264.81
               78.97  229.31
               86.87  132.38
```

		94.77	0.01
POWR	1407	94.77	99.11
		0.00	94.16
		7.90	96.01
		15.79	96.05
		23.69	93.66
		31.59	96.05
		39.49	96.01
		47.38	94.16
		55.28	100.48
		63.18	106.76
		71.08	108.80
		78.97	106.75
		86.87	100.48
		94.77	94.16
POWR	1408	94.77	82.37
		0.00	0.01
		7.90	0.01
		15.79	0.01
		23.69	0.01
		31.59	0.01
		39.49	0.01
		47.38	0.05
		55.28	132.44
		63.18	229.35
		71.08	264.81
		78.97	229.31
		86.87	132.38
		94.77	0.01
POWR	2201	94.77	0.66
		0.00	0.34
		7.90	0.75
		15.79	1.04
		23.69	1.19
		31.59	1.09
		39.49	0.77
		47.38	0.33
		55.28	0.43
		63.18	0.51
		71.08	0.54

	78.97	0.51	
	86.87	0.43	
	94.77	0.34	
POWR	2202	94.77	3.23
	0.00	2.57	
	7.90	3.45	
	15.79	4.38	
	23.69	4.69	
	31.59	3.75	
	39.49	2.88	
	47.38	2.56	
	55.28	2.77	
	63.18	2.95	
	71.08	3.02	
	78.97	2.96	
	86.87	2.78	
	94.77	2.57	
POWR	2203	94.77	1.24
	0.00	0.37	
	7.90	0.70	
	15.79	0.95	
	23.69	1.06	
	31.59	0.99	
	39.49	0.72	
	47.38	1.22	
	55.28	2.04	
	63.18	2.43	
	71.08	2.26	
	78.97	1.57	
	86.87	0.52	
	94.77	0.37	
POWR	2204	94.77	2.82
	0.00	2.55	
	7.90	2.69	
	15.79	3.02	
	23.69	3.19	
	31.59	2.87	
	39.49	2.67	
	47.38	2.54	
	55.28	2.74	

		63.18	2.92
		71.08	2.99
		78.97	2.93
		86.87	2.76
		94.77	2.55
POWR	2205	94.77	2.50
		0.00	2.01
		7.90	1.24
		15.79	0.90
		23.69	0.87
		31.59	1.26
		39.49	2.06
		47.38	2.85
		55.28	3.68
		63.18	4.18
		71.08	4.21
		78.97	3.76
		86.87	2.95
		94.77	2.01
POWR	2206	94.77	2.75
		0.00	2.54
		7.90	2.67
		15.79	2.80
		23.69	2.85
		31.59	2.80
		39.49	2.67
		47.38	2.53
		55.28	2.72
		63.18	2.89
		71.08	2.96
		78.97	2.90
		86.87	2.73
		94.77	2.54
POWR	2207	94.77	2.29
		0.00	2.71
		7.90	1.86
		15.79	1.01
		23.69	0.58
		31.59	0.62
		39.49	1.00

		47.38	1.83
		55.28	2.76
		63.18	3.56
		71.08	4.01
		78.97	4.00
		86.87	3.52
		94.77	2.71
POWR	2208	94.77	2.75
		0.00	2.53
		7.90	2.67
		15.79	2.80
		23.69	2.85
		31.59	2.80
		39.49	2.67
		47.38	2.54
		55.28	2.73
		63.18	2.90
		71.08	2.96
		78.97	2.89
		86.87	2.72
		94.77	2.53
POWR	2209	94.77	0.82
		0.00	1.05
		7.90	0.29
		15.79	0.32
		23.69	0.31
		31.59	0.26
		39.49	0.19
		47.38	0.11
		55.28	0.22
		63.18	1.22
		71.08	1.88
		78.97	2.11
		86.87	1.81
		94.77	1.05
POWR	2210	94.77	2.82
		0.00	2.54
		7.90	2.67
		15.79	2.87
		23.69	3.19

		31.59	3.01
		39.49	2.69
		47.38	2.55
		55.28	2.76
		63.18	2.93
		71.08	2.99
		78.97	2.92
		86.87	2.74
		94.77	2.54
POWR	2211	94.77	0.37
		0.00	0.26
		7.90	0.47
		15.79	0.60
		23.69	0.64
		31.59	0.56
		39.49	0.39
		47.38	0.18
		55.28	0.23
		63.18	0.27
		71.08	0.29
		78.97	0.31
		86.87	0.30
		94.77	0.26
POWR	2212	94.77	3.23
		0.00	2.56
		7.90	2.88
		15.79	3.75
		23.69	4.69
		31.59	4.38
		39.49	3.45
		47.38	2.57
		55.28	2.78
		63.18	2.96
		71.08	3.02
		78.97	2.95
		86.87	2.77
		94.77	2.56
POWR	2213	94.77	1.15
		0.00	0.68
		7.90	1.26

		15.79	1.69
		23.69	1.90
		31.59	1.76
		39.49	1.30
		47.38	0.68
		55.28	0.82
		63.18	0.95
		71.08	0.99
		78.97	0.94
		86.87	0.81
		94.77	0.68
POWR	2214	94.77	5.43
		0.00	2.99
		7.90	7.41
		15.79	10.08
		23.69	9.84
		31.59	8.91
		39.49	6.04
		47.38	2.97
		55.28	3.23
		63.18	3.44
		71.08	3.52
		78.97	3.45
		86.87	3.25
		94.77	2.99
POWR	2215	94.77	1.85
		0.00	0.68
		7.90	1.09
		15.79	1.40
		23.69	1.54
		31.59	1.45
		39.49	2.03
		47.38	2.74
		55.28	3.43
		63.18	3.40
		71.08	2.64
		78.97	1.07
		86.87	0.78
		94.77	0.68
POWR	2216	94.77	3.56

		0.00	2.96
		7.90	4.26
		15.79	4.92
		23.69	4.47
		31.59	3.44
		39.49	3.13
		47.38	2.93
		55.28	3.16
		63.18	3.37
		71.08	3.46
		78.97	3.40
		86.87	3.20
		94.77	2.96
POWR	2217	94.77	5.57
		0.00	4.49
		7.90	3.83
		15.79	3.63
		23.69	3.93
		31.59	4.65
		39.49	5.60
		47.38	6.54
		55.28	7.30
		63.18	7.57
		71.08	7.30
		78.97	6.54
		86.87	5.51
		94.77	4.49
POWR	2218	94.77	3.19
		0.00	2.92
		7.90	3.12
		15.79	3.30
		23.69	3.36
		31.59	3.29
		39.49	3.11
		47.38	2.91
		55.28	3.11
		63.18	3.32
		71.08	3.40
		78.97	3.33
		86.87	3.13

```
                94.77     2.92
POWR          2219      94.77      5.26
                0.00      6.27
                7.90      5.29
               15.79      4.30
               23.69      3.56
               31.59      3.26
               39.49      3.49
               47.38      4.20
               55.28      5.22
               63.18      6.24
               71.08      6.99
               78.97      7.28
               86.87      7.01
               94.77      6.27
POWR          2220      94.77      3.19
                0.00      2.91
                7.90      3.11
               15.79      3.29
               23.69      3.36
               31.59      3.30
               39.49      3.12
               47.38      2.92
               55.28      3.13
               63.18      3.33
               71.08      3.40
               78.97      3.32
               86.87      3.11
               94.77      2.91
POWR          2221      94.77      1.16
                0.00      2.39
                7.90      1.27
               15.79      0.37
               23.69      0.35
               31.59      0.32
               39.49      0.28
               47.38      0.26
               55.28      0.27
               63.18      0.49
               71.08      2.04
```

		78.97	2.86
		86.87	2.99
		94.77	2.39
POWR	2222	94.77	3.56
		0.00	2.93
		7.90	3.13
		15.79	3.44
		23.69	4.47
		31.59	4.92
		39.49	4.26
		47.38	2.96
		55.28	3.20
		63.18	3.40
		71.08	3.46
		78.97	3.37
		86.87	3.16
		94.77	2.93
POWR	2223	94.77	0.57
		0.00	0.49
		7.90	0.67
		15.79	0.78
		23.69	0.79
		31.59	0.72
		39.49	0.56
		47.38	0.37
		55.28	0.42
		63.18	0.47
		71.08	0.49
		78.97	0.53
		86.87	0.52
		94.77	0.49
POWR	2224	94.77	5.43
		0.00	2.97
		7.90	6.04
		15.79	8.91
		23.69	9.84
		31.59	10.08
		39.49	7.41
		47.38	2.99
		55.28	3.25

		63.18	3.45
		71.08	3.52
		78.97	3.44
		86.87	3.23
		94.77	2.97
MASS	0	31.64371000	101
MASS	0	31.64371000	102
MASS	0	31.64371000	103
MASS	0	31.64371000	104
MASS	0	31.64371000	105
MASS	0	31.64371000	106
MASS	0	31.64371000	301
MASS	0	31.64371000	302
MASS	0	31.64371000	303
MASS	0	31.64371000	304
MASS	0	31.64371000	501
MASS	0	31.64371000	502
MASS	0	31.64371000	503
MASS	0	31.64371000	504
MASS	0	31.64371000	701
MASS	0	31.64371000	702
MASS	0	31.64371000	703
MASS	0	31.64371000	704
MASS	0	31.64371000	901
MASS	0	31.64371000	902
MASS	0	31.64371000	903
MASS	0	31.64371000	904
MASS	0	31.64371000	1101
MASS	0	31.64371000	1102
MASS	0	31.64371000	1103
MASS	0	31.64371000	1104
MASS	0	31.64371000	1301
MASS	0	31.64371000	1302
MASS	0	31.64371000	1303
MASS	0	31.64371000	1304
MASS	0	31.64371000	1401
MASS	0	31.64371000	1402
MASS	0	31.64371000	1403
MASS	0	31.64371000	1404
MASS	0	31.64371000	1405

```
MASS   0          31.64371000      1406
MASS   0          31.64371000      1407
MASS   0          31.64371000      1408
MASS   0          31.64371000      2201
MASS   0          31.64371000      2202
MASS   0          31.64371000      2203
MASS   0          31.64371000      2204
MASS   0          31.64371000      2205
MASS   0          31.64371000      2206
MASS   0          31.64371000      2207
MASS   0          31.64371000      2208
MASS   0          31.64371000      2209
MASS   0          31.64371000      2210
MASS   0          31.64371000      2211
MASS   0          31.64371000      2212
MASS   0          31.64371000      2213
MASS   0          31.64371000      2214
MASS   0          31.64371000      2215
MASS   0          31.64371000      2216
MASS   0          31.64371000      2217
MASS   0          31.64371000      2218
MASS   0          31.64371000      2219
MASS   0          31.64371000      2220
MASS   0          31.64371000      2221
MASS   0          31.64371000      2222
MASS   0          31.64371000      2223
MASS   0          31.64371000      2224
NODE   200        199   -5420.00     0.00
NODE   200       2299    -298.00     0.00
NODE   200      20301    -596.00     0.00
POWR   00       20301       0.00     5.00
NODE   200      20302    -596.00     0.00
NODE   200      20303    -596.00     0.00
POWR   00       20303       0.00     5.00
NODE   200      20304    -298.00     0.00
POWR   00       20304       0.00    54.00
NODE   200      20501    -596.00     0.00
POWR   00       20501       0.00     5.00
NODE   200      20502    -596.00     0.00
NODE   200      20503    -596.00     0.00
```

```
POWR   00     20503      0.00      5.00
NODE   200    20504    -298.00     0.00
POWR   00     20504      0.00     54.00
NODE   200    20701    -596.00     0.00
POWR   00     20701      0.00     10.00
NODE   200    20702    -596.00     0.00
POWR   00     20702      0.00     35.00
NODE   200    20703    -596.00     0.00
POWR   00     20703      0.00     10.00
NODE   200    20704    -596.00     0.00
POWR   00     20704      0.00     35.00
NODE   200    20901    -596.00     0.00
POWR   00     20901      0.00     10.00
NODE   200    20902    -596.00     0.00
POWR   00     20902      0.00     35.00
NODE   200    20903    -596.00     0.00
POWR   00     20903      0.00     10.00
NODE   200    20904    -596.00     0.00
POWR   00     20904      0.00     35.00
NODE   200     1199    -298.00     0.00
NODE   200     1299    -894.00     0.00
POWR   00      1299      0.00     20.00
NODE   200     1399    -298.00     0.00
COND   00        100.00000000     1401     1402
COND   00        100.00000000     1403     1404
COND   00        100.00000000     1405     1406
COND   00        100.00000000     1407     1408
COND   00          0.50000000     1401      302
COND   00          0.50000000     1403      502
COND   00          0.50000000     1405      702
COND   00          0.50000000     1407      902
COND   00          0.61000000      301      302
COND   00          0.61000000      301      303
COND   00          0.61000000      501      502
COND   00          0.61000000      501      503
COND   00          0.61000000      701      702
COND   00          0.61000000      701      703
COND   00          0.61000000      901      902
COND   00          0.61000000      901      903
COND   00          0.41000000     1101     1102
```

COND	00	0.41000000	1101	1103
COND	00	0.41000000	1104	1102
COND	00	0.41000000	1104	1103
COND	00	0.41000000	1301	1302
COND	00	0.41000000	1301	1303
COND	00	0.41000000	1304	1302
COND	00	0.41000000	1304	1303
COND	00	100.00000000	301	20301
COND	00	100.00000000	302	20302
COND	00	100.00000000	303	20303
COND	00	100.00000000	304	20304
COND	00	100.00000000	501	20501
COND	00	100.00000000	502	20502
COND	00	100.00000000	503	20503
COND	00	100.00000000	504	20504
COND	00	100.00000000	701	20701
COND	00	100.00000000	702	20702
COND	00	100.00000000	703	20703
COND	00	100.00000000	704	20704
COND	00	100.00000000	901	20901
COND	00	100.00000000	902	20902
COND	00	100.00000000	903	20903
COND	00	100.00000000	904	20904
COND	00	1.00000000	106	1301
COND	00	1.00000000	106	1302
COND	00	1.00000000	106	1303
COND	00	1.00000000	106	1304
COND	00	100.00000000	2299	2201
COND	00	100.00000000	2299	2202
COND	00	100.00000000	2299	2203
COND	00	100.00000000	2299	2204
COND	00	100.00000000	2299	2205
COND	00	100.00000000	2299	2206
COND	00	100.00000000	2299	2207
COND	00	100.00000000	2299	2208
COND	00	100.00000000	2299	2209
COND	00	100.00000000	2299	2210
COND	00	100.00000000	2299	2211
COND	00	100.00000000	2299	2212
COND	00	100.00000000	2299	2213

COND	00	100.00000000	2299	2214
COND	00	100.00000000	2299	2215
COND	00	100.00000000	2299	2216
COND	00	100.00000000	2299	2217
COND	00	100.00000000	2299	2218
COND	00	100.00000000	2299	2219
COND	00	100.00000000	2299	2220
COND	00	100.00000000	2299	2221
COND	00	100.00000000	2299	2222
COND	00	100.00000000	2299	2223
COND	00	100.00000000	2299	2224
COND	00	0.05000000	2299	701
COND	00	0.05000000	2299	1301
COND	00	1000.00000000	101	199
COND	00	1000.00000000	102	199
COND	00	1000.00000000	103	199
COND	00	1000.00000000	104	199
COND	00	1000.00000000	105	199
COND	00	1000.00000000	106	199
COND	00	100.00000000	1199	1101
COND	00	100.00000000	1199	1102
COND	00	100.00000000	1199	1103
COND	00	100.00000000	1199	1104
COND	00	100.00000000	1399	1301
COND	00	100.00000000	1399	1302
COND	00	100.00000000	1399	1303
COND	00	100.00000000	1399	1304
COND	00	12.00000000	1199	1299
COND	00	12.00000000	1299	1399
RAD	00	0.1006893000E+01	101	302
RAD	00	0.1443846000E+01	101	304
RAD	00	0.9314020000E+02	101	1401
RAD	00	0.6716813000E+04	101	63
RAD	00	0.1442412000E+01	102	902
RAD	00	0.1442412000E+01	102	904
RAD	00	0.9304716000E+02	102	1407
RAD	00	0.6716475000E+04	102	63
RAD	00	0.6078452000E+00	103	1403
RAD	00	0.6470630000E+00	103	1405
RAD	00	0.5515839000E+02	103	2201

RAD	00	0.4195664000E+02	103	2203
RAD	00	0.1188134000E+02	103	2205
RAD	00	0.3411785000E+01	103	2207
RAD	00	0.5571794000E+01	103	2209
RAD	00	0.2457188000E+02	103	2211
RAD	00	0.7996828000E+02	103	2213
RAD	00	0.5318195000E+02	103	2215
RAD	00	0.4713123000E+01	103	2217
RAD	00	0.2184513000E+02	103	2223
RAD	00	0.1826218000E+05	103	63
RAD	00	0.1013158000E+01	104	502
RAD	00	0.1450090000E+01	104	504
RAD	00	0.9329594000E+02	104	1403
RAD	00	0.1774404000E+01	104	2207
RAD	00	0.6425112000E+01	104	2209
RAD	00	0.6211922000E+01	104	2211
RAD	00	0.4043107000E+01	104	2221
RAD	00	0.8671329000E+01	104	2223
RAD	00	0.6688377000E+04	104	63
RAD	00	0.1451518000E+01	105	702
RAD	00	0.1448634000E+01	105	704
RAD	00	0.9319384000E+02	105	1405
RAD	00	0.2122554000E+01	105	2203
RAD	00	0.8073335000E+01	105	2205
RAD	00	0.3901613000E+01	105	2207
RAD	00	0.3347648000E+01	105	2215
RAD	00	0.8612158000E+01	105	2217
RAD	00	0.1326407000E+01	105	2219
RAD	00	0.6687671000E+04	105	63
RAD	00	0.1969135000E+04	106	1301
RAD	00	0.1969135000E+04	106	1302
RAD	00	0.1969135000E+04	106	1303
RAD	00	0.1969135000E+04	106	1304
RAD	00	0.1135251000E+02	106	1401
RAD	00	0.1135495000E+02	106	1403
RAD	00	0.1134351000E+02	106	1405
RAD	00	0.1134117000E+02	106	1407
RAD	00	0.8278311000E+03	106	63
RAD	00	0.1022797000E+01	301	302
RAD	00	0.1466652000E+01	301	304

RAD	00	0.9500198000E+02	301	1401
RAD	00	0.1953476000E+04	301	63
RAD	00	0.1022797000E+01	302	303
RAD	00	0.6741600000E+01	302	304
RAD	00	0.4372773000E+03	302	1401
RAD	00	0.1599715000E+04	302	63
RAD	00	0.1466652000E+01	303	304
RAD	00	0.9500198000E+02	303	1401
RAD	00	0.1953476000E+04	303	63
RAD	00	0.6270392000E+03	304	1401
RAD	00	0.2293930000E+04	304	63
RAD	00	0.1023400000E+01	501	502
RAD	00	0.1467218000E+01	501	504
RAD	00	0.9501572000E+02	501	1403
RAD	00	0.5720519000E+00	501	2209
RAD	00	0.7108066000E+00	501	2221
RAD	00	0.6080289000E+00	501	2223
RAD	00	0.1950717000E+04	501	63
RAD	00	0.1023009000E+01	502	503
RAD	00	0.6741857000E+01	502	504
RAD	00	0.4372837000E+03	502	1403
RAD	00	0.1598366000E+04	502	63
RAD	00	0.1466864000E+01	503	504
RAD	00	0.9500698000E+02	503	1403
RAD	00	0.1952514000E+04	503	63
RAD	00	0.6270453000E+03	504	1403
RAD	00	0.2292660000E+04	504	63
RAD	00	0.1466072000E+01	701	702
RAD	00	0.1465766000E+01	701	704
RAD	00	0.9492072000E+02	701	1405
RAD	00	0.5733156000E+00	701	2205
RAD	00	0.8427280000E+00	701	2217
RAD	00	0.1950344000E+04	701	63
RAD	00	0.1465501000E+01	702	703
RAD	00	0.9657964000E+01	702	704
RAD	00	0.6264251000E+03	702	1405
RAD	00	0.5051766000E+00	702	2217
RAD	00	0.2289704000E+04	702	63
RAD	00	0.1465408000E+01	703	704
RAD	00	0.9491216000E+02	703	1405

RAD	00	0.1952173000E+04	703	63
RAD	00	0.6264222000E+03	704	1405
RAD	00	0.2290374000E+04	704	63
RAD	00	0.1465195000E+01	901	902
RAD	00	0.1465195000E+01	901	904
RAD	00	0.9490747000E+02	901	1407
RAD	00	0.1953130000E+04	901	63
RAD	00	0.1465195000E+01	902	903
RAD	00	0.9657597000E+01	902	904
RAD	00	0.6264163000E+03	902	1407
RAD	00	0.2291652000E+04	902	63
RAD	00	0.1465195000E+01	903	904
RAD	00	0.9490747000E+02	903	1407
RAD	00	0.1953130000E+04	903	63
RAD	00	0.6264163000E+03	904	1407
RAD	00	0.2291652000E+04	904	63
RAD	00	0.3077490000E+04	1101	63
RAD	00	0.3077490000E+04	1102	63
RAD	00	0.3077490000E+04	1103	63
RAD	00	0.3077490000E+04	1104	63
RAD	00	0.2223498000E+03	1301	1302
RAD	00	0.2223498000E+03	1301	1303
RAD	00	0.2223498000E+03	1301	1304
RAD	00	0.1282210000E+01	1301	1401
RAD	00	0.1285908000E+01	1301	1403
RAD	00	0.1284473000E+01	1301	1405
RAD	00	0.1280919000E+01	1301	1407
RAD	00	0.2125218000E+03	1301	63
RAD	00	0.2223498000E+03	1302	1303
RAD	00	0.2223498000E+03	1302	1304
RAD	00	0.1282204000E+01	1302	1401
RAD	00	0.1282622000E+01	1302	1403
RAD	00	0.1281759000E+01	1302	1405
RAD	00	0.1280911000E+01	1302	1407
RAD	00	0.2133831000E+03	1302	63
RAD	00	0.2223498000E+03	1303	1304
RAD	00	0.1282202000E+01	1303	1401
RAD	00	0.1283118000E+01	1303	1403
RAD	00	0.1281322000E+01	1303	1405
RAD	00	0.1280914000E+01	1303	1407

RAD	00	0.2133793000E+03	1303	63
RAD	00	0.1282202000E+01	1304	1401
RAD	00	0.1282475000E+01	1304	1403
RAD	00	0.1281173000E+01	1304	1405
RAD	00	0.1280911000E+01	1304	1407
RAD	00	0.2134987000E+03	1304	63
RAD	00	0.4562959000E+04	1401	63
RAD	00	0.5571884000E+04	1402	63
RAD	00	0.1638890000E+01	1403	2201
RAD	00	0.1789869000E+01	1403	2205
RAD	00	0.4016958000E+01	1403	2207
RAD	00	0.5227346000E+01	1403	2209
RAD	00	0.6058942000E+01	1403	2211
RAD	00	0.1137504000E+01	1403	2213
RAD	00	0.1002075000E+01	1403	2217
RAD	00	0.2618959000E+01	1403	2219
RAD	00	0.4990616000E+01	1403	2221
RAD	00	0.6873921000E+01	1403	2223
RAD	00	0.4526355000E+04	1403	63
RAD	00	0.5571884000E+04	1404	63
RAD	00	0.4581543000E+01	1405	2203
RAD	00	0.5761539000E+01	1405	2205
RAD	00	0.4560540000E+01	1405	2207
RAD	00	0.3164492000E+01	1405	2209
RAD	00	0.6577371000E+00	1405	2211
RAD	00	0.4701219000E+01	1405	2215
RAD	00	0.6178950000E+01	1405	2217
RAD	00	0.3654843000E+01	1405	2219
RAD	00	0.1779899000E+01	1405	2221
RAD	00	0.4378534000E+04	1405	63
RAD	00	0.5571884000E+04	1406	63
RAD	00	0.4415142000E+04	1407	63
RAD	00	0.5571884000E+04	1408	63
RAD	00	0.7361633000E+02	2201	63
RAD	00	0.2086344000E+01	2202	2204
RAD	00	0.2504221000E+01	2202	2206
RAD	00	0.2611904000E+01	2202	2208
RAD	00	0.2504221000E+01	2202	2210
RAD	00	0.2086344000E+01	2202	2212
RAD	00	0.2053159000E+01	2202	2214

RAD	00	0.2839348000E+01	2202	2216
RAD	00	0.3025947000E+01	2202	2218
RAD	00	0.3077459000E+01	2202	2220
RAD	00	0.3025947000E+01	2202	2222
RAD	00	0.2839348000E+01	2202	2224
RAD	00	0.1021829000E+03	2202	63
RAD	00	0.8140971000E+02	2203	63
RAD	00	0.2086344000E+01	2204	2206
RAD	00	0.2504221000E+01	2204	2208
RAD	00	0.2611904000E+01	2204	2210
RAD	00	0.2504221000E+01	2204	2212
RAD	00	0.2839348000E+01	2204	2214
RAD	00	0.2053159000E+01	2204	2216
RAD	00	0.2839348000E+01	2204	2218
RAD	00	0.3025947000E+01	2204	2220
RAD	00	0.3077459000E+01	2204	2222
RAD	00	0.3025947000E+01	2204	2224
RAD	00	0.1021829000E+03	2204	63
RAD	00	0.1016663000E+03	2205	63
RAD	00	0.2086344000E+01	2206	2208
RAD	00	0.2504221000E+01	2206	2210
RAD	00	0.2611904000E+01	2206	2212
RAD	00	0.3025947000E+01	2206	2214
RAD	00	0.2839348000E+01	2206	2216
RAD	00	0.2053159000E+01	2206	2218
RAD	00	0.2839348000E+01	2206	2220
RAD	00	0.3025947000E+01	2206	2222
RAD	00	0.3077459000E+01	2206	2224
RAD	00	0.1021829000E+03	2206	63
RAD	00	0.1115072000E+03	2207	63
RAD	00	0.2086344000E+01	2208	2210
RAD	00	0.2504221000E+01	2208	2212
RAD	00	0.3077459000E+01	2208	2214
RAD	00	0.3025947000E+01	2208	2216
RAD	00	0.2839348000E+01	2208	2218
RAD	00	0.2053159000E+01	2208	2220
RAD	00	0.2839348000E+01	2208	2222
RAD	00	0.3025947000E+01	2208	2224
RAD	00	0.1021829000E+03	2208	63
RAD	00	0.1083426000E+03	2209	63

RAD	00	0.2086344000E+01	2210	2212
RAD	00	0.3025947000E+01	2210	2214
RAD	00	0.3077459000E+01	2210	2216
RAD	00	0.3025947000E+01	2210	2218
RAD	00	0.2839348000E+01	2210	2220
RAD	00	0.2053159000E+01	2210	2222
RAD	00	0.2839348000E+01	2210	2224
RAD	00	0.1021829000E+03	2210	63
RAD	00	0.9220393000E+02	2211	63
RAD	00	0.2839348000E+01	2212	2214
RAD	00	0.3025947000E+01	2212	2216
RAD	00	0.3077459000E+01	2212	2218
RAD	00	0.3025947000E+01	2212	2220
RAD	00	0.2839348000E+01	2212	2222
RAD	00	0.2053159000E+01	2212	2224
RAD	00	0.1021829000E+03	2212	63
RAD	00	0.1006598000E+03	2213	63
RAD	00	0.5484510000E+01	2214	2216
RAD	00	0.4255825000E+01	2214	2218
RAD	00	0.4144866000E+01	2214	2220
RAD	00	0.4255825000E+01	2214	2222
RAD	00	0.5484494000E+01	2214	2224
RAD	00	0.1415008000E+03	2214	63
RAD	00	0.1198694000E+03	2215	63
RAD	00	0.5484510000E+01	2216	2218
RAD	00	0.4255825000E+01	2216	2220
RAD	00	0.4144866000E+01	2216	2222
RAD	00	0.4255825000E+01	2216	2224
RAD	00	0.1415008000E+03	2216	63
RAD	00	0.1590222000E+03	2217	63
RAD	00	0.5484494000E+01	2218	2220
RAD	00	0.4255825000E+01	2218	2222
RAD	00	0.4144866000E+01	2218	2224
RAD	00	0.1415008000E+03	2218	63
RAD	00	0.1725270000E+03	2219	63
RAD	00	0.5484510000E+01	2220	2222
RAD	00	0.4255825000E+01	2220	2224
RAD	00	0.1415008000E+03	2220	63
RAD	00	0.1690626000E+03	2221	63
RAD	00	0.5484510000E+01	2222	2224

```
RAD     00    0.1415008000E+03      2222      63
RAD     00    0.1423734000E+03      2223      63
RAD     00    0.1415008000E+03      2224      63
NODE   1 1       63     1.000     0.001
$$$$
!   END OF ITAS-FORMAT THERMAL MATH MODEL
```

FILE 2:

TIME= 0.00

NODE	IR_POWER	UV_POWER	TOT_POWER
101	48.12	0.71	48.83
102	48.12	0.03	48.15
103	409.42	2.83	412.25
104	47.18	186.84	234.02
105	47.17	511.68	558.84
106	6.47	0.99	7.46
301	14.65	0.27	14.92
302	15.45	0.38	15.83
303	14.65	0.27	14.92
304	22.15	0.17	22.33
501	14.54	65.86	80.40
502	15.39	68.38	83.77
503	14.62	65.83	80.45
504	22.12	31.25	53.37
701	14.54	180.39	194.93
702	22.05	85.81	107.87
703	14.62	180.33	194.94
704	22.09	85.80	107.89
901	14.65	0.02	14.66
902	22.13	0.03	22.16
903	14.65	0.02	14.66
904	22.13	0.03	22.16
1101	0.00	0.00	0.00
1102	0.00	0.00	0.00
1103	0.00	0.00	0.00
1104	0.00	0.00	0.00
1301	3.51	0.40	3.90
1302	3.54	0.33	3.87
1303	3.54	0.24	3.78
1304	3.54	0.19	3.74
1401	95.30	1.12	96.41
1402	0.00	0.01	0.01
1403	94.07	25.27	119.34
1404	0.00	0.01	0.01

1405	92.59	73.41	165.99
1406	0.00	0.01	0.01
1407	93.78	0.38	94.16
1408	0.00	0.01	0.01
2201	0.31	0.03	0.34
2202	2.51	0.06	2.57
2203	0.25	0.12	0.37
2204	2.51	0.04	2.55
2205	0.10	1.91	2.01
2206	2.51	0.02	2.54
2207	0.05	2.66	2.71
2208	2.51	0.02	2.53
2209	0.06	0.99	1.05
2210	2.51	0.03	2.54
2211	0.16	0.10	0.26
2212	2.51	0.05	2.56
2213	0.64	0.03	0.68
2214	2.90	0.09	2.99
2215	0.51	0.17	0.68
2216	2.90	0.06	2.96
2217	0.26	4.23	4.49
2218	2.90	0.02	2.92
2219	0.22	6.05	6.27
2220	2.90	0.02	2.91
2221	0.23	2.16	2.39
2222	2.90	0.03	2.93
2223	0.35	0.13	0.49
2224	2.90	0.07	2.97

TIME= 7.90

NODE	IR_POWER	UV_POWER	TOT_POWER
101	48.14	0.57	48.71
102	48.14	0.06	48.20
103	409.41	62.03	471.44
104	47.20	161.11	208.31
105	47.18	508.95	556.14
106	6.47	88.04	94.51
301	14.65	0.66	15.31
302	15.45	3.03	18.48
303	14.65	0.66	15.31
304	22.16	1.38	23.55
501	14.54	57.68	72.22

502	15.40	64.38	79.77
503	14.63	57.65	72.28
504	22.13	29.43	51.55
701	14.55	180.33	194.88
702	22.06	87.82	109.88
703	14.63	180.28	194.91
704	22.10	87.82	109.92
901	14.65	0.06	14.72
902	22.14	0.13	22.27
903	14.65	0.06	14.72
904	22.14	0.13	22.27
1101	0.00	0.00	0.00
1102	0.00	0.00	0.00
1103	0.00	0.00	0.00
1104	0.00	0.00	0.00
1301	3.51	39.41	42.92
1302	3.55	37.65	41.20
1303	3.55	32.65	36.20
1304	3.55	30.33	33.88
1401	95.22	23.55	118.76
1402	0.00	0.01	0.01
1403	94.01	66.80	160.82
1404	0.00	0.01	0.01
1405	92.60	117.65	210.25
1406	0.00	0.01	0.01
1407	93.78	2.23	96.01
1408	0.00	0.01	0.01
2201	0.31	0.44	0.75
2202	2.51	0.94	3.45
2203	0.25	0.46	0.70
2204	2.51	0.17	2.69
2205	0.10	1.15	1.24
2206	2.51	0.16	2.67
2207	0.05	1.81	1.86
2208	2.51	0.16	2.67
2209	0.06	0.22	0.29
2210	2.51	0.15	2.67
2211	0.16	0.31	0.47
2212	2.51	0.37	2.88
2213	0.64	0.62	1.26

2214	2.90	4.52	7.41
2215	0.51	0.58	1.09
2216	2.90	1.37	4.26
2217	0.26	3.57	3.83
2218	2.90	0.22	3.12
2219	0.22	5.07	5.29
2220	2.90	0.22	3.11
2221	0.23	1.05	1.27
2222	2.90	0.23	3.13
2223	0.35	0.32	0.67
2224	2.90	3.14	6.04

TIME= 15.79

NODE	IR_POWER	UV_POWER	TOT_POWER
101	48.13	1.32	49.45
102	48.13	0.06	48.18
103	409.41	105.32	514.73
104	47.19	88.54	135.72
105	47.17	509.43	556.61
106	6.47	44.69	51.16
301	14.65	1.56	16.21
302	15.45	7.17	22.62
303	14.65	1.56	16.21
304	22.16	3.28	25.44
501	14.55	34.78	49.32
502	15.39	44.03	59.42
503	14.62	34.64	49.27
504	22.11	20.13	42.24
701	14.54	181.18	195.72
702	22.05	89.78	111.83
703	14.62	181.14	195.76
704	22.09	89.77	111.87
901	14.65	0.06	14.71
902	22.13	0.13	22.26
903	14.65	0.06	14.71
904	22.13	0.13	22.26
1101	0.00	0.00	0.00
1102	0.00	0.00	0.00
1103	0.00	0.00	0.00
1104	0.00	0.00	0.00
1301	3.51	27.74	31.25
1302	3.54	25.23	28.78

1303	3.54	10.31	13.85
1304	3.54	6.98	10.52
1401	95.21	55.83	151.03
1402	0.00	0.01	0.01
1403	94.01	92.15	186.16
1404	0.00	0.01	0.01
1405	92.64	151.63	244.27
1406	0.00	0.01	0.01
1407	93.86	2.19	96.05
1408	0.00	0.01	0.01
2201	0.31	0.74	1.04
2202	2.51	1.87	4.38
2203	0.25	0.70	0.95
2204	2.51	0.50	3.02
2205	0.10	0.80	0.90
2206	2.51	0.29	2.80
2207	0.05	0.96	1.01
2208	2.51	0.29	2.80
2209	0.06	0.26	0.32
2210	2.51	0.36	2.87
2211	0.16	0.44	0.60
2212	2.51	1.24	3.75
2213	0.64	1.05	1.69
2214	2.90	7.18	10.08
2215	0.51	0.89	1.40
2216	2.90	2.03	4.92
2217	0.26	3.36	3.63
2218	2.90	0.40	3.30
2219	0.22	4.08	4.30
2220	2.90	0.39	3.29
2221	0.23	0.14	0.37
2222	2.90	0.55	3.44
2223	0.35	0.43	0.78
2224	2.90	6.02	8.91

TIME= 23.69

NODE	IR_POWER	UV_POWER	TOT_POWER
101	47.87	2.22	50.09
102	48.09	0.01	48.10
103	409.43	126.64	536.07
104	46.97	2.31	49.28
105	47.15	509.72	556.87

106	6.44	41.22	47.66
301	14.57	2.60	17.18
302	15.38	11.94	27.32
303	14.57	2.60	17.18
304	22.05	5.46	27.51
501	14.48	2.61	17.10
502	15.33	11.95	27.29
503	14.55	2.60	17.16
504	22.02	5.46	27.49
701	14.53	181.53	196.06
702	22.05	90.51	112.56
703	14.61	181.49	196.10
704	22.08	90.51	112.59
901	14.64	0.00	14.64
902	22.12	0.00	22.12
903	14.64	0.00	14.64
904	22.12	0.00	22.12
1101	0.00	0.00	0.00
1102	0.00	0.00	0.00
1103	0.00	0.00	0.00
1104	0.00	0.00	0.00
1301	3.50	25.81	29.31
1302	3.53	25.80	29.33
1303	3.53	6.44	9.96
1304	3.53	6.44	9.96
1401	95.64	92.88	188.52
1402	0.00	0.01	0.01
1403	94.37	93.02	187.39
1404	0.00	0.01	0.01
1405	92.45	164.11	256.56
1406	0.00	0.01	0.01
1407	93.64	0.02	93.66
1408	0.00	0.01	0.01
2201	0.31	0.88	1.19
2202	2.51	2.18	4.69
2203	0.25	0.82	1.06
2204	2.51	0.67	3.19
2205	0.10	0.77	0.87
2206	2.51	0.33	2.85
2207	0.05	0.53	0.58

2208	2.51	0.33	2.85
2209	0.06	0.24	0.31
2210	2.51	0.67	3.19
2211	0.16	0.48	0.64
2212	2.51	2.18	4.69
2213	0.64	1.25	1.90
2214	2.90	6.94	9.84
2215	0.51	1.03	1.54
2216	2.90	1.57	4.47
2217	0.26	3.67	3.93
2218	2.90	0.46	3.36
2219	0.22	3.34	3.56
2220	2.90	0.46	3.36
2221	0.23	0.12	0.35
2222	2.90	1.57	4.47
2223	0.35	0.44	0.79
2224	2.90	6.94	9.84

TIME= 31.59

NODE	IR_POWER	UV_POWER	TOT_POWER
101	48.13	94.18	142.31
102	48.13	0.06	48.18
103	409.41	113.33	522.74
104	47.18	1.42	48.61
105	47.17	509.51	556.69
106	6.47	44.69	51.16
301	14.65	34.77	49.42
302	15.45	44.02	59.47
303	14.65	34.77	49.42
304	22.16	20.12	42.28
501	14.55	1.58	16.12
502	15.40	7.19	22.59
503	14.63	1.57	16.19
504	22.12	3.29	25.40
701	14.54	181.19	195.73
702	22.06	89.78	111.84
703	14.62	181.15	195.77
704	22.09	89.77	111.87
901	14.65	0.06	14.71
902	22.14	0.13	22.26
903	14.65	0.06	14.71
904	22.14	0.13	22.26

1101	0.00	0.00	0.00
1102	0.00	0.00	0.00
1103	0.00	0.00	0.00
1104	0.00	0.00	0.00
1301	3.51	25.25	28.75
1302	3.54	27.73	31.28
1303	3.54	6.98	10.52
1304	3.54	10.31	13.85
1401	95.21	92.01	187.22
1402	0.00	0.01	0.01
1403	93.99	55.95	149.94
1404	0.00	0.01	0.01
1405	92.64	151.63	244.27
1406	0.00	0.01	0.01
1407	93.86	2.19	96.05
1408	0.00	0.01	0.01
2201	0.31	0.78	1.09
2202	2.51	1.24	3.75
2203	0.25	0.74	0.99
2204	2.51	0.36	2.87
2205	0.10	1.17	1.26
2206	2.51	0.29	2.80
2207	0.05	0.57	0.62
2208	2.51	0.29	2.80
2209	0.06	0.20	0.26
2210	2.51	0.50	3.01
2211	0.16	0.40	0.56
2212	2.51	1.87	4.38
2213	0.64	1.12	1.76
2214	2.90	6.02	8.91
2215	0.51	0.94	1.45
2216	2.90	0.55	3.44
2217	0.26	4.39	4.65
2218	2.90	0.39	3.29
2219	0.22	3.04	3.26
2220	2.90	0.40	3.30
2221	0.23	0.09	0.32
2222	2.90	2.03	4.92
2223	0.35	0.37	0.72
2224	2.90	7.18	10.08

TIME= 39.49

NODE	IR_POWER	UV_POWER	TOT_POWER
101	48.14	160.98	209.12
102	48.14	0.06	48.20
103	409.40	66.91	476.31
104	47.20	0.65	47.84
105	47.19	509.13	556.32
106	6.48	88.05	94.53
301	14.65	57.65	72.31
302	15.45	64.35	79.80
303	14.65	57.65	72.31
304	22.16	29.41	51.58
501	14.54	0.68	15.22
502	15.40	3.05	18.45
503	14.63	0.67	15.29
504	22.12	1.39	23.51
701	14.55	180.34	194.89
702	22.07	87.83	109.89
703	14.63	180.29	194.92
704	22.10	87.82	109.92
901	14.65	0.06	14.72
902	22.14	0.13	22.27
903	14.65	0.06	14.72
904	22.14	0.13	22.27
1101	0.00	0.00	0.00
1102	0.00	0.00	0.00
1103	0.00	0.00	0.00
1104	0.00	0.00	0.00
1301	3.51	37.67	41.18
1302	3.55	39.39	42.94
1303	3.55	30.34	33.89
1304	3.55	32.66	36.20
1401	95.22	66.58	161.80
1402	0.00	0.01	0.01
1403	93.98	23.68	117.66
1404	0.00	0.01	0.01
1405	92.57	117.67	210.24
1406	0.00	0.01	0.01
1407	93.78	2.23	96.01
1408	0.00	0.01	0.01
2201	0.31	0.46	0.77

2202	2.51	0.37	2.88
2203	0.25	0.48	0.72
2204	2.51	0.15	2.67
2205	0.10	1.96	2.06
2206	2.51	0.16	2.67
2207	0.05	0.95	1.00
2208	2.51	0.16	2.67
2209	0.06	0.13	0.19
2210	2.51	0.17	2.69
2211	0.16	0.23	0.39
2212	2.51	0.94	3.45
2213	0.64	0.66	1.30
2214	2.90	3.14	6.04
2215	0.51	1.52	2.03
2216	2.90	0.23	3.13
2217	0.26	5.34	5.60
2218	2.90	0.22	3.11
2219	0.22	3.27	3.49
2220	2.90	0.22	3.12
2221	0.23	0.05	0.28
2222	2.90	1.36	4.26
2223	0.35	0.21	0.56
2224	2.90	4.51	7.41

TIME= 47.38

NODE	IR_POWER	UV_POWER	TOT_POWER
101	48.12	186.64	234.76
102	48.12	0.03	48.16
103	409.42	3.24	412.66
104	47.18	0.74	47.92
105	47.17	511.94	559.11
106	6.47	1.03	7.49
301	14.65	65.82	80.46
302	15.45	68.32	83.77
303	14.65	65.82	80.46
304	22.15	31.23	53.39
501	14.54	0.29	14.82
502	15.40	0.41	15.80
503	14.62	0.27	14.90
504	22.12	0.18	22.30
701	14.54	180.41	194.95
702	22.06	85.81	107.87

703	14.62	180.34	194.96
704	22.09	85.81	107.90
901	14.65	0.02	14.66
902	22.13	0.03	22.16
903	14.65	0.02	14.66
904	22.13	0.03	22.16
1101	0.00	0.02	0.02
1102	0.00	0.02	0.02
1103	0.00	0.02	0.02
1104	0.00	0.02	0.02
1301	3.51	0.34	3.85
1302	3.54	0.37	3.91
1303	3.54	0.18	3.73
1304	3.54	0.23	3.78
1401	95.30	24.99	120.29
1402	0.00	0.05	0.05
1403	94.06	1.26	95.32
1404	0.00	0.05	0.05
1405	92.58	73.46	166.04
1406	0.00	0.05	0.05
1407	93.78	0.38	94.16
1408	0.00	0.05	0.05
2201	0.31	0.02	0.33
2202	2.51	0.05	2.56
2203	0.25	0.97	1.22
2204	2.51	0.03	2.54
2205	0.10	2.75	2.85
2206	2.51	0.02	2.53
2207	0.05	1.78	1.83
2208	2.51	0.02	2.54
2209	0.06	0.05	0.11
2210	2.51	0.04	2.55
2211	0.16	0.02	0.18
2212	2.51	0.06	2.57
2213	0.64	0.03	0.68
2214	2.90	0.07	2.97
2215	0.51	2.23	2.74
2216	2.90	0.03	2.93
2217	0.26	6.28	6.54
2218	2.90	0.02	2.91

2219	0.22	3.97	4.20
2220	2.90	0.02	2.92
2221	0.23	0.03	0.26
2222	2.90	0.06	2.96
2223	0.35	0.01	0.37
2224	2.90	0.09	2.99

TIME= 55.28

NODE	IR_POWER	UV_POWER	TOT_POWER
101	48.14	168.23	216.37
102	48.14	3.66	51.81
103	409.40	17.03	426.44
104	47.20	6.11	53.31
105	47.19	519.12	566.31
106	6.48	142.48	148.96
301	14.65	59.37	74.02
302	15.45	53.98	69.43
303	14.65	59.37	74.02
304	22.16	18.20	40.36
501	14.54	2.32	16.86
502	15.40	3.14	18.54
503	14.63	2.32	16.94
504	22.12	1.43	23.55
701	14.55	182.88	197.43
702	22.07	73.35	95.42
703	14.63	182.81	197.43
704	22.10	74.80	96.90
901	14.65	1.41	16.07
902	22.14	0.95	23.10
903	14.65	1.41	16.07
904	22.14	0.95	23.10
1101	0.00	48.31	48.31
1102	0.00	48.31	48.31
1103	0.00	48.31	48.31
1104	0.00	48.31	48.31
1301	3.51	22.85	26.36
1302	3.55	22.92	26.46
1303	3.55	22.57	26.12
1304	3.55	22.65	26.20
1401	95.22	24.64	119.86
1402	0.00	132.44	132.44
1403	93.98	8.09	102.07

1404	0.00	132.44	132.44
1405	92.57	72.55	165.11
1406	0.00	132.44	132.44
1407	93.78	6.71	100.48
1408	0.00	132.44	132.44
2201	0.31	0.12	0.43
2202	2.51	0.26	2.77
2203	0.25	1.80	2.04
2204	2.51	0.23	2.74
2205	0.10	3.59	3.68
2206	2.51	0.20	2.72
2207	0.05	2.71	2.76
2208	2.51	0.21	2.73
2209	0.06	0.15	0.22
2210	2.51	0.25	2.76
2211	0.16	0.07	0.23
2212	2.51	0.27	2.78
2213	0.64	0.17	0.82
2214	2.90	0.33	3.23
2215	0.51	2.92	3.43
2216	2.90	0.26	3.16
2217	0.26	7.03	7.30
2218	2.90	0.21	3.11
2219	0.22	5.00	5.22
2220	2.90	0.24	3.13
2221	0.23	0.04	0.27
2222	2.90	0.31	3.20
2223	0.35	0.06	0.42
2224	2.90	0.35	3.25

TIME= 63.18

NODE	IR_POWER	UV_POWER	TOT_POWER
101	48.13	105.52	153.65
102	48.13	8.79	56.91
103	409.41	28.87	438.28
104	47.18	11.91	59.09
105	47.17	524.33	571.51
106	6.47	75.25	81.73
301	14.65	37.37	52.02
302	15.45	31.76	47.21
303	14.65	35.74	50.39
304	22.16	8.19	30.34

501	14.55	4.48	19.02
502	15.40	5.93	21.33
503	14.63	4.47	19.10
504	22.12	2.71	24.83
701	14.54	184.68	199.22
702	22.06	64.22	86.28
703	14.62	184.61	199.23
704	22.09	65.71	87.80
901	14.65	3.33	17.98
902	22.13	2.11	24.25
903	14.65	3.33	17.98
904	22.13	2.11	24.25
1101	0.00	83.65	83.66
1102	0.00	83.65	83.66
1103	0.00	83.65	83.66
1104	0.00	83.65	83.66
1301	3.51	12.72	16.23
1302	3.54	12.76	16.30
1303	3.54	12.44	15.98
1304	3.54	12.49	16.03
1401	95.21	22.05	117.26
1402	0.00	229.35	229.35
1403	93.99	14.48	108.47
1404	0.00	229.35	229.35
1405	92.64	71.70	164.34
1406	0.00	229.35	229.35
1407	93.86	12.90	106.76
1408	0.00	229.35	229.35
2201	0.31	0.20	0.51
2202	2.51	0.44	2.95
2203	0.25	2.18	2.43
2204	2.51	0.41	2.92
2205	0.10	4.08	4.18
2206	2.51	0.38	2.89
2207	0.05	3.51	3.56
2208	2.51	0.39	2.90
2209	0.06	1.16	1.22
2210	2.51	0.42	2.93
2211	0.16	0.11	0.27
2212	2.51	0.44	2.96

2213	0.64	0.30	0.95
2214	2.90	0.54	3.44
2215	0.51	2.89	3.40
2216	2.90	0.48	3.37
2217	0.26	7.31	7.57
2218	2.90	0.42	3.32
2219	0.22	6.02	6.24
2220	2.90	0.44	3.33
2221	0.23	0.26	0.49
2222	2.90	0.50	3.40
2223	0.35	0.12	0.47
2224	2.90	0.56	3.45

TIME= 71.08

NODE	IR_POWER	UV_POWER	TOT_POWER
101	47.87	14.57	62.44
102	48.09	10.73	58.82
103	409.43	33.09	442.52
104	46.97	14.62	61.59
105	47.15	526.16	573.31
106	6.44	68.86	75.30
301	14.57	5.43	20.01
302	15.38	7.15	22.53
303	14.57	5.43	20.01
304	22.05	3.27	25.32
501	14.48	5.47	19.95
502	15.33	7.19	22.52
503	14.55	5.45	20.00
504	22.02	3.28	25.30
701	14.53	185.32	199.85
702	22.05	60.77	82.82
703	14.61	185.25	199.86
704	22.08	60.76	82.84
901	14.64	4.06	18.69
902	22.12	2.55	24.67
903	14.64	4.06	18.69
904	22.12	2.55	24.67
1101	0.00	96.59	96.59
1102	0.00	96.59	96.59
1103	0.00	96.59	96.59
1104	0.00	96.59	96.59
1301	3.50	11.88	15.37

1302	3.53	11.86	15.38
1303	3.53	11.59	15.12
1304	3.53	11.59	15.11
1401	95.64	17.06	112.69
1402	0.00	264.81	264.81
1403	94.37	17.23	111.60
1404	0.00	264.81	264.81
1405	92.45	70.76	163.20
1406	0.00	264.81	264.81
1407	93.64	15.16	108.80
1408	0.00	264.81	264.81
2201	0.31	0.23	0.54
2202	2.51	0.51	3.02
2203	0.25	2.01	2.26
2204	2.51	0.48	2.99
2205	0.10	4.11	4.21
2206	2.51	0.45	2.96
2207	0.05	3.96	4.01
2208	2.51	0.45	2.96
2209	0.06	1.82	1.88
2210	2.51	0.48	2.99
2211	0.16	0.13	0.29
2212	2.51	0.51	3.02
2213	0.64	0.35	0.99
2214	2.90	0.63	3.52
2215	0.51	2.13	2.64
2216	2.90	0.57	3.46
2217	0.26	7.03	7.30
2218	2.90	0.50	3.40
2219	0.22	6.77	6.99
2220	2.90	0.50	3.40
2221	0.23	1.81	2.04
2222	2.90	0.57	3.46
2223	0.35	0.14	0.49
2224	2.90	0.63	3.52

TIME= 78.97

NODE	IR_POWER	UV_POWER	TOT_POWER
101	48.13	11.97	60.10
102	48.13	8.78	56.91
103	409.41	28.44	437.86
104	47.19	105.66	152.84

105	47.17	524.15	571.33
106	6.47	75.26	81.73
301	14.65	4.47	19.12
302	15.45	5.92	21.37
303	14.65	4.47	19.12
304	22.16	2.70	24.86
501	14.55	37.41	51.96
502	15.39	31.81	47.21
503	14.62	35.77	50.39
504	22.11	8.20	30.32
701	14.54	184.67	199.20
702	22.05	65.71	87.76
703	14.62	184.60	199.22
704	22.10	64.21	86.31
901	14.65	3.33	17.97
902	22.14	2.11	24.25
903	14.65	3.33	17.97
904	22.14	2.11	24.25
1101	0.00	83.64	83.64
1102	0.00	83.64	83.64
1103	0.00	83.64	83.64
1104	0.00	83.64	83.64
1301	3.51	12.77	16.28
1302	3.54	12.71	16.25
1303	3.54	12.49	16.03
1304	3.54	12.44	15.98
1401	95.21	14.36	109.56
1402	0.00	229.31	229.31
1403	94.01	22.28	116.29
1404	0.00	229.31	229.31
1405	92.64	71.64	164.28
1406	0.00	229.31	229.31
1407	93.86	12.90	106.75
1408	0.00	229.31	229.31
2201	0.31	0.20	0.51
2202	2.51	0.44	2.96
2203	0.25	1.33	1.57
2204	2.51	0.42	2.93
2205	0.10	3.66	3.76
2206	2.51	0.38	2.90

2207	0.05	3.95	4.00
2208	2.51	0.38	2.89
2209	0.06	2.05	2.11
2210	2.51	0.41	2.92
2211	0.16	0.15	0.31
2212	2.51	0.44	2.95
2213	0.64	0.30	0.94
2214	2.90	0.56	3.45
2215	0.51	0.55	1.07
2216	2.90	0.50	3.40
2217	0.26	6.28	6.54
2218	2.90	0.43	3.33
2219	0.22	7.06	7.28
2220	2.90	0.42	3.32
2221	0.23	2.63	2.86
2222	2.90	0.48	3.37
2223	0.35	0.17	0.53
2224	2.90	0.54	3.44

TIME= 86.87

NODE	IR_POWER	UV_POWER	TOT_POWER
101	48.14	6.18	54.32
102	48.14	3.66	51.81
103	409.41	16.46	425.87
104	47.20	168.42	215.62
105	47.18	518.84	566.03
106	6.47	142.50	148.97
301	14.65	2.32	16.97
302	15.45	3.12	18.57
303	14.65	2.32	16.97
304	22.16	1.43	23.59
501	14.54	59.42	73.96
502	15.40	54.04	69.43
503	14.63	59.39	74.01
504	22.13	18.23	40.35
701	14.55	182.86	197.41
702	22.06	74.80	96.86
703	14.63	182.79	197.42
704	22.10	73.34	95.45
901	14.65	1.41	16.07
902	22.14	0.95	23.10
903	14.65	1.41	16.07

904	22.14	0.95	23.10
1101	0.00	48.28	48.28
1102	0.00	48.28	48.28
1103	0.00	48.28	48.28
1104	0.00	48.28	48.28
1301	3.51	22.94	26.45
1302	3.55	22.84	26.38
1303	3.55	22.66	26.20
1304	3.55	22.58	26.13
1401	95.22	7.98	103.20
1402	0.00	132.37	132.38
1403	94.01	24.90	118.91
1404	0.00	132.37	132.38
1405	92.60	72.46	165.06
1406	0.00	132.37	132.38
1407	93.78	6.70	100.48
1408	0.00	132.37	132.38
2201	0.31	0.12	0.43
2202	2.51	0.27	2.78
2203	0.25	0.28	0.52
2204	2.51	0.25	2.76
2205	0.10	2.85	2.95
2206	2.51	0.21	2.73
2207	0.05	3.47	3.52
2208	2.51	0.20	2.72
2209	0.06	1.75	1.81
2210	2.51	0.23	2.74
2211	0.16	0.14	0.30
2212	2.51	0.26	2.77
2213	0.64	0.17	0.81
2214	2.90	0.35	3.25
2215	0.51	0.27	0.78
2216	2.90	0.31	3.20
2217	0.26	5.25	5.51
2218	2.90	0.24	3.13
2219	0.22	6.79	7.01
2220	2.90	0.21	3.11
2221	0.23	2.76	2.99
2222	2.90	0.26	3.16
2223	0.35	0.17	0.52

	2224	2.90	0.33	3.23
TIME=	94.77 NODE	IR_POWER	UV_POWER	TOT_POWER
	101	48.12	0.71	48.83
	102	48.12	0.03	48.15
	103	409.42	2.83	412.25
	104	47.18	186.84	234.02
	105	47.17	511.68	558.84
	106	6.47	0.99	7.46
	301	14.65	0.27	14.92
	302	15.45	0.38	15.83
	303	14.65	0.27	14.92
	304	22.15	0.17	22.33
	501	14.54	65.86	80.40
	502	15.39	68.38	83.77
	503	14.62	65.83	80.45
	504	22.12	31.25	53.37
	701	14.54	180.39	194.93
	702	22.05	85.81	107.87
	703	14.62	180.33	194.94
	704	22.09	85.80	107.89
	901	14.65	0.02	14.66
	902	22.13	0.03	22.16
	903	14.65	0.02	14.66
	904	22.13	0.03	22.16
	1101	0.00	0.00	0.00
	1102	0.00	0.00	0.00
	1103	0.00	0.00	0.00
	1104	0.00	0.00	0.00
	1301	3.51	0.40	3.90
	1302	3.54	0.33	3.87
	1303	3.54	0.24	3.78
	1304	3.54	0.19	3.74
	1401	95.30	1.12	96.41
	1402	0.00	0.01	0.01
	1403	94.07	25.27	119.34
	1404	0.00	0.01	0.01
	1405	92.59	73.41	165.99
	1406	0.00	0.01	0.01
	1407	93.78	0.38	94.16
	1408	0.00	0.01	0.01

2201	0.31	0.03	0.34
2202	2.51	0.06	2.57
2203	0.25	0.12	0.37
2204	2.51	0.04	2.55
2205	0.10	1.91	2.01
2206	2.51	0.02	2.54
2207	0.05	2.66	2.71
2208	2.51	0.02	2.53
2209	0.06	0.99	1.05
2210	2.51	0.03	2.54
2211	0.16	0.10	0.26
2212	2.51	0.05	2.56
2213	0.64	0.03	0.68
2214	2.90	0.09	2.99
2215	0.51	0.17	0.68
2216	2.90	0.06	2.96
2217	0.26	4.23	4.49
2218	2.90	0.02	2.92
2219	0.22	6.05	6.27
2220	2.90	0.02	2.91
2221	0.23	2.16	2.39
2222	2.90	0.03	2.93
2223	0.35	0.13	0.49
2224	2.90	0.07	2.97

TIME= -94.77 NODE IR_POWER UV_POWER TOT_POWER < Orbital Averages >

101	48.09	62.76	110.85
102	48.13	3.00	51.12
103	409.41	50.35	459.76
104	47.15	62.36	109.51
105	47.17	515.25	562.42
106	6.47	67.75	74.22
301	14.64	22.69	37.33
302	15.44	25.09	40.53
303	14.64	22.56	37.19
304	22.14	10.40	32.54
501	14.53	22.71	37.25
502	15.39	25.12	40.51
503	14.61	22.55	37.17
504	22.10	10.42	32.52

701	14.54	182.15	196.69
702	22.06	79.68	101.74
703	14.62	182.09	196.71
704	22.09	79.68	101.77
901	14.65	1.15	15.80
902	22.13	0.77	22.91
903	14.65	1.15	15.80
904	22.13	0.77	22.91
1101	0.00	30.04	30.04
1102	0.00	30.04	30.04
1103	0.00	30.04	30.04
1104	0.00	30.04	30.04
1301	3.51	19.98	23.49
1302	3.54	19.97	23.51
1303	3.54	14.07	17.62
1304	3.54	14.07	17.62
1401	95.30	36.92	132.22
1402	0.00	82.37	82.37
1403	94.07	37.09	131.16
1404	0.00	82.37	82.37
1405	92.58	100.72	193.30
1406	0.00	82.37	82.37
1407	93.78	5.33	99.11
1408	0.00	82.37	82.37
2201	0.31	0.35	0.66
2202	2.51	0.72	3.23
2203	0.25	0.99	1.24
2204	2.51	0.31	2.82
2205	0.10	2.40	2.50
2206	2.51	0.24	2.75
2207	0.05	2.24	2.29
2208	2.51	0.24	2.75
2209	0.06	0.75	0.82
2210	2.51	0.31	2.82
2211	0.16	0.21	0.37
2212	2.51	0.72	3.23
2213	0.64	0.50	1.15
2214	2.90	2.53	5.43
2215	0.51	1.34	1.85
2216	2.90	0.66	3.56

```
      2217    0.26    5.31    5.57
      2218    2.90    0.30    3.19
      2219    0.22    5.04    5.26
      2220    2.90    0.30    3.19
      2221    0.23    0.93    1.16
      2222    2.90    0.66    3.56
      2223    0.35    0.21    0.57
      2224    2.90    2.53    5.43
 ITAS ABSORB SUB-PROGRAM FINISHED NORMALLY
**************************************
 ABSORBED HEAT CALC CPU TIME (second) =    605.660
**************************************
 ITAS THERMAL ANALYZER:
vvvvvvvvvvvvvvvvvvvvv ADDING USER NODES vvvvvvvvvvv
IPTR_N=  2522
RECORD  2522=199        -5420 0     2299        -298  0
RECORD  2523=20301       -596  5     20302       -596  0
RECORD  2524=20303       -596  5     20304       -298  54
RECORD  2525=20501       -596  5     20502       -596  0
RECORD  2526=20503       -596  5     20504       -298  54
RECORD  2527=20701       -596  10    20702       -596  35
RECORD  2528=20703       -596  10    20704       -596  35
RECORD  2529=20901       -596  10    20902       -596  35
RECORD  2530=20903       -596  10    20904       -596  35
RECORD  2531=1199        -298  0     1299        -894  20
RECORD  2532=1399        -298  0
^^^^^^^^^^^^^^^^^END OF USER NODES^^^^^^^^
^^^^^^^^^^^^^^^^END OF FLUID^^^^^^^^^^^^^
^^^^^^^^^^^^^^^^END OF FLUID^^^^^^^^^^^^^
 NODE   101 (REL NODE    1 ) IS BEING ADDED TO THE CURRENT
LIST
 NODE   102 (REL NODE    2 ) IS BEING ADDED TO THE CURRENT
LIST
 NODE   103 (REL NODE    3 ) IS BEING ADDED TO THE CURRENT
LIST
 NODE   104 (REL NODE    4 ) IS BEING ADDED TO THE CURRENT
LIST
 NODE   105 (REL NODE    5 ) IS BEING ADDED TO THE CURRENT
LIST
```

APPENDIX J - STRUCTURAL DESIGN CALCULATIONS

A. CENTRAL CYLINDER

Assuming the payload mass to be concentrated at its center and the spacecraft bus mass to be concentrated at its center as shown in Figure J.1, the axial load, P, and the bending moment, M, at the bottom of the cylinder are determined as follows:

$$P = (363+900)(7.2)(9.81)(1.5) = 1.34\times10^5 \text{ N}$$

$$M = 363(2.5)(9.81)(1.5)(0.762) = 1.02\times10^5 \text{ Nm}$$

The critical axial buckling load and critical bending moment are:

$$P_{cr} = 1.2\gamma Et^2$$

$$M_{cr} = 0.6\gamma\pi Ert^2$$

where $\gamma = 1 - 0.9(1 - e^{-\phi})$

$$\phi = \frac{1}{16}\sqrt{\frac{r}{t}}$$

Using the radius of the cylinder, r = 0.254 m, Young's Modulus for 6061-T6 Aluminum, E = 67 x 10^9 N/m^2, and assuming a thickness, t = 2 mm, the critical buckling load and bending moment are

$$P_{cr} = 1.75\times10^5 \text{ N}$$

$$M_{cr} = 6.99\times10^4 \text{ Nm}$$

The margin of safety is thus:

$$MS = (P/P_{cr} + M/M_{cr})^{-1} - 1 = 0.100$$

B. ADAPTER CONE

The axial load, P, and the bending moment, M, at the bottom of the adapter cone are determined as follows:

$$P = (363+900)(7.2)(9.81)(1.5) = 1.34\times10^5 \text{ N}$$

$$M = 363(2.5)9.81(1.5)1.27 + 900(2.5)9.81(1.5)0.508 = 3.38\times10^4 \text{ Nm}$$

The critical buckling load and bending moment are given by

$$P_{cr} = 2\,\pi\, r_1\, t\, \sigma_c \cos\alpha$$

$$M_{cr} = \pi\, r_1^2 t\, \sigma_b \cos\alpha$$

where

$$\sigma_c = 0.19972\, E \frac{t}{r_e}$$

$$\sigma_b = 0.24814\, E \frac{t}{r_e}$$

$$r_e = r_2 / \cos\alpha$$

Using $\alpha = 41.85\,^\circ$ (Figure J.1) , the smaller radius, $r_1 = 0.254$ m, the larger radius, $r_2 = 0.709$ m, and assuming the shell thickness, $t = 5$ mm,the critical buckling load and bending moment are

$$P_{cr} = 4.18\times10^5 \text{ N}$$

$$M_{cr} = 6.59\times10^4 \text{ Nm}$$

The margin of safety is therefore: MS = 0.201.

C. HONEYCOMB PANELS

1. Payload Panel

This panel supports the load of the payload (363 kg). It transmits this load to the central cylinder by being clamped to the top of the cylinder. To determine the dimensions of the panel, it was assumed to be made up of two panels, each clamped on one side and simply supported on the other three as shown in Figure J.2. Each of these panels supports half the payload or approximately 185 kg. The mass per unit area, γ, is

$$\gamma = \frac{185}{(0.762)(1.524)} = 159.3\ \frac{\text{kg}}{\text{m}^2}$$

Assuming a natural frequency of 50 Hz to avoid coupling with the launch vehicle, the panel stiffness, D, can be found from

$$f = \frac{1}{2\pi}\beta_1\sqrt{\frac{D}{\gamma a^4}}$$

$$50 = \frac{1}{2\pi}17.33\sqrt{\frac{D}{159.3(0.762)^4}}$$

$$\therefore \quad D = 17650 \text{ Nm}$$

Assuming that the skin thickness, t, of the honeycomb is 1.0 mm, the heighth of the honeycomb can be found from the following equation:

$$D = \frac{E\,t\,h^2}{2(1-\vartheta^2)}$$

$$= \frac{67\times10^9(0.001)\,h^2}{2(.89)} \Rightarrow h = 2.34 \text{ cm}$$

Assuming a uniform dynamic acceleration of 36 g's across the panel, the maximum stress in the face skin at the center of the panel is given by:

$$\sigma_{max} = \frac{\beta_2\,\gamma g\,(\text{dyn accel})\,a^2}{6\,t\,h}$$

$$= \frac{0.6102(159.3)(9.81)(36)(.762^2)}{6(.001)(0.0234)}$$

$$= 141.9 \text{ N/mm}^2$$

This maximum stress is below the allowable yield stress of aluminum which is 240 N/mm^2. Hence, the panel design is acceptable.

2. Equipment Panels

There are two equipment panels which must support the loads from the various subsystems which total approximately 600 kg. It was assumed that 300 kg must be supported by each equipment panel. The top panel was modeled identically to the payload panel. The mass per unit area is 129.2 kg/m^2. Following

a procedure similar to that above, the maximum stress is 115.1 N/mm^2. This is again below the allowable yields stress.

The bottom equipment panel was assumed to be made of four panels, each clamped on one end and simply supported on the other three as shown in Figure J.3. Each of these panels supports 1/4 of the 300 kg. Using the same honeycomb as above, the maximum stress was determined to be 54.2 N/mm^2, which is again below the yield stress considerably.

3. Side Panels

Each of the side panels are manufactured from the same honeycomb as the other panels. The panels are simply supported on all sides and are attached to the frame's square tubing. The panels adequately support any components attached to them.

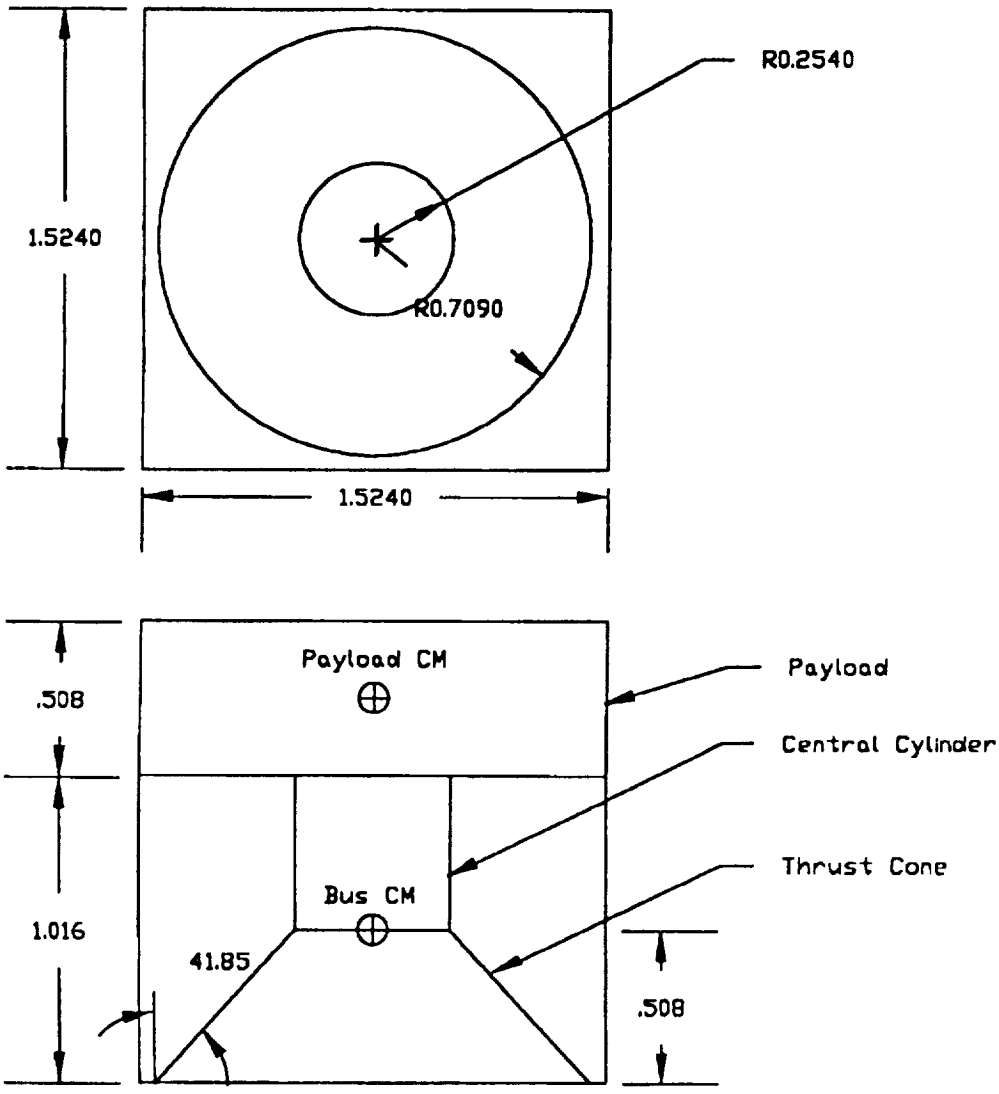

Figure J.1 Structure Diagram

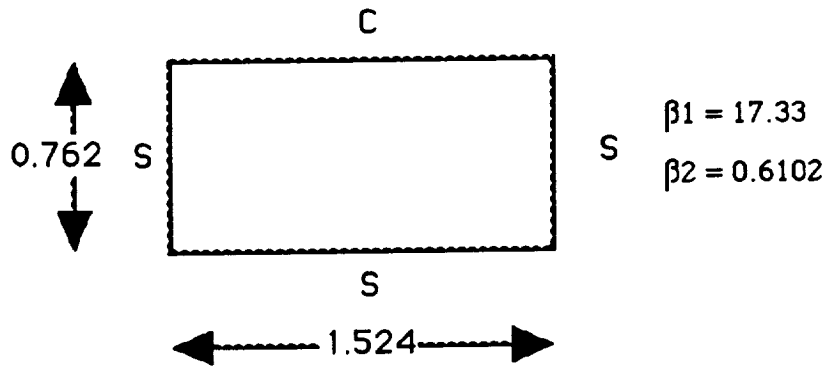

Figure J.2 Side Pannel Diagram

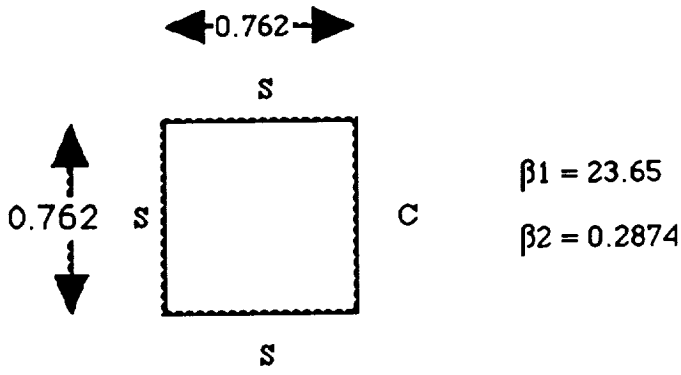

Figure J.3 Top Pannel Diagram

APPENDIX K - COST ANALYSIS

The following are a few of the definintions used in cost analysis

(A) Component: A component is a functional unit that is viewed as an entity for purposes of analysis, manufacturing, maintenance, or record keeping. Examples are hydraulic actuators, valves, batteries, electrical harnesses, and individual electronics packages such as transmitters, receivers, or multiplexers.

(B) Subsystem: A subsystem is an assembly of two or more components including the supporting structure to which they are mounted, and any interconnecting cables or tubing. A subsystem is composed of functionally related components that perform one or more prescribed functions. Typical space vehicle subsystems are electrical power, attitude control, thermal control, telemetry, structure, and propulsion.

(C) Space Vehicle: A space vehicle is a complete, integrated set of subsystems and components capable of supporting an operational role in space. A space vehicle may be an orbiting vehicle, a major portion of an orbiting vehicle, or a payload which performs its mission while attached to a recoverable launch vehicle.